



The composition of root-associated microbiomes and their beneficial effects on plant growth under stress conditions Z. Yan 2022

The composition of root-associated microbiomes and their beneficial effects on plant growth under stress conditions

Zhichun Yan
严志纯



Invitation

You are cordially invited to
attend the public defence
of my PhD thesis entitled:

**The composition of root-
associated microbiomes
and their beneficial effects
on plant growth under
stress conditions**

On Friday the 2nd of December 2022
at 4.00 p.m.
in the Omnia Auditorium

Zhichun Yan

zhichun.yan@wur.nl

Paranymphs

Siqi Yan

siqi.yan@wur.nl

Jundi Yan

jundi.yan@wur.nl



Propositions

1. Formation of the root-sleeve does increase tolerance to drought.
(this thesis)
2. Biodiversity is a key to the success of a synthetic community to confer tolerance to abiotic stress.
(this thesis)
3. The expression patterns of HvHOX1 and HvHOX2 do not justify the conclusion of Thirulogachandar *et al.* (*bioRxiv* 2021.11.08.467769) that they have antagonistic activities.
4. Using psyllids to transfer Huanglongbing does not support the conclusion of Lee *et al.* (PNAS, 2015, 112.24: 7605-7610) that *Liberibacter* is the cause of the disease symptoms.
5. Improving animal welfare will reduce productivity, but it is essential to achieve the United Nations sustainable development goal No.2, zero hunger.
6. Lifelong learning is crucial to delay the decrease in cognitive functioning.

Propositions belonging to the thesis, entitled

The composition of root-associated microbiomes and their beneficial effects on plant growth under stress conditions.

Zhichun Yan

Wageningen, 2 December 2022

The composition of root-associated microbiomes and their beneficial effects on plant growth under stress conditions

Zhichun Yan

Thesis committee

Promotor

Prof. Dr A.H.J. Bisseling

Professor at the Laboratory of Molecular Biology

Wageningen University & Research

Co-promotor

Prof. Dr X. Cheng

Professor of Agricultural Genomics Institute at Shenzhen

Chinese Academy of Agricultural Sciences

Other members

Prof. Dr W.H. van der Putten, Wageningen University & Research

Prof. Dr J. Raaijmakers, NIOO-KNAW, Wageningen

Dr R.B. Karlova, Wageningen University & Research

Dr V.J. Carrion Bravo, Leiden University

This research was conducted under the auspices of the Graduate School Experimental Plant Sciences.

The composition of root-associated microbiomes and their beneficial effects on plant growth under stress conditions

Zhichun Yan

Thesis

submitted in fulfilment of the requirement for the degree of doctor

at Wageningen University,

by the authority of the Rector Magnificus,

Prof. Dr A. P. J. Mol,

in the presence of the

Thesis Committee appointed by the Academic Board

to be defended in public

on Friday 2nd December, 2022

at 4 p.m. in the Omnia Auditorium.

Zhichun Yan

The composition of root-associated microbiomes and their beneficial effects on plant growth under stress conditions

264 pages

PhD thesis, Wageningen University, Wageningen, the Netherlands (2022)

With references, with summary in English

ISBN 978-94-6447-481-7

DOI <https://doi.org/10.18174/580377>

Contents

Chapter 1	1
General introduction	
Chapter 2	19
Root-sleeve, an adaptation to drought and a niche for a distinct microbiome	
Chapter 3	45
High salt levels reduced dissimilarities in root-associated microbiomes of two barley genotypes	
Chapter 4	89
Longevity correlates with similar composition of root associated bacterial microbiomes in a chrono-series of Chinese chestnut	
Chapter 5	137
Synthetic bacterial community derived from a desert rhizosphere confers salt stress resilience to tomato in the presence of a soil microbiome	
Chapter 6	193
General discussion	
References	207
Summary	243

Chapter 1

General introduction

Introduction

Plants have a multitude of niches to host a diversity of microorganisms. These communities of microorganisms include, for example, bacteria, fungi, protists, nematodes and viruses and are referred to as microbiomes (Marchesi & Ravel, 2015). In the belowground, they are called root-associated microbiomes. Plant roots assemble two distinct microbiomes: in the rhizosphere (microbes in the soil surrounding roots) and in the endophytic compartment (microbes within roots) (Lundberg *et al.*, 2012). These root-associated microbiomes have complex interactions with their host and can promote growth and health of the plant at "normal" conditions as well as under (a)biotic stresses (Mendes *et al.*, 2013). Although root-associated microbiomes have been known for a long time, till recently they could only be studied by, for example, culture-dependent approaches, which created serious limitations (Su *et al.*, 2012). However, since last two decades, next-generation DNA sequencing technologies and data analyses (known as culture-independent approaches) have markedly expanded the ability to study microbiomes, including those associated with plant roots (Fitzpatrick *et al.*, 2020). Among the members of root-associated microbiomes, bacteria are relatively well-studied compared to others (Mendes 2013, Leach 2017). In this thesis, I will focus on bacteria, and the root-associated microbiomes mentioned in this thesis are in general bacterial microbiomes.

Determinants that affect the composition of root-associated microbiomes

The composition of root-associated microbiomes is determined by various factors and these can be grouped as host-related factors and environmental factors, respectively. The host-related factors include plant compartment and genotype effects (Lundberg *et al.*, 2012; Schnejderberg *et al.*, 2020). The environmental factors can be separated into biotic factors such as the presence of pathogens and abiotic factors such as soil physiochemical properties, drought and salinity (Bulgarelli *et al.*, 2012; Lundberg *et al.*, 2012; Philippot *et al.*, 2013; Edwards *et al.*, 2015; Lebeis *et al.*, 2015).

Chapter 1

The plant compartment effect

Members of the root-associated microbiomes can be transferred horizontally or vertically, i.e. they are derived from either the bulk soil or inherited via seeds. Soil contributes to most members of the root-associated microbiome and functions as a microbial reservoir containing highly diverse microorganisms (Berg, Gabriele & Smalla, Kornelia, 2009). The soil bacterial microbiome is in general dominated by Acidobacteria, Verrucomicrobia, Bacteroidetes, Planctomycetes, Proteobacteria and Actinobacteria (Lennon & Jones, 2011; Fierer, 2017). In general, the composition of microbiomes in the rhizosphere (RH) and endophytic compartment (EC) are different from that in the bulk soil, and that of the endophytic microbiome differs most (Fonseca-Garcia *et al.*, 2016; Fitzpatrick *et al.*, 2018). The microbiomes of RH and EC are structured by a common principle across various environments and host species, i.e. the microbial diversity is significantly reduced from soil to RH and this becomes, in general, even lower in the EC (Vieira *et al.*, 2020). These differences indicate an increasing influence of the plant host on microbiome composition from "around the root" to "in the root" (Coleman-Derr *et al.*, 2016).

The plant genotype effect

A second host-related factor, i.e. the plant genotype, can strongly influence the composition of the root-associated microbiomes. The effect of plant genotype was, for example, demonstrated by growing different plant species in the same soil. For example, Schneijderberg *et al.* (2020) compared the root-associated microbiomes of *Arabidopsis thaliana* (Arabidopsis) to eight other plant species from the same habitat. Principal coordinate analyses showed that both RH and EC microbiomes were significantly different between these species. This was also the case in a comparative study of grapevine and four weed species growing in the same vineyard, showing that they formed different root-associated microbiomes in RH and EC, respectively (Samad *et al.*, 2017). Next to a species-specific effect, the genotype effect has even been detected between accessions or cultivars of single species. This has been shown, for example, in Arabidopsis, maize and rice (Peiffer *et al.*, 2013; Schlaeppi *et al.*, 2014; Edwards *et al.*, 2015).

The plant genotype effect can be caused by several aspects, like the differences in plant morphology and physiology under normal or stressed conditions, which induce metabolic diversification of root exudates (Trivedi *et al.*, 2020). Mutagenesis has been widely used to demonstrate the causal relationship between plant-derived metabolites and the assembly of microbial communities. Mutations that affected the biosynthesis of metabolites like triterpenes, coumarin and benzoxazinoids proved that these root exudate compounds play a role in the formation of the root microbiomes (Hu *et al.*, 2018; Stringlis *et al.*, 2018; Huang *et al.*, 2019).

Some studies showed that the phylogenetic distance between plant species is positively correlated with the dissimilarity of root-associated microbiomes. For example, a comparative study of seven Poaceae species revealed that the larger the phylogenetic distance of the host plants, the larger the dissimilarity of the RH microbiome (Bouffaud, ML *et al.*, 2014). Further, a study on 18 Poaceae species showed that this positive correlation also existed for the EC microbiome (Naylor, Dan *et al.*, 2017). However, some studies showed that this correlation was not so strict. Schlaeppi *et al.* (2014) investigated the root microbiomes of hosts following a phylogenetic framework, i.e. three *Arabidopsis* species (*A. thaliana*, *A. halleri* and *A. lyrata*) and one *Cardamine hirsuta*, a species from a closely related genus. The dissimilarity of root microbiomes was larger between the *Arabidopsis* species and *C. hirsuta*. However, it did not correlate with the phylogenetic distance within the genus *Arabidopsis*. It has been suggested that the recent speciation event of *Arabidopsis*, coupled to the adaptation to a distinctive lifestyle would result in this incongruent correlation. So both phylogenetic distance and plant environmental adaptation could influence the microbiome diversification (Schlaeppi *et al.*, 2014).

Environmental effects

Environmental factors can influence the composition of the root-associated microbiomes. These include abiotic factors such as: physicochemical characteristics of the soil, salinity, drought and nutrient deficiencies (Peiffer *et al.*, 2013; Naylor, D. *et al.*, 2017; Finkel *et al.*, 2019). Such determinants can either directly influence the soil microbiome, due to adaptation of microorganisms to it, or indirectly by affecting, for example, the root

Chapter 1

morphology, physiology and the composition of root exudates. This as an adaptation of plants, which in turn influences the composition of the root-associated microbiomes (Hartman & Tringe, 2019). In addition to abiotic factors, biotic factor like the presence of pathogens or herbivory can also affect the composition of the microbiomes (Berendsen *et al.*, 2018). To withstand these abiotic or biotic stresses, plants attract beneficial (micro)organisms for protection, which is referred to as the "cry for help" response. This is mediated, to some extent, by quantitative and/or qualitative changes of root exudates (Rizaludin *et al.*, 2021). How the beneficial microbes can confer some tolerance to stress will be described later.

Plant-soil feedback

The interaction between soil microbiome and plants is dynamic. Plants change the biotic and abiotic properties of the soil (e.g. soil microbiome, and chemical and physical soil properties). These plant-mediated changes, especially in the soil microbiome, can modulate local growth conditions for themselves, as well as for their own offspring and other plants, and these plant-induced changes are known as "plant-soil feedback" (van der Putten *et al.*, 2013; Hannula *et al.*, 2021). One well-known plant-soil feedback is the apple replant disease, which is defined as a disturbed physiological reaction of newly planted apple trees to soils that have altered (micro-)biomes due to previous apple growth (Winkelmann *et al.*, 2019). The plant-soil feedback is not always negative, sometimes it can be positive. For instance, Hannula *et al.* (2021) found that plant-soil feedback consistently lead to a negative effect on plants grown in their own soil, but had a positive effect on other plant species grown in this soil. Another example is the feedback between maize and soil which affected the composition of the soil microbiome (Hu *et al.*, 2018). When maize was grown in this soil their growth was reduced in comparison to the soil lacking the legacy of the feedback. However, when exposed to herbivory by caterpillars, the growth of maize was positively affected. In this case, the plant-soil feedback was caused by the secretion of benzoxazinoids in the soil which alters the root-associated microbiomes inducing an increase in the jasmonate defence system (Hu *et al.*, 2018). This caused contrasting effects on growth in the absence and presence of herbivory, showing

that plant-soil feedback is not just simply negative or positive, but it depends on the plant species as well as the environment.

Core microbiome

Environmental factors do affect the composition of the root-associated microbiomes. However, the relative abundance of some microbial profiles, are consistently enriched in the RH or EC, of a certain plant species, compared to the bulk soil, irrespective to the sampling environment (Lundberg *et al.*, 2012; Yeoh *et al.*, 2016; Xu, J *et al.*, 2018). These microbes form the "core" plant microbiome. The core root-associated microbiomes have been identified in non-crop and crop plants like grapevine, potato, tomato, sugarcane and citrus grown in diverse environments. The identified members of the core microbiome include, for example, *Pseudomonas*, *Bradyrhizobium*, *Agrobacterium*, *Burkholderia* and *Bacillus* (Zarraonaindia *et al.*, 2015; Yeoh *et al.*, 2016; Pfeiffer *et al.*, 2017; Tian *et al.*, 2017; Xu, J *et al.*, 2018).

It seems probable that core microbes are strongly selected by the plant and they can be shared by different species, but can also be more species specific. The fact that the host selects these core species makes it probable that they are beneficial to their host. Several core microbiome members have been isolated and have been shown to have beneficial properties, for example, enhancing nutrient uptake, modulating hormonal balances and improving biotic or abiotic stress resistance (Lemanceau *et al.*, 2017; Tian *et al.*, 2017; Xu, J *et al.*, 2018). So identification of core microbiomes is an effective way to select putative beneficial root microbes (Compant *et al.*, 2019).

Beneficial root-associated microbiomes

The root-associated microbiomes comprise beneficial, neutral and pathogenic microorganisms. Beneficial bacteria are collectively termed plant growth-promoting rhizobacteria (PGPR) (Lugtenberg, Ben & Kamilova, Faina, 2009). These bacteria can be in the RH and inside the root. The latter can be hosted intracellular or intercellular. Intracellular PGPR refer to bacteria interacting intimately with the plant by forming, in general, specialized structures. A well-studied example is a symbiosis between legumes

Chapter 1

and rhizobia (e.g. *Rhizobium* and *Bradyrhizobium*) which results in the formation of root nodules (Bisseling & Geurts, 2020). Such nodules have specialised cells that contain thousands of rhizobia in membrane compartments made by the host. There they can fix atmospheric nitrogen into ammonia. Intercellular PGPR are more diverse than intracellular PGPR, including a broad range of genera, for example, species belonging to the genera *Bacillus*, *Burkholderia*, *Enterobacter*, *Streptomyces* and *Pseudomonas* (Afzal *et al.*, 2019).

The effects of PGPR on plant

PGPR have been shown to promote plant growth, nutrient uptake and can confer tolerance to stress (Lugtenberg, B. & Kamilova, F., 2009). These beneficial traits can be direct or indirect (Oleńska *et al.*, 2020). PGPR can directly transform compounds into nutrients and translocate essential nutrients by which they can be used by plants (Richardson & Simpson, 2011). Also, by producing phytohormones, they can directly stimulate plant growth (Richardson & Simpson, 2011; Sarkar *et al.*, 2018). Indirect effects can be the production of antimicrobial compounds to inhibit the growth of soil pathogenic organisms (Raaijmakers *et al.*, 2008). Another mechanism by which PGPR can protect against a broad range of pathogens and insect herbivores is priming the host for enhanced defence, called induced systemic resistance (ISR) (Pieterse *et al.*, 2014). In the following paragraphs I will discuss some of these properties in more detail.

Nutrient uptake

PGPR can improve plant nutrition by creating nutrients or facilitating the uptake of nutrients. An example of the former are nitrogen-fixing bacteria, free-living or in a root nodule symbiosis with, for example, legumes, can produce ammonia by reducing atmospheric nitrogen (Dobbelaere *et al.*, 2003; Remans *et al.*, 2007; Bisseling & Geurts, 2020). Under phosphate limiting conditions, phosphate solubilizing bacteria can mobilize insoluble phosphate from inorganic mineral phosphate and organophosphate (phytate) by which it becomes accessible to plants. This involves solubilization and mineralization via the production of organic acids and phosphatases, respectively (Richardson 2011). In addition, bacteria can enhance the expression of plant genes involved in the phosphate

starvation response, thereby increasing inorganic phosphate uptake (Castrillo *et al.*, 2017). Under potassium limiting conditions, potassium solubilizing bacteria can solubilize K-bearing minerals and convert insoluble potassium to soluble forms through the production of organic and inorganic acids (Etesami *et al.*, 2017). Further, PGPR can excrete siderophores to mediate iron uptake (Sadeghi *et al.*, 2012). Most bacteria that facilitate such iron uptake belong to genera such as *Pseudomonas*, *Bacillus*, *Enterobacter* and *Streptomyces* (Oleńska *et al.*, 2020).

PGPR can improve nutrient uptake in an indirect manner. For example, by changing the root architecture of host plants, thus increasing the exploratory capacity of the root for water and mineral nutrients (Richardson & Simpson, 2011). An example is *Pseudomonas simiae* WCS417 which promoted *Arabidopsis* secondary root formation and induced the formation of longer root hairs (Pieterse *et al.*, 2021). It induces an auxin response in *Arabidopsis* roots, where the auxin accumulation in root pericycle cells could play a role in specifying lateral root founder cells in the meristem and altering root architecture (Dubrovsky *et al.*, 2008; Li *et al.*, 2022).

In addition to interfering with the auxin signalling of the plant, PGPR can directly produce plant hormones such as auxins, cytokinin and gibberellin (Patten & Glick, 1996; Hayat *et al.*, 2010; Spaepen & Vanderleyden, 2011). One example is a study on *Azospirillum brasilense*, which showed that inoculation with the wild-type strains resulted in a decreased root length and an increase in root hair number (Dobbelaere *et al.*, 1999). But this effect was lost by an *ipdC* mutant of *A. brasilense*, where the *IPDC* gene is a key enzyme in the *IPyA* pathway of IAA synthesis (Dobbelaere *et al.*, 1999). So by producing plant hormones or inducing hormone signalling responses, PGPR can affect the root architecture and influence the plant nutrient uptake.

Abiotic stress tolerance

The role of PGPR in conferring tolerance to certain abiotic stresses has been studied, for example, for drought, flood, low or high temperatures and heavy metals. In this thesis, I focus on salt tolerance and therefore I will introduce this in more detail. Plants are in

Chapter 1

general sensitive to salt (NaCl) and the stress causes damage due to ion toxicity and osmotic stress. Sodium (Na⁺) and potassium (K⁺) are related alkali metals. However, Na⁺ is not an essential element for plant growth and development, whereas K⁺ is (Wang & Wu, 2017). Maintaining a high K⁺/Na⁺ ratio in the shoots has been suggested to be a major strategy for plants to cope with salt stress (Hauser & Horie, 2010). Several PGPR have been shown to improve Na⁺ exclusion and K⁺ uptake in plants, thereby increasing the K⁺/Na⁺ ratio (Rojas-Tapias *et al.*, 2012; Han *et al.*, 2014).

The ability of PGPR to enhance the uptake of nutrients, including K⁺, has been introduced in the previous section of this chapter. Further, PGPR can directly affect the uptake of Na⁺ or they can stimulate mechanisms of the plant that contribute to salt tolerance. An example of such direct effect is that the exopolysaccharides secreted by some PGPR may bind the toxic Na⁺ and restrict Na⁺ influx into roots (Ashraf *et al.*, 2004; Qin *et al.*, 2016). A mechanism by which some PGPR regulate the Na⁺ uptake of the plant concerns the expression level of *HIGH AFFINITY K⁺ TRANSPORTER 1 (HKT1)* that mediates the Na⁺/K⁺ homeostasis in plants. Two classes of HKT transporters have been found in plants. Class II has been identified as a K⁺ uptake transporter, but later it was shown to have Na⁺/K⁺ co-transport activity (Schachtman & Schroeder, 1994; Rubio *et al.*, 1995). In contrast, class I HKTs are Na⁺ selective transporters (Uozumi *et al.*, 2000; Maser *et al.*, 2002). Several PGPR can regulate the expression level of a class I HKT transporter. For example, *Bacillus subtilis* strain GB03 can repress in Arabidopsis roots *HKT1*, reducing Na⁺ entry into the roots. In contrast, it stimulates *HKT1* expression in the shoot facilitating shoot-to-root Na⁺ recirculation, which is critical to reduce Na⁺ levels in the shoot by which plant salt tolerance is increased (Zhang *et al.*, 2008).

Another mechanism by which plant cells protect themselves against salinity is sequestering Na⁺ into the vacuoles or secreting it into the apoplast (Qiu *et al.*, 2004; Bassil & Blumwald, 2014). Na⁺/H⁺ antiporters in the plasma membrane (*SOS1*, salt overly sensitive) and in the tonoplast (*NHX1*, Na⁺/H⁺ exchanger) control Na⁺ secretion and vacuolar sequestering, respectively (Kronzucker & Britto, 2011). Some PGPRs confer salt tolerance by enhancing the expression of these genes (Chen *et al.*, 2016; Haroon *et al.*,

2021). Other indirect mechanisms by which PGPR confer salt tolerance concern the damage caused by Na⁺. Under salt stress conditions, reactive oxygen species (ROS) accumulate that could damage plant cells (Kronzucker & Britto, 2011). This accumulation of ROS can be reduced by some PGPR, for example, *Bacillus amyloliquefaciens* NBRISN13 which increased the expression of catalase in rice and consequently reduced the ROS level under saline conditions (Nautiyal *et al.*, 2013).

When subjected to salinity, plants produce ethylene, which retards root growth (Morgan & Drew, 1997). Several microbes can counteract this by secreting, 1-aminocyclopropane-1-carboxylate (ACC) deaminase, which cleaves ACC, the precursor of ethylene. So the ethylene accumulation can be reduced (Morgan & Drew, 1997; Glick, 2005). It has been shown that inoculation with, for example, *Pseudomonas*, *Bacillus*, *Ochrobactru*, *Arthrobacter*, *Brachy bacterium*, *Brevibacterium* or *Haerero halobacter* secreting ACC-deaminase promote the growth of plants under saline conditions (Shukla *et al.*, 2012; Chang *et al.*, 2014; Aslam & Ali, 2018; Saikia *et al.*, 2018). However, root growth retardation by ethylene is a common adaptation to salt. It is controlled by DELLA transcription factors and it is not just the result of a poor physiology of the plant (Achard *et al.*, 2006; Tao *et al.*, 2015). When this growth retardation is blocked, plants are killed more easily by the stress conditions. Therefore, it can be questioned who is benefitting from the secretion of ACC deaminase, the host plant or the bacterium? So in contrast to commonly held assumptions, ACC deaminase-producing microbes are not necessarily beneficial (Ravanbakhsh *et al.*, 2018).

Tolerance to pathogens

Disease-suppressive soils provided an indication that microbes could protect plants against pathogens. The formation of disease-suppressive soils requires a disease outbreak after which a certain crop grown in such soil is markedly more tolerant to the pathogen (Weller *et al.*, 2002; Haas & Defago, 2005). For example, Mendes *et al.* (2011) investigated a disease-suppressive soil from a Dutch arable land where sugar beet plants were protected against *Rhizoctonia solani*, whereas in the past sugar beet grown in this area became diseased. When tested under greenhouse conditions, this soil maintained its

Chapter 1

disease-suppressive activity, whereas soil with similar physical-chemical properties collected from the margin of this area, where sugar beet had not been grown, did not suppress disease. Further, it was shown that inoculation with disease-suppressive soils can confer tolerance to a disease-conducive soil. However, when the disease-suppressive soil was sterilized this was no longer the case, strongly indicating that microbes were responsible for the tolerance to a pathogen (Mendes *et al.*, 2011).

It has been postulated that plants can actively recruit beneficial soil microorganisms in their rhizosphere when under attack by pathogens (Cook *et al.*, 1995). This is well in line with the engineering of a disease-suppressive soil, for example, by growing wheat for several years on a field (Weller *et al.*, 2002). This resulted in the development of a soil that conferred tolerance to the disease “take-all decline” caused by *Gaeumannomyces graminis* var. *tritici*. This disease suppression was the result of the accumulation of an antagonistic *Pseudomonas* spp. However, other studies showed that the activity of disease-suppressive soil is more complex (Cordovez *et al.*, 2015; Carrión *et al.*, 2019). For example, by a combination of a high throughput sequencing approach and studies on antagonistic activities of isolated bacteria, it was shown that most likely the disease suppressing properties of the sugar beet soil was controlled by a microbial consortium and not a single strain (Mendes *et al.*, 2011).

The mechanisms by which antagonistic microorganisms of disease-suppressive soils confer resistance have been studied in several cases. These mechanisms involve the production of antibiotics, siderophores and pathogen-inhibiting volatile organic compounds (VOCs) (Mendes *et al.*, 2011; Verbon *et al.*, 2017). For example, the *Pseudomonas* spp. of the wheat suppressive soil has been shown to suppress soil pathogens by producing the antimicrobial compound 2,4-diacetylphloroglucinol (de Souza *et al.*, 2003). Members of the Pseudomonadaceae, identified from the sugar beet suppressive soil, protected plants from fungal infection by producing a putative chlorinated lipopeptide encoded by NRPS genes (Mendes *et al.*, 2011). Later on, from the same sugar beet suppressive soil, *Streptomyces* species and *Paraburkholderia graminis* PHS1 have been shown to produce VOCs to inhibit hyphal growth of *Rhizoctonia solani* (Cordovez *et al.*, 2015; Carrion *et al.*,

2018). The *Streptomyces* can produce methyl 2-methylpentanoate and 1,3,5-trichloro-2-methoxybenzene, whereas the *Paraburkholderia* can produce sulphurous volatile compounds (Carrion *et al.*, 2018). This suggests that the disease-suppressing properties of soil is created by a microbial consortium with multiple mechanisms.

Another way by which PGPR can improve plant resistance to pathogens is by induced systemic resistance (ISR). This primes the whole plant for a faster and stronger defence against a broad range of pathogens and insect herbivores (Pieterse *et al.*, 2014). ISR has been demonstrated in numerous plant species and in addition to PGPR, beneficial fungi such as mycorrhizal fungi and *Trichoderma spp.* have been shown to induce ISR (Pieterse *et al.*, 2014). Induction of ISR in Arabidopsis by the PGPR *Pseudomonas simiae* WCS417 is well studied. Inoculation with *P. simiae* WCS417 stimulates the activity of root-specific transcription factor MYB72. MYB72 regulates the expression of genes involved in biosynthesis of coumarin in the roots as well as β -glucosidase BGLU42 which is involved in the excretion of coumarin into the rhizosphere (Van der Ent *et al.*, 2008; Zamioudis *et al.*, 2014; Stringlis *et al.*, 2018). Coumarin selectively inhibits the growth of the soil-borne fungal pathogens *Fusarium oxysporum* and *Verticillium dahliae*, whereas the growth-promoting and ISR-inducing *P. simiae* WCS417 and *Pseudomonas capeferrum* WCS358 are highly tolerant to its antimicrobial effect (Stringlis *et al.*, 2018). So MYB72-dependent coumarin secretion shapes the root microbiome where the PGPRs are selectively enriched. This can provide a strategy to identify such PGPR by especially focusing on root-associated microbes that enrich under biotic stress conditions.

The application of root-associated microbiomes

In the former part of this introduction I have described a broad range of PGPR that have properties that can be very beneficial for crops in an agricultural setting. They have the potential to reduce the use of fertilizer and pesticides which have negative effects on the environment. Growth-promoting microbes that increase stress tolerance and crop yield could be a valuable tool for helping mitigate these problems.

Chapter 1

Single strain inoculation

Till recently, the application of PGPR in agriculture has been done with single strains. Single strains can stimulate plants when they are grown under sterile conditions in the lab or greenhouse. However, success in a field setting with single strains is rare, most likely because they are outcompeted by the soil microbiome (Backer *et al.*, 2018; Sessitsch *et al.*, 2019; Trivedi *et al.*, 2020). For example, the growth of maize and wheat inoculated with *Azospirillum brasilense* (strain Ab-V5 and Ab-V6) was significantly increased under controlled conditions, but not in the field (Fukami *et al.*, 2016). Similarly, the biomass of rice inoculated with *Rhizobium leguminosarum* *bv. trifolii* was significantly increased in the greenhouse, but not in the field (Kecskés *et al.*, 2016). Therefore, instead of this "one-microbe-at-a-time" approach, an alternative would be to create so-called synthetic microbial communities (SynComs) (Raaijmakers, 2015).

Synthetic microbial communities

The application of SynComs is an emerging strategy to overcome problems during lab-to-field transition, as a community of microbes probably has a better chance to survive and function in a non-sterile environment (Vorholt *et al.*, 2017). However, this will heavily depend on the composition of the SynCom. The selection of microbial members will be essential for SynCom construction. One strategy largely depends on the functional properties of microbial isolates. Individual microbial isolates can be cultured using high-throughput platforms and characterized through genomic, metabolic and physiological analysis *in vivo/vitro* with plant hosts (Oleńska *et al.*, 2020). Referring to the desired effect of SynCom, such as abiotic stress tolerance, microbial isolates with the best performance would be selected for SynCom construction. This is more a collection of microbes than a community that can withstand the competitive pressure of the soil microbiome.

Other strategies are based on the read counts from meta-amplicon sequencing. One of them is related to a host-mediated selection approach, where the dominant and enriched members in the root-associated compartments were selected to create a SynCom. For example, after two rounds of host selection, Niu *et al.* (2017) selected seven strains from

the genera which were enriched and dominant in the maize root. The SynCom constructed by these seven strains had the ability to inhibit the phytopathogenic fungus *Fusarium verticillioides*, indicating a clear benefit to the host. Recently, selection for keystone strains has been emphasized as another strategy for selecting microbial members of SynCom (Lemanceau *et al.*, 2017). Keystone taxa represent microbes that frequently co-occur with many others and can be identified through topological networks derived from correlation analysis on sequencing output (Hartman *et al.*, 2018). The use of keystone strains may maximize SynCom persistence in natural settings. Some studies have attempted to combat salt stress with SynComs following these strategies and succeed under sterile conditions (Ahmad *et al.*, 2011; Egamberdieva *et al.*, 2017; Finkel *et al.*, 2020). However, to our knowledge, there are no studies yet where a SynCom has been shown to promote growth or provide protection against stresses to plants grown under field conditions.

Thesis outline

Root-associated bacteria are the most dominant composition and are relatively well-studied compared to other community members, such as fungi and archaea (Mendes 2013, Leach 2017). Stretching our knowledge from ‘who is there’ to ‘what they are doing (or can do)’ offers us a good opportunity to apply these root-associated bacterial microbiomes in sustainable agricultural practices. In this study, I have investigated various aspects of root-associated microbiomes by both culture-independent and -dependent approaches. I began with characterising the plant-microbial interaction of plant species adapted to drought conditions by studying a newly determined plant compartment and the composition of its bacterial microbiome. Then I studied the interaction between the plant genotype and environment on influencing the microbiome composition. In addition, one of my studies was focussed on trees to investigate the relationship between root-associated microbiomes and longevity, as microbiomes have been shown to provide protection against biotic stress. Lastly, I constructed a SynCom derived from a saline desert, to study whether this can confer salt tolerance to a crop growing under non-sterile conditions.

Chapter 1

In **chapter 2**, we studied the effect of host-related factors, i.e. plant compartment, on the composition of the root-associated microbiome. We showed that the microbiome composition in the root-sleeve (RS), a peculiar root structure that can be moved along the root in 2 desert grass species, was significantly different from that in the bulk soil, RH and EC, albeit it was most similar to that in EC. Actinobacteria and Proteobacteria ASVs were enriched with the highest abundance in both RS or/and EC compartments. Further, we studied the developmental and cellular processes underlying the formation of the RS and we showed that the RS contains outer cortical cells, epidermis and tightly adhered sandy layer at the root surface. We suggested that the formation of RS was an adaptation of arid tolerant grasses by integrating, from outside to inside, rhizosheath formation, formation of lacunae in the inner cortex and endodermal cell wall modification and hydrolysis.

In **chapter 3**, we compared the effects of plant genotype and environment on the root-associated microbiome composition. We showed a reduced dissimilarity of the composition of root-associated microbiomes of two distinct barley (*Hordeum vulgare* L.) genotypes, i.e. the reference cultivar Golden Promise (GP) and the Algerian landrace barley (AB), in response to salt stress (200 mM), especially in the EC. These findings indicated that the plant genotype-dependent microbiome composition was reduced by abiotic stress.

In **chapter 4**, we showed that the root-associated bacterial microbiomes of a chronoseries of Chinese chestnut trees (*Castanea mollissima*), ranging from 8 to 830 years old, were rather similar, although based on the models we could not exclude that tree age has a weak correlation with the composition of root-associated microbiomes. The similarity of the root-associated microbiome indicated the absence of a negative plant-soil feedback. To test this, chestnut seedlings were grown in soil that had been associated with young and old chestnut trees, respectively. We observed that these chestnut plants were healthy and their growth was similar. Furthermore, a *Pseudomonas* OTU representing more than 50% of the rhizosphere community strongly inhibited the growth of chestnut pathogens and stimulated plant growth. We suggested that such properties of the Chinese chestnut

root microbiome and the absence of negative plant-soil feedback contributed to the longevity of chestnut.

In **chapter 5**, we tested the effect of single strain and SynCom inoculation on plant growth under abiotic stress conditions in a non-sterile environment. We created a 15 strain SynCom, using the core members and verified plant-growth promoting rhizobacteria originating from the root of desert plant *Indigofera argentea*. The SynCom protected tomato plants growing in a non-sterile substrate against high salt stress. Furthermore, we simplified this SynCom to 5 strains and such simplified SynCom even outperformed the plant growth promoting effect observed from the initial SynCom under non-sterile condition. We proposed that more advanced methods, such as metagenomics, metatranscriptomics and metabolomics sequencing, should be used to unveil the mechanism of such phenotype.

In **chapter 6**, I summarized and discussed the results described in this thesis within a broader perspective.

Chapter 2

Root-sleeve, an adaptation to drought and a niche for a distinct microbiome

Zhichun Yan^{1,#}, Huchen Li^{1,#}, Lucas Schmitz¹, Carolien Franken¹, Bin Zhang², Jirong Qiao², Fang Tang², Min Li³, Zhiqing, Qu², Cuiping Gao², Xu Cheng^{1,4}, Feng Zhang², Jiahua Zheng², Guodong Han², Ton Bisseling^{1,2*}, Mengli Zhao^{2*}

¹ Laboratory of Molecular Biology, Cluster of Plant Developmental Biology, Plant Science Group, Wageningen University and Research (WUR), Droevendaalsesteeg 1, 6708PB Wageningen, The Netherlands

² College of Grassland and Resources Science, Inner Mongolia Agricultural University, Hohhot, China

³ College of Horticulture and Plant protection, Inner Mongolia Agricultural University, Hohhot, China

⁴ Shenzhen Branch, Guangdong Laboratory for Lingnan Modern Agriculture, Genome Analysis Laboratory of the Ministry of Agriculture, Agricultural Genomics Institute at Shenzhen, Chinese Academy of Agricultural Sciences, Shenzhen, China

These authors contributed equally.

* Corresponding authors: nmgmlzh@126.com; ton.bisseling@wur.nl

Abstract

In 1887 Volkens first described peculiar structures on the roots of some grasses growing in arid regions (Volkens, 1887). These are cylinders composed of sand grains and mucilage. What makes them special is that they can slide along the root, like an arm in a sleeve. Therefore we will name them root-sleeves. Here we show, for 2 perennial grasses from arid areas, that the formation of a root-sleeve starts with the formation of a rhizosheath. This is followed by the formation of cortical lacunae, that are known to protect the plant against drought, by reducing radial hydraulic conductivity (Cuneo et al., 2016). Ultimately, the lacunae encompass the complete inner cortex. The anticlinal cell walls of endodermal cells are lysed but their inner periclinal wall, together with pericycle cell wall become strongly lignified and forms a protective laminae around the vasculature. So root-sleeve formation is an adaptation to drought. Further, we show that it is a unique niche for bacteria as its microbiome is different from rhizosphere and endophytic compartment. This microbiome is dominated by Actinobacteria which are known to be positively correlated with drought (Naylor, D. et al., 2017).

Main

We selected 2 grass species, that were collected in semi-arid grasslands in Inner Mongolia, to study how root-sleeves are formed. These are *Agropyron mongolica* (Agropyron) and *Stipa breviflora* (Stipa). Both plant species, developed numerous roots covered with sandy cylinders. These cylinders were continuous alongside the whole root except for the tip (Fig. 1a, b; Fig. S1a, b). They could easily slide along the root (Fig. 1a, Fig. S1a), similar to the structures described by Volkens (1887). Recently, it has been shown that roots of the majority of angiosperms can be covered by a sticky cylinder of sand grains as a response to mild drought. However, it cannot slide along the root and is named rhizosheath (Wullstein *et al.*, 1979).

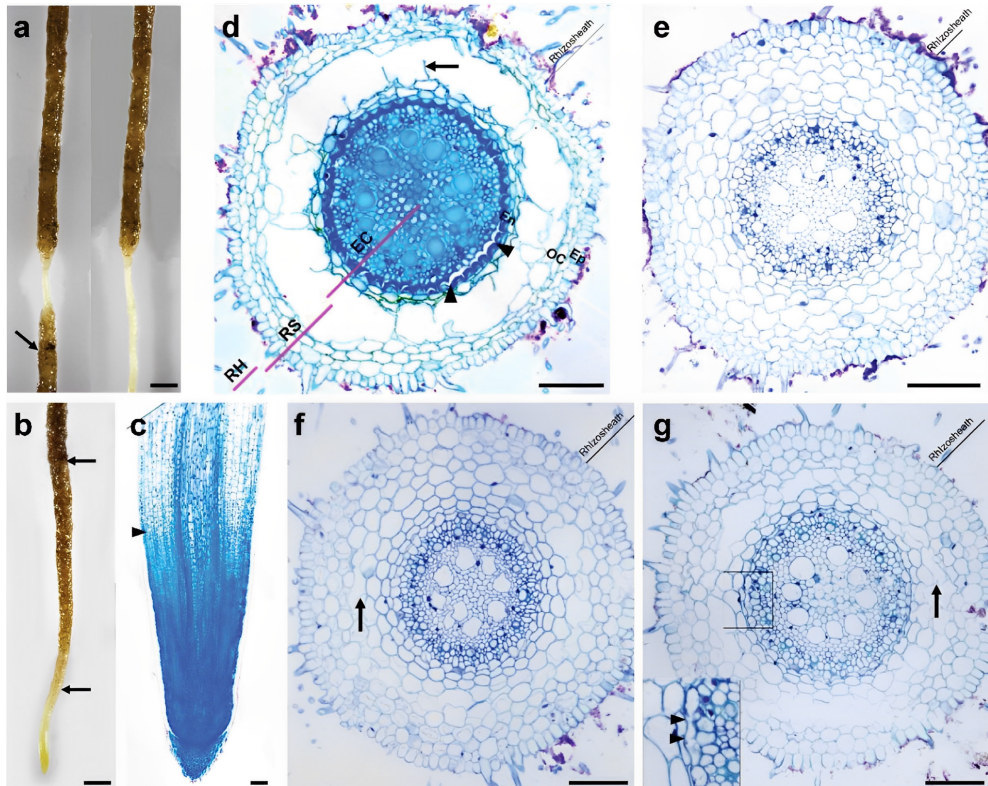


Fig. 1 | Development of root-sleeves of *Agropyron*. **a**, Overview of *Agropyron* root segments before (left) and after (right) removing the sandy cylinder (arrow). **b**, Overview of

Chapter 2

Agropyron root tip. Arrows indicate the beginning (lower) and the place where root/rhizosheath radial diameter reach to the maximum thickness (upper). **c**, Sections of *Agropyron* sand-free root tip. Arrowhead indicates the boundary between root meristem and elongation zone. **d-g**, Sections of *Agropyron* root segments at different positions. Position of segments is indicated in Fig. S3. Rhizosheath region where sand grains are carefully brushed off prior to sectioning, the thickness of rhizosheath are marked on the upper right corner. Images **e** to **g** are from the same root. Arrows in **d**, **f** and **g** indicate the lysed inner cortical cell walls. Arrowheads in **d** and **g** (within the magnified box) indicate the lysed radial cell walls of endodermis cells. In **d**, rhizosphere (RH), root-sleeve (RS) and endophytic compartment (EC) are indicated at lower left corner. En, endodermis; OC, outer cortex; Ep, epidermis. For all images, 15 roots are analysed and representative images are shown. Scale bars = 1 mm in **a** and **b**, or 100 μ m in **c** to **g**.

So the root-sleeve has a rhizosheath at its surface. To determine which tissues contribute to root-sleeves, we analyzed root cross sections of both species. This showed that cell walls of the inner cortex were lysed, resulting in a big hollow space between endodermis and outer cortex (Fig. 1d, Fig. S1d). The anticlinal walls of endodermis were also lysed. So the root-sleeve is formed by the outer cortex and the epidermis with root hairs embedded in a rhizosheath (Fig. 1d, Figs. S1d, S2).

To obtain insight in how root-sleeves are formed, we made use of the indeterminate growth of roots by which a gradient of developmental stages are present along the longitudinal axis. Longitudinal sections through the tip, that was not covered by sand, showed that in *Agropyron* it included meristem and elongation zone (Fig. 1c). Next, cross sections were made of the root segment, where the formation of the rhizosheath had just been initiated, here endodermis and cortex were still intact (Fig. 1e, Fig. S3; rhizosheath formation zone, Stage I). In the area where the rhizosheath has just reached its full thickness, anticlinal walls of some inner cortical cells were lysed. This resembles the formation of lacunae, structures that have previously been shown to be rapidly induced by drought stress (Cuneo *et al.*, 2016). At this stage the endodermis was still intact (Fig. 1f, Fig. S3; lacunae formation zone, Stage II). At a later stage the lysis of anticlinal walls started in the endodermis, and the inner cortex showed larger lysed regions (Fig. 1g, Fig. S3;

endodermal lysis zone, Stage III). Further towards the shoot, inner cortex was completely lysed, the anticlinal walls of the endodermal cells were lysed, and the inner periclinal wall of the endodermis had become very thick (Fig. 1d, Fig. S3; mature zone, Stage IV). The formation of root-sleeves in *Stipa* involved similar steps (Fig. S1).

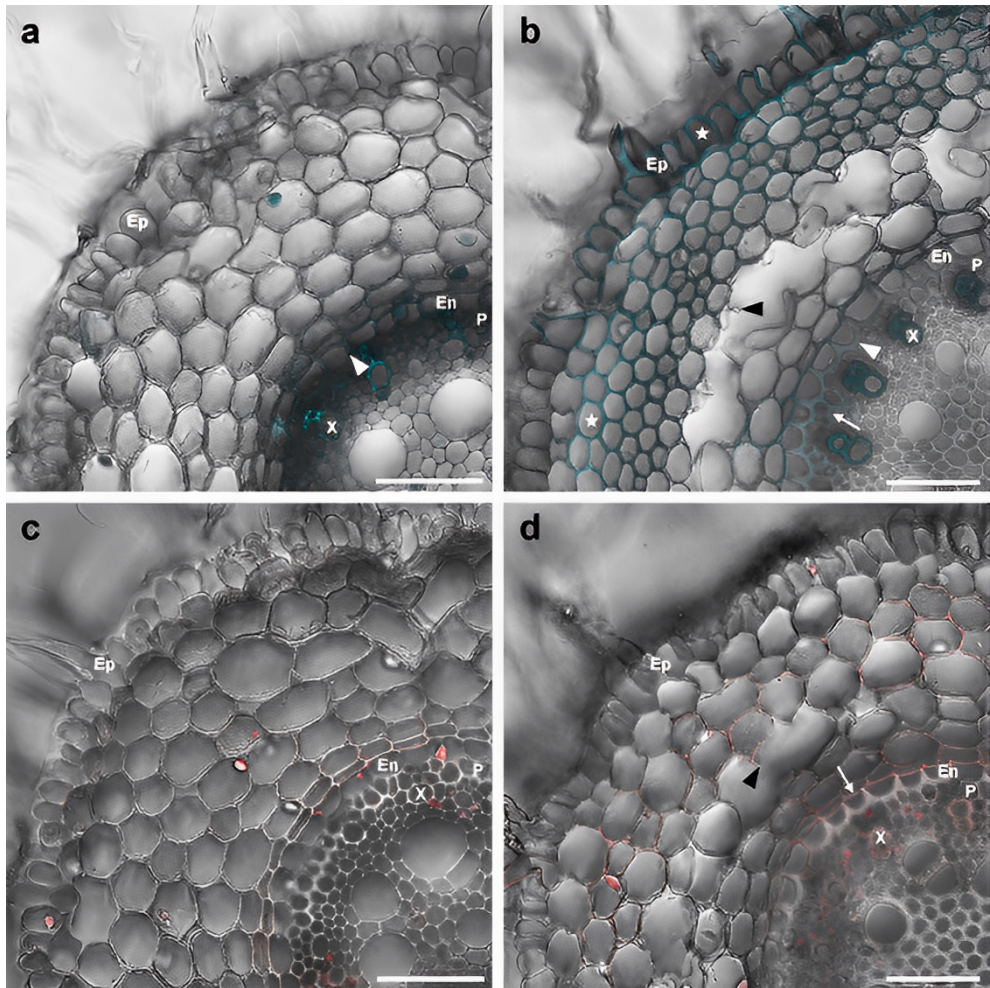


Fig. 2 | Secondary cell wall formation during *Agropyron* root-sleeve formation. a and b, Lignin staining of cross sections of *Agropyron* roots at stage I (a) and stage II (b). White arrowheads in a or b indicate the anticlinal cell wall, the inner periclinal cell wall of endodermis, respectively. In b, stars indicate the epidermal and outer cortical cells, white arrow indicates the cell wall of pericycle, all accumulate lignin. c and d, Suberin staining of

Chapter 2

cross sections of Agropyron root segment with root-sleeve at stage I (c) and stage II (d). White arrow in d indicates the outer periclinal cell wall of endodermis cell. In b and d, black arrowheads indicate where cell lysis has started in inner cortex, At this stage it has not yet started in endodermis. X, xylem; P, pericycle; En, endodermis; Ep, epidermis. Basic fuchsin or nile red signal is demonstrated in cyan (a and b) or in red (c and d), respectively. For all images, 7 roots are analysed and representative images are shown. Scale bars = 100 μ m.

The endodermis forms a barrier between cortex and vasculature. This barrier is formed by casparian strips (composed of lignin) surrounding the anticlinal walls, by which the apoplastic space is sealed, and a secondary cell wall formed by a suberin laminae (Naseer *et al.*, 2012; Andersen *et al.*, 2018). As the inner periclinal wall of the endodermis had become very thick, we investigated whether lignin and/or suberin accumulated in this wall. To study this we stained with basic fuchsin (lignin) and nile red (suberin) (Ursache *et al.*, 2018). At stage I, lignin of the casparian strips was visible between anticlinal walls of endodermis (Fig. 2a). Here the suberin laminae had not yet been formed (Fig. 2c). At stage II, the inner periclinal wall of endodermis had already become thick. Lignin had accumulated in this wall (Fig. 2b), but not suberin (Fig. 2d). In contrast, the outer periclinal wall of endodermis was suberized, as in “normal” endodermal cells (Fig. 2d). There was no suberin accumulation in other tissues (Fig. 2d). In addition, at stage II the lignin also accumulated in the complete cell wall of pericycle cells, as well as of a few epidermal and outer cortex cells (Fig. 2b). Similar lignified cell walls of endodermis and pericycle were also formed during root-sleeve formation in *Stipa* (Fig. S4).

The root stele covered by the lignified pericycle and inner periclinal wall of the endodermis forms the endophytic compartment. As root-sleeve and this endophytic compartment are composed of different tissues (Fig. 1d), we expected that the composition of their microbiomes would be distinct. To test this, we harvested bulk soil (SO), rhizosphere (RH), root-sleeve (RS), as well as endophytic compartment (EC) of both *Agropyron* and *Stipa*. We analysed the bacterial communities by 16S rRNA gene amplicon (V4 region) sequencing.

First, we determined the relative abundance of the major bacterial phyla. In both species, the phylum distribution in their RH resembled that of their corresponding soil (Fig. 3a, b). In contrast, the phylum distribution in RS of both species markedly differed from that in the soil and RH. However, it was similar to that in EC in both species. In EC and RS of both species, Proteobacteria and Actinobacteria were dominant and encompassed around 25% and 70% of the total reads. So at the phylum level, the composition of the microbiomes of RS and EC seem similar.

To compare the composition of RS and EC microbiomes with a greater resolution, we performed Principal Coordinate Analyses (PCoAs). Using the Bray-Curtis dissimilarity measure on a rarefied ASV table, samples of the four compartments were plotted along the first two principal coordinates (PCs) (Fig. 3c, d). Along the first PC (70% and 63% of the variance for *Stipa* and *Agropyron*, respectively), samples from the four compartments formed two clusters at the ends of PC1. One cluster encompassed the soil and RH and the other contained RS and EC. Within these two clusters, samples from the two compartments were separated along the second PC (11% and 10% of variance, respectively). Pair-wise permutational multivariate analysis of variance (PERMANOVA) was performed to determine whether the composition of the microbiome of RS was significantly different from that of other compartments (Fig. 3c, d). In both species, the differences between RS and each other compartment were significant ($p\text{-FDR} < 0.05$). Also, the difference between RS and EC was significant, indicating that the composition of the microbiomes of RS and EC were distinct. However, the closer relationship was also demonstrated by the pair-wise PERMANOVA, as the R^2 values of RS-EC were smaller than that of, for example, RS-RH and RS-SO (Fig. 3c, d). Further, the relatively high R^2 values of RS-SO imply that in both species (Fig. S5), the selection/exclusion of root-sleeve in bacterial community assembly is stronger than that of rhizosphere and it is similar to that of endophytic compartment.

Chapter 2

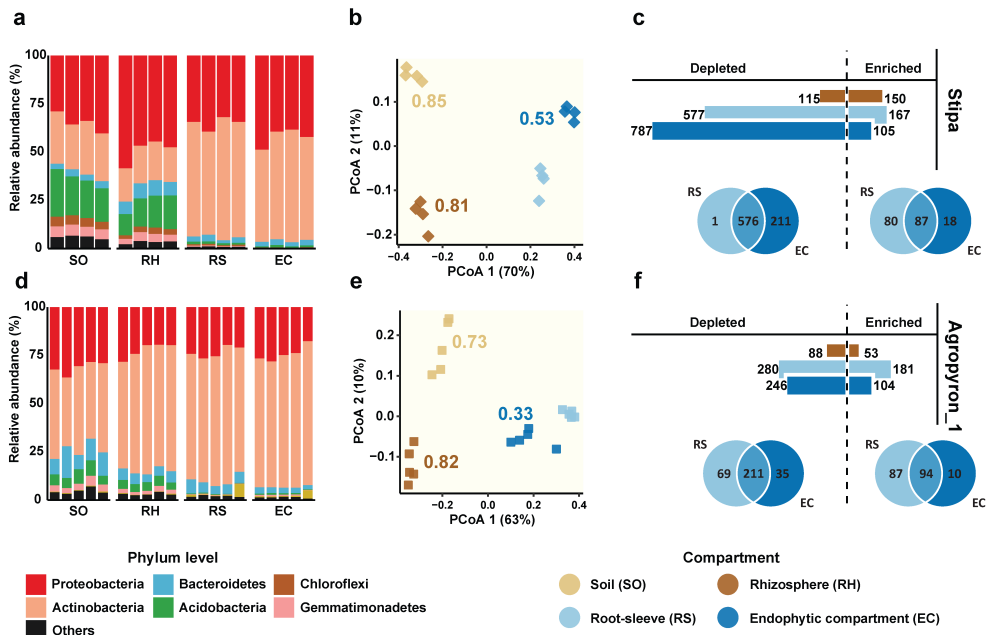


Fig. 3 | Bacterial community composition in different compartments of *Stipa* and *Agropyron*. **a** and **b**, The relative abundance of the dominant phyla (more than 5% of the total reads in at least one compartment) are shown for the soil (SO), rhizosphere (RH), root-sleeve (RS) and endophytic compartment (EC) of *Stipa* (**a**) and *Agropyron* (**b**). **c** and **d**, Principal Coordinates Analysis (PCoA) of bacterial communities in the four compartments of *Stipa* (**c**) and *Agropyron* (**d**). The R^2 values of PERMANOVA by comparing SO, RH, EC to RS are shown in the figures, coloured as same as for the compartments accordingly. **e** and **f**, the number of ASVs with a changed relative abundance (enriched and depleted) in comparison to that in the soil are shown for *Stipa* (**e**) and *Agropyron* (**f**). This was done by the *edgeR* package with threshold values of a p -value 0.05 and a log₂-fold change of 1. Furthermore, Venn diagrams show the number of shared and unique ASV with a changed relative abundance in RS and EC.

The PCoA analysis showed that the RS microbiome was distinct from that of the other compartments at the community level, albeit it seems closely related to that of EC. We next compared the RS and EC microbiomes by analyzing the ASVs with a changed relative abundance (enriched and depleted) in comparison to that in the soil. In both species, the

number of these changed ASVs was markedly higher in RS (744 in *Stipa* and 461 in *Agropyron*) than in RH (265 and 141) and similar to that in ECs (Fig. 3e, f; Table S1). To compare the RS and EC microbiomes, we focused on the enriched ASVs as the majority of the depleted ASVs were shared (Fig. 3e, f). Half of the RS enriched ASVs was unique for this compartment, in both species, and the other half was shared with EC. The number of enriched ASVs in EC was lower than that in RS and more than 80% of EC enriched ASVs was shared with RS. Only a minor fraction was unique for EC (17% in *Stipa* and 10% in *Agropyron*) (Fig. 3e, f), which was much less than the fraction of unique enriched ASVs of the RS (about 50%).

Among the enriched RS ASVs of both species, the Actinobacteria ASVs were highest in number and relative abundance (collectively they encompassed about 70% of the reads). This was the case for enriched RS ASVs that were shared with EC as well as those that were unique for RS (Fig. S6) and the number of shared and unique Actinobacteria ASVs was similar (55 and 46 in *Stipa*, respectively, 47 and 33 in *Agropyron*, respectively). The enriched ASVs unique for EC especially belonged to Proteobacteria (Fig. S6).

Two additional accessions of *Agropyron* were collected in different grasslands (see Methods). Their RS had a similar distinct microbiome (Fig. S5, S6 & S7). So the analyses of bacterial community composition and assembly, as well as the enriched ASVs in both *Agropyron* and *Stipa* underline that the RS has a distinct microbiome.

Taken together, we showed that in the root-sleeve formation three processes are integrated: rhizosheath formation, formation of lacunae in the inner cortex and endodermal cell wall modification and hydrolysis. The formation of a rhizosheath is a property shared with many angiosperms, as a study including species from different orders distributed throughout the phylogeny of angiosperms showed that more than 80% of these species could form a rhizosheath (Brown *et al.*, 2017). The formation of a rhizosheath has been shown to be induced by drought and to provide some protection against it (Zhang *et al.*, 2020b; Karanja *et al.*, 2021). Formation of lacunae have previously been shown to be a response to drought in desert succulents and grapevine (North & Nobel, 1991; North & Nobel, 1992; Cuneo *et al.*, 2016). As we collected *Stipa* and

Chapter 2

Agropyron from semi-arid grasslands, we postulate that the lacunae formed in the inner cortex is also induced by drought. In grapevine it was shown that lacunae are formed within a few hours after exposure to drought, at modest drought this is the only response and up to 30% of the cortex is lysed. This was already sufficient to reduce radial hydraulic conductivity by more than 50% and this reduced water loss to the dry soil (Cuneo *et al.*, 2016). Most likely the massive lysis of the inner cortex provides an even stronger reduction of this conductivity. Further, the stele becomes covered by a continuously lignified lamellae formed from the pericycle, as well as the major part of internal periclinal walls of the lysed endodermal cells.

To our knowledge this is the first time that the microbiome of a root-sleeve has been characterized. In contrast, the microbiomes of RH and EC have been studied in many plant species. The composition of bacterial communities of RH and especially of EC are markedly different from that of bulk soil (Hartmann *et al.*, 2009; Bakker, Peter AHM *et al.*, 2013). The microbiome of the rhizosheath was shown to be most similar to that of RH (Marasco *et al.*, 2018). Here we show that the root-sleeve is a niche with a distinct microbiome. This became especially clear by comparing the enriched ASVs in RS (root-sleeve) and EC. This showed that about 50% of the enriched ASVs of the RS are unique for this compartment and the other 50% is shared with the EC. A striking property of the shared and RS unique enriched ASVs is the very high number and abundance of ASVs that are classified as Actinobacteria. This is well in line with previous studies showing that the relative abundance of actinobacteria increases during drought (Naylor, D. *et al.*, 2017; Simmons *et al.*, 2020).

By forming a root-sleeve which includes a rhizosheath integrated with a completely lysed inner cortex and a stele sealed by a lignin laminae, the root vasculature most likely becomes well protected from the dry environment. Further, the Actinobacteria rich microbiome of the root-sleeve might contribute to drought tolerance. Therefore we conclude that the formation of a root-sleeve is an adaptation to drought.

Methods

Site description and plant materials sampling

We used four sites in Inner Mongolia Autonomous Region, China (Fig. S8). One was for the *Stipa breviflora* collection named 'Stipa' in our study. This is an experimental field at Siziwang Banner which is located in a desert steppe (41°46'43.6"N, 111°53'41.7"E). Three were used to collect samples of *Agropyron mongolica*, named 'Agropyron_1', '_2' and '_3' in our study. loc 1 is near the Inner Mongolia Grassland Ecosystem Research Station, located in Xilinhot city (43.55°N, 116.67°E). loc 2 is near the Horinger county which located in the southeast of Hohhot city (39.59°N, 111.35°E). loc 3 is an extension of the Maowusu sandy land where wind erosion and desertification are serious. It is located near Dongsheng district in Ordos city (39.43°N, 110.12°E).

These four locations are separated by more than 600 kilometres (Fig. S8), albeit all these area are around 1200 m above the sea level. Their mean annual temperature are generally below 6 °C and their annual precipitation are ranging from 300 to 500 mm.

We sampled at each site at locations that were ~ 50 m apart from each other. Plant collected at a location was one of the replicates; 4 replicates for *Stipa* and 5 replicates for *Agropyron*. The plants were excavated to a depth of 20 cm and then the plant, together with soil around its roots were put into one plastic bag and immediately placed into an ice box. Soil samples of about 20 cm depth were collected by an auger (5 cm diameter) nearby but from areas without plants.

Root Embedding and Sectioning

Root segments were fixed in 4% (v/v) paraformaldehyde, 3% (v/v) glutaraldehyde and 3% (w/v) sucrose in 0.1 M phosphate buffer (7.0), by overnight incubation under vacuum at room temperature. The sand grains at root surface were then carefully washed away in 0.1 M phosphate buffer (7.0) by using a brush. Roots were washed three times with phosphate buffer to get clean roots, to allow sectioning. Then, the root was cut in 0.5 cm segments. For studying the anatomy, root segments were dehydrated in an ethanol series and embedded in Technovit 7100 (Heraeus-Kulzer, Hanau, Germany according to the

Chapter 2

manufacturer's protocol. 5 and 15 μm thick longitudinal or 15 μm cross sections were made with a microtome (Leica Microsystems 2035). For studying cell wall components, root segments were embedded in 6% low melting agarose at 42 °C. After solidification, 80 μm thick cross sections were made with a vibratome (Leica VT1000).

Microscopy

5 μm thick longitudinal/cross sections were stained with 0.05% Toluidine Blue (Sigma), mounted in euparal, and were analyzed using a light microscope (Leica DM5500) equipped with a camera. For confocal fluorescence microscopy imaging (Leica SP8), 15 μm thick cross sections were stained and mounted in 10 μM propidium iodide dissolved in milli q H_2O ; 80 μm cross sections were stained with 0.5% basic fuchsin or 0.1% Nile red solution in 0.1M phosphate buffer (7.0) for 2 hours, then transferred to ClearSee solution (Ursache *et al.*, 2018) for 15 mins before mounted in Milli-Q water. The excitation wavelength for propidium iodide, Nile red and basic fuchsin detection was 552 nm, for autofluorescence detection 405 nm was used.

Soil, rhizosphere, root-sleeve and endophytic compartment harvesting

Loose soil was removed from the roots by kneading and shaking by hand. Soil still sticking to the roots was defined as rhizosphere soil. Roots including the rhizosphere soil were put into a 50 ml Falcon tube containing 25 ml sterile phosphate buffer (PB, per litre: 6.33 g $\text{NaH}_2\text{PO}_4 \cdot \text{H}_2\text{O}$, 10.96 g $\text{Na}_2\text{HPO}_4 \cdot 2\text{H}_2\text{O}$; after autoclaving, 200 μl Silwet L-77) and vortexed for 15 seconds. The roots were transferred to a new Falcon tube containing PB, and briefly vortexed. This procedure was repeated twice to clean the roots until the PB stayed clear. The clean roots were then transferred to a 15 ml tube containing 12 ml PB and sonicated for 10 mins (with a 30 seconds pause in every minute). After one more brief vortexing, the root-sleeve was removed with sterilized forceps along the root. The “naked” roots, where the central vascular bundle were covered with and pericycle and remains of endodermis. This was defined as the endophytic compartment sample. Both root-sleeve and endophytic compartment samples were then placed on a filter paper for drying. The solution, with rhizosphere soil, from the first vortexing step was filtered through a 100 μm cell strainer (Falcon) into a new Falcon tube and spun down for 10 mins at 4,000x g.

Root-sleeve harbours a unique microbiome

Supernatant was quickly poured off and the pellet was rinsed with 1.5 ml PB then transferred to a 2 ml tube (Eppendorf). After spinning down for 5 mins at 10,000x g, supernatant was poured and the additional liquid residues were removed. The pellet was defined as rhizosphere sample. Soil samples were washed in the PB buffer and were collected in the same way as the rhizosphere samples. Samples from these four compartments were then weighed, frozen in liquid nitrogen and stored at -80 °C.

DNA isolation and 16S rRNA gene amplicon sequencing

DNA from soil and rhizosphere samples was isolated using the Mo Bio PowerSoil kit (Qiagen) according to manufacturer's instructions. According to the procedures described previously (Lundberg *et al.*, 2012), DNA from the root-sleeve and endophytic compartment samples was isolated using Fast DNA Spin Kit for Soil (MP Biomedicals). Quality and quantity of the DNA was checked by nanodrop and gel electrophoresis. Per sample, around 400ng was sent for 16S rRNA gene sequencing. Agropyron and Stipa samples were sequenced using the HiSeq sequencing platform at Beijing Genomics Institute (BGI) and Novogene, respectively. For Stipa samples, the V4 region of the 16S rRNA gene was sequenced by the primers 515F and 806R; For Agropyron samples, the V3-V4 region of the 16S rRNA gene was sequenced by the primers 341F and 806R.

Processing of the sequencing results

The forward and reverse primer sequences were trimmed from the FASTQ reads with cutadapt (v1.18). Afterwards, amplicon sequence variants (ASVs) were inferred from the Illumina paired-end FASTQ reads with the DADA2 pipeline (v.1.12.1) (Callahan *et al.*, 2016). FASTQ reads were filtered with the filterAndTrim function allowing for only one expected number of errors (maxEE=1) and discarding reads with any ambiguous nucleotides (maxN=0). Error rates were learned separately with the first 1x10⁸ nucleotide bases of the filtered forward and reverse reads. The pseudo-pooling algorithm from the dada function together with the learned error rates predicted the ASVs in both orientations of the filtered reads after dereplication. Afterwards, the paired reads were merged with the mergePairs function. This workflow involving DADA2 was applied separately on each sequencing run of which there were one and nine for the Agropyron and Stipa datasets,

Chapter 2

respectively. Afterwards, the sequence tables from the different runs of the Stipa sequencing data were merged with the `mergeSequenceTables` function. Chimeras were removed by the consensus method with the `removeBimeraDenovo` function. In order to merge the Agropyron and Stipa ASV tables, the V4 regions were extracted from the original Agropyron ASV sequences by finding the downstream 515F primer sequence. Then the read counts of the unique V4 regions were summed together and forming a new ASV table for Agropyron data. Finally, the RDP Naive Bayesian Classifier algorithm (Wang *et al.*, 2007) as implemented in the `assignTaxonomy` function assigned the taxonomy of the ASVs against the GreenGenes dataset (v.13.8).

Meta amplicon sequencing data analysis

All analyses were performed in the R environment (v.3.6.3). First, ASVs related to mitochondrial and chloroplast sequences were removed. Then, ASVs with sequence length smaller than 253 or bigger than 254 bps were excluded. After this, data relating to our study were subset and named as “raw ASVs”. The “raw ASVs” table was then filtered and ASVs which have more than 25 reads in at least 5 samples were named as “measurable ASVs”. For Stipa, the dataset included 1.27 million reads representing 1076 measurable bacterial ASVs. For Agropyron, it was 1.23 million reads and 622 measurable ASVs. We did similar analyses with two additional Agropyron accessions collected at two other locations (Agropyron_2 and _3) and these data were included in the Agropyron dataset. The custom R commands were used in these analyses based on the R packages *tidyr* (v.1.1.1), *reshape2* (v.1.4.4), *ggplot2* (v.3.3.2) and *fmsb* (v.0.7.0).

To determine the taxonomic composition of the different compartments, analyses in which read counts based on “measurable ASVs” table were assessed. For the Phylum level distribution, all reads were aggregated according to different phyla. The “Others” category was created to include low abundance phyla which did not reach at least 5% in any compartment (Wagner *et al.*, 2016). For β -diversity analyses, a subset of “measurable ASVs” table was generated, containing samples for the research question. Then, using the Bray-Curtis dissimilarity method, measures on the rarefied ASV table, principal coordinate analysis (PCoA) was executed. This was largely done with the *vegan* package (v.2.5.6).

Root-sleeve harbours a unique microbiome

Permutational Multivariate Analysis of Variance (PERMANOVA) and multiple pairwise PERMANOVA were performed using the functions `adonis` and `pairwise.adonis`, respectively. To reduce the false discovery rate (FDR), we used the Benjamini-Hochberg method to adjust the p-values of pairwise comparisons. Differential abundance test was performed with the *edgeR* package in R based on custom scripts of a previously published pipeline (Hartman *et al.*, 2018). In this analysis, “measurable ASVs” were tested by the threshold values with a p-value of 0.05 and a log2-fold change of 1.

Chapter 2

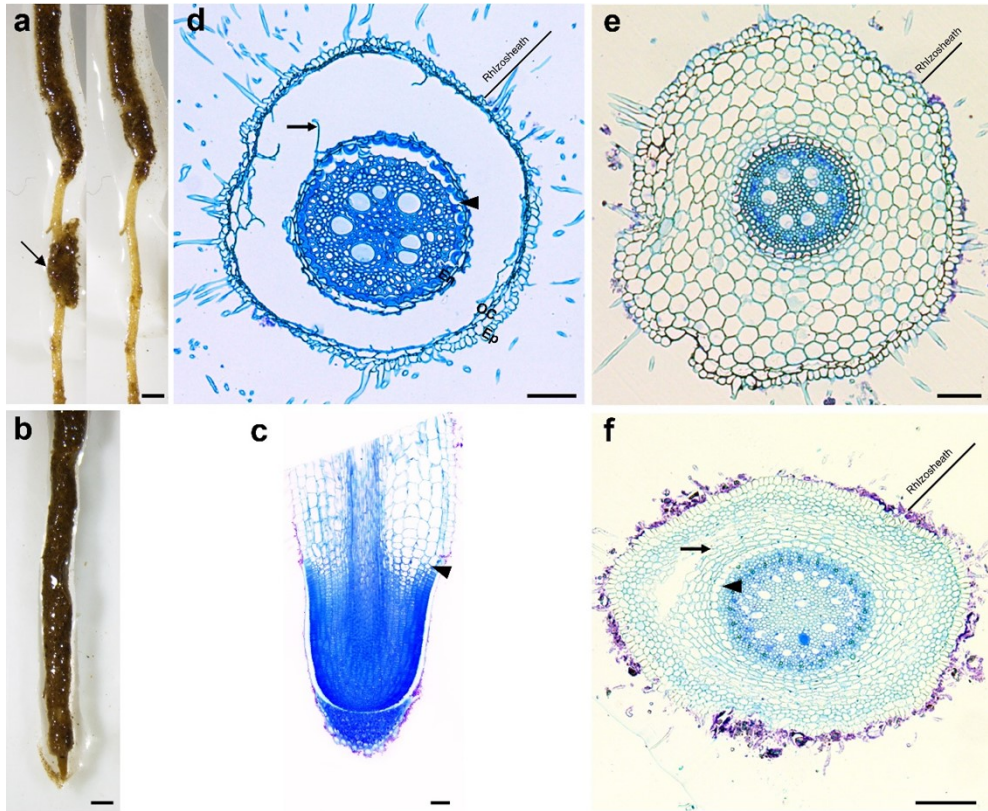
Acknowledgements

This work was supported by the National Natural Science Foundation of China (No. 32192463; No. 31861143001 to M.Z.), National Scientific and Technological Program on Basic Resources Investigation (No. 2019FY102000 to M.Z.), Natural Science Foundation of Inner Mongolia (2020ZD03 to M.Z.) and National Key Laboratory of Grassland Resources, National Key Laboratory of Forage, Inner Mongolia Agricultural University, Hohhot, China.

Author contributions

ZY, HL, BZ, JQ, XC, ML executed the experiments. HL, CF performed microscopy analysis. LS, ZY constructed and implemented the bioinformatics pipelines. ZQ, FZ, JZ, collected field samples. FT, CG, CF helped on sample preparation. LS, ZY, XC conducted in silico analyses. MZ, GH and TB initiated this project and XC helped setting up this study. ZY, HL and TB wrote the manuscript.

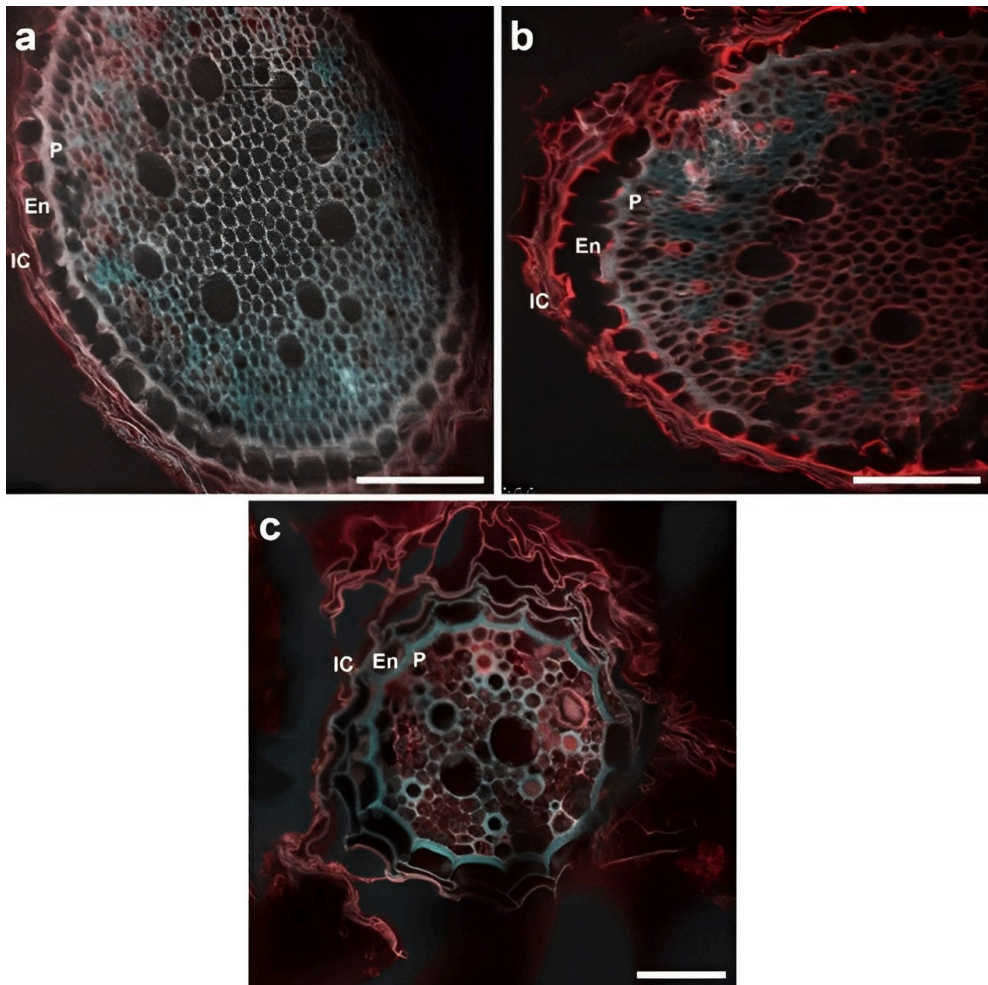
Supplementary information:



Supplementary Fig. 1 | Development of root-sleeves of *Stipa*. **a**, Overview of *Stipa* root segment before (left) and after (right) removing the sandy cylinder (arrow). **b**, Overview of *Stipa* root tip. **c**, Sections of *Stipa* sand-free root tip. Arrowhead indicates the boundary between root meristem and elongation zone. **d-f**, **Cross** Sections of *Stipa* root segments from different positions along the root axis. They are collected from a section close to the shoot (d) slightly above the sandy-free root tips (e), and a moderately old segment roots (f, between e and d). Rhizosheath region where sand grains are carefully brushed off prior to sectioning, the thickness of rhizosheath are marked with a black line in the upper right corner. In d and f, arrows indicate lysed inner cortical cell walls. Arrowheads indicate lysed radial cell walls of endodermis cells. In d, En, endodermis; OC, outer cortex; Ep, epidermis.

Chapter 2

Images d to f are not from the same root. 5 roots are analysed and representative images are shown. Scale bars = 1 mm in a and b, or 100 μ m in c to f.



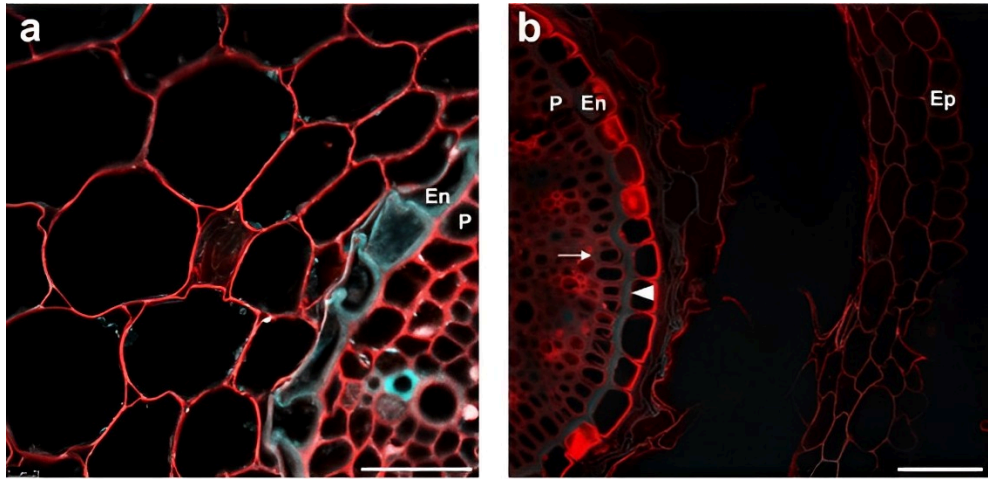
Supplementary Fig. 2 | Structure of root central bundles after removing root-sleeves.

Confocal images of root central bundle in *Agropyron* (a and b) or *Stipa* (c). In both species the surface of root central bundle is formed by remains of inner cortex (IC) and endodermis (En), and occasionally by the pericycle (P) when endodermis is damaged (b). Cyan colour is from lignin autofluorescence, red is from cell walls stained by propidium iodide. 15 *Agropyron* and 5 *Stipa* roots are analysed and representative images are shown. Scale bars = 100 μ m.

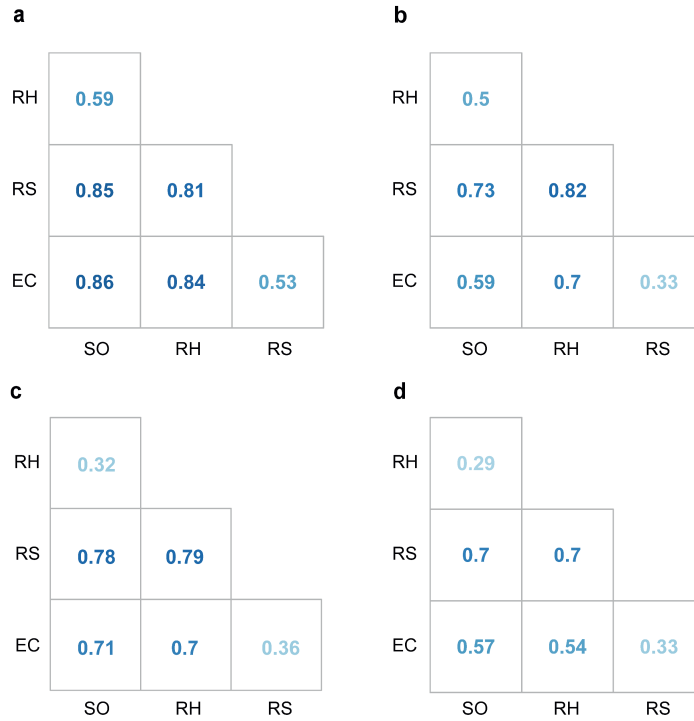


Supplementary Fig. 3 | Position of the 4 developmental stages of root-sleeve formation.

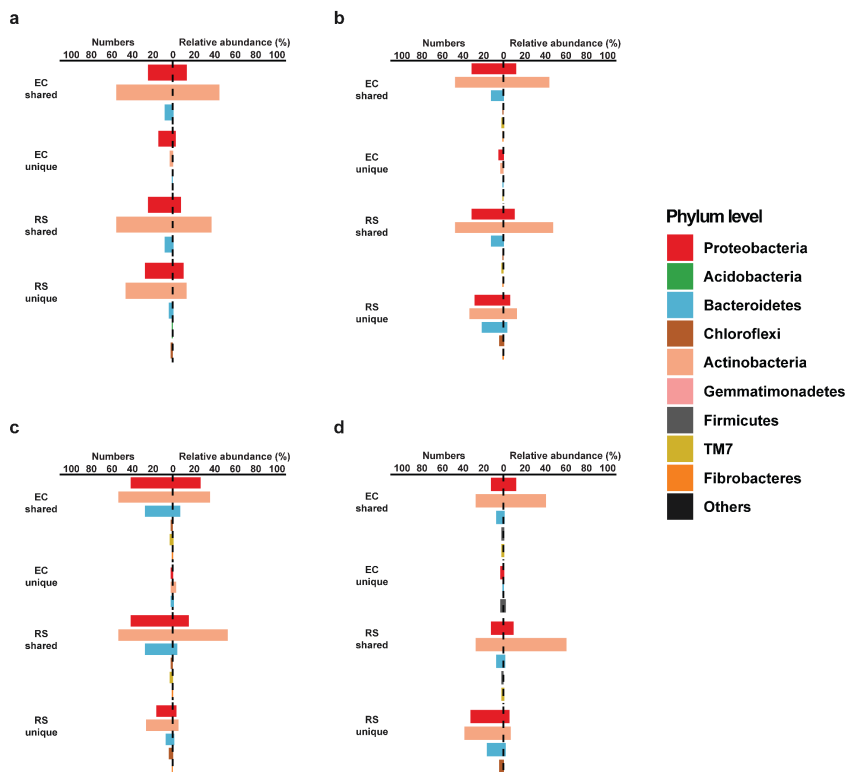
Agropyron plant with a root that has a short sand-free root tip, followed by a long sand-covered part. Positions of the 4 developmental zones/stages are indicated.



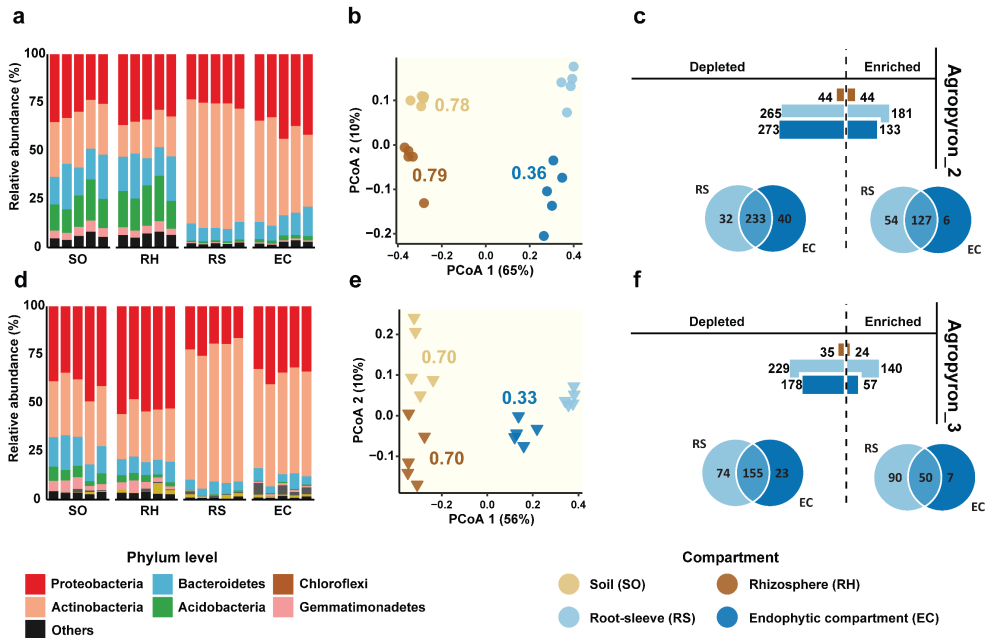
Supplementary Fig. 4 | Lignin deposition during root-sleeve formation of *Stipa*. Cross sections of *Stipa* roots at stage I (a) and stage IV (b). Cyan colour is from lignin autofluorescence, red is from cell walls stained by propidium iodide. In b, the inner periclinal wall of endodermis cells (arrowhead) and pericycle cell wall (arrow) are lignified. P, pericycle; En, endodermis; Ep, epidermis, 5 roots are analysed and representative images are shown. Scale bars = 25 μ m.



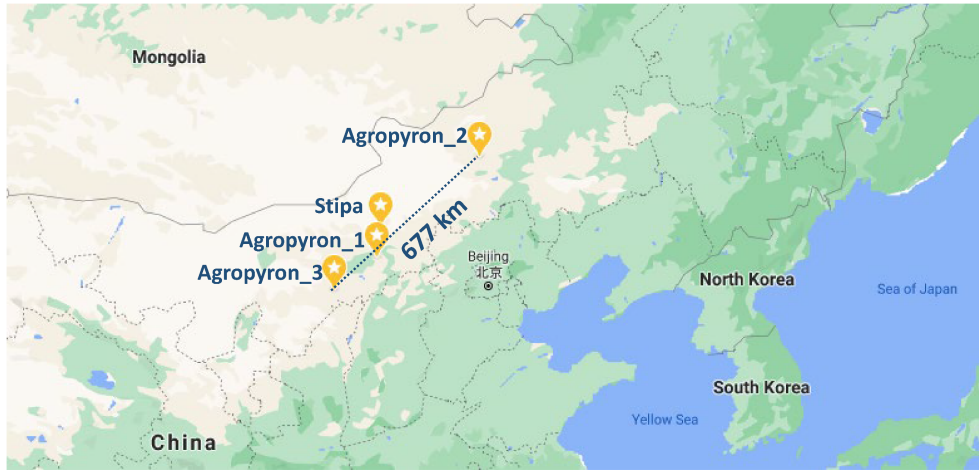
Supplementary Fig. 5 | The R² values obtained by pair-wise PERMANOVA of bacterial community composition of the four compartments. Results from Stipa (a) and three Agropyron accessions (b, c, d for Agropyron_1, _2 and _3). SO, soil; RH, rhizosphere; RS: root-sleeve; EC: endophytic compartment.



Supplementary Fig. 6 | Distribution of enriched ASVs in the root. ASVs in the root-sleeve (RS) and endophytic compartment (EC) with an increased relative abundance in comparison to that in soil are studied at phylum level, for *Stipa* (a) and three *Agropyron* accessions (b, c, d for *Agropyron*_1, _2 and _3, respectively). The number and relative abundance of these enriched ASVs in these two compartments are shown. Furthermore, among these enriched ASVs, the shared and unique ones are shown separately.



Supplementary Fig. 7 | Bacterial community composition in different compartments of two additional Agropyron accessions. **a** and **b**, The relative abundance of the dominant phyla (more than 5% of the total reads in at least one compartment) are shown for soil (SO), rhizosphere (RH), root-sleeve (RS) and endophytic compartment (EC) of Agropyron_2 (**a**) and Agropyron_3 (**b**). Detailed information is described in Methods; **c** and **d**, Principal Coordinates Analysis (PCoA) of bacterial communities in the four compartments of Agropyron_2 (**c**) and Agropyron_3 (**d**). The R² values of PERMANOVA by comparing SO, RH, EC to RS are shown in the figures, coloured as the compared compartment. **e** and **f**, the number of ASVs with a changed relative abundance (enriched and depleted) in comparison to that in soil are shown for Agropyron_2 (**e**) and Agropyron_3 (**f**). This was done by the *edgeR* package with threshold values of a p-value 0.05 and a log₂-fold change of 1. Venn diagrams show the overlap or unique part of these changed ASVs in RS and EC.



Supplementary Fig. 8 | Locations where *Stipa* and three *Agropyron* accessions were collected in grassland of Inner Mongolia, China.

Sample	Compartment	Number of changed ASVs
Stipa	RH	265
	RS	744
	EC	892
Agropyron_1	RH	141
	RS	461
	EC	350
Agropyron_2	RH	88
	RS	446
	EC	406
Agropyron_3	RH	59
	RS	369
	EC	235

Supplementary Table 1 | Number of ASVs with a changed relative abundance (enriched and depleted) in comparison to that in soil. This was done by the *edgeR* package with threshold values of a p-value 0.05 and a log2-fold change of 1.

Chapter 3

High salt levels reduced dissimilarities in root-associated microbiomes of two barley genotypes

Asma Kherfi-Nacer^{1,2,#}, Zhichun Yan^{2,#}, Amina Bouherama^{1,3}, Lucas Schmitz², Saadia Ouled Amrane^{1,4}, Carolien Franken², Martinus Schneijderberg², Xu Cheng^{2,5}, Said Amrani¹, Rene Geurts², Ton Bisseling^{2,6*}

¹ Laboratory of Biology and Physiology of Organisms (LBPO), Biological Sciences Faculty, Houari Boumediène Sciences and Technology University (USTHB), BP 32, El-Alia, Bab Ezzouar, Algiers 16111, Algeria.

² Laboratory of Molecular Biology, Plant Science Group, Wageningen University and Research (WUR), Droevendaalsesteeg 1, Wageningen 6708PB, The Netherlands.

³ Sciences Faculty, Yahia Farès University, Médéa 26000, Algeria.

⁴ Research Experimental Field Station, Belbachir, El-Meniaa, Ghardaïa 47001, Algeria.

⁵ Agricultural Genome Institute at Shenzhen, Chinese Academy of Agricultural Sciences, Shenzhen 518124, China.

⁶ Beijing Advanced Innovation Centre for Tree Breeding by Molecular Design, Beijing University of Agriculture, Beijing 102206, China.

These authors contributed equally to this work.

* Corresponding author: ton.bisseling@wur.nl

Published: *Molecular Plant-Microbe Interactions* volume 35.7, pages 592-603 (2022).

Abstract

Plants harbour in and at their roots bacterial microbiomes that contribute to their health and fitness. The microbiome composition is controlled by the environment and plant genotype. Previously, it was shown that the plant genotype-dependent dissimilarity of root microbiome composition of different species becomes smaller under drought stress. However, it remains unknown whether this reduced plant genotype-dependent effect is a specific response to drought stress or a more generic response to abiotic stress. To test this, we studied the effect of salt stress on two distinct barley (*Hordeum vulgare* L.) genotypes; the reference cultivar Golden Promise and the Algerian landrace AB. As inoculum, we used soil from a salinized and degraded farmland on which barley was cultivated. Controlled laboratory experiments showed that plants inoculated with this soil display growth stimulation under high salt stress (200 mM) in a plant genotype-independent manner, whereas the landrace AB also showed significant growth stimulation at low salt concentrations. Subsequent analysis of the root microbiomes revealed a reduced dissimilarity of the bacterial communities of the two barley genotypes in response to high salt, especially in the endophytic compartment. High salt level did not reduce α -diversity (richness) in the endophytic compartment of both plant genotypes, but associates with an increased number of shared strains that respond positively to high salt. Among these, *Pseudomonas* species were most abundant. These findings suggest that the plant genotype-dependent microbiome composition is altered generically by abiotic stress.

Keywords: barley, Golden Promise, abiotic stress, meta-amplicon sequencing, salinity, root microbiome.

Introduction

Plants have microbes associated with their roots, of which bacteria are prominent (Hacquard *et al.*, 2017; Jacoby *et al.*, 2017; Compant *et al.*, 2019; Babalola *et al.*, 2020; Bakker *et al.*, 2020). Bacteria are highly abundant in the rhizosphere (RH), which is the soil closely associated with the root, whereas the root interior -the endophytic compartment (EC)- is less accessible (Iniguez *et al.*, 2005; Mendes *et al.*, 2013; Edwards *et al.*, 2015; Wang *et al.*, 2016). The composition of these two root-associated bacterial microbiomes is generally different from that of the bulk soil and this difference is always biggest in the EC (Bulgarelli *et al.*, 2012; Lundberg *et al.*, 2012; Bulgarelli *et al.*, 2015; Fernández-González *et al.*, 2019; Alegria Terrazas *et al.*, 2020). The composition of these root microbiomes is, controlled by the plant genotype, the composition of the soil microbiome as well as environmental conditions (Berg, G. & Smalla, K., 2009; Bakker, P. A. *et al.*, 2013; Philippot *et al.*, 2013; Lebeis *et al.*, 2015; Sasse *et al.*, 2018; Tang *et al.*, 2021). The effect of the plant genotype has been observed in several studies. For example, a comparative analysis of Poaceae species showed that the differences in the composition of the root-associated microbiomes correlated with the phylogenetic distance of the host plants (Bouffaud, M-L *et al.*, 2014; Naylor, Dan *et al.*, 2017). This plant genotype effect on the root-associated microbiome is detected even between accessions/cultivars of single species, e.g. maize (*Zea mays* L.) and barley (*Hordeum vulgare* L.) (Peiffer *et al.*, 2013; Bulgarelli *et al.*, 2015; Pérez-Jaramillo *et al.*, 2018).

Several abiotic factors like salinity, drought, extreme temperatures, nutrient deficiencies, and flooding affect the composition of the root-associated microbiomes (for reviews see: Hussain *et al.* (2018), Hartman and Tringe (2019), Sandrini *et al.* (2022)). Interestingly, a study on the root microbiomes of 18 Poaceae species, including barely, showed that the plant genotype effect is reduced by drought as the composition of the root-associated microbiomes became more similar (Naylor, Dan *et al.*, 2017). However, it remains elusive whether this reduced dissimilarity is a generic response to abiotic stress, or alternatively, a drought stress-specific response, because some specific bacterial taxa do become dominant in the root microbiomes under drought stress, e.g. Actinobacteria (Naylor, Dan

Chapter 3

et al., 2017; Fitzpatrick *et al.*, 2018). In this study, we questioned whether salt stress reduces the differences in the composition of the root microbiomes between two barley genotypes and if so, which genera it might involve.

Salt changes the physiology of most plant species, which affects the composition of the root-associated microbiomes (Li *et al.*, 2021; Rizaludin *et al.*, 2021). As these microbiomes have the potential to protect plants to some extent from salt stress (Ilangumaran & Smith, 2017; Egamberdieva *et al.*, 2019), it is important to know how salt affects their composition. This is relevant as many areas in the world are affected by salinization (Hassani *et al.*, 2020). It has been reported that 33% of the irrigated land used for agriculture has an increased salinity, which represents 20% of the total cultivated land worldwide (Otlewska *et al.*, 2020). This salinization can have various causes like; flooding with seawater (Gould *et al.*, 2020), the upward transport of salts from the groundwater (Shi *et al.*, 2005), and the use of water with a poor quality (Abdenmour *et al.*, 2021). Salinity also can be the result of a combination of inappropriate irrigation practices and excessive evapotranspiration, especially in arid and semi-arid areas (Hassani *et al.*, 2020). Soil salinity causes reduced plant growth, as it affects crop physiology in several ways. For example, ions in the soil affect osmosis and this makes water less available to the plant. Furthermore, excessive uptake of Na^+ and Cl^- causes cytotoxicity for the plant and salinity also leads to the accumulation of reactive oxygen species damaging the plant cells (Munns & Tester, 2008; Julkowska & Testerink, 2015; Julkowska *et al.*, 2017; Isayenkov & Maathuis, 2019; Lamers *et al.*, 2020; Van Zelm *et al.*, 2020; Awlia *et al.*, 2021; Karlova *et al.*, 2021). Thus, soil salinization is a major problem as it causes loss of arable land.

We aimed to test the host plant genotype effect on the root-associated microbiome of barley under salt stress. Although barley is moderately salt tolerant, its growth is reduced to about 50% at 110 mM exogenously applied NaCl (Munns & Tester, 2008). Extensive studies on the barley root-associated microbiomes showed that the microbiome compositions of the RH and EC differ significantly from bulk soil samples (Bulgarelli *et al.*, 2015; Mitter *et al.*, 2017; Liu, Z *et al.*, 2019). The barley EC microbiome is low in diversity, indicating this compartment is highly selective (Bulgarelli *et al.*, 2015). Furthermore, host plant genotype effects on the microbiome have been found (Bulgarelli *et al.*, 2015; Liu, Z

et al., 2019; Alegria Terrazas *et al.*, 2020). As barley is selective and shows a genotype effect, it is suited to study the salt effect on the composition of the root-associated microbiomes. We used a barley landrace from Algeria -named AB (Algerian Barley)- and the barley reference cultivar (*cv.*) Golden Promise for our study, as we expected that their microbiomes would be sufficiently different in absence of salt to allow us to study the effect on the level of dissimilarity at high salt. The landrace AB is adapted and cultivated by farmers for example in the oasis of El-Golea (Algeria), while *cv.* Golden Promise was selected as it is a model for which molecular, genetic, and genomics tools have been developed (Schreiber *et al.*, 2019; Schreiber *et al.*, 2020).

We argued that we could test our hypothesis in the best way when using a microbiome that is adapted to a saline environment as well as to barley as a host plant. Communities adapted to a certain trait have previously been created by an approach named host-mediated selection on microbiome (Mueller & Sachs, 2015). This involves the growth of the host plant of choice for several cycles on a microbiome and selection of the property of interest. This approach was used to create for example microbiomes that induce increased drought tolerance in wheat (*Triticum aestivum*) (Jochum *et al.*, 2019). We aimed to select an adapted microbiome for barley grown on saline soil. Therefore, we used a soil from a degraded farmland in El-Golea and grew two cycles of barley landrace AB in the presence of salt before we used this soil as inoculum. Additionally, we compared the microbiome of this landrace to the microbiome of the reference *cv.* Golden Promise when grown on this 'AB soil trained microbiome'.

Here we show that landrace AB and *cv.* Golden Promise formed distinct root-associated microbiomes under control conditions. Salt stress reduced the differences in the composition of the bacterial communities in the root-associated microbiome of landrace AB and *cv.* Golden Promise. These findings suggest that reduction in dissimilarity caused by plant genotype is a more generic response to abiotic stress.

Results

The barley root-associated microbiome shows distinct responses to mild and severe salt stress.

To determine the effect of salt on the composition of the bacterial communities of the 'bulk soil', the rhizosphere (RH), and the endophytic compartment (EC), barley landrace AB was grown on different concentrations of salt (see materials and methods) and to compare the compositions of the bacterial root-associated microbiome, we performed Principal Coordinate Analyses (PCoAs) using the rarefied ASV dataset (see materials and methods). This analysis was based on the Bray-Curtis dissimilarity matrix between all samples. RH and EC samples were separated from 'barley soil' along the first component (36% of variance) and along the second component especially RH and EC samples were separated (30% of variance) (Figure 1a). By including the 'barley soil', the RH and EC samples clustered more closely. To increase the resolution between these samples, we repeated the analysis now excluding the 'barley soil' samples (Figure 1b). This showed that bacterial communities from the RH were distinct from the EC along the first coordinate (47% of the variance). Permutational Multivariate Analysis of Variance (PERMANOVA) confirmed that the difference between the two compartments was significant ($R^2=0.42$, $p<0.001$). Along the second coordinate (16% of variance), a gradual distribution of bacterial communities in both RH and EC was observed, in accordance with the salt gradient.

Differences in the barley root-associated bacterial communities were most pronounced when comparing compartments. As we aim to study the effect of the salt gradient on the composition of the bacterial communities in RH and EC, we analysed these two compartments separately using Constrained PCoA (CPCoA), constrained by salt. The RH samples have a gradual distribution along the first coordinate (52% of variance) with 0mM on the left and 250 mM on the right (Figure 1c). Along the second coordinate (23% of variance), such a gradual distribution occurred up to 150 mM. However, the samples of 200 and 250 mM positioned markedly closer to 0 and 50 mM. In case of the EC, the first two coordinates of the CPCoA analysis explained 47 and 25% of the variance (Figure 1d).

High salt reduces microbiomes' dissimilarities

Also, in the EC there was a gradual change in the position of samples along the first coordinate, with 0 and 250 mM at the extreme ends. Along the second coordinate, EC samples from 0 and 100 mM were separated and at higher salt concentrations the samples were positioned gradually closer to 0 mM. Comparisons by pairwise PERMANOVA showed that most of the EC samples of different salt levels form clusters significantly distinct from each other (adjusted $p < 0.05$) (Table 1). The adjusted p values of pairwise comparisons ordinations of samples of RH were in most cases slightly higher than 0.05 (Table 1).

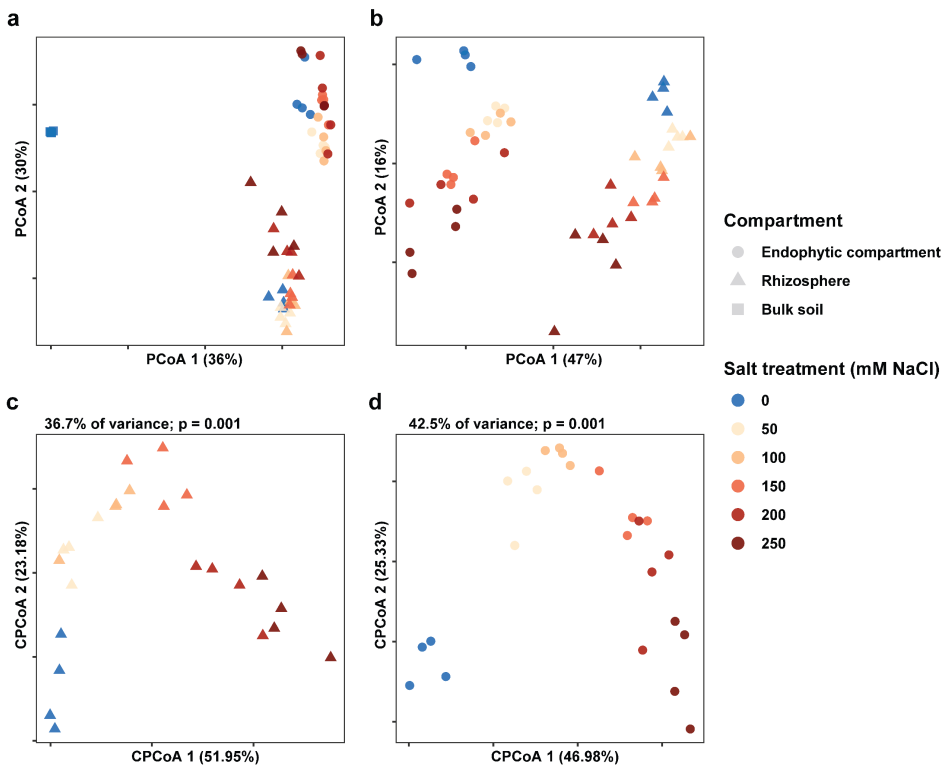


Figure 1. Effects of a salt gradient on barley root-associated microbiome. (a) Principal Coordinates Analysis (PCoA) of bacterial communities in the bulk soil, rhizosphere and endophytic compartment of Algerian barley landrace AB exposed to six different salt concentrations; 0, 50, 100, 150, 200 and 250 mM NaCl. Bray-Curtis dissimilarities were calculated with ASV read counts after rarefaction and standard filtering. **(b)** PCoA

Chapter 3

excluding bulk soil samples. (c & d) Constrained PCoA of bacterial communities by the salt treatment in the rhizosphere (c) and endophytic compartment samples (d). For each sample type, four biological replicates were analysed. Shape of the data point indicates the compartment and their colour corresponds to the salt concentration. Permutational Multivariate Analysis of Variance (PERMANOVA) and pairwise PERMANOVA were used to test significant differences among the samples.

So, in both the RH and the EC the effect of the first coordinates became bigger with increasing salt concentrations (up to 250 mM NaCl). In contrast, the two second coordinates have most effect at modest salt levels (100 and 150 mM NaCl). This indicates that the physiological response to mild salt stress is distinct from that of severe salt stress. In the following experiment, aimed to compare the microbiomes of the landrace AB and cv. Golden Promise, we used 0, 100, and 200 mM salt to cover mild and severe stress and increase the chance to obtain significant differences between microbiome of plants grown at different salt levels.

‘Algerian barley soil trained microbiome’ promotes growth of two barley genotypes under saline conditions.

To study the effect of mild and severe salt stress on the root-associated microbiomes, we cultured landrace AB and cv. Golden Promise at 0, 100 and 200 mM.

To test whether the microbiome might stimulate growth we cultured the plants with and without the ‘AB soil trained microbiome’. Shoots were harvested when the plants were four weeks old and so had been exposed to salt for 2 weeks. Both barley genotypes were sensitive to salt as a gradual drop of the biomass took place with increasing salt concentrations (Figure 2), although cv. Golden Promise was affected more severely than landrace AB (at 200 mM 51% vs 27% reduction of shoot weight). The difference in shoot biomass between 0 and 200 was for both genotypes significant ($p < 0.05$, t-test). Inoculation with 10% ‘AB soil trained microbiome’ resulted in more than 50% growth promotion of landrace AB at 0, 100 and 200 mM NaCl and in all cases this increased growth was significant ($p < 0.05$, t-test). Growth promotion in cv. Golden Promise also occurred at all conditions. At 0 and 100 mM the growth promotion was relatively minor

High salt reduces microbiomes' dissimilarities

and not significant. At 200 mM the shoot fresh weight almost doubled when the microbiome was present and it was significant (Tables 2 and 3).

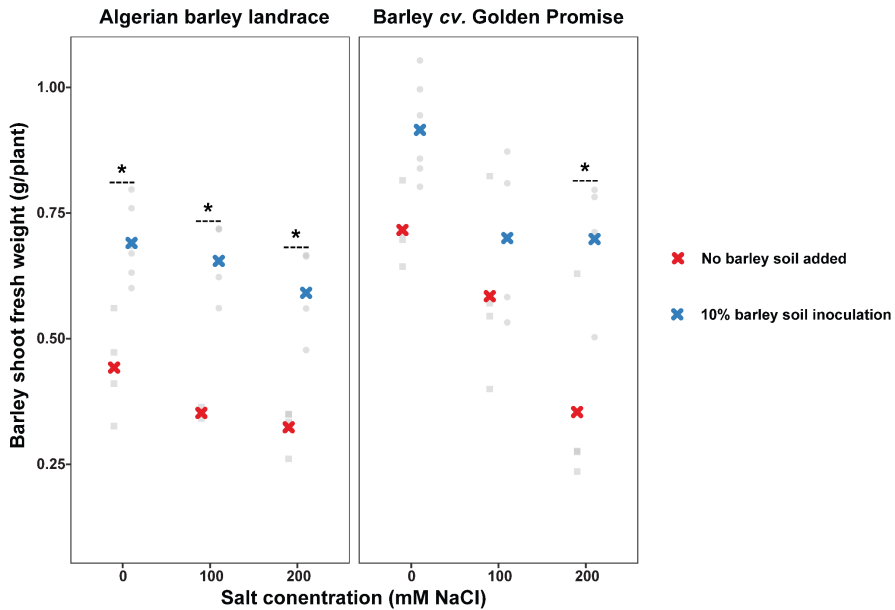


Figure 2. 'Barley soil trained microbiome' promotes growth of barley under salt stress conditions. The shoot fresh weight (g/plant) of Algerian barley landrace AB and Barley cv. Golden Promise grown under three salt levels in two soils. Barley seedlings were transplanted into the sterile river sand with or without the 10% 'barley soil trained microbiome'. After two weeks of growth, plants were exposed to salt (0, 100, and 200 mM NaCl) and harvested two weeks later. The weight of each replicate is shown by a grey dot, shaped differently (square for no 'barley soil trained microbiome' added, circle for 10% 'barley soil trained microbiome' inoculation). The mean value of each sample type is shown by a cross symbol and coloured accordingly. Asterisks indicate statistical significance ($p < 0.05$, t-test) between soil treatments.

This indicates that 'AB soil trained microbiome' promotes growth of both barley genotypes at all three salt concentrations. However, at 0 and 100 mM growth stimulation of cv. Golden Promise is rather small and not significant, whereas growth of landrace AB

Chapter 3

was significantly stimulated. At a high salt level growth of both genotypes was significantly stimulated.

The α -diversity of root-associated bacterial microbiomes in response to salt.

To compare the effect of salt on the root-associated microbiomes of landrace AB and cv. Golden Promise we analysed the α -diversity, compared the phyla distribution, and performed PCoAs.

We have calculated richness (ASVs) and evenness based on a rarefied dataset of ASVs. Salinity had no strong effect on richness and evenness in the root-associated microbiomes (Figure 3). In the RH of landrace AB, the evenness was reduced with 3%, whereas the decrease in the richness at 200 mM was not significant. In EC of landrace AB at 200 mM, α -diversity increased with about 20 and 8%, richness and evenness, respectively. There was also no significant effect in EC of cv. Golden Promise (Figure 3).

In both RH and EC there was no significant effect on the α -diversity ($p < 0.05$, ANOVA with Tukey HSD test).

Salt decreases the dissimilarity between the root-associated bacterial microbiomes of Algerian Barley landrace and cv. Golden Promise

Next, we determined the effect of salt on the composition of the root-associated bacterial microbiomes of the two barley genotypes. The two genotypes had a similar phylum distribution in their RH and also the composition of their EC was comparable. Proteobacteria and Bacteroidetes were the two major phyla and Actinobacteria, Verrucomicrobia, Acidobacteria and Gemmatomonadeles had a modest relative abundance. In the EC, the relative abundance of Actinobacteria increased and that of Verrucomicrobia, Acidobacteria and Gemmatomonadeles decreased in comparison to RH (Supplementary Figure 1). Salt did not affect the phyla distribution in the root-associated bacterial microbiomes of each genotype. The differences were, in both genotypes, primarily due to the compartment effect.

High salt reduces microbiomes' dissimilarities

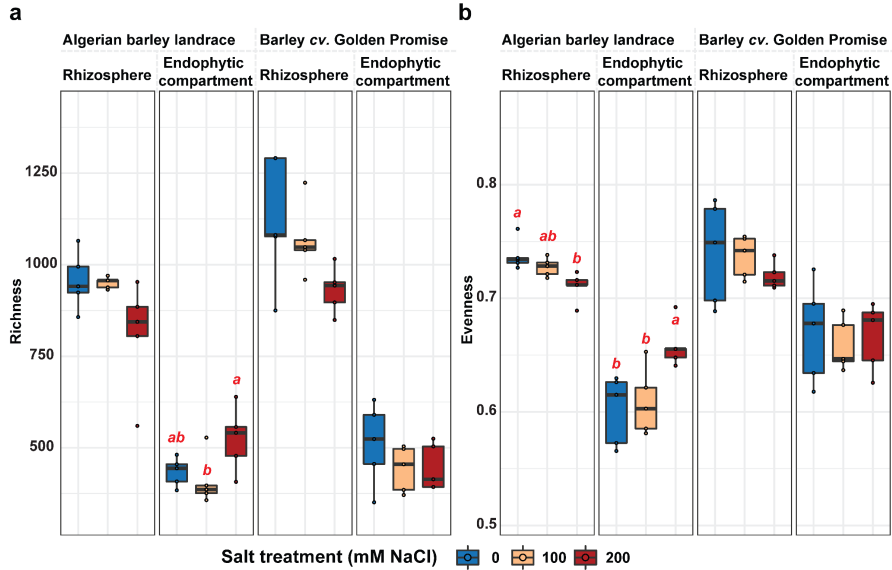
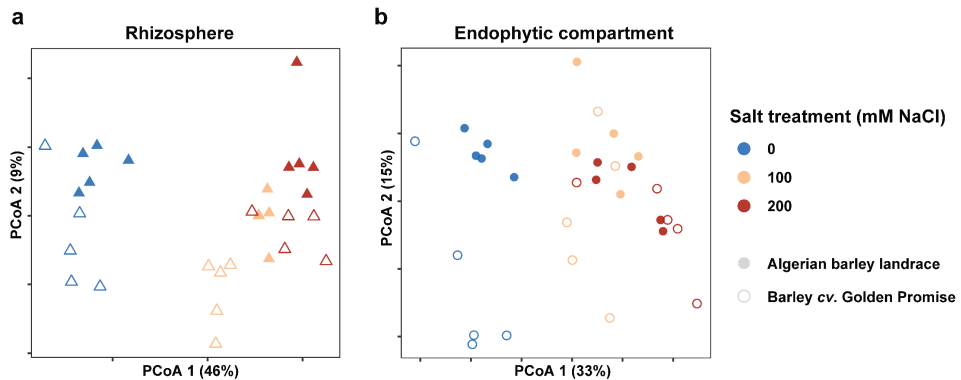


Figure 3. α -diversity of barley root-associated microbiomes at different salt concentrations. The α -diversity of bacterial communities in the rhizosphere and endophytic compartment of Algerian barley landrace AB and Barley cv. Golden Promise grown at three salt levels. The α -diversity is measured by two indices; Richness (a) and Evenness (b). Indices are calculated using the rarefied ASV table. For each sample type, five biological replicates were included. Colour of the box corresponds to a specific salt concentration (0, 100, and 200 mM NaCl). Red italic letters above the box indicate statistical significance ($p < 0.05$, ANOVA with Tukey HSD test) between salt treatment.



Chapter 3

Figure 4. Root microbiomes of the Algerian barley landrace AB and cv. Golden Promise become more similar upon salt treatment. PCoAs of bacterial communities in the rhizosphere **(a)** and endophytic compartment **(b)** of both landrace AB and cv. Golden Promise grown at three salt concentrations. For each sample type, five biological replicates were analysed. Filled shape (circle/triangle) refers to landrace AB and open shape refers to cv. Golden Promise samples. Colour of the dot corresponds to salt concentrations (0, 100, and 200 mM NaCl).

To compare the effect of salt on the community level in the RHs and ECs, we performed PCoA analyses. This was based on the Bray-Curtis dissimilarity matrix between all RH samples of the two genotypes (Figure 4a) and all samples of the ECs (Figure 4b), respectively. The RH samples of both genotypes separated along the first principal coordinate (46% of variance) by salt concentration and at the different salt concentrations the samples of the two genotypes, positioned similarly along this axis. The samples were separated by genotype along the second principal coordinate, which represents 9% of variance. The EC samples of both genotypes separated in a similar way. Along the first coordinate (33% of variance) by salt concentration and along the second coordinate by genotype (15%). However, at 200 mM salt the EC samples of the two genotypes were almost not separated. To quantify the differences between samples of the two genotypes, pairwise PERMANOVA analyses were performed for landrace AB and cv. Golden Promise samples of a certain condition and compartment (Table 4). This showed the lowest R^2 value for the comparison of EC samples obtained from plants treated with 200 mM NaCl (0 mM $R^2=0.28$, 100 mM $R^2=0.20$ and 200 mM $R^2=0.11$). Whereas differences in bacterial root microbiome between cv. Golden Promise and landrace AB were significant for plants treated with 0 and 100 mM, it was not for plants treated with 200 mM NaCl. This demonstrates that at 200 mM NaCl, the EC bacterial microbiomes of the barley genotypes landrace AB and cv. Golden Promise became similar. A comparable pattern is observed for the bacterial microbiome in the RH, albeit less strong than in the EC (Table 4).

To further analyse whether the dissimilarity between the root-associated microbiomes of the two genotypes became smaller at high salt, we did abundance analysis. We identified ASVs with more than 4-fold increased relative abundance at 100 or 200 mM in comparison

to 0 mM with $p < 0.05$. To compare the root-associated microbiomes, we determined which of these enriched ASVs are shared by the two genotypes and which are unique. This showed that there are less unique enriched ASVs in both RH and EC at high salt, whereas the number of shared enriched ASVs increased (Table 5). To test this in an independent manner indicator species analysis was performed. This analysis was visualized in bipartite networks summarizing the identified indicator ASVs within the RH and EC samples that are positively and significantly ($p < 0.05$) correlated with one or two salt concentrations (Supplementary Figure 2). In both, landrace AB and cv. Golden Promise, about 40% of the ASVs were salt responsive in the RHs, whereas in the ECs this was 22 to 24% of the ASVs (Supplementary Table 1). Indicator species analysis showed that the majority of the indicator ASVs positively responding to salt (salt cluster in 100, 200 and 100-200 mM NaCl) were shared by the two genotypes (Table 5, Supplementary Table 2). This confirmed the differential abundance analysis, showing that salt stress decreases the dissimilarity of root-associated bacterial microbiomes of the two barley genotypes.

Next, we wanted to know what are the dominant ASVs of each genotype under different salt conditions and whether there are more overlaps of dominant ASVs between the two genotypes under high salinity. Therefore, we compared the 10 most abundant ASVs from both genotypes under different salt conditions, in different compartments. These 10 most abundant ASVs generally represented about 30% and 40% of the total reads in RH and EC, respectively. First, this showed that *Pseudomonas* species are most dominant in RH and EC of both genotypes, whereas none of the abundant 10 ASVs belong to Actinobacteria (Figure 5, Supplementary Figure 3). Both landrace AB and cv. Golden Promise shared 6-7 abundant ASVs in RH and EC when grown in 0 or 100 mM NaCl, but also possessed plant genotype-specific ASVs that are abundant in the root microbiome. However, the genotype-specific effect decreased when plants were exposed to 200 mM NaCl, resulting in the recruitment of the same 10 most abundant strains in the EC of the landrace AB and cv. Golden Promise (Figure 5).

Taken together, these findings show that the genotype-effect on the root microbiome composition in barley, decreases with increasing salt concentration.

Chapter 3

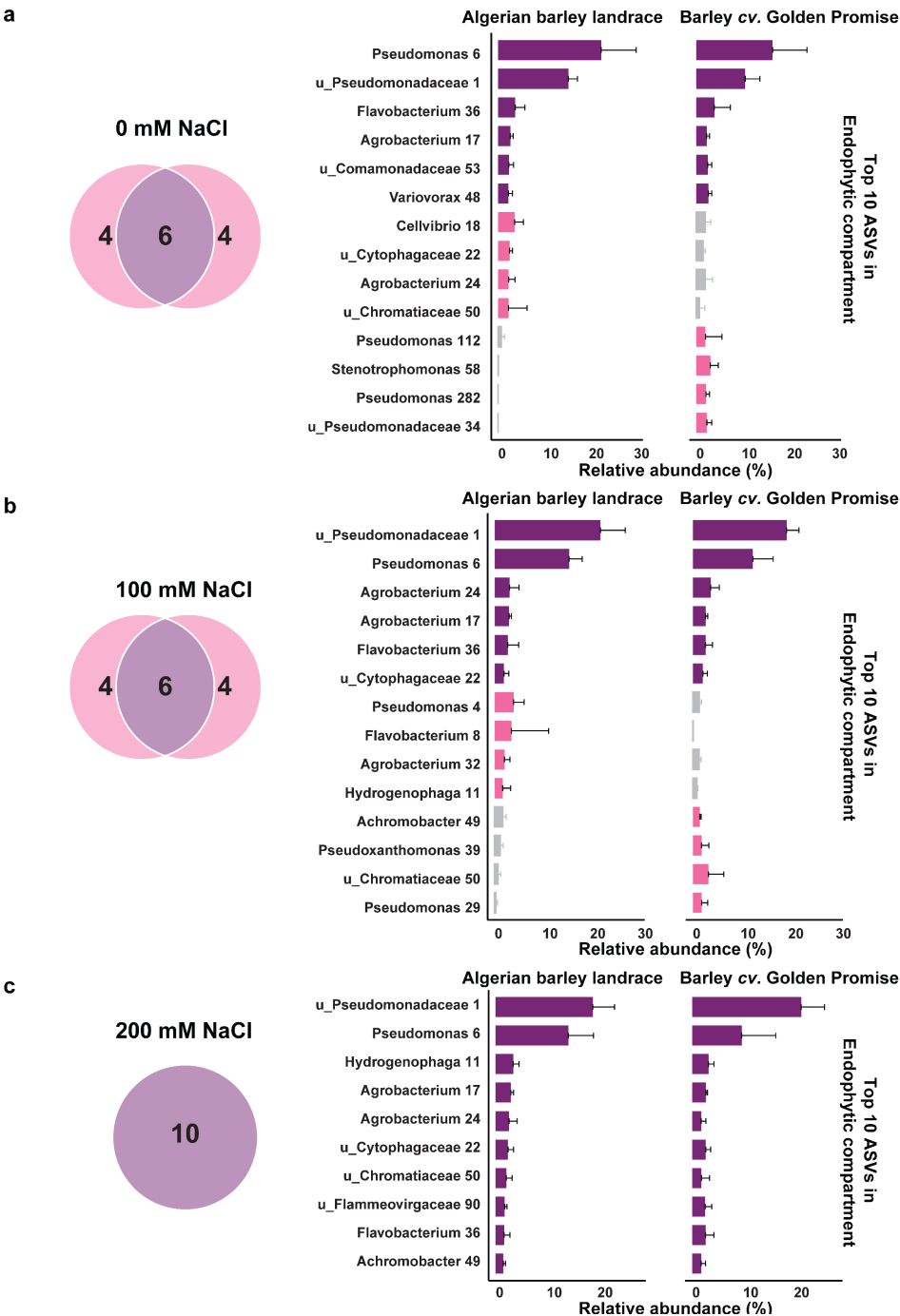


Figure 5. Abundant bacterial ASVs in the endophytic compartment of two barley genotypes become similar upon salt application. Ten most abundant ASVs (top-10) in the EC of Algerian barley landrace AB and cv. Golden Promise at three salt concentrations (0, 100, and 200 mM NaCl). On the left, Venn diagram represents the number of shared and unique top-10 ASVs between the two genotypes. On the right, Y-axis of the bar chart taxonomic information and the ASV number assigned in this study. X-axis represents the mean relative abundance of ASV in the EC of the genotype. The top-10 ASVs are coloured, ASVs shared by two genotypes are given in dark purple, and non-shared ASVs are given in pink (top-10 ASV) or grey (non-top-10 ASV). ASVs were ordered by their relative abundance in the EC of Algerian barley landrace AB. In all EC samples, ASV_1 (unclassified Pseudomonadaceae) and ASV_6 (Pseudomonas) were the two most abundant ASVs. In the EC of roots grown at 200 mM NaCl, all top-10 ASVs were shared and their relative abundance was similar in both genotypes.

Chapter 3

Discussion

Here we show that exogenously applied salt reduces the dissimilarity of the root-associated microbiomes of two barely accessions. The Algerian Barley landrace (AB) and the reference cultivar (cv.) Golden Promise, displayed distinct plant genotype effects on the root microbiome composition, when plants were grown under low salt conditions. However, application of 200 mM NaCl resulted in a decrease of the dissimilarity of the root microbiomes, an increase in the number of shared ASVs that positively responded to high salt in both genotypes, and an increased similarity in ASVs that were abundantly present in the rhizosphere (RH) and/or the endophytic compartment (EC).

Principal coordinate analyses showed that at the population level the bacterial microbiomes of landrace AB and cv. Golden Promise responded similarly to salt. The differences caused by the plant genotype were smaller than those caused by salt. Additionally, the genotype effect became smaller at higher salt levels. This reduction of the dissimilarity between the root microbiomes of the two plant genotypes at high salt was most severe in the EC. At 200 mM salt, the EC microbiomes of both samples had similar positions along the first and second coordinates and the small difference was not significant. In contrast, at 0 and 100 mM salt the differences between the root-associated microbiomes of the two genotypes were significantly different. The reduced dissimilarity at high salt can be caused by a reduced plant genotype effect, or alternatively a result of a reduced richness of the soil microbiome due to salt application. To discriminate between these two scenarios, ideally the microbiome of the bulk soils after salt treatment needed to be quantified. However, the chosen experimental setup did not allow such approach. Because, at the end of the experiment pots were well filled with roots and so it is not feasible to collect soil samples that had not been in close contact with roots. To obtain insight into the salt effect on the microbiome, we studied the richness in rhizosphere soils. As these were only slightly reduced upon salt application, we postulate that the microbiome of the bulk soil may respond similarly. In contrast to the slightly reduced richness in rhizosphere soil, the richness of EC showed a slight increase or stayed similar

(Figure 3). As richness (diversity) of the EC microbiomes is not reduced, the reduced dissimilarity at high salt is most probably caused by a reduced plant genotype effect.

The constrained principal coordinate analyses (Figure 4) indicated that the response of barley to mild salt stress has aspects that are distinct from that of severe salt stress. The analysis of the salt gradient experiment showed that the strongest shift along the second coordinate occurred with the mild salt samples. That mild salt involves some specific changes is further supported by the presence of indicator ASVs specific for the 100mM NaCl clusters (Supplementary Table 2). It has not been well studied whether plants have distinct physiological responses to mild and severe salt stress. In contrast, variation in response has been well documented for mild and severe drought stress. It was shown that about 25% of the genes differentially expressed under mild drought stress are not induced during severe drought stress (Clauw *et al.*, 2015). Based on our findings, we postulate the plant's physiological response may be salt concentration dependent, similarly as reported for drought.

At high salt (200 mM), the 10 ASVs with the highest relative abundances in the EC microbiomes were identical for both barely accessions and even the relative abundances of the strains were similar. Also, the ASVs positively responding to high salt were similar in both genotypes. The underlying mechanism of this effect remains still elusive. The two barley accessions could vary for example in physiology or in secondary metabolites produced by the root at low salt, whereas the physiological response to high salt is similar. This might have caused the composition of the microbiomes at high salt become more similar.

The salt stress dependent reduction of the plant genotype effect on the root-associated microbiomes is in line with a study on drought on Poaceae species. This showed that drought decreased the dissimilarity between the microbiomes of these species (Naylor, Dan *et al.*, 2017). In the case of drought, this reduction of the plant genotype effect correlates with an increase in the relative abundance of Actinobacteria (Naylor, Dan *et al.*, 2017; Santos-Medellín *et al.*, 2017; Simmons *et al.*, 2020). In our study, the relative abundance of Actinobacteria remained low under saline conditions. For example, in the

Chapter 3

RH of landrace AB, 2 out of 208 positively responding ASVs and in its EC 7 out of 119 were Actinobacteria (Supplementary Figure 2). Thus, Actinobacteria seem to play a minor role in the observed dynamics in the root microbiome induced by salinity.

We found that the salt effect on the α -diversity the bacterial root microbiome was limited. In other studies, it has been reported that the α -diversity of the root microbiome is affected upon salt application (Li *et al.*, 2021). It has been hypothesized that an increase of the α -diversity is due to a decrease of abundant strains, which gives room to more rare strains (Yang *et al.*, 2016; Benidire *et al.*, 2020; Santos *et al.*, 2021). In our study, this is not the case as the relative abundance of dominant ASVs is not affected by the treatment. Indicator species analyses showed that the number of ASVs of which the relative abundance increased or decreased upon salt treatment was comparable (Supplementary Table 1, Supplementary Figure 2). This most probably explains why in barley the α -diversity was only slightly affected upon salt treatment.

The 'AB soil trained microbiome' used in our experiment resulted in root microbiomes in which *Pseudomonas* related ASVs were abundant. Collectively *Pseudomonas* sp. represented more than 30% relative abundance under all the conditions. However, the response to salt of these strains varied. For example, of the top-3 most abundant *Pseudomonas* strains, two responded positive and one negative to salt (Figure 5; Supplementary Figure 3). This is consistent with an earlier study, where *Pseudomonas* sp. was highly abundant in the root microbiome of *Medicago truncatula*, while individual strains responded differently to salt (Yaish *et al.*, 2016). This suggests occurrence of genetic variation in *Pseudomonas* in the capacity to colonize plant roots under high salt conditions.

Previous studies have shown that inoculation with individual bacterial strains, including *Pseudomonas* sp., can confer growth promotion to various crops under saline conditions (Cardinale *et al.*, 2015; Egamberdieva *et al.*, 2019). *Pseudomonas* strains have been shown to alleviate salt stress in a diverse range of species; including chickpea (Jatan *et al.*, 2019), cucumber (Egamberdieva *et al.*, 2011), cotton (Egamberdieva *et al.*, 2015), red pepper (Chatterjee *et al.*, 2017), soybean (Egamberdieva *et al.*, 2017), sunflower (Fatima & Arora,

2021), citrus (Vives-Peris *et al.*, 2018), arabidopsis (Chu *et al.*, 2019), mustard (Phour & Sindhu, 2020), and garlic (Zhuang *et al.*, 2021). However, it was also reported that a growth promoting *Pseudomonas* strain inoculated on the roots of barley did not result in a significant growth increase under salt conditions (Rahman *et al.*, 2018). This shows that plant growth promotion under saline conditions is dependent on the plant genotype and the bacterial inoculum. We showed that the 'AB soil trained microbiome' promoted plant growth especially at high salt, but we did not demonstrate which bacteria contributed to this response. To answer this question, it requires the isolation and testing of bacterial strains. Our study provides some indications which ASVs are potential candidates to be tested for growth promoting effects under high salt conditions. ASVs relatively abundant in a root-associated microbiome of both barley genotypes under all conditions represent such candidates (in bold in Table 6). These include *Pseudomonas* and *Agrobacterium*, genera of which species have previously been shown to confer salt tolerance to their host plants (Chatterjee *et al.*, 2017; Chu *et al.*, 2019; Egamberdieva *et al.*, 2019).

The growth of cv. Golden Promise was significant at 200 mM salt whereas barley landrace AB also showed a significant increase of growth at 0 and 100 mM. As the microbiomes of these two genotypes are more different at these concentrations, the landrace AB microbiomes could stimulate growth better. This might be the result of a better adaptation of landrace AB to the 'AB soil trained microbiome'. At 200 mM the microbiomes of the two genotypes became less different and could stimulate growth in both barley genotypes in a similar way. It is possible that growth stimulation of cv. Golden Promise at low salt concentration could be higher, when this cultivar would have been used to create a host-selected 'barley soil trained microbiome'.

In conclusion, we showed that salt stress reduced the dissimilarity of the root-associated microbiomes of two barley genotypes, which most probably is caused by a reduced plant genotype effect. This salt-induced decrease in microbiome dissimilarity is similar to what is observed with drought stress. However, in contrast to drought stress, the salt-induced decrease in microbiome dissimilarity didn't correlate with an increase of the relative abundance of Actinobacteria, but members of *Pseudomonas*. So, the reduction of plant genotype-dependent dissimilarity is not strictly correlated with Actinobacteria but can

Chapter 3

involve species from other genera. We postulate that the reduction of the plant genotype-dependent dissimilarity of the root-associated microbiomes is a more generic response to abiotic stress.

Materials & Methods

'Algerian barley soil trained microbiome' preparation

To create a soil with a microbiome that might stimulate growth of barley under saline conditions, we have made use of a soil of a saline field that in the past was a farmland on which several crops, including barley, had been cultured. Inappropriate irrigation practices in the past have led to a degraded land where crops could no longer effectively be grown there. During a few decades only some halophytes like *Zygophyllum* and *Imperata* grew in this field. The selected saline area (30°37'01.4"N 2°52'42.7"E) was located in the Université des Sciences et de la Technologie Houari Boumediene (USTHB) Research Experimental Field Station located in the El-Golea oasis, in the Sahara of Algeria, (Supplementary Figure 4). Soil from this station was saline (5.6dS/m \approx 56 mM NaCl), sandy and poor in nutrients, this is named 'starting soil'. El-Golea local landrace barley seeds, bought from the local market, were used as this landrace is probably well adapted to the local conditions. We named it Algerian barley landrace (AB). To enhance the microbiome in the starting soil, we cultivated the local landrace AB for two cycles. In the first cycle, landrace AB was grown on this starting soil for four weeks without additional salt. After harvesting barley, the resulting soil was collected and homogenized. One plot of 100*100*50 cm (for control plants) and three plots of 50*50*50 cm (for salt-treated plants) were created and covered with plastic and subsequently filled with this soil. Landrace AB was grown in these plots and irrigated with water. After one week of growth, plants were subjected to salt treatment by irrigation with a NaCl solution by which salt concentrations of about 50, 100 and 200 mM were created. Plants were grown for an additional three weeks. Two kilograms of soil were collected from each salt condition and stored at 4.0 °C for further use in experiments under controlled conditions. For the lab experiments, soils collected from the four different plots were mixed in equal amounts, this is named 'AB soil trained microbiome'.

Experiments under controlled conditions

Barley seeds were surface sterilized as follows: dry seeds were soaked in 4% commercial bleach for five min, then washed with sterile distilled water at least five times. Sterile

Chapter 3

seeds were placed in Petri dishes on wet sterile filter paper at 4.0 °C for 24 h and then moved to 28.0 °C for 24 h to germinate in the dark. Subsequently, they were exposed to light for 24 h at 28.0 °C. Five uniform size seedlings were planted into pots containing 1.5kg of soil composed of 90% sterile (Gamma irradiated) river sand and 10% of the 'AB soil trained microbiome'. The soil was saturated with Fårhæus nutrient solution (per liter: 0.12 g $\text{MgSO}_4 \cdot 7\text{H}_2\text{O}$, 0.1 g KH_2PO_4 , 0.15 g $\text{Na}_2\text{HPO}_4 \cdot 2\text{H}_2\text{O}$, 1 ml 15 mM Fe-citrate, 2.5 ml trace-elements B. Add after autoclaving: 0.75 ml 1 M Ca $(\text{NO}_3)_2$, 0.7 ml 1 M $\text{CaCl}_2 \cdot 2\text{H}_2\text{O}$ (Fårhæus, 1952). The Water Holding Capacity (WHC) of this soil is 150 ml water per 1 kg of soil. Plants were grown at 25.0 °C, 40% humidity and 16-h light/8-h dark photoperiod using a plant growth cabinet (Weiß Kast). Three times per week, the pots were weighed, and their water content was adjusted to 70% WHC, using sterile distilled water. Each time, the position of the pots was randomized in the growth cabinet. After two weeks plants were treated with salt. Prior to salt treatment, water was added to $\approx 70\%$ of WHC. Salt application was done as previously described (Awlia *et al.*, 2016).

To determine the concentrations of salt that we could use in an experiment in which we aimed to compare the root-associated microbiomes of the barley landrace AB and cv. Golden Promise, we first did a pilot experiment in which landrace AB was grown in a salt gradient. In short, pots with AB landrace plants were submerged for 30 mins in saline solutions of 0, 75, 150, 225, 300 and 375 mM NaCl and were let to drain. In this way the salt concentration became 0, 50, 100, 150, 200 and 250 mM NaCl increased when the WHC is back to 70%. This was maintained by adding distilled water for two weeks after which plant growth was scored by measuring the Fresh Shoot Weight (Supplementary Figure 5).

In a second experiment, barley cv. Golden Promise and AB landrace were grown using the same setup as described above. This cultivar was selected, because it can be transformed (Schreiber *et al.*, 2019; Schreiber *et al.*, 2020), which will facilitate future functional analyses. Salt concentrations were limited to 0, 100 and 200 mM NaCl. In all cases when plants were inoculated with 10% 'AB soil trained microbiome' the concentrations of NaCl were about 17.6 mM higher as the 'AB soil trained microbiome' contained about 176 mM NaCl (Supplementary Figure 6).

Collecting soil and harvesting plant materials

For both experiments, bulk and rhizosphere soil and roots were collected as described by Schneijderberg *et al.* (2020), which was based on Lundberg *et al.* (2012). Four biological replicates were made for each treatment by pooling five individual plants into one sample. Rhizosphere soil was collected by washing roots using sterile phosphate buffer (per liter: 6.33 g $\text{NaH}_2\text{PO}_4 \cdot \text{H}_2\text{O}$, 10.96 g $\text{Na}_2\text{HPO}_4 \cdot 2\text{H}_2\text{O}$ and 200 μL Silwet L-77) according to Schneijderberg *et al.* (2020). Subsequently, roots were cleaned by several washes with phosphate buffer until the washing solution remained clean and roots were placed in an ultrasonic water bath by alternating 30 s bursts followed by 30 s rest, for a total of 10 mins. Then they were dried on filter paper in the flow cabinet. Soil and root samples were frozen in liquid nitrogen and stored at -80°C till DNA isolation.

DNA extraction, Illumina meta-amplicon sequencing and data processing

DNA was isolated from bulk and rhizosphere soil using the Mo Bio PowerSoil® kit (Qiagen) and from the root (endophytic compartment) using the Fast DNA Spin® Kit for Soil (MP Biomedicals), following the manufacturer's instructions. DNA quality and quantity check were done by Thermo Scientific™ NanoDrop and 1% agarose gel electrophoresis, respectively. About 300ng per sample was sent to Beijing Institute of Genomics (BGI). The V4 region of the 16S rRNA gene was amplified and sequenced using 515F and 806R primers with an Illumina HiSeq 2500 sequencer as described by Illumina HiSeq System guidelines (Illumina 2020). Raw sequence data were processed using the DADA2 microbiome pipeline (Callahan *et al.*, 2016). As the complete dataset was composed of multiple sequencing runs, DADA2 was run separately on each one. For each sequencing run, raw reads were inspected (Supplementary Figure 7) cleaned with the '*filterAndTrim*' function from DADA2 with $\text{maxEE}=2$. Reads matching the phiX genome were also removed. The error rates were learned by randomly taking $1\text{e}8$ bases from all the samples (i.e. pools). These error profiles were used to infer ASVs by the *dada* function with default settings on the dereplicated sequences. The sequence tables from each run were merged together into one with the '*mergeSequenceTables*' function. Chimeras were then removed with the '*removeBimeraDenovo*' function from DADA2, using the "consensus" method.

Chapter 3

Finally, taxonomy was assigned with the '*assignTaxonomy*' function using the Green Genes database. In this way, we generated a table where each ASV is assigned to a unique number coupled to its taxonomical information at the genus level. For example, '6_*Pseudomonas*' means the ASV number 6 in the whole dataset belonging to the genus *Pseudomonas*. When an ASV is not assigned to any genus, it will have the mention 'unclassified' in addition to its known taxonomy at a higher rank than the genus level, for example: '1_*unclassified Pseudomonadaceae*'.

Microbiome analyses

All analyses were performed in the R environment (v.3.6.3). First, ASVs assigned to mitochondria and chloroplasts were removed. Then, ASVs with sequence lengths smaller than 253 or bigger than 254 bps were excluded. After this, data relating to our study were selected and named as "raw ASVs". The "raw ASVs" table was then filtered, and ASVs (which have more than 25 reads in at least five samples) were kept (46.2% of the total reads number) and named as "measurable ASVs", this corresponded to 42.6 M reads. The custom R commands were used in these analyses, mainly retrieved from the R packages *tidyr* (v.1.1.1), *reshape2* (v.1.4.4), *ggplot2* (v.3.3.2) and *agricolae* (v.1.3-5).

For the α - and β -diversity analyses, a subset of "measurable ASVs" table was generated, containing samples according to the research question. α -diversity was estimated by the evenness and richness. The richness was calculated using the '*Observed*' function in the *phyloseq* package (v.1.36.0) (McMurdie & Holmes, 2013) after rarefying the subset ASV table by the lowest read counts of samples (at least 36k reads), while the Shannon index was calculated by the '*Shannon*' function. We calculated the evenness of the same sample by its Shannon index and richness, following the equation: $\text{evenness} = \text{Shannon index} / \log(\text{richness})$. The data was assessed to meet the basic assumptions on the distribution of populations using the '*leveneTest*' function for homogeneity and '*shapiro.test*' for normality, then tested by ANOVA with Tukey HSD test for significant differences. Then, using the Bray-Curtis dissimilarity method, measures on the same rarefied ASV table, principal coordinate analysis (PCoA) was executed. This was largely done with the *vegan* package (v.2.5.6). Constrained Principal Coordinates Analysis (CPCoA) was performed

using the function '*capscale*'. Permutational Multivariate Analysis of Variance (PERMANOVA) and multiple pairwise PERMANOVA were performed using the functions '*adonis*' and '*pairwise.adonis*' respectively. To reduce the false discovery rate (FDR), we used the Benjamin-Hochberg method to adjust the *p*-values of pairwise comparisons.

For the indicator species analysis, differential abundance analysis and the bipartite network, we used a custom implementation of the scripts (Hartman *et al.*, 2018; Schnejderberg *et al.*, 2020). For the differential abundance test, we used a standard pipeline as implemented in the *metagenomeSeq* package (v.1.28.2) (Paulson *et al.*, 2013). We first used the default settings to create a normalized ASV table from the "raw ASVs". Then we used '*fitzig*' function and default settings in the *metagenomeSeq* package (v.1.28.2) to test ASVs differentially abundant between 100mM salt and 0mM, and 200mM and 0mM in RH and EC, respectively. For indicator species analysis, we employed correlation-based analysis to identify individual bacterial ASVs in barley root communities which abundances varied between the different salt levels using the *indicspecies* package (v.1.7.9) (De Cáceres *et al.*, 2010). The analysis was conducted with 999 permutations and considered significance at $p < 0.05$. Finally, we visualized the indicator ASVs associated with one or more of the salt levels by the bipartite networks, constructed using the Kamada-Kawai layout as implemented in the *igraph* package (v.1.2.6) (Csardi & Nepusz, 2006).

Chapter 3

Acknowledgements

This work was supported by Wageningen University & Research (WUR) – Netherlands and by the PNE scholarship (2019-2020) offered by the Algerian Ministry of Higher Education and Scientific Research (MESRS) - Algeria. We thank Dr. Wilma van Esse (WUR) for providing barley cv. Golden Promise seeds used in this study. We also acknowledge the support of the Research Experimental Field Station workers (El-Golea, Algeria) during the field trials as well as UniFarm staff for their help (Wageningen, the Netherlands).

Tables and legends:

Table 1. Pairwise PERMANOVA of the bacterial community changes in the roots of barley Algerian landrace (AB) under a gradient of salt levels.

Pairwise comparisons	Rhizosphere		Endophytic compartment	
	R ²	p.adjusted	R ²	p.adjusted
0 vs 50 mM	0.29	0.078	0.47	0.045
0 vs 100 mM	0.35	0.078	0.57	0.045
0 vs 150 mM	0.52	0.068	0.66	0.045
0 vs 200 mM	0.47	0.068	0.6	0.045
0 vs 250 mM	0.52	0.068	0.6	0.045
50 vs 100 mM	0.1	0.607	0.27	0.045
50 vs 150 mM	0.32	0.068	0.44	0.045
50 vs 200 mM	0.39	0.068	0.4	0.045
50 vs 250 mM	0.47	0.068	0.48	0.045
100 vs 150 mM	0.18	0.302	0.32	0.069
100 vs 200 mM	0.31	0.068	0.34	0.045
100 vs 250 mM	0.41	0.068	0.47	0.045
150 vs 200 mM	0.27	0.090	0.2	0.058
150 vs 250 mM	0.34	0.068	0.32	0.045
200 vs 250mM	0.14	0.528	0.19	0.229
P-value adjusted by the false discovery rate (FDR) method of Benjamin-Hochberg. Marked in bold: $p < 0.05$.				

Chapter 3

Table 2. Growth promotion of barley Algerian landrace AB and barley cv. Golden Promise by the 'Algerian barley soil trained microbiome'.

Plant genotype	Barley Algerian landrace			Barley cv. Golden Promise		
Salt level (mM NaCl)	0	100	200	0	100	200
FW-RS (g/plant)	0.442	0.352	0.324	0.716	0.585	0.354
FW-BS (g/plant)	0.69	0.655	0.591	0.916	0.7	0.698
Growth promotion (%)	56.11	86.08	82.41	27.93	19.66	97.18
FW-RS: mean fresh shoot weight per plant, grown on sterile river sand.						
FW-BS: mean shoot fresh weight per plant, grown on sterile river sand mixed with 10% 'Algerian barley soil trained microbiome'.						
Growth promotion: (BS-RS)/RS.						

Table 3. Growth difference of two barley genotypes in two soil types and three salt levels.

	Barley Algerian landrace AB						Barley cv. Golden Promise					
	RS			BS			RS			BS		
	0 mM	100 mM	200 mM	0 mM	100 mM	200 mM	0 mM	100 mM	200 mM	0 mM	100 mM	200 mM
Barley Algerian landrace AB	0 mM	0.09	0.12	-0.25	-0.21	-0.15	0 mM	0.03	0.36	-0.2	0.02	0.02
	RS 100 mM		0.03	-0.34	-0.3	-0.24	RS 100 mM		0.23	-0.033	-0.12	-0.11
	200 mM			-0.37	-0.33	-0.27	200 mM		-0.56	-0.35	-0.34	
	0 mM				0.04	0.1	0 mM			0.22	0.22	
	BS 100 mM					0.06	BS 100 mM					0
Barley Algerian landrace AB	200 mM						200 mM					
Value indicates the difference of mean fresh shoot weight per plant, of the treatment on the left versus that of the treatment on the top												
RS: barley on sterile river sand												
BS: barley on sterile river sand mixed with 10% barley soil												
Multiple T-tests are adjusted by Benjamini-Hochberg (BH)												
Marked in red: p < 0.05												

Chapter 3

Table 4. Pairwise PERMANOVA of the bacterial community changes in the roots of two barley genotypes under three salt levels.

Comparisons	Rhizosphere		Endophytic compartment	
	R ²	<i>p</i> .adjusted	R ²	<i>p</i> .adjusted
AB.0 vs AB.100	0.56	0.013	0.35	0.020
AB.0 vs AB.200	0.63	0.013	0.44	0.018
AB.0 vs GP.0	0.29	0.013	0.28	0.018
AB.0 vs GP.100	0.49	0.013	0.37	0.018
AB.0 vs GP.200	0.62	0.013	0.47	0.018
AB.100 vs AB.200	0.28	0.013	0.21	0.033
AB.100 vs GP.0	0.60	0.013	0.45	0.018
AB.100 vs GP.100	0.27	0.013	0.20	0.042
AB.100 vs GP.200	0.26	0.013	0.22	0.027
AB.200 vs GP.0	0.64	0.013	0.49	0.018
AB.200 vs GP.100	0.42	0.013	0.25	0.018
AB.200 vs GP.200	0.25	0.020	0.11	0.399
GP.0 vs GP.100	0.48	0.013	0.38	0.018
GP.0 vs GP.200	0.63	0.013	0.49	0.018
GP.100 vs GP.200	0.33	0.013	0.20	0.042
<p>Comparisons: abbreviation of the treatment is used as Genotype.Salt level.</p> <p>AB: barley Algerian landrace.</p> <p>GP: barley cv. Golden Promise.</p> <p><i>p</i> values, adjusted by the false discovery rate (FDR) method of Benjamin-Hochberg.</p> <p>Marked in bold: <i>p. adjusted</i><0.05.</p>				

Table 5. Number of ASVs enriched in saline condition in the roots of two barley genotypes.

Comparison	Rhizosphere						Endophytic compartment					
	Algerian barley landrace			Barley cv. Golden Promise			Algerian barley landrace			Barley cv. Golden Promise		
	unique	shared	total	unique	shared	total	unique	shared	total	unique	shared	total
100 mM vs 0	106	89	195	55	89	144	82	59	141	58	59	117
	54.36%	45.64%		38.19%	61.81%		58.16%	41.84%		49.57%	50.43%	
200 mM vs 0	91	128	219	73	128	201	77	97	174	72	97	169
	41.55%	58.45%		36.32%	63.68%		44.25%	55.75%		42.60%	57.40%	

Comparison: the relative abundance of ASV increased under saline condition (100 mM or 200 mM) in comparison to that under non-saline condition (0 mM)

unique: enriched ASVs only detected in one genotype

shared: enriched ASVs detected in both genotypes

Table 6. Indicator species analysis of ASVs with a high relative abundance in the roots of Algerian barley landrace AB and/or Barley cv. Golden Promise.

Plant genotype Compartment ASVs	Algerian barley landrace				Barley cv. Golden Promise			
	Rhizosphere	Endophytic compartment	Rhizosphere	Endophytic compartment	Rhizosphere	Endophytic compartment	Rhizosphere	Endophytic compartment
	Top 10	Cluster	Indicator	Top 10	Cluster	Indicator	Top 10	Cluster
U_Pseudomonadaceae 1	T	100-200	+	T	100	+	T	100-200
Pseudomonas 4	T	100	+	T			T	
Pseudomonas 6	T		-	T	0	-	T	
Flavobacterium 8	T			T			T	
Hydrogenophaga 11	T	100-200	+	T	100-200	+	T	200
Agrobacterium 17	T			T			T	
Cellvibrio 18	T	0	-	T	0	-	T	0
U_Cytophagaceae 22	T			T			T	
Agrobacterium 24	T			T			T	
Pseudomonas 29	T			T			T	
Agrobacterium 32	T			T			T	
U_Pseudomonadaceae 34	T			T			T	
Flavobacterium 36	T			T			T	
Pseudoxanthomonas 39	T			T			T	
Variovorax 48	T			T			T	
Achromobacter 49	T			T			T	
U_Chromatiaceae 50	T	200	+	T	0	-	T	0
U_Comamonadaceae 53	T		-	T			T	
U_Stenotrophomonas 58	T	0	-	T	0	-	T	0
U_Alteromonadaceae 66	T			T			T	
Dyadobacter 73	T	0	-	T			T	
Flavobacterium 78	T		-	T			T	
Janthinobacterium 83	T	0	-	T			T	
Halomonas 89	T	200	+	T	100-200	+	T	200
U_Flammeovirgaceae 90	T			T			T	
Pseudomonas 112	T			T			T	
Cellvibrio 134	T			T			T	
Rheinheimera 166	T	200	+	T	200	+	T	200
U_Flavobacteriaceae 195	T	200	+	T			T	
Pseudomonas 282	T			T			T	

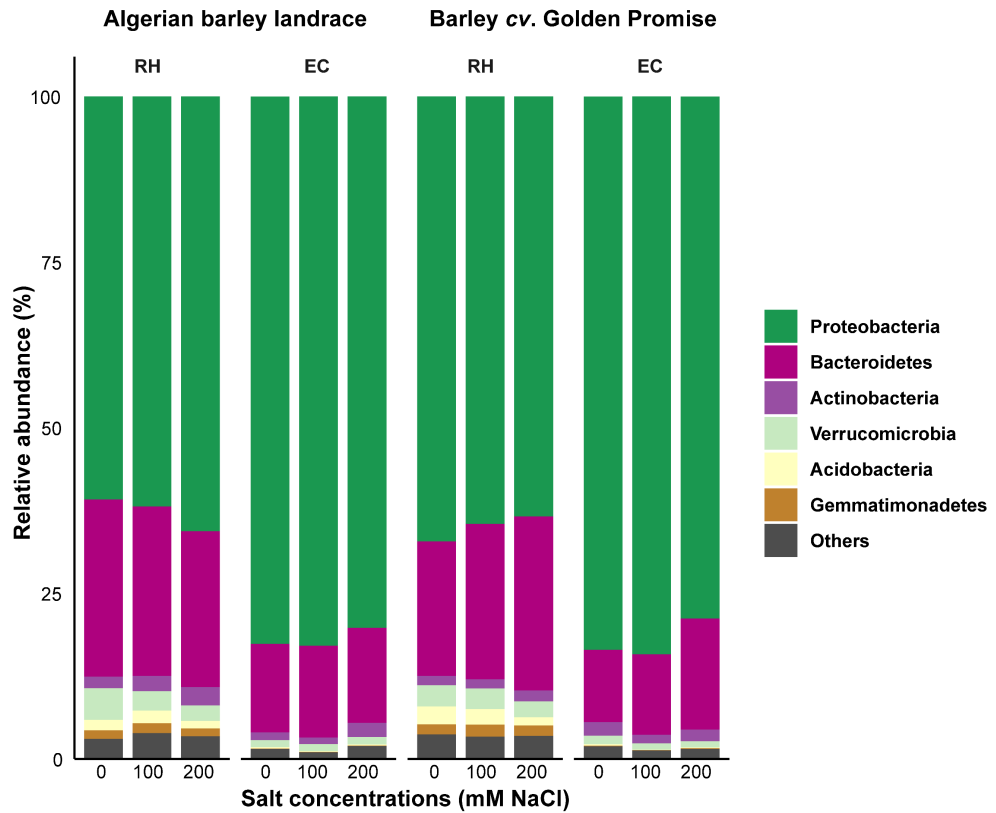
ASVs: information assigned in this study, including the taxonomic and number; the bold and underline ones are candidates for further functional study (see discussion)

Top10: ASVs belong to the 10 most abundant ASVs ("T")

Indicator: Identified indicator ASVs, grouped by positively responds to salt ("+") or negatively responds to salt (" - ")

Cluster: Indicator ASVs correlate with one or two salt concentrations

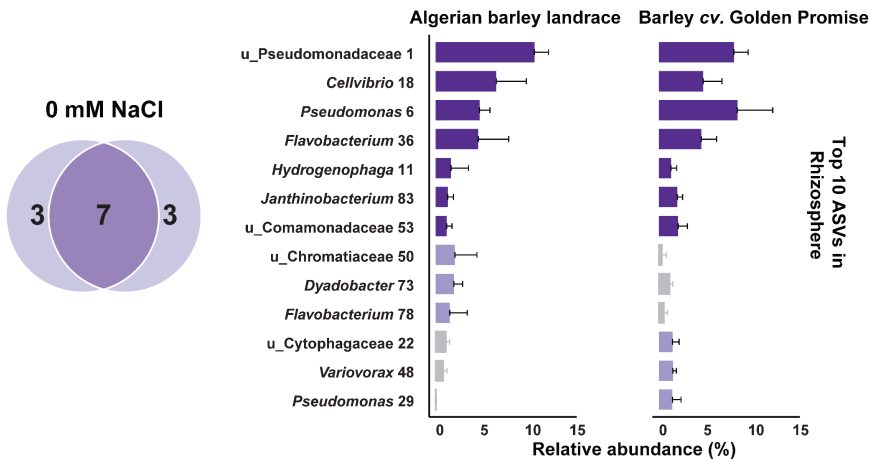
Supplementary information:



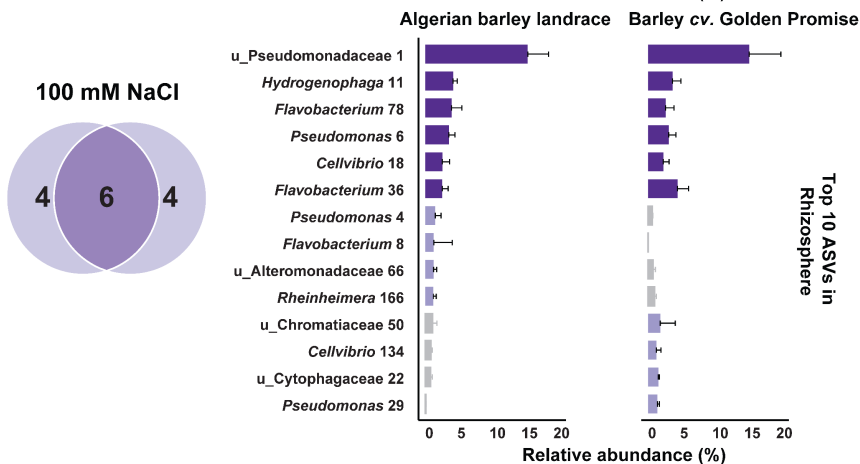
Supplementary Figure 1. Bacterial phyla distribution in the roots of Algerian barley landrace AB and cv. Golden Promise grown at 0, 100, and 200 mM NaCl. Bacterial phyla with low abundances ($\leq 1\%$) are referred to as 'Others'. RH: rhizosphere, EC: Endophytic compartment.

Chapter 3

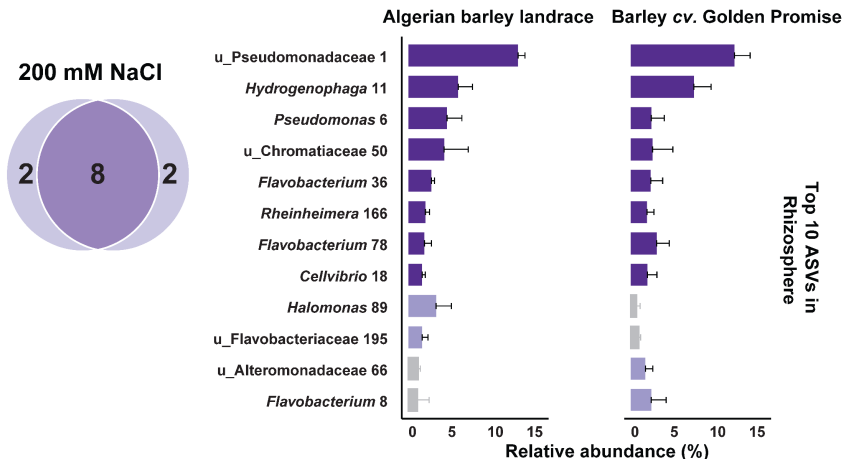
a



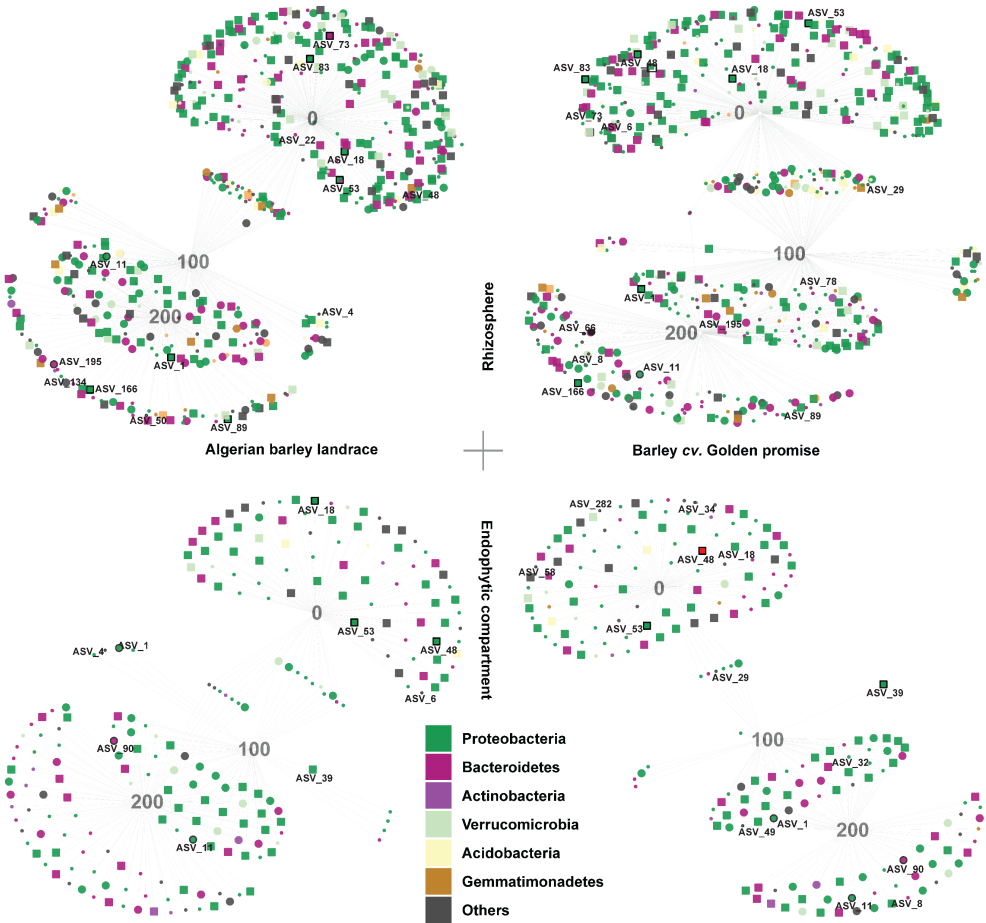
b



c



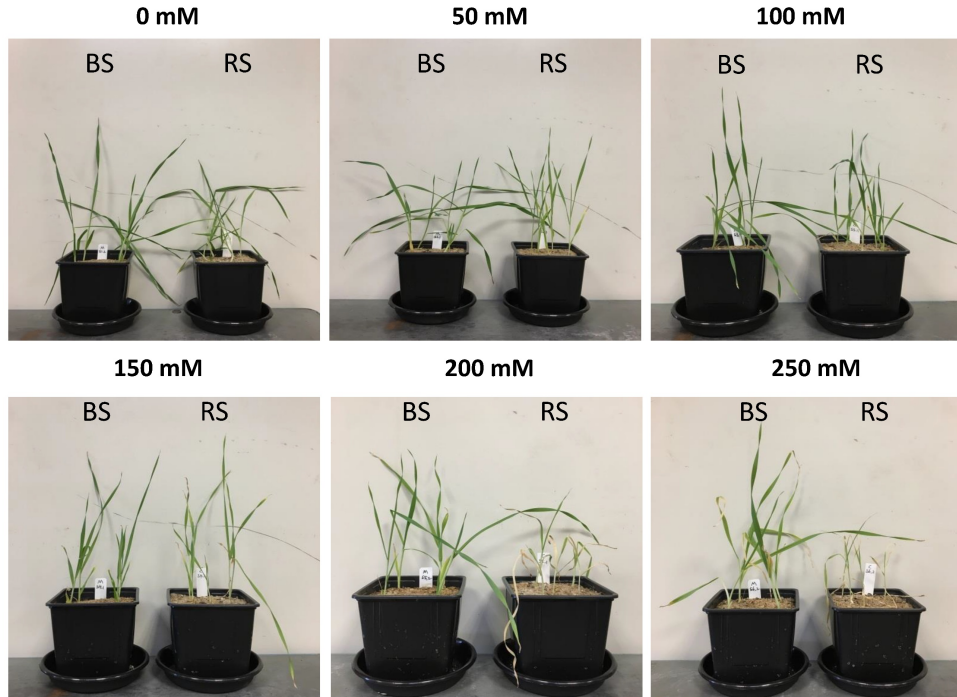
Supplementary Figure 2. Salt cluster specific ASVs in the roots of Algerian barley landrace AB and cv. Golden Promise. Bipartite networks visualizing ASVs positively and significantly ($p < 0.05$) correlate with salt cluster, i.e. a single or two salt concentrations (0, 100, 200 mM NaCl), in the rhizosphere and endophytic compartment of two barley genotypes, as identified by indicator species analysis. Indicator ASVs are coloured according to their phylum association. Squares and circles represent that ASVs of both genotypes are indicator ASVs. Squares are in the same cluster, i.e. ASVs correlate with same salt concentration(s), whereas circles are not. Dots are indicator ASVs that are genotype unique. Exact numbers of indicator ASVs are listed in Supplementary Table 2. A black bold frame surrounding the indicator ASV means that it is a “highly abundant” ASV.



Supplementary Figure 3. Abundant ASVs in the rhizosphere of two barley genotypes become similar upon salt application. Ten most abundant ASVs (top-10) in the rhizosphere of Algerian barley landrace AB and cv. Golden Promise for three salt levels (0, 100, and 200 mM NaCl). On the left, Venn diagram with the number of shared and unique top-10 ASVs between both barley genotypes. On the right, Y-axis of the bar chart shows taxonomic information and the ASV number assigned in this study. X-axis shows the mean relative abundance of ASVs in the rhizosphere of the genotype. The top-10 ASVs are coloured (purple or pink). ASVs shared by both genotypes are given in purple and the non-shared top-10 ASVs are given in pink. Not top-10 ASVs of the genotype are given in grey. ASVs were ordered by their relative abundance in the rhizosphere of Algerian barley landrace AB.



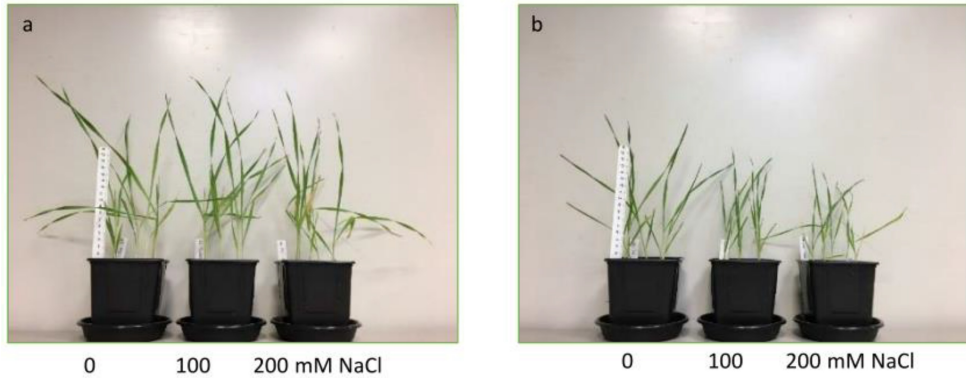
Supplementary Figure 4: Field location of used 'Algerian barley soil trained microbiome'.
The GPS coordinates of the El-Golea Research Experimental Field Station in Algeria;
30°37'01.4"N 2°52'42.7"E (Figure made with google maps).



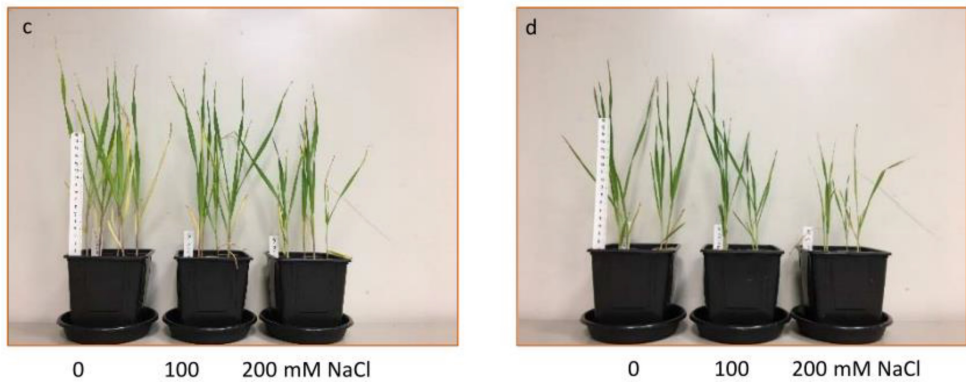
Supplementary Figure 5: Growth of Algerian barley landrace AB on a gradient of salt: 0, 50, 100, 150, 200 & 250 mM NaCl. Photographs were captured two weeks post salt treatment. BS: sterile river sand mixed with 10% of 'Algerian barley soil trained microbiome', RS: sterile river sand.

High salt reduces microbiomes' dissimilarities

Algerian barley landrace



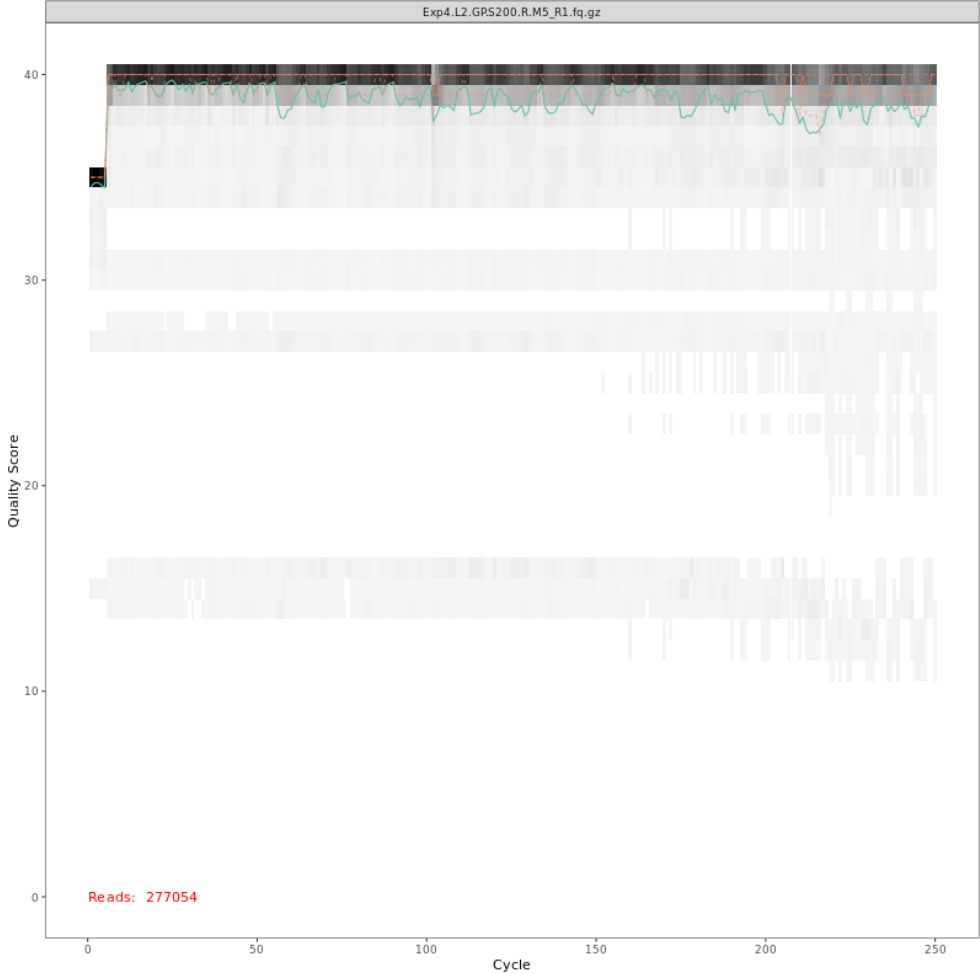
Barley cv. Golden promise



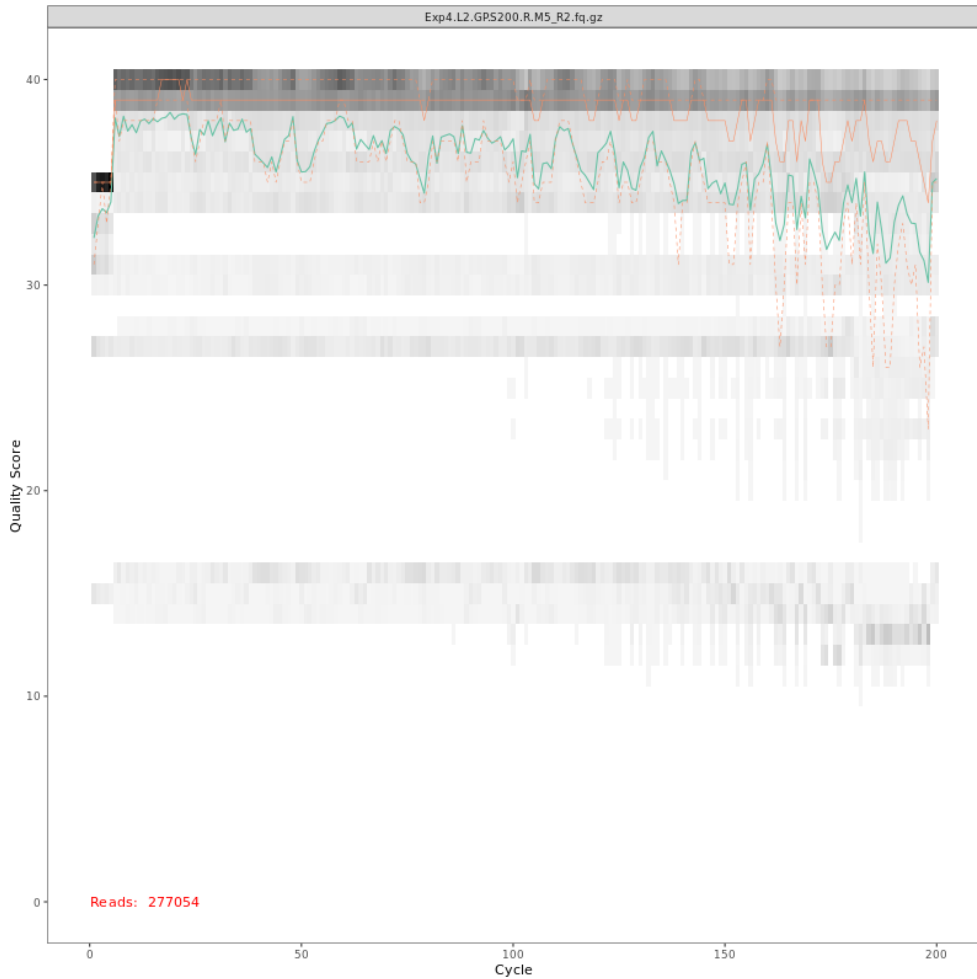
Supplementary Figure 6: Growth of Algerian barley landrace AB and cv. Golden Promise grown on a gradient of salt: 0, 100 & 200 mM NaCl. Photographs were captured two weeks post salt treatment. **(a & c)** Barley grown in the sterile river sand mixed with 10% of 'Algerian barley soil trained microbiome'. **(b & d)** Barley grown in the sterile river sand.

Chapter 3

a.



b.



Supplementary Figure 7: FASTQ read quality scores after filtering, (a) forward, (b) reverse. The read quality scores of a sample are shown as an example. The solid green and orange lines show the mean and median quality score at that position of the read. The dashed orange lines are the 25th and 75th quantiles. Plots were drawn with the DADA2 function `plotQualityProfile` with the default settings.

Chapter 3

Supplementary Table 1. Number of indicator ASVs identified in the roots of barley Algerian landrace AB and cv. Golden Promise.

Compartment	Rhizosphere		Endophytic compartment	
Plant genotype	AB	GP	AB	GP
Indicator ASVs	533	621	217	204
Total ASVs	1360	1372	889	919
Percentage of indicator ASVs	39,20%	45,30%	24,40%	22,40%
AB: barley Algerian landrace. GP: barley cv. Golden Promise.				

Supplementary Table 2. Properties of indicator ASVs correlated with salt cluster in the roots of two barley genotypes.

Plant genotype	Salt cluster (mM NaCl)	Rhizosphere				Endophytic compartment			
		Dots	Circles	Squares	sum	Dots	Circles	Squares	sum
Algerian barley landrace	0	92	25	166	283	34	1	46	81
	100	14	9	8	31	7	1	1	9
	200	28	11	24	63	38	11	14	63
	0-100	26	8	7	41	7	3	0	10
	0-200	0	1	0	1	6	1	0	7
	100-200	27	44	43	114	10	17	20	47
	sum	187	98	248	533	102	34	81	217
Barley cv. Golden Promise.	0	98	4	166	268	55	3	46	104
	100	16	7	8	31	4	1	1	6
	200	53	45	24	122	12	17	14	43
	0-100	41	26	7	74	5	1	0	6
	0-200	2	0	0	2	0	0	0	0
	100-200	65	16	43	124	13	12	20	45
	sum	275	98	248	621	89	34	81	204

Dots: indicator ASVs that are genotype unique
Circles: indicator ASVs that are indentified from both genotypes but correlated with different salt cluster
Squares: indicator ASVs that are indentified from both genotypes and correlated with same salt cluster

Chapter 4

Longevity correlates with similar composition of root-associated bacterial microbiomes in a chrono-series of Chinese chestnut

Xu Cheng^{1,2,6,†}, Zhichun Yan^{2,†}, Qian Li¹, Lucas Schmitz², Jundi Yan^{2,3}, Yueyang Ge^{2,3}, Yanping Lan⁴, Yaceng Zhao⁵, Yiyang Wang³, Guangdong Li³, Yang Liu³, Martinus Schneijderberg², Liu Yang³, Huihui Bian^{1,3}, Aalt D J van Dijk⁵, Ling Qin^{1,3}, Qingqin Cao^{1,3,*} and Ton Bisseling^{1,2,*}

¹ Beijing Advanced Innovation Center for Tree Breeding by Molecular Design, Beijing University of Agriculture, Beinong Rd. #7, Beijing 102206, China

² Laboratory of Molecular Biology, Wageningen University, Droevendaalsesteeg 1, 6708PB Wageningen, The Netherlands

³ Beijing Key Laboratory of New Technology and Agricultural Application, College of Plant Science and Technology, Beijing University of Agriculture, Beinong Rd. #7, Beijing 102206, China

⁴ Beijing Academy of Forestry and Pomology Sciences, Beijing 100093, China

⁵ Bioinformatics Group, Wageningen University and Research, Wageningen, The Netherlands

⁶ Shenzhen Branch, Guangdong Laboratory for Lingnan Modern Agriculture, Genome Analysis Laboratory of the Ministry of Agriculture, Agricultural Genomics Institute at Shenzhen, Chinese Academy of Agricultural Sciences, Shenzhen, China

[†] These authors contributed equally to the manuscript.

* Corresponding authors: ton.bisseling@wur.nl; caoqingqin@bua.edu.cn

Chapter 4

Summary

- Certain tree species can reach ages of centuries, whereas lifespan of species like apple are markedly shorter. The latter is caused by negative plant-soil feedback that results in microbiome changes. We hypothesized that tree species capable of a long lifespan will be able to avoid such negative feedback and their root-associated microbiomes will be similar in trees of different ages.
- To test this, we used a chrono-series of Chinese chestnut (*Castanea mollissima*) trees, ranging from 8 to 830 years old, from a Ming orchard at the Great Wall. Their root-associated microbiomes were analysed by using illumina meta-amplicon sequencing analysis.
- We showed that their root-associated bacterial microbiomes are rather similar although based on the linear regression models we cannot exclude that age has a weak correlation with the composition of root-associated microbiomes. When chestnut seedlings were grown in soil associated with young and old chestnut trees and control soil for 3 months, the chestnut plants were healthy and their growth was similar. This strongly supported that negative feedback had not occurred. A member of core microbiome *Pseudomonas* OTU1 that represents more than 50% of the rhizosphere community strongly inhibited growth of chestnut pathogens and stimulated plant growth.
- Such properties of the microbiome, in combination with a high number of resistance genes can contribute to longevity of chestnut.

Key words: Chinese chestnut, chrono-series, Ming orchard, plant-soil feedback, *Pseudomonas*, root-associated microbiome, tree longevity

Introduction

Longevity of plant species can vary markedly. For example, some annuals can have a lifespan of only several weeks, whereas perennials can live for decades or even centuries. Especially some tree species can become very old and reach ages of hundreds or even thousands of years (Branch, 1999). This implies that mechanisms must be in place by which these plant species with a long lifespan can cope with rapidly evolving pathogens, as well as with mutations that will accumulate in their stem cells upon division (Burian *et al.*, 2016).

Although trees have in general a longer lifespan than herbaceous perennials, there is a remarkable difference in longevity between tree species. Trees like, for example, oak, chestnut and ginkgo can become hundreds of years and some pine species even thousands of years (Branch, 1999; Plomion *et al.*, 2018). In contrast, several fruit trees, for example, apple and peach, in general only reach ages of decades. The latter is caused by negative plant-soil feedback by which root/soil microbiomes change (Winkelmann *et al.*, 2019). We hypothesise that tree species that can have a long lifespan will be able to avoid such negative plant-soil feedback and as a consequence their root-associated microbiomes will be similar in trees of different ages. However, to our knowledge this has never been studied. Here we tested this hypothesis in a chrono-series of Chinese chestnut (*Castanea mollissima*). This series included trees ranging from several years to centuries of age and they are located in an orchard at the Great Wall.

Longevity of trees is most likely controlled at several levels. To keep the number of mutations that accumulate in their stem cells rather low, the mitotic activity in the apical meristem appears to be reduced (Ljubuncic & Reznick, 2009; Burian *et al.*, 2016; Plomion *et al.*, 2018). Short living plants cope with their rapidly evolving pathogens by diversifying selection of their resistance genes like, for example, the nucleotide-binding site leucine-rich repeat (NBS-LRR) resistance gene family. However, long living perennials, like trees, have to defend themselves against these rapidly evolving pathogens with a static number of resistance genes. In part they can cope with such rapidly evolving pathogens, because in general they have a higher number of resistance genes than short living annuals. For

Chapter 4

example, oak and Chinese chestnut have about 1000 and 700 NBS-LRR genes, respectively (Plomion *et al.*, 2018; Xing *et al.*, 2019), whereas in most short living annuals this family has 50-200 members (Meyers *et al.*, 2003). Apple has a relatively high number of resistance genes, for example, ~1000 NBS-LRRs (Jia *et al.*, 2015). However, its life expectancy is in general only some decades, so markedly shorter than that of, for example, oak and chestnut. It is due to the soil legacy causing the apple replant disease. The definition of this disease is, according to Winkelmann *et al.* (2019), a disturbed physiological reaction of newly planted apple plants to soils that have altered (micro-)biomes due to negative plant soil feedback during previous apple cultures. This causes a markedly reduced production or death of the trees and has left a legacy of biotic nature in the soil causing apple replant disease. It can develop in a few decades. For example, a study in an orchard in Beijing showed that within 30 years a microbiome causing apple replant disease had developed (Sun *et al.*, 2014). Microbiome changes occur, for example, in the bacterial, fungal and oomycete communities. However, which organisms cause the replant disease is not known (Balbín-Suárez *et al.*, 2020). Other Rosacea species, like peach, cherry and strawberry can develop a similar replant disease, but the negative effect on growth is species/genus specific (Bent *et al.*, 2009; Zhao *et al.*, 2009; Si *et al.*, 2017). So, the relative short lifespan and apple replant disease are not due to a low number of resistance genes, but it is caused by negative feedback between plant and soil which affects the composition of the (micro)biome of soil (Mazzola & Manici, 2012; Winkelmann *et al.*, 2019).

Plants sustain thousands of microorganisms around and inside their roots. These microbiomes are of major importance for plant growth and can contribute to tolerance to biotic stresses (Mendes *et al.*, 2013). The composition of bacterial communities in the rhizosphere, the thin layer of soil that is in direct contact with the root, and the endophytic compartment is to some extent determined by the plant genotype (Berg, G. & Smalla, K., 2009). We hypothesise that the root-associated microbiomes of individuals of a tree species that range in age from decades to centuries, will be rather similar and they will contain microorganisms that can protect the trees against its major pathogens and/or stimulate growth. To test this hypothesis, we made use both culture independent and

Longevity correlates with similar root microbiomes

culture dependent methods to analyse the bacterial root-associated microbiomes of Chinese chestnut trees from an orchard at the Huanghuacheng Lakeside Great Wall in China.

The Wall at this site was built during the Ming dynasty and started in A.D. 1404 under the command of Emperor Yongle (Zhu Di). It aimed to strengthen defence against tribes from the north. The oldest trees at this orchard are even older than the current Great Wall at this site. The chestnut orchard provided food for the military people that were active at this Great Wall. The Great Wall has remained functional as a defence barrier till 1644. Further, the region in which this ancient orchard is located had developed into an important production area for chestnut. This can explain why this orchard has been maintained for centuries. This orchard is unique as it contains a broad chrono-series of trees up to more than 800 years old. In nature very old chestnut trees are rare, among others by competition with other species. This is an orchard with a single species, in this case chestnut. In this respect it is similar to apple orchards, so the growth conditions are similar to orchards in which replanting disease would happen. This makes it most suited to test our hypothesis, as effects caused by other tree species are avoided.

In this study, we used chestnut trees ranging from 8 to 830 years old and Illumina meta-amplicon sequencing analysis showed that their root-associated bacterial microbiomes are rather similar, although based on the linear regression models we cannot exclude that age has a weak correlation with the composition of root-associated microbiomes. Further, soils in which these chestnut trees were growing had no negative effect on the growth of replanted seedlings, showing that negative feedback had not occurred. Concerning the occurrence of bacteria with antagonistic activity we showed that a *Pseudomonas* OTU, that can represent more than 50% of the rhizosphere community, strongly inhibited growth of chestnut pathogens and stimulated plant growth.

Chapter 4

Materials and Methods

Samples collection

The Chinese chestnut orchard that dates from the Ming dynasty locates at the Huanghuacheng Lakeside Great Wall (Beijing, China), which at this site was built during the Ming dynasty. This Orchard has trees of various ages ranging from centuries to tens of years and the oldest tree in this orchard is more than 800 years old. The canopies of the old trees, with ages ranging from 3 to 8 centuries, have a similar size. From each tree, fine roots were sampled from 20-30cm in depth (surface soil were removed), where located just below the edge of the canopy. Soil was collected at a similar location and depth, but in a part where chestnut roots were not present. All samples were collected in around 4 replicates. A young tree was also sampled from the chestnut research station that is nearby this orchard. Detailed sample information has been described in **Table S1**.

Tree age determination

The age of the trees was determined in 2011 by analyzing dendrochronology. To do so, firstly, position an increment borer at 1.3 meters high above the ground. Then, drill a 5 mm hole through the pith and collect a sample that contains tree-rings. At last, age of the tree is determined by measuring tree-ring width using LINTAB™ Series 6 (Germany).

Soil, rhizosphere and endophytic compartment harvesting

The soil that was sticking tightly to the roots was defined as rhizosphere soil (RH). The harvesting protocol closely followed the procedures described previously with minor modifications (Lundberg *et al.*, 2012; Schneijderberg *et al.*, 2020). Detailed procedures are described as following: roots including the rhizosphere soil was put into a 50 ml Falcon tube containing 25 ml phosphate buffer (PB, per litre: 6.33 g $\text{NaH}_2\text{PO}_4 \cdot \text{H}_2\text{O}$, 10.96 g $\text{Na}_2\text{HPO}_4 \cdot 2\text{H}_2\text{O}$ and 200 μl Silwet L-77) and vortexed for 15 seconds. The root was transferred to a new Falcon tube containing PB, and briefly vortexed. This procedure was repeated twice, until the PB stayed clear. Roots were sonicated for 10 mins (with a 30 seconds pause in every minute). After vortexing briefly, clean roots were defined as the endophytic compartment (EC) samples and were placed on filter paper for drying. In the

Longevity correlates with similar root microbiomes

meanwhile, wash-offs after the first vortexing were filtered through a 100 µm cell strainer (Falcon) and spun down for 10 minutes at 4000x g. Supernatant was quickly poured off, and the pellet was transferred to a 2 ml tube. The additional liquid residues were removed and these were defined as the RH samples. Soil (SO) samples were washed in the PB buffer and were collected in the same way as the RH samples. SO, RH and EC samples were then weighed, frozen in liquid nitrogen and stored at -80 °C.

DNA isolation and 16S rRNA gene amplicon sequencing

DNA from SO and RH samples was isolated using the MoBio PowerSoil kit (Qiagen) according to manufacturer's instructions. From EC samples, DNA was isolated using Fast DNA Spin Kit for Soil (MP Biomedicals). Quality and quantity of the DNA was checked by nanodrop and gel electrophoresis. Around 300ng DNA per sample was sent for meta-amplicon sequencing at Beijing Genomics Institute (BGI). Using primers 515F and 806R, the V4 region of the 16S rRNA gene was sequenced by using the HiSeq2500 PE250 sequencing platform (Illumina).

Processing of the sequencing data

Paired-end reads were merged into contigs using the RDP (Ribosomal Database Project) extension to PANDASeq (Masella *et al.*, 2012), named Assembler (Cole *et al.*, 2014) with a minimum overlap of 50 bp, Phred score of 25, and contig length of 100 bp. Contigs were converted to fasta format using the fastx-toolkit and combined in a single file. Then, contigs were clustered into operational taxonomic units (OTUs) according to the UPARSE pipeline (Edgar, 2013) implemented in VSEARCH 1.1.3 (Rognes *et al.*, 2016). In short, the pipeline consisted of de-replication, sorting by abundance and discarding singletons before clustering them into OTUs using the UPARSE algorithm (Edgar, 2013), discarding chimeric sequences using the UCHIME algorithm (Edgar *et al.*, 2011) and mapping contigs to the OTUs using the usearch_global algorithm. The resulting OTU table was then converted into BIOM format using QIIME 1.9.1 (Caporaso *et al.*, 2010). Finally, we added taxonomic information for each OTU based on the GreenGenes database release 13_8 97% (Caporaso *et al.*, 2010) using the RDP classifier 2.10.1 (Cole *et al.*, 2014). All processing steps were implemented in a SnakeMake workflow (Köster & Rahmann, 2012).

Chapter 4

Microbiome analyses

All analyses were performed in the R environment (v.3.6.3). First, OTUs related to mitochondrial and chloroplast sequences were removed and it was named as “raw OTUs”. Next, the OTUs that have more than 25 reads in at least 5 samples were kept and they were named as “measurable OTUs” for further analysis.

For the α - and β -diversity analyses, a subset of "measurable OTUs" table was generated, containing samples according to the research question. α -diversity was estimated by the Shannon index which was calculated using the ‘Shannon’ function in the *phyloseq* package (v.1.36.0). The relationship between tree age and Shannon index has been tested with the linear regression model (**Table S2**). Then, using the Bray-Curtis dissimilarity method, measures on the same rarefied OTU table, principal coordinate analysis (PCoA) was executed. This was largely done with the *vegan* package (v.2.5.6). Permutational Multivariate Analysis of Variance (PERMANOVA) was performed using the functions ‘adonis’. The occurrence of increasing delta tree age patterns in all 3 compartments has been tested using the linear regression between the dissimilarity of bacterial communities (Bray-Curtis) and the tree age differences (Marasco *et al.*, 2018) (**Table S3 & 4**).

To compare the taxonomic composition between different compartments of all trees, read counts based on Phylum, Family, Genus and OTU level were assessed separately. For the Phylum, Family and Genus level distribution, all the reads were aggregated according to different phyla, families and genera, respectively. The “Others” category was created to include low abundance taxonomies which did not reach at least 5% in any one compartment (Wagner *et al.*, 2016).

For the OTU level analysis, a core microbiome was identified based on the following two criteria: First, OTUs in the RH or EC that were enriched compared to the bulk soil, were identified. This was done from the trees with at least three replicates in each compartment (i.e. the trees with age 10, 440 in 2016 and 10, 372, 440, 620, 830 in 2017). The significance ($p < 0.05$) of enrichment was determined by the Dunnett’s test using “measurable OTUs” table. Second, the enrichment of an OTU should occur in at least 70% of the samples of the RH or EC (Xu, J *et al.*, 2018). The custom R commands were used in

Longevity correlates with similar root microbiomes

this analysis, mainly retrieved from the R packages *tidyverse* (v.1.3.0) and *reshape2* (v.1.4.3).

Plant soil feedback assay

To test whether the soils associated with chestnut trees for a long time will cause negative feedback to chestnut growth, we collected soil around a young tree (10 years old) and two old trees (372 and 620 years old) as well as soil from an open field never cultivated with chestnut trees that was defined as the control. Chestnut seeds were pre-germinated and planted in each soil. Chestnut seedlings were cultivated in a greenhouse for more than 3 months. Plant height was measured. Leaves were randomly selected (0.5 g) from 10 seedlings grown in each soil and cut into 2 mm slices. Chlorophyll was extracted from leaf samples by using acetone and absorption was measured at 663 nm and 645 nm (Richardson *et al.*, 2002).

Bacteria isolation and OTU correlation analysis

To isolate strains belonging to the *Pseudomonas* OTU1 from the rhizosphere of chestnut trees grown in the orchard for centuries. Serial dilutions of the rhizosphere glycerol stocks obtained from the 440 years old trees were plated on 1/10th strength TSA (1/10th TSA) and King's B agar media. Plates were incubated at 28 °C for 7 days. According to the morphologies, approximately 90 independent colonies were picked and re-streaked on 1/10th TSA plates. Colonies were re-streaked on fresh 1/10th TSA plates once more to ensure purity. Fresh colonies were used for identification. The isolate collection was replicated and 16S rRNA genes were amplified by using the primers 63F 5'-CAGGCCTAACACATGCAAGTC-3' and 1389R 5'-ACGGGCGGTGTGTACAAG-3' (Hongoh *et al.*, 2003). PCR products were sequenced Sanger sequencing at Macrogen (Amsterdam, Netherlands). All 16S rRNA sequences were processed with Geneious 8.1.9 (<https://www.geneious.com>) and submitted to RDP database for taxonomic identification. *Pseudomonas* Isolates were selected for correlation analysis with meta-amplicon data. The V4 region of their 16S rRNA gene sequences were extracted and aligned with consensus sequences of all OTUs. Isolates with the V4 region matching OTU1 with more than 97% identity were kept and further aligned with raw reads of OTU1. Isolates with the V4 region

Chapter 4

that 100% identical to any raw reads of OTU1 were kept for strain level analysis by using BOX-PCR with primer BOXA1R 5'-CTACGGCAAGGCGACGCTGACG-3' (Rademaker, 1997). By comparing genetic profiling of these isolates, repetitive strains were removed and 11 different *Pseudomonas* strains belonging to OTU1 were then obtained. Glycerol stocks were prepared and stored at -20 °C and -80 °C.

Genome assembly

Genomes were sequenced at BGI, using the Illumina HiSeq2500 PE150 platform with paired end reads and a 350 bp insert size. Reads were cleaned with Trimmomatic v. 0.35 (Bolger *et al.*, 2014) by using a sliding window approach that trimmed bases below a PHRED quality score of 28. Next, reads were assembled using SPAdes v. 3.9.0 (Bankevich *et al.*, 2012) with default parameters and contigs smaller than 1,000bp were removed. Assembly quality was assessed with QUAST which included BUSCO gene detection as an indicator of genome completion (Gurevich *et al.*, 2013). These results can be found in Table S5.

Phylogeny of *Pseudomonas* strains

A *Pseudomonas* strain collection was selected from a study published by Jun *et al.* (2016). In this paper, a tree was reconstructed based on an average amino acid identity (AAI) score of reciprocal conserved protein-coding sequences between genome pairs. Genomes were clustered if they shared at least a 95% AAI. For our purposes, we selected one representative from each cluster which had a completed genome available on NCBI. These were downloaded from RefSeq in December 2018. Additionally, the *Populus*- and *Castanea*-associated isolates from the above and present study, respectively, were also included. One tree was inferred based on a multiple sequence alignment of the AMPHORA genes. HMMs were used to identify the 32 single-copy genes with the HMMER suite. The nucleotide sequences were individually aligned with Clustal Omega and trimmed with Gblocks to remove poorly aligned bases in the flanking regions of the conserved domains. The genes were concatenated to create a multiple sequence alignment from which a maximum likelihood tree was reconstructed using FastTree with a general time reversible model of DNA evolution. Another tree was inferred based on a multiple protein sequence

Longevity correlates with similar root microbiomes

alignment of shared single copy orthologues. Single copy orthologues (n=711) were identified with OrthoFinder which were further filtered based on a chi-square test. Only orthologues without sequences deviating significantly (p-value > 0.05) from the overall composition (n=468) were considered. The aligned protein sequences were concatenated into a multiple sequence alignment from which a maximum likelihood tree was reconstructed using IQ-TREE. The tool ModelFinder, included in IQ-TREE, was used to find the best-fit partition model for the multi-gene alignment by only considering the invariable site and Gamma rate heterogeneity. IQ-TREE reconstructed the tree under the best-fit partition model using *Cellvibrio Japonicus* Ueda107 as the out-group (Jun *et al.*, 2016; Hesse *et al.*, 2018). The AMPHORA and single copy orthologues trees resembled each other in their topology. Trees were visualized and annotated with the Python ETE3 library.

Genome Annotation and Functional Diversity Inference

To determine functional similarity between genomes, we predicted Open Reading Frames (ORFs) with Prodigal. These putative coding domain sequences were annotated with the KEGG orthology (KO) database (Bai *et al.*, 2015). Hidden Markov Models (HMMs) (Eddy, 1998) of the KO groups were used to assign homology to each ORF with hmmsearch from the HMMER suite. The threshold for homology was set at an E-value below 1.0×10^{-4} and a coverage of at least 90%. In case of multiple hits, the best scoring KO group was preferred. Subsequently, a binary matrix for the presence/absence of each KO group per genome was generated. This presence/absence matrix was projected into a 2D space using Singular Value Decomposition as a PCA plot with the Python scikit-learn library (Schneijderberg *et al.*, 2018).

Phenotypic traits of *Pseudomonas* strains

Several phenotypic traits of the 11 *Pseudomonas* strains isolated from chestnut rhizosphere (strains CM1-11) were tested in this study and the protocols closely followed the procedures described previously (Cheng *et al.*, 2013). For the siderophore detection, strains were grown in KB broth overnight at 28 °C. Cells were washed twice with KB broth and the cell density was set to an OD600 of 1.0. 5 µl cell suspension was spotted on a CAS

Chapter 4

agar plate (Schwyn & Neilands, 1987). After 48 h of incubation at 28 °C, siderophore production was visualized by a color change of the CAS medium from blue to orange (Hartney *et al.*, 2011). For the P-solubilization test, strains CM1-CM11 were spot inoculated to the National Botanical Research Institute's phosphate growth medium (NBRIP) contained per liter: glucose, 10 g; $\text{Ca}_3(\text{PO}_4)_2$, 5 g; $\text{MgCl}_2 \cdot 6\text{H}_2\text{O}$, 5 g; $\text{MgSO}_4 \cdot 7\text{H}_2\text{O}$, 0.25 g; KCl, 0.2 g and $(\text{NH}_4)_2\text{SO}_4$, 0.1 g. A clear halo around the colonies indicates the P-solubilization ability (Nautiyal, 1999). The antagonistic activities of these strains were tested as follows: strains CM1-CM11 were grown in 5 ml KB broth overnight at 28°C. 2 µl bacterial suspension ($\text{OD}_{600} = 1.0$) was spotted on a 1/5th strength PDA plate near the edges of the plate. After 24 h of incubation at 28 °C, a mycelial plug of 4-mm diameter of pathogenic strains *Cryphonectria parasitica* and *Phytophthora cinnamon* was placed in the center of the 1/5th PDA plate and incubated at their appropriate temperature. Radial hyphal growth was monitored for several days depending on the pathogen's growth (Trifonova *et al.*, 2009; Cheng *et al.*, 2013).

Plant assays

Pseudomonas sp. CM11 strain was grown in 5 ml KB broth at 28 °C, 200 rpm for 12 hours. Bacterial cells were washed and resuspended with 10 mM MgSO_4 . Bacterial suspension was adjusted to $\text{OD}_{600} = 1.0$ ($\sim 10^9$ cfu/ml). Chestnut seeds were pre-germinated and planted in potting soil. 50 ml bacterial suspension was inoculated to each seedling and 10 days later, the second time inoculation was performed. Chestnut seedlings were cultivation in greenhouse condition for 45 days. Leaf area, chlorophyll content, and fresh weight of shoot and root were measured. Leaves of 8 seedlings per treatments were imaged and leaf area was measured by using the Intelligent Leaf Area Meter (Model: YMJ-C). A destructive method was used for Chlorophyll content measurement. Leaves were randomly selected (0.5 g) from 8 seedlings per treatments and cut into 2 mm slices. Chlorophyll was extracted from leaf samples by using acetone and absorption, and was measured at 663 nm and 645 nm (Richardson *et al.*, 2002). Chlorophyll a and b concentrations (mg/g fresh weight) were then calculated by using the equations (Arnon, 1949):

Longevity correlates with similar root microbiomes

$$\text{Chlorophyll a} = (12.7 * A_{663} - 2.697 * A_{645}) * V / 1000W$$

$$\text{Chlorophyll b} = (22.77 * A_{645} - 4.687 * A_{663}) * V / 1000W$$

(A₆₆₃: absorbance at 663 nm; A₆₄₅: absorbance at 645 nm; V: volume of extracting solvent; W: fresh weight of leaf materials)

Seeds of *Arabidopsis thaliana* Columbia-0 (*Arabidopsis*) were surface sterilized by washing with ethanol and soaking in ¼ bleach for 10 minutes. Seeds were transferred on water-saturated filter paper in petri dishes. After incubating at 4°C for 3 days, 8 seeds were sown on plates containing 50ml 1/2th Murashige Skoog (MS) medium. Plates were transferred and positioned vertically in a growth chamber under a long-day photoperiod (16 h of light, relative humidity 60%) at 22 °C. In *in vitro* assay, 2 µl bacterial suspension (10⁹ cfu/ml) was applied to the root tips of one-week-old seedlings. Control plants were inoculated with 2 µl of 10 mM MgSO₄ (van de Mortel *et al.*, 2012; Cheng *et al.*, 2017). In the soil assay, one-week-old seedlings were transferred to 60 ml PVC pots carrying: vermiculite-soil mixture (2:1 v/v) that was autoclaved twice for 20 min at 120 °C with a 24 h interval. After transplanting, 50 ml bacterial suspension (10⁶ cfu/ml) was inoculated to each seedling (one seedling per soil pot). Seedlings treated with the same amount of 10 mM MgSO₄ were the controls. For both experiments, *Arabidopsis* was cultivated under the same conditions and 11 days after inoculation with bacterial suspension, fresh weight of shoot and root was quantified.

Chapter 4

Results

A chrono-series of chestnut trees ranging from 8 years to 8 centuries

To select a chrono-series of chestnut trees, we made use of the Great Wall orchard (**Fig. S1**). The age of the old trees at this orchard was determined in 2011 by dendrochronology (see Materials and Methods). For the younger trees, it was recorded when they were planted. In addition to the orchard, we also collected samples from some young trees at the chestnut research station which is located in the vicinity of the orchard. In this way, we could select a chrono-series with the oldest tree being more than 800 years (**Table S1**). The canopies of the old trees, with ages ranging from 8 years to 8 centuries, have a similar size, due to pruning. Young roots primarily grow in the soil directly below the edge of the canopy. This implies that these young roots grow in soil where plant-soil feedback has taken place for centuries.

The bacterial community composition of a young and three old chestnut trees are similar

In 2016, we did a small-scale experiment by harvesting bulk soil (SO), rhizosphere (RH) and endophytic compartment (EC) of 3 old trees (372, 440 and 620 years) in the orchard and one young tree (~10 years) at the chestnut research station. From each tree, fine roots were collected from 3 positions (referred to as replicates) which were 20-30 cm deep and located just below the edge of the canopy. Soil was collected at a similar location and depth, but in a part where chestnut roots were not detected. We focussed on the bacterial communities, as analysis of fungal communities would have been difficult due to the massive presence of ectomycorrhiza. We analysed the bacterial community by 16S rRNA gene V4 region meta-amplicon sequencing using a HiSeq2500 platform (Illumina). Operational Taxonomic Units (OTUs) were identified by a 97% identity threshold of sequences (Lundberg *et al.*, 2012; Schneijderberg *et al.*, 2020), and filtering produced 3161 “measurable” OTUs. This also included the samples of the second experiment (see below) and together we collected 111 samples.

Longevity correlates with similar root microbiomes

We first determined the relative abundance of major bacterial phyla in the SO, RH and EC, respectively, of the young and old trees. The majority of the OTUs were distributed across eight dominant phyla, and these contained approximately 80-90% of the reads of all compartments (Fig. 1a). The phylum distribution of the 3 old trees and the young tree were very similar, where OTUs belonging to Proteobacteria were dominant in both EC and RH, and Actinobacteria OTUs were dominant in EC. We observed taxonomic shifts from soil to the root-associated compartments, by comparing relative abundance of the major phyla (Supplementary file 1). In the RH community, Proteobacteria was enriched, whereas Acidobacteria, Chloroflexi and Verrucomicrobia were markedly reduced. In the EC community, the relative abundance of Actinobacteria was increased, whereas that of Bacteroidetes and Acidobacteria was reduced.

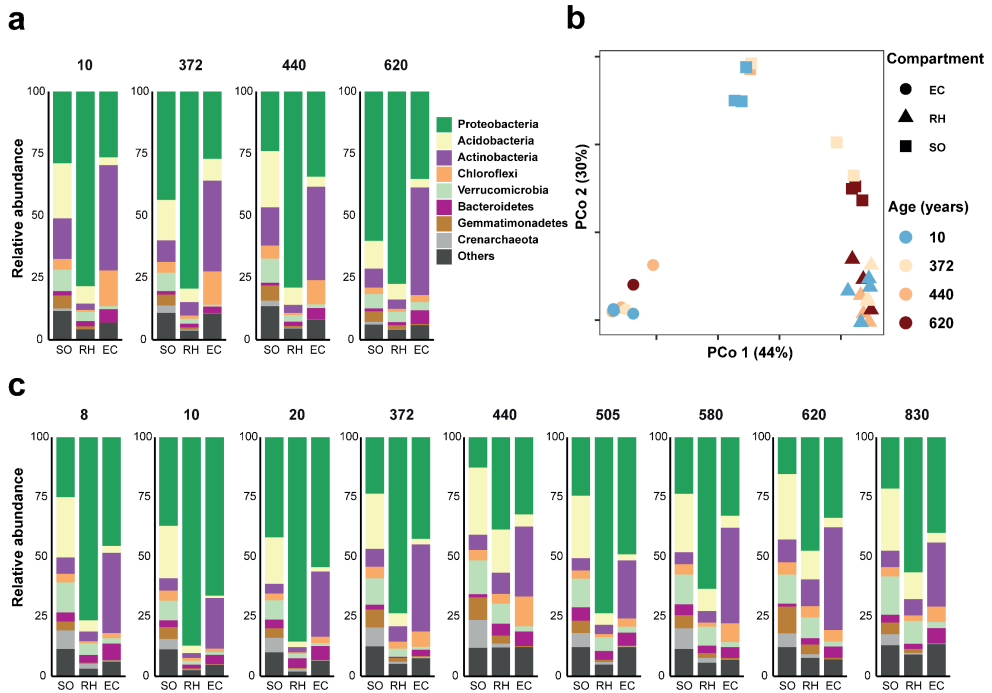


Fig. 1: The plant compartment drives the composition of the bacterial communities. a, c, The relative abundance of the dominant (more than 5% of the total reads in at least one compartment) phyla are shown for the soil (SO), rhizosphere (RH) and endophytic compartment (EC) samples harvested in 2016 (a) and 2017 (c); **b,** Principal Coordinates

Chapter 4

Analysis (PCoA) of samples harvested in 2016. Samples of 2016 were harvested from 1 young tree (~10 years old) and 3 old trees (372, 440 and 620 years). In 2017, the same trees were sampled as well as 2 additional young trees (8 and 20 years) and 3 additional old trees (505, 580 and 830 years).

To compare the microbiomes at the community level, we used the Bray-Curtis dissimilarity measure on rarefied OTUs. We plotted SO, RH, and EC samples along the first two principal coordinates (PCo), which explained 44% (PCo 1) and 30% (PCo 2) of the variance, respectively (**Fig. 1b**). Especially the microbiomes of the RHs as well as ECs of the 3 old trees and the young tree clustered very well. SO microbiomes were distinct from the microbiomes of the RH and EC, but formed two sub clusters. The two SO clusters were formed due to the uneven distribution of OTU1 (see below). When OTU1 was excluded and PCoA was repeated, then SO samples formed one cluster (**Fig. S2a**). RH and EC communities were well separated along the PCo 1 and the RH samples of the old and young trees clustered well together. This was also the case for the EC samples. This suggests that chestnut shaped very different bacterial communities in and around the root. However, their composition seemed not or only slightly to depend on tree age. To test to what extent the compartment and tree age, respectively, would influence the bacterial community, Permutational Multivariate Analysis of Variance (PERMANOVA) was performed. It showed that the impact of the compartment is the largest ($p < 0.05$) and forms 64% of the variance (**Table S6**). The difference between bacterial communities of different tree ages was significant, albeit tree age explains only 6.4% of variance (**Table S6**). This suggests that the tree age has a small impact on the community composition.

The age of chestnut trees within a chrono-series has only a small impact on the distribution of OTUs at a high taxonomic level

We repeated the analyses in August 2017 by analyzing the same trees as in 2016 as well as 2 additional young trees and 3 additional old trees (**Table S1**). In this way, we could study a more complete chrono-series. We first determined the relative abundance of bacterial phyla (**Fig. 1c**). The taxonomic shifts from soil to the root-associated microbiomes were analyzed in the same way as in 2016. Phylum distribution showed that compared to the

Longevity correlates with similar root microbiomes

SO microbiome, the relative abundance of Proteobacteria was enriched, whereas that of Acidobacteria, Verrucomicrobia, Gemmatimonadetes and Crenarchaeota was reduced in the RH (**Supplementary file 1**). In the EC community, the relative abundance of Proteobacteria and Actinobacteria was increased, and that of Bacteroidetes and Acidobacteria was reduced. The phylum distribution within the microbiomes of these trees within the chrono-series was very similar (**Fig. 1c**). This shows that the tree age has only a small impact on the phylum distribution.

We then determined the effect of tree age on the distribution of OTUs at lower taxonomic levels and this was done for the samples collected in 2016 as well as 2017. At the family level, we found 137 classified families in total. 136 of them were detected in the soil, and 135 and 132 of them occurred in RH and EC, respectively (**Fig. S3**). This shows that the vast majority of the members of the root microbiomes originated from soil, suggesting that horizontal transfer contributes most to the composition of the microbiomes. Also, at the genus and OTU level, this major contribution of horizontal transfer was visible. Vertical transfer was also shown as OTU1201, member of Thermaceae, only occurred in EC (**Fig. S3**).

Three families had a relative abundance of at least 5% in RH or EC and they occurred in all trees. Their relative abundance is presented in **Fig. 2** and it shows that Pseudomonadaceae was the most dominant family in RH with a relative abundance that can reach over 60%. Micromonosporaceae and Streptomyetaceae were dominant in EC, where they generally occupied 5% and 10% of reads, respectively. At the genus level, *Pseudomonas* was the only classified genus with at least 5% in RH and occurred in all trees. The relative abundance of *Pseudomonas* was similar to that of Pseudomonadaceae in the trees, suggesting that especially the genus *Pseudomonas* contributed to the dominance of Pseudomonadaceae (**Fig. S4**).

In most cases the relative abundance of these taxa are rather similar. However, in some trees the relative abundances differed markedly. For example, the relative abundance of Streptomyetaceae in EC was far below the average in the 372-year-old tree in 2016 and

Chapter 4

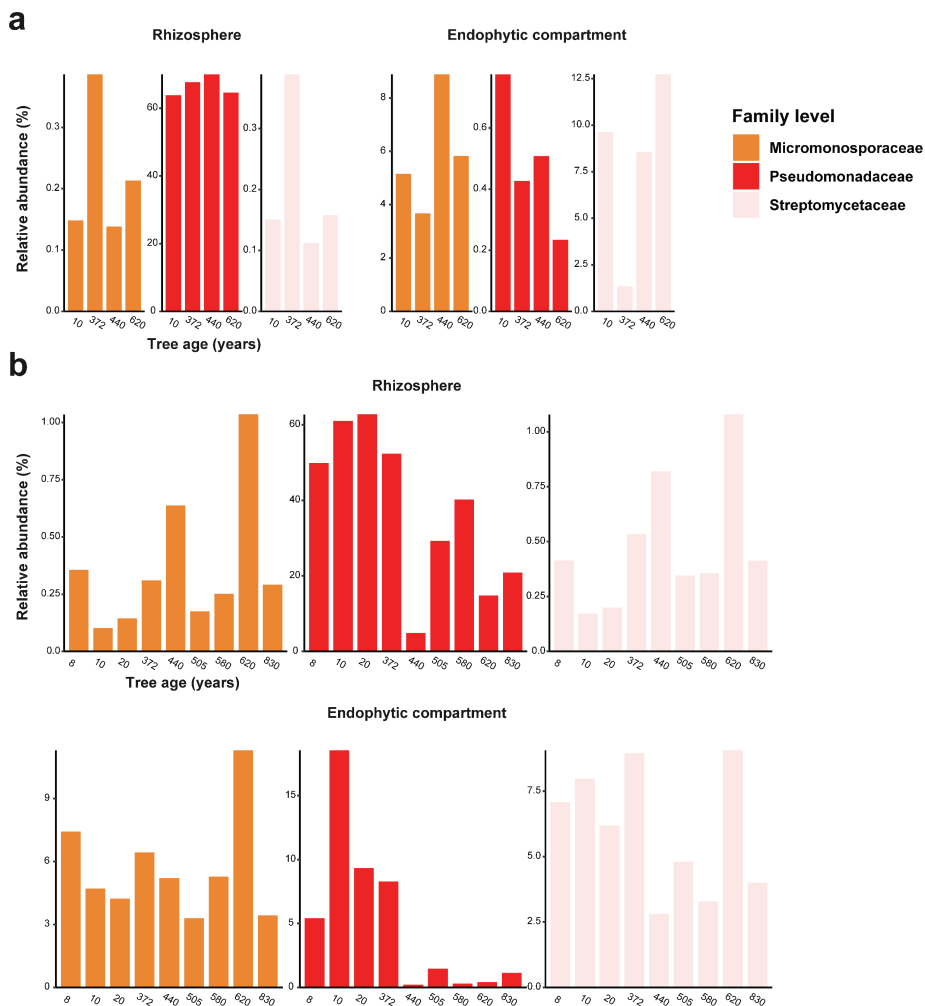


Fig. 2: Occurrence of dominant classified families in RH & EC. Three dominant classified families were identified with a relative abundance of at least 5% in RH or EC. Their occurrence in RH and EC were showed in all trees sampled in 2016 (a) and 2017 (b).

this was the same for Pseudomonadaceae in RH of the 440-year-old tree in 2017 (Fig. 2). However, these variations were present in one year but absent in the other year. The relative abundance of Pseudomonadaceae was higher in the EC of trees collected in 2017 than in 2016. In 2017, its relative abundances varied between trees of different ages. It was markedly higher in the 8 to 372-year-old trees, than in the older trees (Fig. 2). Also in this case, this difference did not occur for the trees also collected in 2016 as the relative

Longevity correlates with similar root microbiomes

abundance of Pseudomonadaceae in the 440- and 620-year-old tree was similar to that of the younger ones. We expect that the sampling year dependent variation might be due to some variation in the microenvironment that is more critical in one of the two years (for example, water availability).

So the distribution of these dominant taxa, especially at the higher taxonomic level, is similar in chestnut trees within the chrono-series. At a lower taxonomic level, some trees, for certain families/genera, showed an aberrant relative abundance, but this seems more correlated with sampling year than age of the tree.

The alpha diversity of root associated bacterial microbiomes in the chestnut trees are similar although the alpha diversity has a weak correlation with tree age

To investigate the alpha diversity of the root associated bacterial communities in the chestnut trees of the chrono-series, the Shannon diversity index (H) was calculated. We plotted the results along tree age, and this was done for all samples collected at both years and for each compartment (**Fig. 3**). The H index was in general higher in the SO than that in the RH and EC. But within each compartment, the H index was rather similar for the different trees. Analysis of Variance (ANOVA) has been performed to test the effect of sampling year and tree age, respectively, on the H index in three compartments (**Table S7**). It showed that sampling year has a significant influence in all three compartments. The differences in H index of trees of different ages were small. However, these differences were significant in SO and RH but not in EC. The sampling year appeared to have a big impact on the H index of old trees, especially in RH. This is due to the difference in the relative abundance of OTU1 in RH and SO of both years, as if OTU1 was excluded, the H index of trees collected in both years is similar (**Fig. S5**).

To investigate whether the small differences of H index between trees with different ages correlated with tree age, we tested the relationship of the H index of the trees and their age with linear regression. Models indicated positive correlations between the H index and tree age in RH ($R^2 = 0.195$, $p = 0.0026$) and EC ($R^2 = 0.095$, $p = 0.048$), but not for SO (**Table S2**). However, the small R^2 values suggested that models do not fit well with the actual data points. So the correlations determined by the models were very weak.

Chapter 4

Nevertheless, in case the models were correct, the changes would develop very slowly, as the regression coefficients of models of RH and EC were extremely small (2.1×10^{-3} and 5.1×10^{-4} , respectively). This means the H index increased with a speed of around 6%/century (0.208/century) in RH and 0.2%/century (0.005/century) in EC. So the alpha diversity of their root-associated bacterial microbiomes is rather similar, although the linear regression models do not exclude that the tree age has a very weak correlation with the alpha diversity of the root-associated microbiomes.

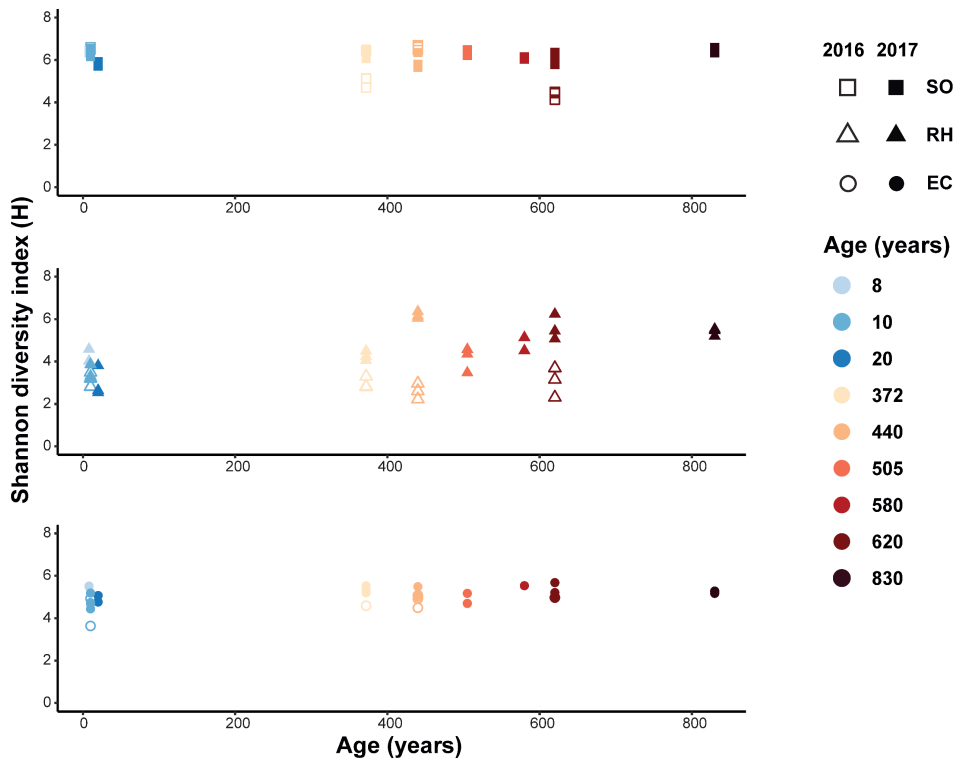


Fig. 3: Root-associated bacterial alpha diversities of a chrono-series chestnut trees are rather similar. Relationships between bacterial alpha diversities (Shannon diversity index) in each compartment (SO, RH and EC) of trees sampled in 2016 (empty symbols) and 2017 (solid symbols). Each symbol indicates the Shannon diversity index value of one sample (Y-axis) with correlated tree age (X-axis).

PCoA shows that sampling year has a larger effect on the composition of RH microbiome than tree age

Our analysis at family and genus level showed there can be some variation between trees and this seems to depend on the sampling year. To study in more detail the effect of the sampling year on the root-associated bacterial community composition, we performed PCoA by plotting SO, RH and EC samples of the 10, 372, 440 and 620 year-old trees, which were collected in both 2016 and 2017 (**Fig. 4a**). It showed that samples of different compartments clustered along PCo1 (27% of variance), suggesting that the plant compartment is the main driver of bacterial community composition. Along PCo2 (22% of variance), samples, especially of RH, were clearly separated by the sampling year, whereas the separation along PCo2 is markedly less for the EC samples. This suggests that for the RH samples, the effect of sampling year is larger than that of tree age on microbiome composition. The effect of the sampling year on the composition of the EC microbiome seems markedly less than in RH (**Table S8**). Furthermore, the difference in relative abundance of OTU1 markedly contributed to the variance caused by of sampling year, as PCoA after excluding OTU1 showed that samples of the two years are closer (**Fig. 4b**) than that in the PCoA including OTU1 (**Fig. 4a**).

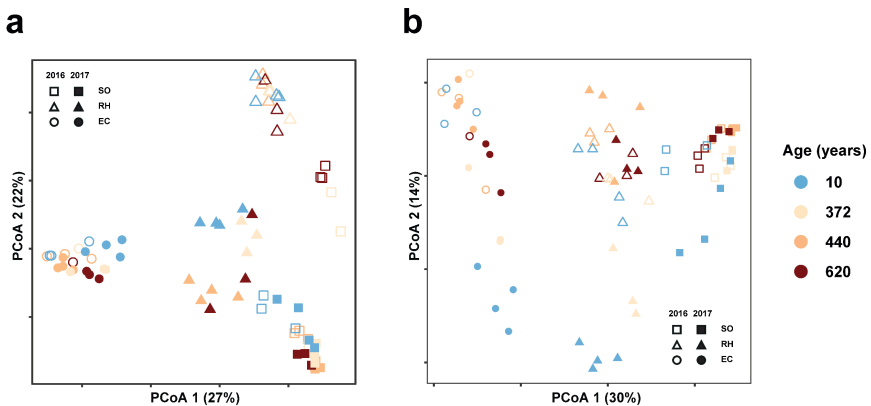


Fig. 4: Sampling year has a larger effect on the composition of RH microbiome than tree age. PCoA of samples from 4 trees, i.e. 1 young tree (~10 years old) and 3 old trees (372, 440 and 620 years), collected in both 2016 (empty symbols) and 2017 (solid symbols) (a) and the same analysis was shown by excluding the OTU1 from the communities (b).

Chapter 4

PCoA shows that root-associated bacterial microbiomes of a chrono-series of chestnut trees are similar although their composition has a weak correlation with tree age

To investigate how tree age influenced the bacterial community composition, we made use of the samples of all chestnut trees collected in 2016 and 2017. The first two principal coordinates of PCoA explained 27% (PCo 1) and 20% (PCo 2) of the variance, respectively (**Fig. 5a**). The EC samples of the young and old trees clustered well together. This was also the case for the SO samples, except for the samples of 2016 with the high relative abundance of OTU1. It suggests that the microbiome communities of trees with different ages are similar in these two compartments. All RH samples clustered well along PCo 1. However, the samples of 2017 spread along PCo 2, whereas the RH samples of 2016 had a similar ordinate. From this PCoA it is unclear whether there is a correlation between the microbiome composition of RH and tree age.

To quantify the putative compositional changes of microbiomes of SO, RH and EC when trees become older, we plotted the relationships between community dissimilarities (Bray-Curtis) and age differences, obtained by pair-wise comparisons of all individual samples (**Fig. 5b**). For example, the age difference between the 8 and 830-year-old trees was 822, and the average community dissimilarity between these two trees was 0.451 in SO, 0.563 in RH and 0.58 in EC (**Table S3**). The community dissimilarities among the replicates were analysed as well by pair-wise comparison of replicates of each tree (age difference of “0”). If the small microbiome composition differences would depend on tree age, we would expect that a bigger tree age difference correlated with a larger community dissimilarity. Further, community dissimilarities between trees of different ages should be larger than those among replicates. In fact, the differences in community dissimilarities between trees of different ages, as well as those among replicates were small (**Fig. 5b**).

To statistically analyse whether these small differences depend on tree age, linear regression was performed to quantify the relationship between the community dissimilarities and tree age differences in three compartments, respectively (**Fig. S6**). Models indicated a positive correlation between the community dissimilarity and tree age difference ($p < 0.01$). However, the R^2 values are very small (0.03, 0.013, 0.028,

Longevity correlates with similar root microbiomes

respectively), indicating that the models do not fit well with the actual data points. So the correlation determined by the models are very weak. Nevertheless, assuming the models are correct, the changes due to increasing tree age develop very slowly as the regression coefficients of the models are small (7.5×10^{-5} , 8.9×10^{-5} , 8.2×10^{-5} , respectively) (**Table S4**). This would imply that in 100 years the dissimilarity values would increase only 1.48% in SO (0.507 to 0.5145), 1.55% in RH (0.574 to 0.5829) and 1.44% in the EC (0.569 to 0.5772).

Taken together, we have shown that the phylum distribution was similar in chestnut trees within a chrono-series. The analysis of the relative abundance of dominant families and genera shows similarities, but also in some trees sampling year correlated with variation. However, the clustering of compartments of different trees in the PCoAs shows that the overall composition of the root-associated microbiomes, especially that of EC, still are similar. Further, although the linear regression models do not exclude that increasing tree age does affect the composition of the root-associated microbiomes, the effect was with a very slow speed. Therefore, the overall composition of root-associated microbiomes was similar among these chestnut trees with age difference of 8 centuries', albeit with small changes. Next, we decided to test whether such small changes (including what was observed on the relative abundance at family and genus level) might in part be due to negative plant-soil feedback.

Growth of chestnut for centuries has not resulted in negative plant soil feedback

When growth of chestnut has resulted in negative plant-soil feedback, this will cause a reduced growth when seedlings are planted in such soil, whereas growth will not be affected in the absence of such negative feedback. To test whether growth for centuries did result in negative plant-soil feedback, a plant assay was performed by growing chestnut seedlings in soils collected from young and old trees. We collected soil around a young tree (10 years old) and two old trees (372 and 620 years old) as well as soil from an open field that was defined as the control. In case negative feedback would have occurred, chestnut seedlings planted in such soil would grow less than in control soil. Chestnut seedlings were planted in each above-mentioned soil. After three months of

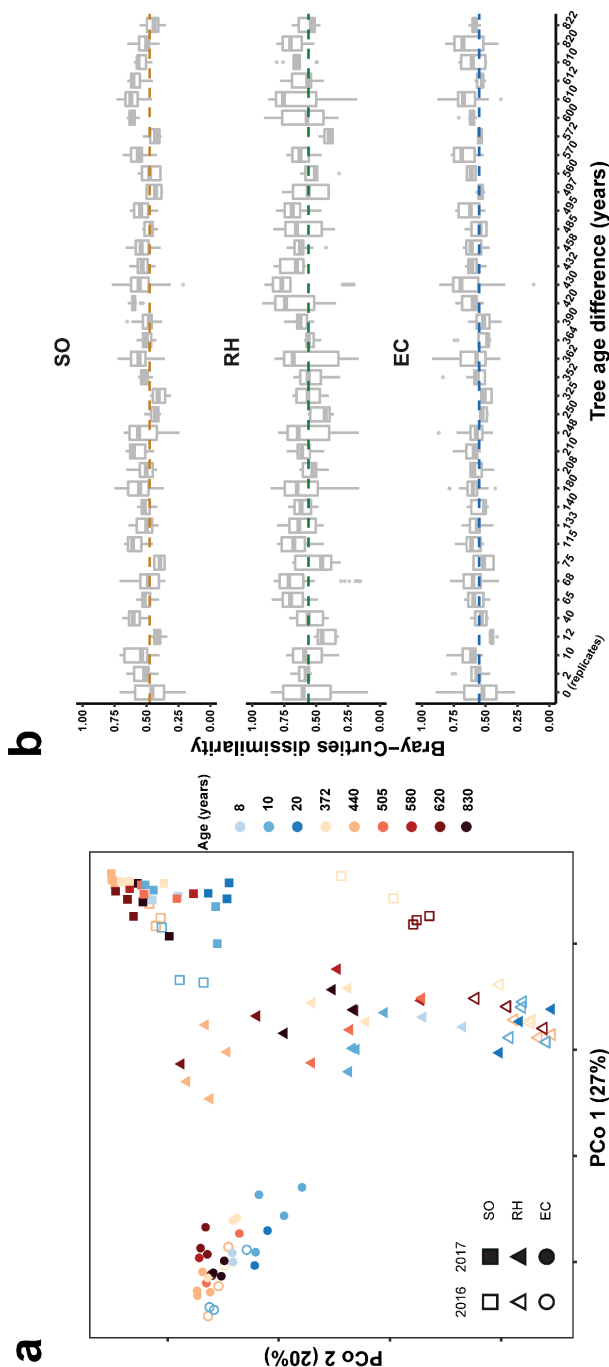


Fig. 5: Root associated bacterial community composition of a chrono-series chestnut trees are rather similar. Three young trees (8, 10 and 20 years) and six old trees (372, 440, 505, 580, 620 and 830 years) were sampled in 2016 and 2017. a, PCoA of SO, RH and EC samples of trees harvested in 2016 (empty symbols) and 2017 (solid symbols); b, By pair-wise comparisons of samples collected in three compartments, respectively, the relationships between the bacterial community dissimilarities (Bray-Curtis) and corresponding tree age differences of each pair were shown by a boxplot. Box of “0” tree age difference represents the dissimilarities between replicates of each tree. Horizontal dash lines are added to show the mean dissimilarity values of pair-wise comparisons of replicates.

growth, the chestnut plants were very similar (**Fig. S7**). Plant height and leaf chlorophyll content of these chestnut seedlings grown in the control and 3 chestnut soils were determined and the values were very similar (**Fig. 6**). This suggests that the chestnut soils with similar composition of bacterial microbiomes had not accumulated microorganisms that negatively affect growth of chestnut. Therefore, it confirmed our hypothesis that Chinese chestnut can avoid negative plant-soil feedback during centuries of growth.

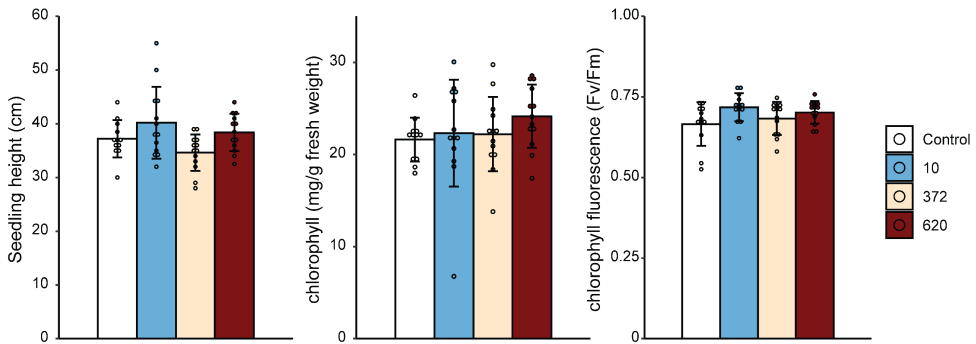


Fig. 6: Similar growth of chestnut seedlings replanted in soils cultivating chestnut trees for up to six centuries. Chestnut seedlings have been grown on the soils collected from the orchard and its margin, respectively. In the orchard, soils have been cultivated with chestnut trees for 10, 372 and 620 years, respectively. In the margin of the orchard, soils which have never been cultivated with trees were collected (defined as Control soil). Chestnut seedlings were grown for 3 months. Their growth was monitored and physiological parameters were quantitatively analyzed. No significant differences of seedling height, chlorophyll content and chlorophyll fluorescence were detected between these chestnut seedlings (one-way ANOVA).

***Pseudomonas* OTU1, the most abundant OTU of the core microbiome, was selected for functional tests**

Root bacterial core microbes of a certain plant species are composed of bacteria frequently enriched in the RH or EC compared to the bulk soil, irrespective to the sampling environment, in our case the tree age and sampling year (Lundberg *et al.*, 2012). We followed the criteria defined by Xu, J *et al.* (2018) that a member of core microbiome should be enriched in vast majority of samples collected in RH or EC (see Materials &

Chapter 4

Methods). Core members have been often shown to be beneficial to their host, for example, improving biotic stress resistance (Tian *et al.*, 2017). To identify bacterial taxa that could contribute to longevity, we determined the core microbiome of chestnut trees and focussed on core members with a high relative abundance.

Performing analysis on samples of all trees, we identified 326 and 483 OTUs that are enriched in the RH and EC, respectively, compared to the soil. Among the 326 RH enriched OTUs, 3 of them occur in more than 70% of the RH samples collected in both years from the different trees. These 3 OTUs all belonged to Proteobacteria and OTU1 belonged to the genus *Pseudomonas* and the other two belonged to unclassified Pseudomonadaceae and Ellin329, respectively (**Table S9**). In the EC, 40 of the 483 enriched OTUs occurred in more than 70% of the EC samples. They predominantly belonged to Actinobacteria and Proteobacteria. So core microbiome, contained 3 and 40 OTUs in the RH and EC, respectively. Next, the relative abundance of these core members was determined (**Fig. 7**). It showed that *Pseudomonas* OTU1 occupied, on average, 30% of reads in the RH community of all trees, whereas the other two core microbes in the RH accounted for less than 1%. In the EC, the mean relative abundance of 10 most abundant core microbes was ranging from 4.4% to 0.7%, where the OTU12, *Bradyrhizobium*, was the highest.

Pseudomonas (OTU1) was selected for further studies, because of it is the member of the core microbiome with the highest relative abundance and several species of this genus have previously been shown to confer stimulation of growth or have antagonistic activities (Cheng *et al.*, 2017; Hesse *et al.*, 2018; Rigling & Prospero, 2018). This genus harbours also several pathogens, but it seems unlikely that an OTU with such high abundance in the RH of healthy trees could be a pathogen. For the EC, *Bradyrhizobium* (OTU12) seemed to be a good choice based on its core membership as well as its relatively high abundance. However, a clear antagonistic activity of *Bradyrhizobium* has not yet been reported. Therefore, we decided to focus on *Pseudomonas* (OTU1).

Longevity correlates with similar root microbiomes

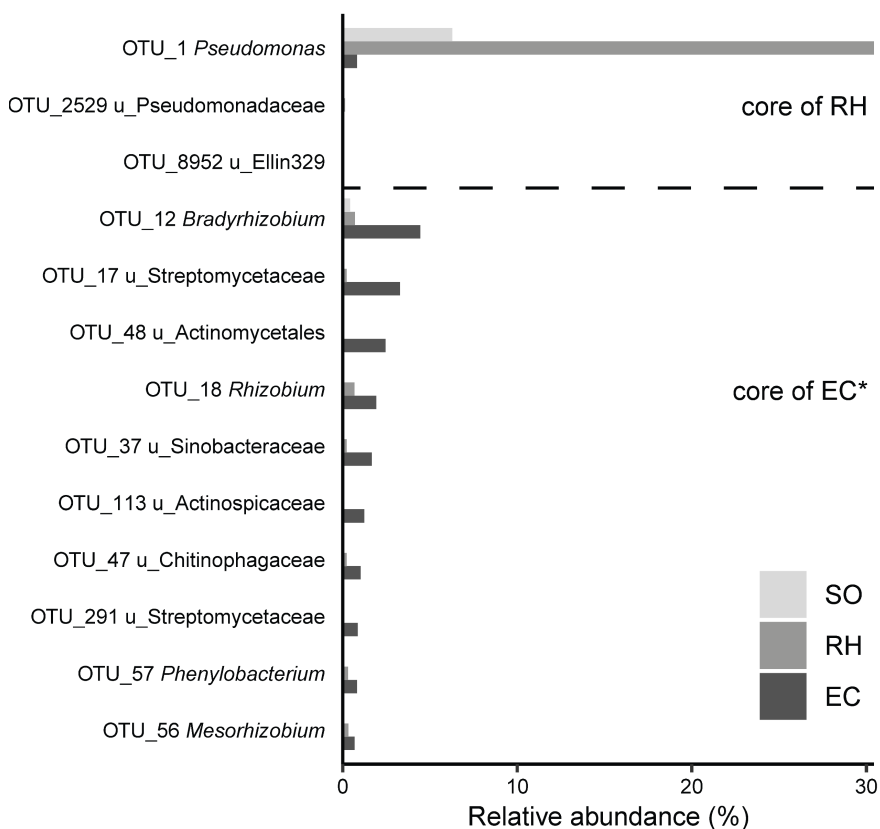


Fig. 7: The relative abundance of core microbes in RH and EC. OTUs that consistently enriched in more than 70% of RH and EC samples, respectively, compared to that in the soil were defined as members of core microbiome. Core microbiome contained 3 and 40 OTUs in the RH and EC, respectively. The relative abundance of the 3 RH and top 10 EC core OTUs in the three compartments were shown.

Pseudomonas strains were isolated from the RH of the 440-year-old tree. Eleven different *Pseudomonas* strains, CM1-CM11, were identified by Sanger sequencing of 16S rRNA gene and Box PCR technic. Based on the V4 region of their 16S rRNA gene sequences, they all belonged to OTU1. Among these 11 CM strains, the V4 region of CM11 matched the most abundant raw sequence of OTU1 in all rhizosphere samples. It encompassed 38.8-46.1% of all OTU1 reads in the rhizosphere samples. The V4 regions of other CM strains matched low abundant raw sequences of OTU1 and were less than 0.7% of all OTU1 reads. Further,

Chapter 4

the genomes of these 11 strains were sequenced (**Table S5**). The core genome of these 11 *Pseudomonas* strains was determined to contain 3328 coding sequences and each genome contained hundreds of unique coding sequences reflecting a high genetic diversity (**Table S10**). A maximum likelihood phylogeny of these 11 strains and 74 reference strains based on protein sequences of 468 single-copy genes revealed 15 groups of *Pseudomonas* (**Fig. 8**). The 11 strains belong to 6 groups, they do not cluster with pathogenic strains, but all with known plant growth-promoting rhizobacteria and non-pathogens, suggesting that they have plant beneficial traits.

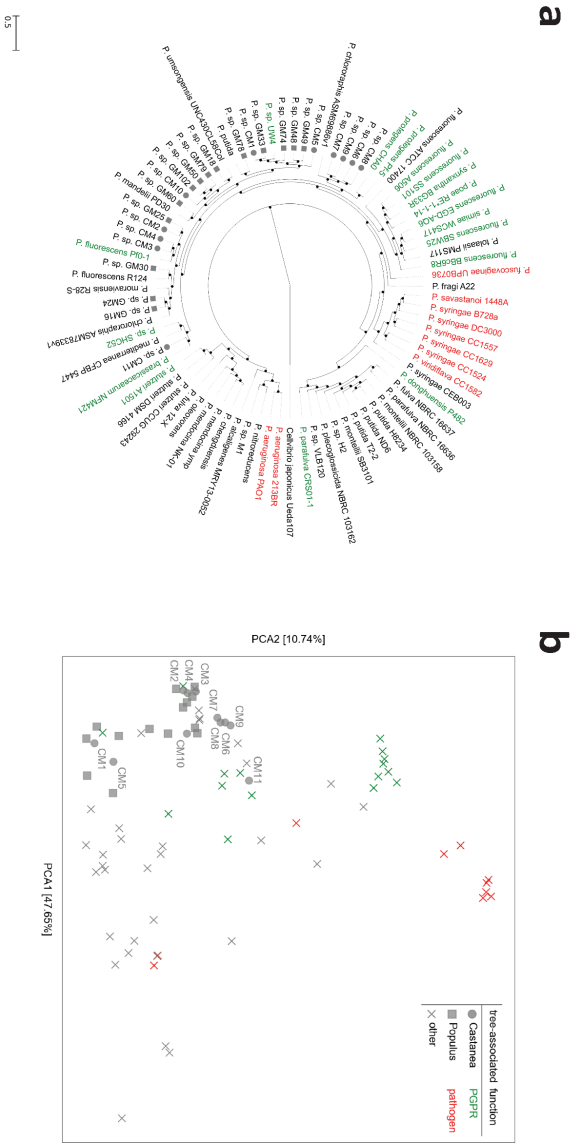
***Pseudomonas* OTU1 harbours strains with strong antagonistic and growth stimulating abilities**

To test our hypothesis that the root microbiome can confer resistance to pathogens, we tested the antagonistic activity of these 11 strains on 2 major chestnut pathogens *Cryphonectria parasitica* and *Phytophthora cinnamom*, which cause chestnut blight and ink disease, respectively (Vettraino *et al.*, 2005; Rigling & Prospero, 2018). The 4 *Pseudomonas* strains (CM6-9) had the strongest antagonistic activity (**Fig. 9**). They are close relatives of *P. protegens* CHA0 and *P. protegens* Pf-5 which are two well-known biological control agents with antifungal activities (Keel *et al.*, 1992; Hartney *et al.*, 2011; Hesse *et al.*, 2018). Strains CM1-CM10 have at least antagonistic activity on one of the 2 major chestnut pathogens. The antagonistic activity of these CM strains supports the hypothesis that the microbiome of chestnut can provide additional defence.

Strain CM11 had a rather low antagonistic activity, but it was the most abundant strain in the rhizosphere of all chestnut trees that we analysed. The latter showed it was a good root colonizer and it could have other plant growth promoting properties including P-solubilization and siderophore production (**Fig. S8**). We tested the effect of CM11 on chestnut grown in a potting system (**Fig. 10a**). CM11 inoculated seedlings were in general bigger, leaf area was larger (**Fig. 10b**) and chlorophyll content was significantly higher (**Fig. 10d**) compared to the non-inoculated plants. CM11 seemed also to enhance biomass formation of chestnut seedlings, however, due to a large variation between individual

seedlings, the biomass difference with and without CM11 inoculation was not significant (Fig. 10c).

Fig. 8: *Pseudomonas* OTU1 strains cluster with PGPR and non-pathogenic strains. **a**, Phylogenetic tree of isolated *Pseudomonas* strains (CM1 to CM11) based on single copy gene (n=468) alignment; **b**, Principal Component Analysis of KEGG functional group by presence or absence amongst the 74 selected *Pseudomonas* strains. Green: strains experimentally proved as plant-growth promoting rhizobacteria (PGPR); Red: strains experimentally proved as pathogenic strains (Pathogen); Gray: non-pathogenic strains. Full filled circle indicates the 11 *Pseudomonas* strains obtained in this study.



Chapter 4

Therefore, the model plant *Arabidopsis* was used to analyse the growth promotion trait. *Arabidopsis* was grown on plates as well as in soil. Biomass analysis of plants grown on plates showed that 11 days after CM11 inoculation, shoot and root fresh weight increased 3.4- and 2.4-fold, respectively, compared to mock inoculated plants (**Fig. 10e**). Inoculation with CM11 of plants grown in soil increased shoot and root fresh weight 3.9- and 2.8-fold, respectively (**Fig. 10f**). This showed that OTU1, in addition to strains with strong antagonistic activity, harbours a strain with strong growth stimulating abilities.

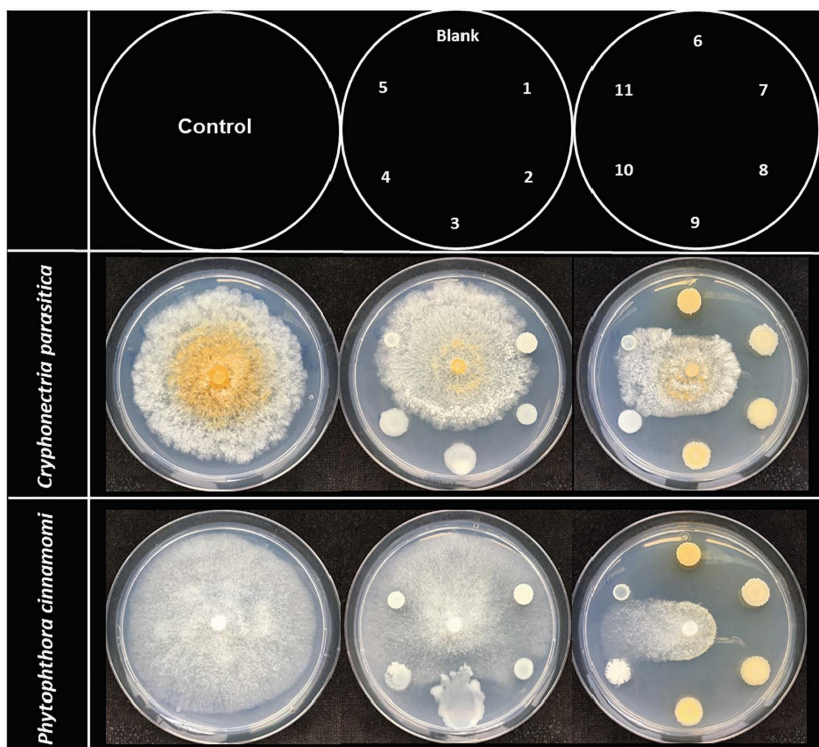


Fig. 9: *Pseudomonas* OTU1 strains inhibit growth of two major chestnut pathogens. In *in vitro* condition, *Pseudomonas* strains CM1-CM11 and their potential antagonistic activity against the Chestnut fungal pathogen, *Cryphonectria parasitica* (chestnut blight) and oomycete pathogen, *Phytophthora cinnamoni* (chestnut ink disease) are shown. Blank is the 0.9% NaCl solution used for washing and suspending bacterial cells. The number indicates different *Pseudomonas* strains used in these assays.

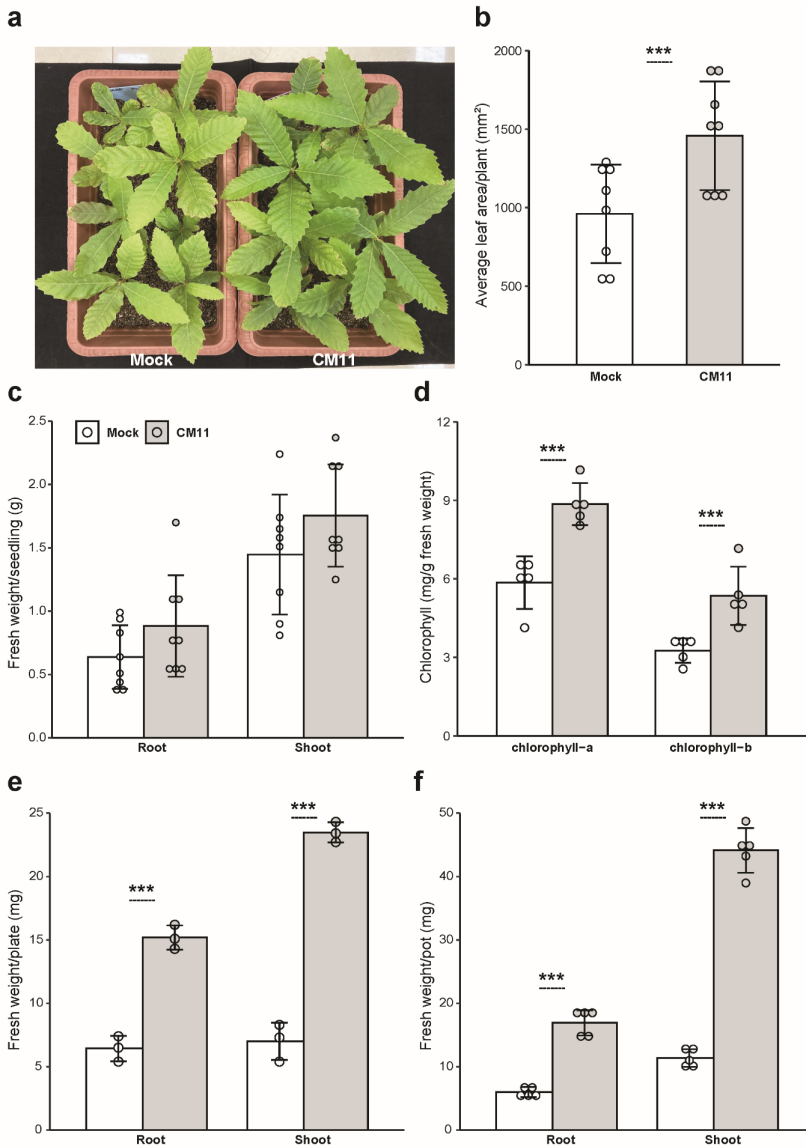


Fig. 10: *Pseudomonas* strain CM11 stimulates growth of chestnut seedlings and *Arabidopsis*. **a-d**, Chestnut assay in potting system: the phenotypical observation of plant growth (**a**); Quantitative analysis of leaf area ($n = 8$) (**b**), the fresh weight of root and shoot ($n = 8$) (**c**), and chlorophyll content ($n = 5$) (**d**); **e, f**, *Arabidopsis* assay on plates ($n = 3$) (**e**) and in potting system ($n = 5$) (**f**): fresh weight of root and shoot are plotted. Bars indicate means (\pm SD). Asterisks indicate statistical significance (***: $p < 0.001$, t-test).

Chapter 4

Discussion

In this study, we showed that the overall composition of the root associated bacterial microbiomes of a chrono-series of chestnut trees, ranging from 8 to about 800 years, is rather similar, although based on the models we cannot exclude that tree age has a weak correlation with the composition of root associated microbiomes. Chestnut seedlings were grown in soil that had been associated with young and old chestnut trees, respectively. We observed that these chestnut plants were healthy and their growth was similar. This provided strong indications that Chinese chestnut is able to avoid negative feedback with its soil. The root associated microbiomes, contain a highly abundant *Pseudomonas* OTU, harbouring strains with antagonistic activity against 2 major chestnut pathogens and another that can markedly stimulate plant growth. This together with the absence of negative plant soil feedback can contribute to its longevity.

PCoA of Bray-Curtis dissimilarity values showed that SO, RH and EC have clearly distinct microbiomes. The PCoA showed that the overall composition of the microbiomes was similar among different trees, although their age could differ more than 800 years. This despite that, in a few trees, the relative abundance of two dominant families and one dominant genus could vary most likely due to the sampling year. These studies could not exclude that there were small differences that were correlated with age. To test this, we could not perform a pair-wise permutation ANOVA analysis on the dissimilarity values between the trees of different ages, due to the uneven and small number of replicates. Therefore, we performed linear regression analyses to determine whether there is a relation between the community dissimilarities and tree age differences (Marasco *et al.*, 2018). The models do not exclude that increasing tree age does affect the composition of the root associated microbiomes, albeit with a very slow speed. The speed by which the soil and root associated microbiomes change, due to negative apple soil feedback, has not been accurately quantified. However, some studies indicate that it occurs relatively fast (Mazzola & Manici, 2012; Sun *et al.*, 2014; Winkelmann *et al.*, 2019). The microbiome of soil in which apple had grown for about 30 years is significantly different from that of the soil where no apples were grown in the same orchard. Young apple trees were planted in

Longevity correlates with similar root microbiomes

both soils, and this showed that within half a year, the microbiome of the apple soil caused a 40-50% reduction of shoot and root biomass of newly planted apple trees. Further, the difference between the two soil microbiomes had even become markedly bigger, underlining the strong feedback between apple and soil (Sun *et al.*, 2014). This means in a time span that apple replant disease can develop (~30 years), the dissimilarity values of the chestnut root associated bacterial communities might increase with only about 0.4%.

Moreover, when chestnut seedlings were grown in soil that had been associated with chestnut roots for up to 620 years, they all are healthy and have a very similar growth compared to those in soil that had been either associated for shorter periods or had not been in contact with chestnut trees. It showed that the small changes in root associated microbiomes do not negatively affect the growth of replanted chestnut seedlings. This in combination with the healthy nature of the trees, strongly indicates that Chinese chestnut is able to avoid negative feedback with its soil.

Considering the potential beneficial properties of the core microbiome to plant growth and health, in depth analysis was focused on the most abundant core microbiome member, which is *Pseudomonas* OTU1 that especially occurred in the RH. Its relative abundance varied in the 2 years that we did analyses. This fluctuation is in line with a study on a highly abundant *Pseudomonas* in maize root associated microbiome (Peiffer *et al.*, 2013). This also illustrates that, although microbiomes at a certain time point are similar, it does not imply that they are static. Changes might occur due to environmental conditions that can vary between years. High abundance of OTU1 in the RH is the reason why the Shannon index of the RH is lower than that of EC. Its relative abundance is also high in 2 soil samples that we collected in 2016. We assume that this is due to variation in the distance to the root system.

It is probable that the root-associated microbiomes contribute to protection against pathogens and can stimulate growth. *Pseudomonas* spp. are ubiquitous bacteria in soils and is one of the bacterial genera most used as biocontrol agent for soilborne pathogens as well as plant growth stimulator (Van Loon, 2007; Mendes *et al.*, 2013). In combination

Chapter 4

with the highest abundance of the *Pseudomonas* OTU 1 among the core microbiome of RH, *Pseudomonas* isolates, i.e. the 11 *Pseudomonas* strains that belong to OTU1, were selected for functional analysis. Especially one strain stimulated growth and in a recent study its effect on root architecture has been studied in more detail (Li *et al.*, 2022). In addition, several other strains have strong antagonistic activities against the 2 major diseases of chestnut. Since the core microbiome contains other members as well, we expect that this is just the tip of the iceberg and probably several other strains of the microbiomes have antagonistic or plant growth promoting activities individually or in consortia.

In our study, we showed that the root associated bacterial microbiomes of a chrono-series of Chinese chestnut are similar despite 8 centuries' difference in age, although the models do not exclude that age has a weak correlation with the composition of root associated microbiomes. The *Pseudomonas* OTU1 is highly abundant in the chestnut rhizosphere. Such an abundance points to a beneficial effect on its host. This is well in line with the observation that strains belonging to this OTU have a strong antagonistic activity on 2 major chestnut pathogens and one member can stimulate growth of chestnut as well as *Arabidopsis*. Such properties of the “second genome” (the microbiomes), in combination with a high number of resistance genes can markedly contribute to the longevity of chestnut.

Acknowledgements

We thank our colleagues and collaborators who provided us with valuable feedbacks and assistance at all stages of this study. We thank grant support from the National Key Research, Development Program of China (Grant NO. 2018YFD1000605) & the NWO-TTW Perspectief project “Back to the Roots” (Grant NO. 14220).

Authors' contributions

XC, ZY, QL, JY, YG, YW, GL, YZ, YL, LY, HB and QC executed the field and lab experiment. ZY, LS, MS, AD and XC conducted *in silico* analyses. YL determined Chestnut tree age. LQ and QC provided access to the Ming orchard, joined sample collection and contributed to the data analysis. XC, ZY and TB wrote the manuscript.

Supplementary information:



Fig. S1: Chestnut trees grown at the Huanghuacheng Lakeside Great Wall, Beijing, China.
Root samples of three old chestnut trees were collected in 2016 & 2017.

Longevity correlates with similar root microbiomes

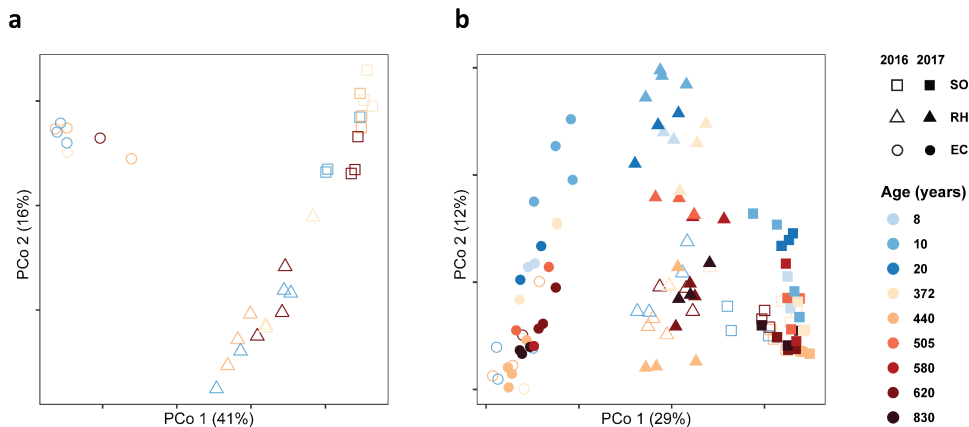


Fig. S2: PCoA of samples collected in two years, while the OTU1 was removed from the communities. **a**, a young tree (~10 years old) and 3 old trees (372, 440 and 620 years) were sampled in 2016. When OTU1 was excluded and PCoA was repeated, then SO samples formed one cluster; **b**, with additional 2 young trees (8 and 20 years) and 3 old trees (505, 580 and 830 years) were sampled in 2017. High abundance of OTU1 in the RH is the reason why the Shannon index of the RH is lower than that of EC. Its relative abundance is also high in 2 SO samples that we collected in 2016. We assume that this was due to variation in the distance to the roots system.

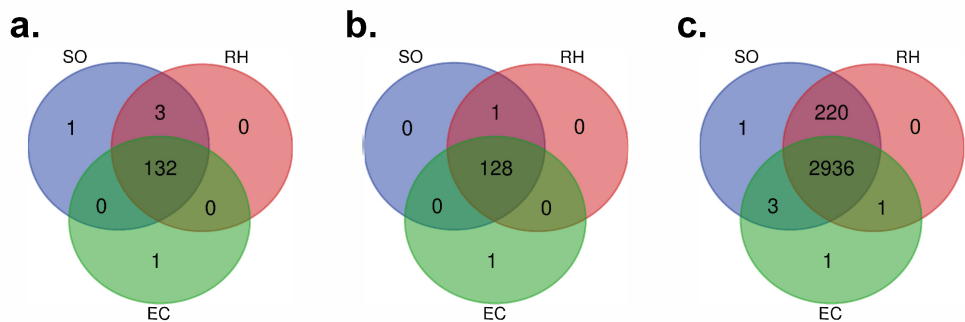


Fig. S3: Venn diagrams show the occurrence of classified families (a), genera (b) and measurable OTUs (c) among the three compartments.

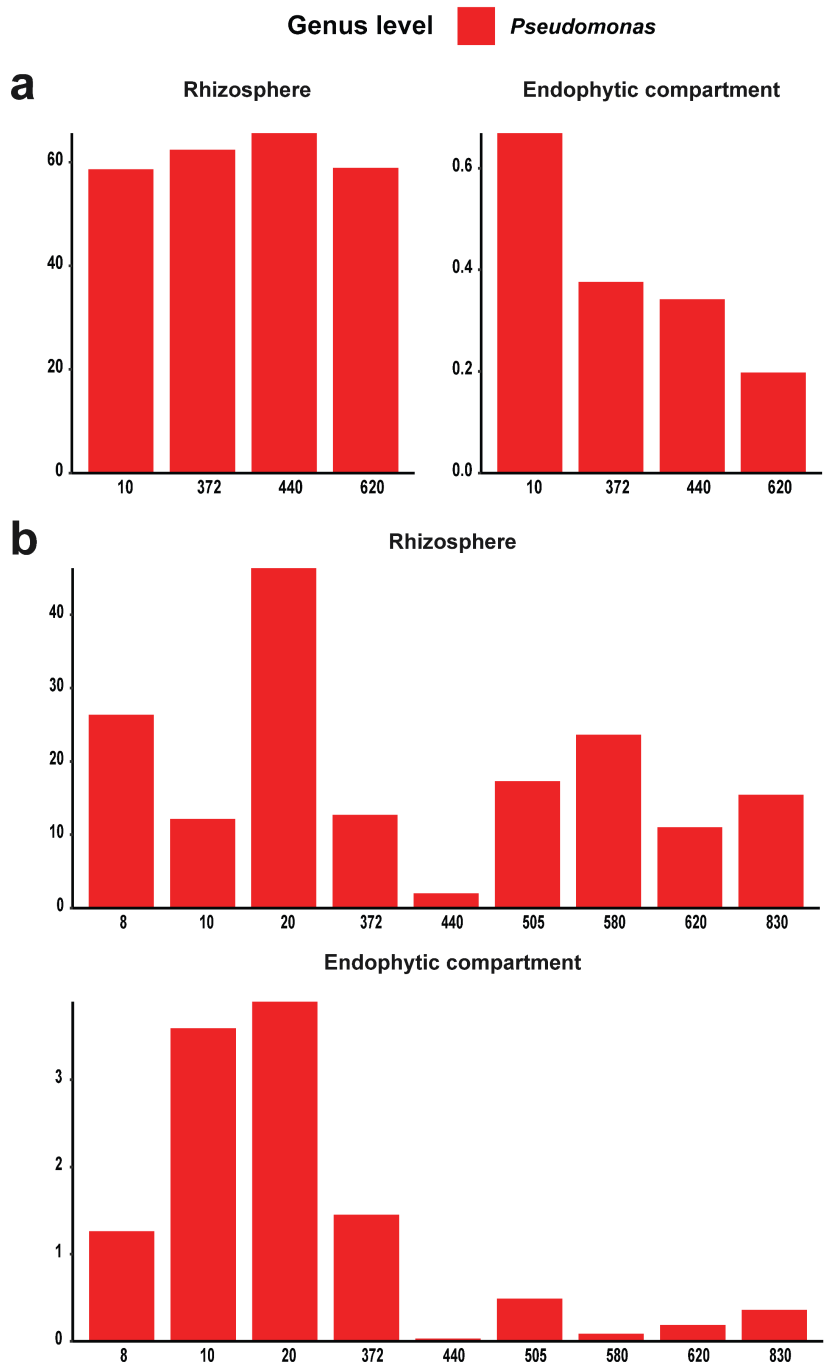


Fig. S4: Dominant *Pseudomonas* in RH & EC. One dominant classified genus with a relative abundance of at least 5% in RH or EC and occurred in all trees of 2016 (a) and 2017 (b).

Longevity correlates with similar root microbiomes

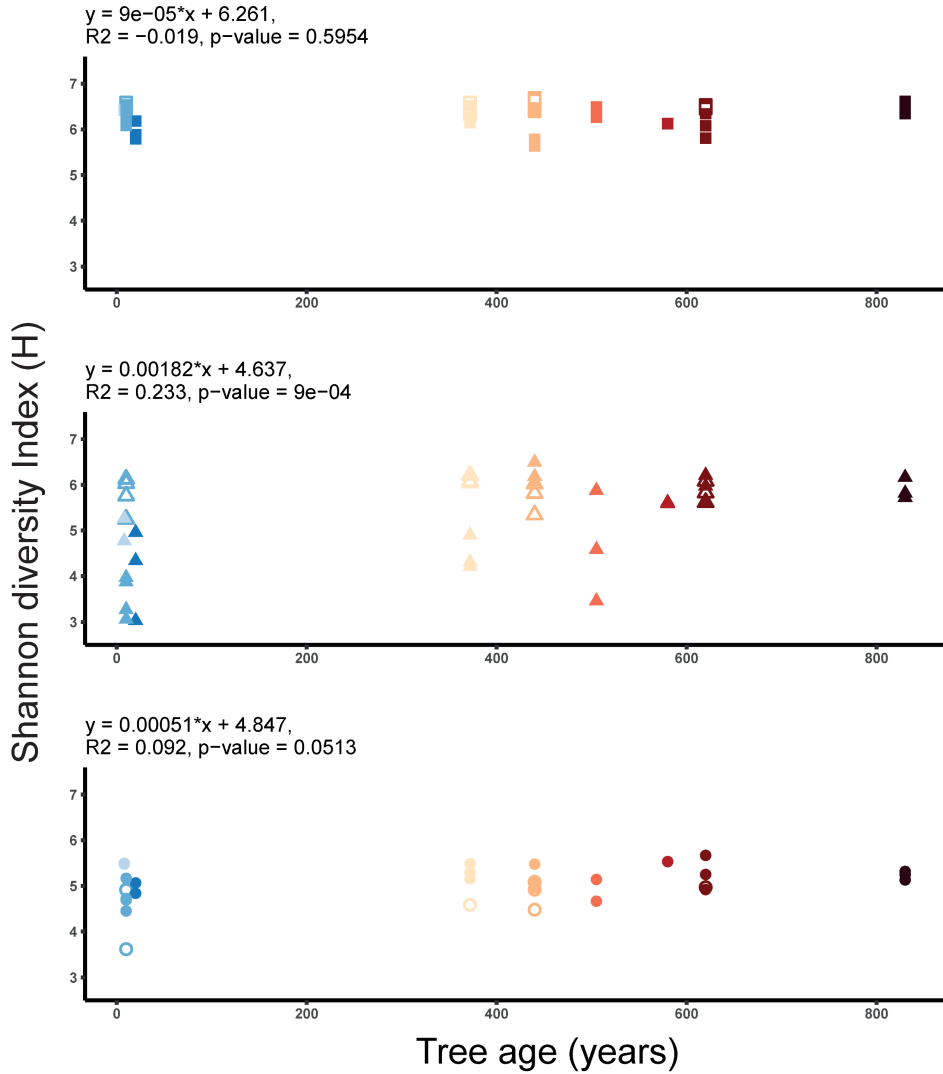


Fig. S5: The relationship between alpha diversities and chestnut tree ages while the OTU1 was removed from the communities. Relationships between bacterial alpha diversities (Shannon diversity index) in each compartment (SO, RH and EC) of trees sampled in 2016 (empty symbols) and 2017 (solid symbols). Each symbol indicates the Shannon diversity index value of one sample (Y-axis) with correlated tree age (X-axis).

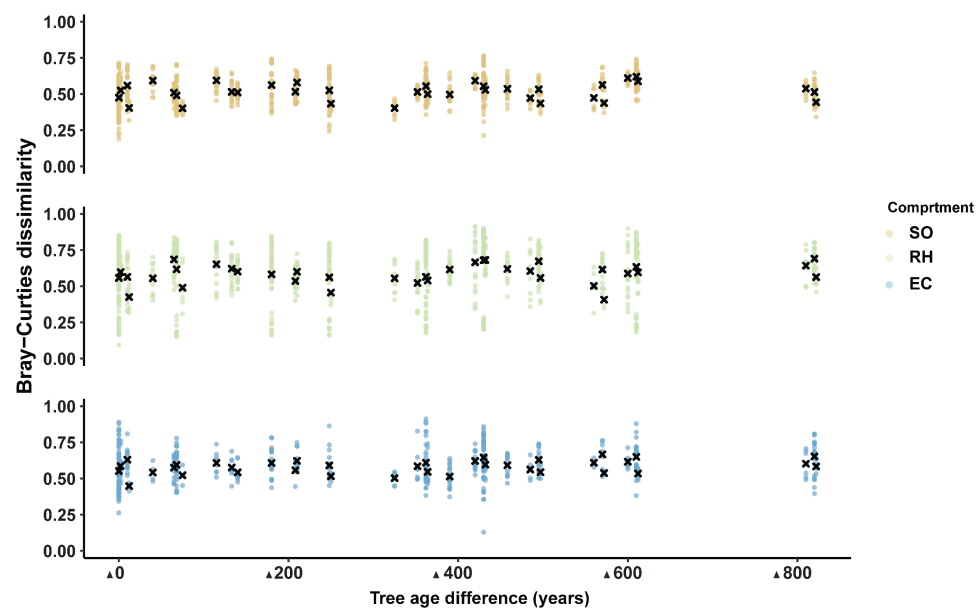


Fig. S6: The relations between the chestnut root bacterial communities and tree ages. Relationships between bacterial communities' dissimilarities (Bray-Curtis) in each compartment of trees sampled in two years and the tree age differences by pair-wise comparisons are shown. Each dot indicates the Bray-Curtis dissimilarity value of two samples (Y-axis) with correlated tree age differences (X-axis, Δ years). Black cross highlights the mean values of Bray-Curtis dissimilarities regarding specific tree age differences.

Longevity correlates with similar root microbiomes

Control



10 Years



372 Years



620 Years



Fig. S7: Phenotypical observation of the plant-soil feedback assay. Chestnut seedlings were cultivated on different soils, control: soil from the margin of the orchard where no chestnut or other trees have been cultivated; 10, 372 and 620: soils around the chestnut trees with ages of 10, 372 and 620 years old. After 3 months, plant phenotypes were captured.

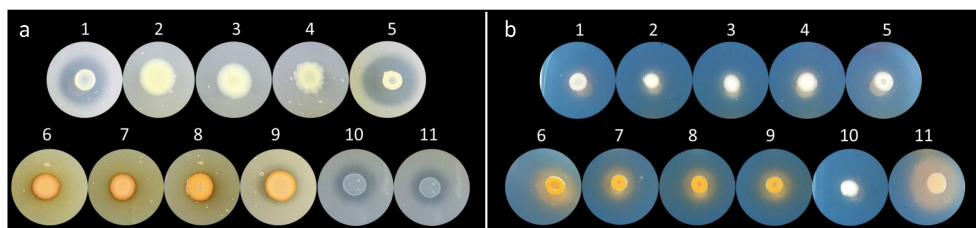


Fig. S8: Biological activities of *Pseudomonas* OTU1 strains. **a**, P-solubilization activity test on NBRIP medium. Transparent halo surrounding the colonies shows P-solubilization of each strains; **b**, detection of siderophore production on CAS medium. Number indicates different *Pseudomonas* strains used in these assays.

Table S1: Detailed information of samples collected in 2016 and 2017.

Sampling time	Determined Age (years)	Replicates	Location (Beijing, China)	GPS
August 2016	10	4	Chestnut research station	N40°25'13.42",E116°31'51.61"
	372	4	Orchard, Great Wall	N40°24'44.74",E116°18'09.49"
	440	4	Orchard, Great Wall	N40°24'46.06",E116°18'07.49"
	620	4	Orchard, Great Wall	N40°24'41.79",E116°18'10.50"
July 2017	8	2	Orchard, Great Wall	N40°24'43.64",E116°18'08.65"
	10	4	Chestnut research station	N40°25'13.42",E116°31'51.61"
	20	3	Orchard, Great Wall	N40°24'45.09",E116°18'05.17"
	372	3	Orchard, Great Wall	N40°24'44.74",E116°18'09.49"
	440	4	Orchard, Great Wall	N40°24'46.06",E116°18'07.49"
	505	3	Orchard, Great Wall	N40°24'45.03",E116°18'04.48"
	580	2	Orchard, Great Wall	N40°24'43.65",E116°18'07.88"
	620	3	Orchard, Great Wall	N40°24'41.79",E116°18'10.50"
	830	3	Orchard, Great Wall	N40°24'43.78",E116°18'09.10"

Table S2: Linear regression test between Shannon diversity index and tree age.

Compartment	p-value	R2	Equation
SO	0,274	0,006	$y = -0.00043 * x + 6.187$
RH	< 0.01	0,195	$y = 0.00208 * x + 3.311$
EC	0,048	0,095	$y = 0.00051 * x + 4.848$

Longevity correlates with similar root microbiomes

Table S3: Mean Bray-Curtis dissimilarity values regarding to tree age differences.

Tree age difference (Year)	Compartment		
	SO	RH	EC
0	0.475	0.559	0.551
2	0.528	0.591	0.587
10	0.564	0.567	0.629
12	0.413	0.418	0.442
40	0.59	0.557	0.541
65	0.506	0.691	0.574
68	0.49	0.618	0.592
75	0.4	0.495	0.524
115	0.588	0.656	0.607
133	0.511	0.626	0.576
140	0.509	0.607	0.547
180	0.558	0.582	0.605
208	0.515	0.538	0.56
210	0.577	0.6	0.621
248	0.522	0.562	0.588
250	0.438	0.454	0.524
325	0.403	0.561	0.504
352	0.518	0.525	0.583
362	0.554	0.565	0.609
364	0.499	0.536	0.546
390	0.5	0.616	0.513
420	0.597	0.667	0.618
430	0.556	0.681	0.645
432	0.533	0.681	0.595
458	0.537	0.62	0.591
485	0.477	0.607	0.56
495	0.533	0.674	0.626
497	0.437	0.557	0.538
560	0.475	0.505	0.609
570	0.562	0.617	0.666
572	0.445	0.401	0.542
600	0.611	0.592	0.612
610	0.617	0.636	0.65
612	0.585	0.594	0.537
810	0.548	0.644	0.599
820	0.517	0.69	0.651
822	0.451	0.563	0.58

Chapter 4

Table S4: Linear regression test between Bray-Curtis dissimilarity and tree age difference.

Compartment	p-value	R2	Equation
SO	< 0.01	0,03	$y = 0.000075 * x + 0.507$
RH	< 0.01	0,013	$y = 0.000089 * x + 0.574$
EC	< 0.01	0,028	$y = 0.000082 * x + 0.569$

Table S5: Genome assembly statistics.

Strain	Contig count	Largest contig (bp)	Total length (bp)	N50 (bp)	L50	BUSCO (%)
CM1	44	888292	6492253	393766	6	100
CM2	16	1280022	6316609	656198	4	100
CM3	22	981261	6158082	555952	5	100
CM4	23	995079	6140400	511348	5	100
CM5	42	742621	6096348	388146	6	100
CM6	15	1200717	6867146	799881	4	100
CM7	18	1538942	6686490	683511	4	100
CM8	19	1412009	6820682	759831	4	100
CM9	13	2468088	6813630	1022324	2	100
CM10	40	932747	6642803	357918	7	100
CM11	32	1303846	5878492	572018	4	100

Table S6: PERMANOVA of the bacterial communities in three compartments of chestnut trees collected in 2016.

	Df	SumsOfSqs	MeanSqs	F.Model	R2	Pr(>F)
Compartment	2	4.991	2.496	30.381	0.645	0.001
Tree Age	3	0.497	0.166	2.016	0.064	0.031
Residuals	27	2.218	0.082		0.288	
Total	32	7.705			1.000	

Table S7: ANOVA of bacterial alpha diversities in three compartments of chestnut trees collected from both two years.

SO	Df	Sums Of Sqs	Mean Sqs	F. Model	Pr(>F)	
Sampling year	1	1.047	1.047	7.533	0.01332	*
Tree age	3	4.894	1.631	11.74	0.00017	***
Sampling year : Tree age	3	5.774	1.925	13.851	6.33E-05	***
Residuals	18	2.501	0.139			

RH	Df	Sums Of Sqs	Mean Sqs	F. Model	Pr(>F)	
Sampling year	1	25.569	25.569	156.73	1.26E-10	***
Tree age	3	6.801	2.267	13.89	4.95E-05	***
Sampling year : Tree age	3	9.447	3.149	19.3	5.43E-06	***
Residuals	19	3.1	0.163			

EC	Df	Sums Of Sqs	Mean Sqs	F. Model	Pr(>F)	
Sampling year	1	0.9027	0.9027	6.191	0.0261	*
Tree age	3	0.8667	0.2889	1.981	0.1631	
Sampling year : Tree age	3	0.1342	0.0447	0.307	0.8201	
Residuals	14	2.0413	0.1458			

Signif. codes: 0 '***' 0.001 '**' 0.01 '*' 0.05 '.' 0.1 ' ' 1

Chapter 4

Table S8: PERMANOVA of the bacterial communities in three compartments of chestnut trees collected from both two years.

SO	Df	SumsOfSqs	MeanSqs	F.Model	R2	Pr(>F)
Sampling Year	1	0.886	0.886	9.467	0.235	0.001
Tree Age	3	0.918	0.306	3.269	0.243	0.001
Residuals	21	1.965	0.094		0.521	
Total	25	3.768			1.000	

RH	Df	SumsOfSqs	MeanSqs	F.Model	R2	Pr(>F)
Sampling Year	1	2.260	2.260	24.062	0.417	0.001
Tree Age	3	1.096	0.365	3.887	0.202	0.002
Residuals	22	2.067	0.094		0.381	
Total	26	5.423			1.000	

EC	Df	SumsOfSqs	MeanSqs	F.Model	R2	Pr(>F)
Sampling Year	1	0.736	0.736	5.226	0.181	0.002
Tree Age	3	0.942	0.314	2.229	0.231	0.007
Residuals	17	2.394	0.141		0.588	
Total	21	4.072			1.000	

Remarks: In each compartment, the sampling year and tree age significantly influence the bacterial community composition ($p < 0.001$). In RH, the sampling year explained most of the variance ($R^2 = 0.417$) and tree age did the least ($R^2 = 0.202$). In SO, the sampling year and tree age showed similar influence ($R^2=0.235$ and 0.243 , respectively), where in EC, the sampling year showed less effect than the tree age ($R^2=0.181$ and 0.231 , respectively).

Table S9: Taxonomic information of OTUs consistently enriched in more than 70% of RH and EC samples, respectively, compared to the soil.

RH core microbes	phylum	class	order	family	genus
OTU_1	Proteobacteria	Gammaproteobacteria	Pseudomonadales	Pseudomonadaceae	Pseudomonas
OTU_2529	Proteobacteria	Gammaproteobacteria	Pseudomonadales	Pseudomonadaceae	unclassified_Pseudomonadaceae
OTU_8952	Proteobacteria	Alphaproteobacteria	Elin329	unclassified_Elin329	unclassified_Elin329
EC core microbes	phylum	class	order	family	genus
OTU_113	Actinobacteria	Actinomycetia	Actinomycetales	Actinospiraceae	unclassified_Actinospiraceae
OTU_118	Proteobacteria	Alphaproteobacteria	Rhizobiales	Hyphomicrobiaceae	Rhodoplanes
OTU_1193	Actinobacteria	Actinomycetia	Actinomycetales	Streptomycetaceae	unclassified_Streptomycetaceae
OTU_12	Proteobacteria	Alphaproteobacteria	Rhizobiales	Bradyrhizobiaceae	Bradyrhizobium
OTU_132	Actinobacteria	Actinomycetia	Actinomycetales	Micromonosporaceae	Dactylosporangium
OTU_1375	Actinobacteria	Actinomycetia	Actinomycetales	unclassified_Actinomycetales	unclassified_Actinomycetales
OTU_1390	Proteobacteria	Alphaproteobacteria	Rhizobiales	unclassified_Rhizobiales	unclassified_Rhizobiales
OTU_1641	Actinobacteria	Actinomycetia	Actinomycetales	Micromonosporaceae	unclassified_Micromonosporaceae
OTU_17	Actinobacteria	Actinomycetia	Actinomycetales	Streptomycetaceae	unclassified_Streptomycetaceae
OTU_18	Proteobacteria	Alphaproteobacteria	Rhizobiales	Rhizobiaceae	Rhizobium
OTU_19262	Proteobacteria	Alphaproteobacteria	Rhizobiales	unclassified_Rhizobiales	unclassified_Rhizobiales
OTU_212	Proteobacteria	Alphaproteobacteria	Rhizobiales	Hyphomicrobiaceae	unclassified_Hyphomicrobiaceae
OTU_216	Proteobacteria	Alphaproteobacteria	Rhizobiales	Hyphomicrobiaceae	Rhodoplanes
OTU_218	Proteobacteria	Alphaproteobacteria	Rhizobiales	Xanthobacteraceae	Labrys
OTU_2421	Actinobacteria	Gammaproteobacteria	Xanthomonadales	Sinobacteraceae	unclassified_Sinobacteraceae
OTU_247	Actinobacteria	Actinomycetia	Actinomycetales	Nocardiodaceae	Kribbella
OTU_252	Proteobacteria	Gammaproteobacteria	Xanthomonadales	Xanthomonadaceae	Dokdonella
OTU_283	Actinobacteria	Actinomycetia	Actinomycetales	Streptomycetaceae	unclassified_Streptomycetaceae
OTU_291	Actinobacteria	Actinomycetia	Actinomycetales	Streptomycetaceae	unclassified_Streptomycetaceae
OTU_3528	Proteobacteria	Alphaproteobacteria	Sphingomonadales	Sphingomonadaceae	unclassified_Sphingomonadaceae
OTU_37	Proteobacteria	Gammaproteobacteria	Xanthomonadales	Sinobacteraceae	unclassified_Sinobacteraceae
OTU_400	Actinobacteria	Actinomycetia	Actinomycetales	Micromonosporaceae	unclassified_Micromonosporaceae
OTU_40972	Proteobacteria	Alphaproteobacteria	Rhizobiales	Hyphomicrobiaceae	Devosia
OTU_427	Actinobacteria	Actinomycetia	Actinomycetales	Micromonosporaceae	unclassified_Micromonosporaceae
OTU_47	Bacteroidetes	[Saprospirae]	[Saprospirae]	Chitinophagaceae	unclassified_Chitinophagaceae
OTU_48	Actinobacteria	Actinomycetia	Actinomycetales	unclassified_Actinomycetales	unclassified_Actinomycetales
OTU_559	Actinobacteria	Actinomycetia	Actinomycetales	unclassified_Actinomycetales	unclassified_Actinomycetales
OTU_56	Proteobacteria	Alphaproteobacteria	Rhizobiales	Phyllobacteriaceae	Mesorhizobium
OTU_57	Proteobacteria	Alphaproteobacteria	Caulobacterales	Caulobacteraceae	Phenylobacterium
OTU_6012	Proteobacteria	Alphaproteobacteria	Rhizobiales	Xanthobacteraceae	Labrys
OTU_65	Actinobacteria	Actinomycetia	Actinomycetales	Bradyrhizobiaceae	Mycobacterium
OTU_7143	Proteobacteria	Alphaproteobacteria	Rhizobiales	Actinospiraceae	unclassified_Actinospiraceae
OTU_8025	Actinobacteria	Actinomycetia	Actinomycetales	Actinospiraceae	unclassified_Actinospiraceae
OTU_846	Actinobacteria	Actinomycetia	Actinomycetales	Actinospiraceae	unclassified_Actinospiraceae
OTU_87	Proteobacteria	Alphaproteobacteria	Myxococcales	Actinospiraceae	unclassified_Actinospiraceae
OTU_881	Proteobacteria	Gammaproteobacteria	Xanthomonadales	Actinospiraceae	unclassified_Actinospiraceae
OTU_8999	Proteobacteria	Alphaproteobacteria	Rhizobiales	unclassified_Rhizobiales	unclassified_Rhizobiales
OTU_901	Proteobacteria	Gammaproteobacteria	Xanthomonadales	Sinobacteraceae	unclassified_Sinobacteraceae
OTU_954	Actinobacteria	Thermoplasma	Solirubrobacterales	unclassified_Solirubrobacterales	unclassified_Solirubrobacterales
OTU_994	Proteobacteria	Alphaproteobacteria	Rhizobiales	Bradyrhizobiaceae	unclassified_Bradyrhizobiaceae

Table S10: Summary information of OrthoFinder run on Chestnut strains.

Accession	unique orthogroups	unique genes	ORFs
CM1	253	288	6313
CM2	118	206	5991
CM3	83	224	5958
CM4	81	335	5973
CM5	166	329	6259
CM6	57	204	6365
CM7	33	178	6226
CM8	74	216	6408
CM9	82	251	6518
CM10	337	494	6694
CM11	256	342	5669
shared orthogroups	3328		

Remarks:

- The number of orthogroups or genes found in only one assembly are shown in the "unique orthogroups/genes" columns
- The number of open reading frames are shown in the "ORFs" column
- The complete set of orthogroups which had at least one gene from each assembly was defined as the core genome, its count is shown as "shared orthogroups"

Chapter 5

Synthetic bacterial community derived from a desert rhizosphere confers salt stress resilience to tomato in the presence of a soil microbiome

Lucas Schmitz^{1, #}, Zhichun Yan^{1, #}, Martinus Schneijderberg¹, Martijn de Roij¹, Rick Pijnenburg¹, Qi Zheng¹, Carolien Franken¹, Annemarie Dechesne², Luisa M. Trindade², Robin van Velzen³, Ton Bisseling¹, Rene Geurts^{1, *}, and Xu Cheng^{1, 4, *}

¹ Laboratory of Molecular Biology, Cluster of Plant Developmental Biology, Plant Sciences Group, Wageningen University, Droevendaalsesteeg 1, 6708PB Wageningen, The Netherlands

² Laboratory of Plant Breeding, Plant Sciences Group, Wageningen University & Research, Droevendaalsesteeg 1, 6708 PB Wageningen, The Netherlands.

³ Biosystematics, Plant Sciences Group, Wageningen University & Research, Droevendaalsesteeg 1, 6708 PB Wageningen, The Netherlands.

⁴ Shenzhen Branch, Guangdong Laboratory for Lingnan Modern Agriculture, Genome Analysis Laboratory of the Ministry of Agriculture, Agricultural Genomics Institute at Shenzhen, Chinese Academy of Agricultural Sciences, Shenzhen, China

These authors contributed equally.

* Corresponding authors: rene.geurts@wur.nl; xu.cheng@wur.nl

Published: *The ISME Journal* volume 16, pages 1907–1920 (2022)

Abstract

The root bacterial microbiome is important for the general health of the plant. Additionally, it can enhance tolerance to abiotic stresses, exemplified by plant species found in extreme ecological niches like deserts. These complex microbe-plant interactions can be simplified by constructing synthetic bacterial communities or SynComs from the root microbiome. Furthermore, SynComs can be applied as biocontrol agents to protect crops against abiotic stresses such as high salinity. However, there is little knowledge on the design of a SynCom that offers a consistent protection against salt stress for plants growing in a natural and, therefore, non-sterile soil which is more realistic to an agricultural setting. Here we show that a SynCom of five bacterial strains, originating from the root of the desert plant *Indigofera argentea*, protected tomato plants growing in a non-sterile substrate against a high salt stress. This phenotype correlated with the differential expression of salt stress related genes and ion accumulation in tomato. Quantification of the SynCom strains indicated a low penetrance into the natural soil used as the non-sterile substrate. Our results demonstrate how a desert microbiome could be engineered into a simplified SynCom that protected tomato plants growing in a natural soil against an abiotic stress.

Introduction

Plants sustain microorganisms around and inside their roots (Mendes *et al.*, 2013). These communities of root-associated microorganisms are referred to as the root microbiome. There is increasing evidence showing that the root microbiome is vital to plant health, growth and development and plays a prominent role in plant fitness under diverse environmental growth conditions (Lemanceau *et al.*, 2017). The root microbiome can promote growth and development by modulating plant hormone homeostasis, promoting nutrient acquisition, or improving resilience to abiotic stresses (Mayak *et al.*, 2004; Yang *et al.*, 2009).

The microbes that make up the root microbiome can sometimes succeed where other methods such as gene engineering have failed. For example, the HIGH-AFFINITY K⁺ TRANSPORTER 1;1 (HKT1;1) is proposed to facilitate the shoot-to-root recirculation of Na⁺, but both loss-of-function and overexpression in *Arabidopsis thaliana* (arabidopsis) does not improve salt tolerance (Maser *et al.*, 2002; Rus *et al.*, 2004). Interestingly, a strain of the soil bacterium *Bacillus subtilis* did confer salt tolerance by concurrently down- and upregulating the expression of *AtHKT1* in the roots and shoots of arabidopsis, respectively (Zhang *et al.*, 2008). This finding of tissue-specific regulation of *AtHKT1* mediated by a microbe being critical to Na⁺ homeostasis in salt-stressed plants demonstrates the potential of plant-microbe interactions.

It is generally hypothesized that the root microbiome is also important in the case of desert plants to cope with multiple and critical threats such as nutrient deficiency, drought and salinity (Saad *et al.*, 2020). So far, only a limited number of studies have been conducted to characterize microbial communities associated with desert plants and their contribution to plant fitness. *Indigofera argentea* (indigofera) is a legume species that can be found in multiple desert regions (Schrire *et al.*, 2009). It is a perennial subshrub that grows as pioneer vegetation in scattered populations in well-drained and sandy soils. Also, indigofera has a certain resilience to salt stress and can grow like a weed on former agricultural fields that suffer from high salinity due to extensive irrigation practices. For example, former agricultural areas in the Jizan desert, Saudi Arabia, are scarcely populated

Chapter 5

with indigofera (Fig. S1). We questioned whether the microbiome present in this Jizan soil plays a pivotal role in conferring abiotic stress tolerance to indigofera growing under such conditions.

Indigofera root bacterial strains of Jizan origin have been isolated and resulted among others in the identification of *Pseudomonas argentinensis* SA190, *Acinetobacter radioresistens* SA188, *Enterobacter* sp. SA187, and *Ochrobactrum intermedium* SA148. For these bacteria, plant-growth promoting effects have been predicted and experimentally verified for *Enterobacter* sp. SA187 (Lafi *et al.*, 2016; Andres-Barrao *et al.*, 2017; Lafi *et al.*, 2017a; Lafi *et al.*, 2017c).

Most studies focus on single strains applied to plants grown in essentially sterile conditions. This is not the case in a field setting where the presence of the local microbiome naturally implies a non-sterile environment. This non-sterile environment is suspected to explain the failure of a single strain in the field due to the competition with the local microbiome (Bashan *et al.*, 2014; Baez-Rogelio *et al.*, 2017). Therefore, instead of this “one-microbe-at-a-time” approach (Raaijmakers, 2015), an alternative would be to create so-called synthetic microbial communities (SynComs), which as a community stands a better chance to survive and function in a non-sterile environment. However, it remains elusive to what extent a SynCom derived from a natural microbiome is effective in improving plant growth in a non-sterile environment, especially with the inclusion of an abiotic stress such as high salinity. And an efficient methodology of constructing and simplifying a functional SynCom is also unclear.

We characterized the bacterial microbiome of indigofera grown in Jizan soil under mimicked desert conditions and isolated strains representing the core root bacterial microbiome. Growth promoting effects of single strains and SynComs were studied on indigofera as well as the non-related crop tomato (*Solanum lycopersicum*). A SynCom of five bacterial strains promoted tomato growth under saline and non-sterile conditions. This increased salt tolerance was associated with both the differential expression of salt stress-related genes and ion accumulation in the shoot. Subsequent quantification of the relative abundance of SynCom strains revealed a low penetrance of the added SynCom,

Salt tolerance conferred by a SynCom

indicating that growth promotion can be triggered without affecting a native root microbiome.

Results

Growth promotion of indigofera by the microbiome in the Jizan soil

To find support for the importance of the root microbiome to plant fitness, we established an assay to study the growth of indigofera mimicking native growing conditions. Indigofera did not survive when grown in sterilized Jizan soil, suggesting that the soil microbiome is essential for plant growth. Since indigofera is a legume that, under native conditions, relies on nitrogen-fixing nodule symbiosis, we repeated the growth assay now adding a compatible rhizobium microsymbiont isolated from the Jizan soil sample (strain *Bradyrhizobium* sp. SA281). This rescued plant growth and could therefore serve as an axenic control. Next, we compared plant growth in sterilized Jizan soil complemented with *Bradyrhizobium* sp. SA281 and non-sterile Jizan soil. This revealed the plants in non-sterile soil produced more biomass compared to the control condition (Figure 1), suggesting that the native root microbiome is conducive to the growth of indigofera.

The bacterial root microbiome of indigofera is relatively simple but distinct

We questioned whether indigofera recruits specific bacteria. To study its root microbiome composition, indigofera was grown in Jizan soil under mimicked native conditions. Samples from the soil, rhizosphere (Rhizo) and endophytic compartment (EC) of 42-days-old indigofera plants were collected in at least three biological replicates from which DNA was extracted. An OTU table was constructed from the Illumina sequencing reads of the 16S rRNA gene V4 regions in these samples. Using the Bray-Curtis dissimilarity measure on the rarefied OTU table, the Soil, Rhizo, and EC samples were plotted with Principal Coordinate Analysis (PCoA) in two-dimensional space (Figure 2a). The first two principal coordinates explained 60% and 14% of the total variance, respectively. Rhizo and EC bacterial microbiomes hardly separated along the first coordinate but were clearly distinct from the Soil community. Conversely, the Rhizo and EC samples did form separate clusters along the second coordinate. This revealed that indigofera grown in Jizan soil possessed a distinct root microbiome when compared to the soil (PCoA1 60%) and with different bacterial communities in the rhizosphere and endophytic compartment (PCoA2 14%).

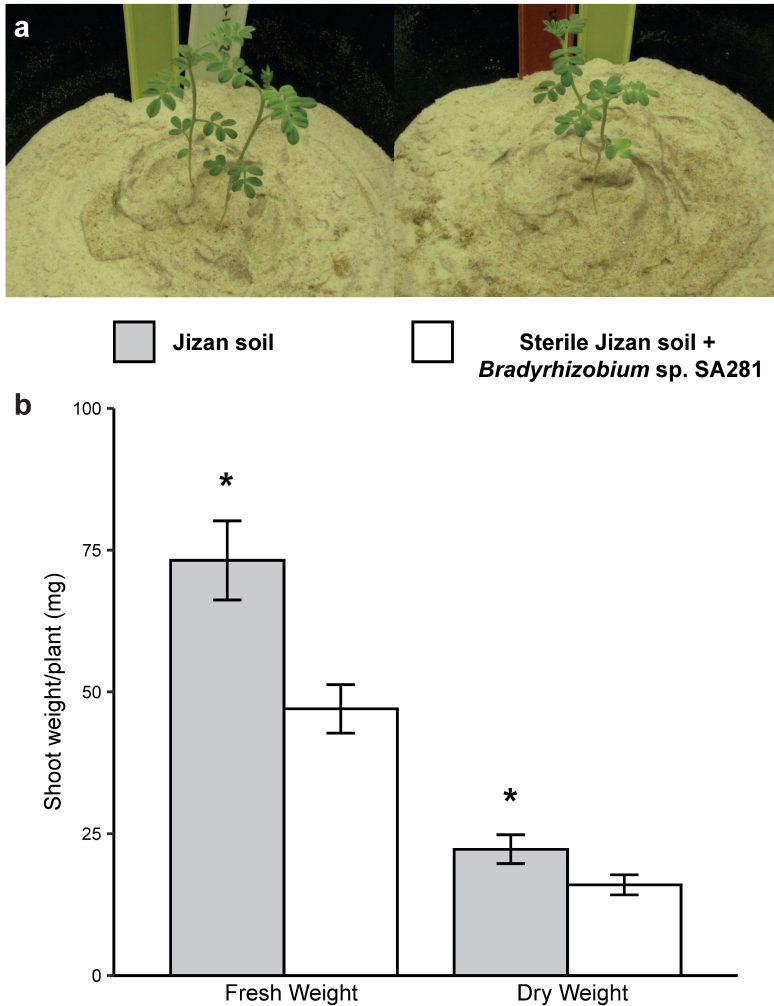


Figure 1: Jizan soil microbiome promotes growth of *Indigofera argentea*. (a) Six-week-old indigofera plants in Jizan soil (left) or sterile Jizan soil supplemented with the strain *Bradyrhizobium* sp. SA281 (right). There were four pots per treatment and each pot contained two indigofera seedlings. *Bradyrhizobium* sp. SA281 was isolated from nitrogen-fixing indigofera nodules grown in Jizan soil. (b) Fresh and dry shoot weight of indigofera plants at six weeks old show increased growth promotion triggered by the Jizan soil, when compared to sterile Jizan soil complemented with *Bradyrhizobium* sp. SA281. Asterisks indicate statistical significance ($p < 0.05$) as per one-way ANOVA.

Chapter 5

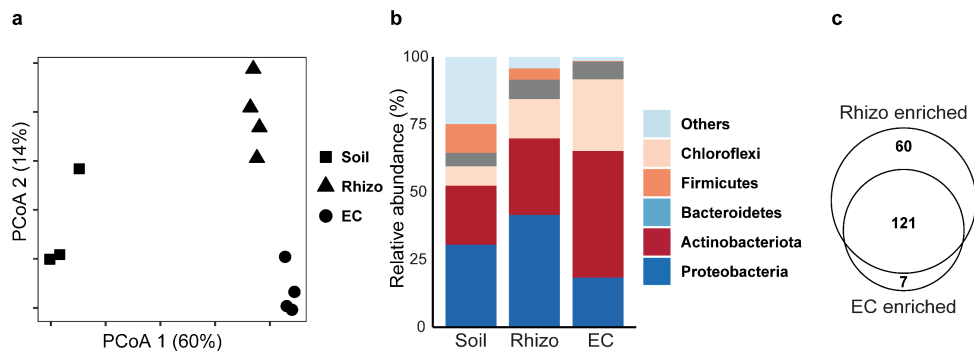


Figure 2: *Indigofera argentea* root microbiome in Jizan soil. (a) Principal coordinates analysis (PCoA) of the bacterial microbiomes in the soil, rhizosphere (Rhizo) and endophytic compartment (EC) of *indigofera* grown in Jizan soil for six weeks. The Soil is distinct from the Rhizo and EC along the first principal component. While the second component separates the Rhizo and EC. Bray-Curtis dissimilarities were calculated with OTU read counts after rarefaction and standard filtering. **(b)** Taxonomic classification of bacterial OTUs with relative abundance greater or equal to 5% grouped at the phylum level. The three bars represent the relative abundance of bacterial phyla in Soil, Rhizo and EC. There is a drop in bacterial diversity or number of rare phyla (indicated as "others") from the Soil to EC. **(c)** Venn diagram showing number of enriched OTUs in the Rhizo and EC of *indigofera*.

In line with the PCoA, the bacterial communities in each compartment also differed at the phylum level (Figure 2b). In the transition from the Soil to the EC, the biodiversity reduced due to a drop in the number of rare phyla (indicated as "Others"). Firmicutes and Proteobacteria were significantly depleted in the two root compartments compared to Soil, whereas the phyla of Chloroflexi and Actinobacteriota were significantly enriched in these compartments. Next, we determined the number of OTUs from the Soil that increased in their relative abundance in the Rhizo and EC. Compared to the Soil, 181 and 128 were enriched ($p < 0.001$) in the root compartments, of which 121 OTUs were shared between the Rhizo and EC (Figure 2c & Dataset S1). Also, a similar number of OTUs was depleted in the Rhizo and EC compartments when compared to the Soil (Dataset S1 & Fig. S2). This suggests a strong rhizosphere effect of *indigofera*, even though the Jizan soil

microbiome is relatively simple. Furthermore, there is strong commonality of bacterial community selection between the rhizosphere and endophytic compartment.

Plant growth promotion triggered by a Jizan SynCom in indigofera and tomato

To study the function of the root bacterial microbiome, we aimed to isolate the bacterial strains that showed an increased abundance in the indigofera root microbiome as determined by the OTU data described above. By applying a culture-dependent approach using different cultivation media, roughly two thousand bacterial isolates were obtained. All isolates were grouped by morphology and designated with the prefix SA (Saudi Arabia) followed by a strain number. Sanger sequencing of the full length 16S rRNA gene amplicon provided the V4 region of each isolate which could then be mapped back to an OTU found on the roots of indigofera. Ultimately, representative strains for nine of the most abundant OTUs shared between the Rhizo and EC could be identified. According to their relative abundance, these OTUs (Figure 3a) represented approximately 40% and 30% of the Rhizo and EC, respectively, and were collectively considered the core bacterial root microbiome of indigofera. We also included the isolates *Ensifer* sp. SA403 and *Bacillus* sp. SA436, which showed promise in promoting plant growth (Fig. S3) even though they belonged to the less abundant OTUs 38 and 49 – respectively. Additionally, previous work of culture-dependent isolation on a different sample batch but from the same ecological niche culminated in four growth promoting isolates that were also included in this study: *Pseudomonas argentinensis* SA190, *Acinetobacter radioresistens* SA188, *Enterobacter* sp. SA187 and *Ochrobactrum intermedium* SA148. (Lafi *et al.*, 2016; Lafi *et al.*, 2017a; Lafi *et al.*, 2017c; Lafi *et al.*, 2017b). The V4 sequences of the first three could be found in the indigofera microbiome (matching the OTUs 1333, 17 and 955 – respectively) though they did not belong to a dominant OTU.

Together, a total collection of 15 strains was used in further studies. It included species of the genera *Acinetobacter* and *Streptomyces* (phylum Actinobacteriota), *Bacillus* (phylum Firmicutes), and *Ensifer*, *Enterobacter*, *Massilia*, *Ochrobactrum*, *Pseudomonas*, and *Ralstonia* (phylum Proteobacteria) (Table 1). Draft genome sequencing was conducted to further characterize the selected strains (Table S1). Subsequently, maximum likelihood

Chapter 5

phylogeny was inferred from the nucleotide alignment of the 31 AMPHORA genes. This consisted of two separate analyses. First, the nine genera covering the 15 selected Jizan strains were analysed separately with reference and other root-associated strains (Dataset S2). This showed that several isolated Jizan strains are close relatives of species with reported plant-growth promoting effects. For example, *Bacillus* sp. SA436 is a close relative of the plant-growth promoting species *Bacillus megaterium* and *Bacillus aryabhattai* (Zhou *et al.*, 2016; Park *et al.*, 2017), *Ensifer* sp. SA403 to the nitrogen-fixing legume symbionts *Ensifer sojae* and *Ensifer alkanisoli*, and the five *Streptomyces* sp. to *Streptomyces leeuwenhoekii*, a species known to produce a variety of specialised metabolites (Gran-Scheuch *et al.*, 2018)(Fig. S4). Next, the 15 selected Jizan strains were compared to 61 earlier studied desert bacterial species of the same genera (Dataset S3). This revealed that the Jizan strains clustered together with the selected desert microbes at the genus level but diverged at the species or strain level (Figure 3b). Taken together, this shows that the selected Jizan strains are novel yet representative of species found in desert environments.

We questioned whether these isolated Jizan strains as a community triggered a similar plant growth promotion previously observed with indigofera grown in Jizan soil. Therefore, plants were grown in sterilized river sand that was inoculated with *Bradyrhizobium* sp. SA281. Half of the plants were also inoculated with an equal mixture of the 15 selected strains (the Jizan SynCom). Indigofera inoculated with the Jizan SynCom produced significantly more shoot biomass (42 days post-inoculation), when compared to the plants that were only inoculated with *Bradyrhizobium* sp. SA281 (Figure 3c). This showed that the Jizan SynCom triggered increased plant growth promotion when compared to only a diazotrophic and nodulating *Bradyrhizobium* strain. Next, we questioned whether this growth response was specific to indigofera or more generic, which would be of more practical significance in translating these results to agriculture. We tested the growth response of the Jizan SynCom on tomato (Moneymaker cultivar). The Jizan SynCom also triggered a significant growth response in tomato (Figure 3d). This demonstrated that the growth-promoting effect of the bacterial Jizan strains is a generic effect on plants.

Salt tolerance conferred by a SynCom

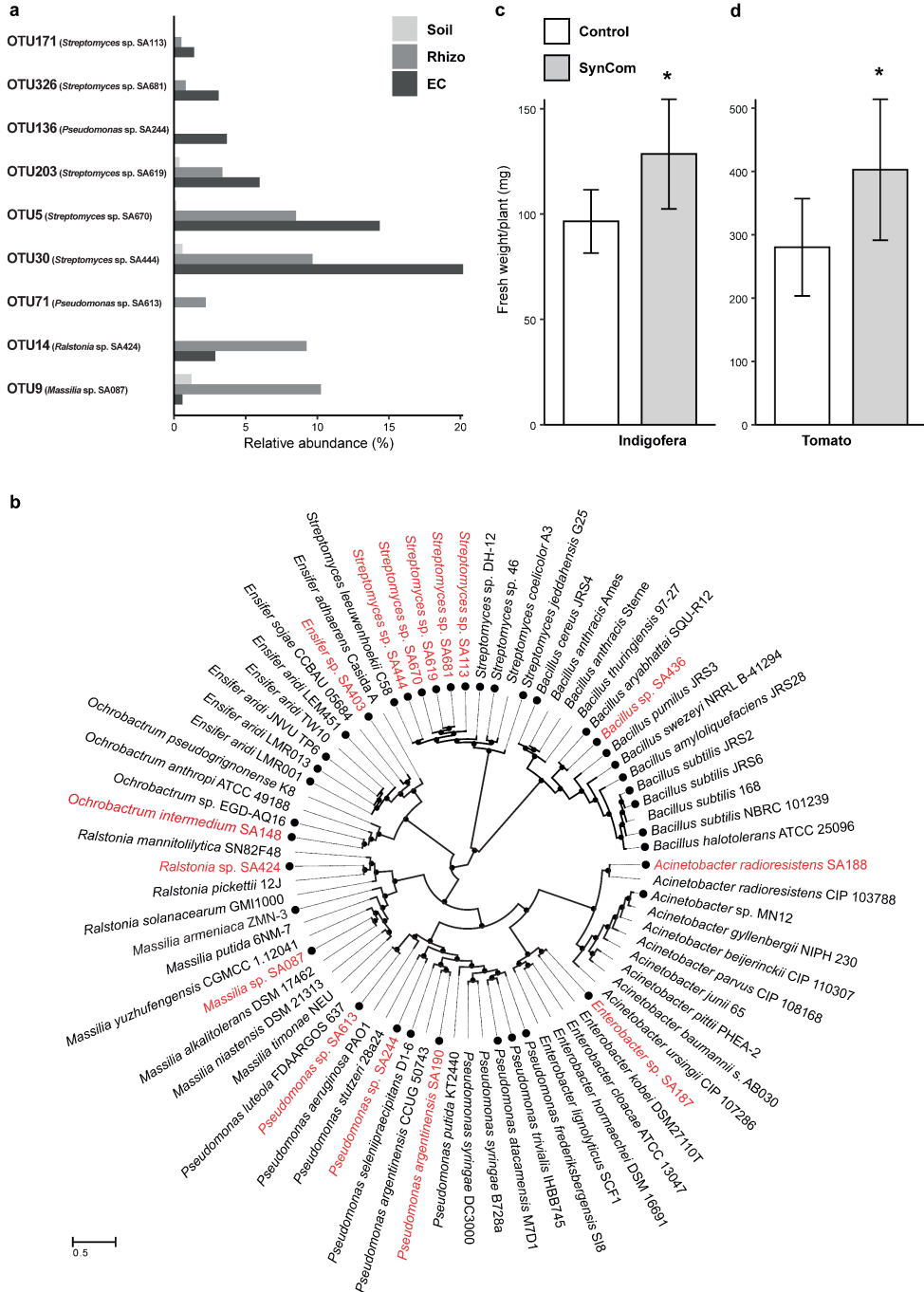


Figure 3: Relative abundance, phylogeny and plant growth promotion of the Jizan strains isolated from *Indigofera argentea*. (a) Jizan strains belonged to highly abundant OTUs in either the Rhizo or EC of *indigofera*. The x-axis shows the relative abundance of the best matching OTU for each Jizan strain. (b) Maximum likelihood tree based on the AMPHORA gene alignments of 15 Jizan strains - colored in red. The black filled circles on the outer perimeter indicate desert-associated strains. Representative strains for each genus were also included. The distance scale indicates the number of differences between sequences. (c, d) Quantitative analysis of shoot fresh weight of seven-week-old *indigofera* (c) and three-week-old tomato (d) plants grown under sterile conditions with or without the Jizan SynCom. In both cases, the Jizan Syncom led to a better plant yield compared to the control. Asterisks indicate statistical significance ($p < 0.05$) as per one-way ANOVA.

Jizan SynCom promotes tomato growth under salt stress and non-sterile conditions

We questioned whether the Jizan SynCom is also effective in promoting abiotic stress tolerance in other plant species and under non-sterile conditions. To test this, we used tomato and established a generic assay for analysing microbial effects on plant fitness under various conditions with the focus on salt stress in this study (Fig. S5). A controlled and reproducible non-sterile substrate was created by mixing sterilized river sand with 10% of a well characterized soil and supplemented with nutrient solution. We wanted to exclude interference from the endogenous SynCom strains present in the soil and evaluate SynCom effectiveness in the presence of another natural microbial community outside its native habitat. So, we collected soil from an ecological field station (the Mossel area at Veluwe, the Netherlands), referred to as the Mossel soil, of which the rhizosphere effect was characterized on a series of plant species (Schneijderberg *et al.*, 2020). Diluting the soil with sand allowed us to design a synchronized growth assay in which the effects of soil nutrients were reduced. The physical properties of the sand were also more suitable for the salt stress assay. Tomato seeds were sown in the 10% soil - 90% sand mixture and inoculated with/without the Jizan SynCom (approximately 10^9 cells per plant). After one week of growth in this soil mixture, plants were exposed to various salt levels (0, 100, 200 and 300 mM NaCl) (Fig. S5). Two weeks post salt imposition, the total plant biomass was quantified. First, we noted that under non-sterile conditions the Jizan SynCom promoted

tomato growth in the absence of salt (Fig. S6). Furthermore, the biomass was not significantly different between control and SynCom treated plants except for those exposed to 200 mM NaCl. In contrast, tomato plants without Jizan SynCom inoculation showed a clear decline in biomass proportional to the salt concentration. These results showed that the Jizan SynCom not only promoted tomato growth but also conferred tolerance to salt imposition. Since the 200 mM salt level provided a clear contrast in plant growth between the Jizan SynCom inoculated plants and non-inoculated control plants, it was set as the standard salt concentration for subsequent experiments in this study.

Bacterial SynCom triggered salt stress resilience associates with differential expression of salt stress related marker genes and ion content accumulation

We questioned whether a simplified Jizan SynCom can trigger salt tolerance under non-sterile conditions. First, individual strains were tested. Tomato plants were grown as described above, inoculated with 15 strains individually and exposed to 200 mM NaCl. Plants growing only in the non-sterile substrate served as an inoculum-free control. Of the 15 strains tested, *Ensifer* sp. SA403, *Ralstonia* sp. SA424, *Massilia* sp. SA087, and *Bacillus* sp. SA436 promoted tomato growth compared to the non-inoculated plants. The remaining strains did not significantly affect plant growth when compared to the control plants (Figure 4a). Interestingly, the Jizan SynCom inoculated plants showed the highest shoot biomass compared to other inoculated plants.

Next, we tested simplified SynComs containing a subset of the 15 strains from the Jizan core microbiome. Instead of using a targeted approach, we decided to randomly combine the strains. We did avoid taxonomic redundancy so that none of the simplified SynComs would have two or more strains of the same genus. In total, 20 combinations of 3 to 5 strains were tested on tomato plants growing in the non-sterile substrate and exposed to 200 mM NaCl (Table S2). This revealed that SynCom C, which consisted of *Massilia* sp. SA087, *Enterobacter* sp. SA187, *Ensifer* sp. SA403, *Bacillus* sp. SA436, and *Streptomyces* sp. SA444 led to the strongest growth response, having a 34% increase in dry shoot biomass compared to the non-inoculated control (Figure 4b) and even outperforming the 15 strain Jizan SynCom.

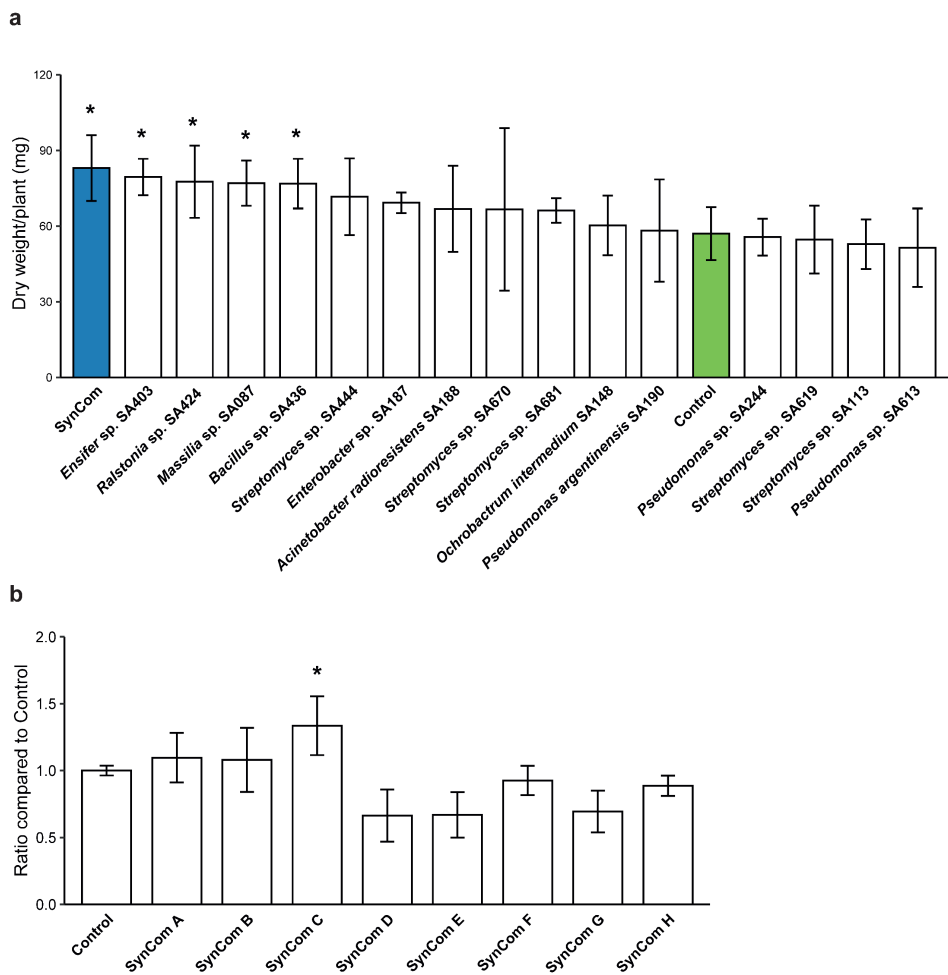


Figure 4: Growth promotion of the SynComs and individual Jizan strains on salt-stressed tomato plants. (a) The dry shoot weight of three-week-old tomato plants grown in the non-sterile substrate and inoculated with either a single Jizan strain or the SynCom as an equimolar mixture. Salt imposition was with 200 mM NaCl according to the assay described previously (Fig. S4). The SynCom (colored in blue) performed best and together with the strains *Ensifer* sp. SA403, *Ralstonia* sp. SA424, *Massilia* sp. SA087, *Bacillus* sp. SA436 were significantly different from the control plants (colored in green) which were not inoculated. **(b)** Ratios of the shoot dry weight of tomato plants treated with simplified SynComs to the control. Each SynCom contained four or five Jizan strains and the control was not inoculated. The five member SynCom C performed the best and was the only one

significantly different to the control. Asterisk indicates statistical significance ($p < 0.05$) as per Dunnett's test.

We questioned whether the increased biomass of salt-treated tomato plants inoculated with SynCom C is the result of a generic growth response, or alternatively, associated with salt stress-related physiological factors such as ion homeostasis or the expression of salt stress-related marker genes. To this end, leaf and root tissues were sampled from tomato at four, seven and ten days post salt imposition. Plants were grown either sterile (control), inoculated with SynCom C or with the five individual strains which compose this best performing SynCom. By including the five strains as separate inoculums, we aimed to validate that simultaneous presence of different strains as a SynCom is a prerequisite for the observed growth response. Quantification of the fresh shoot biomass showed that SynCom C was the only inoculum that significantly promoted tomato growth compared to the inoculum-free control (Figure 5a). Transcriptional analysis was then performed on root and shoot tissue for the salt stress related marker genes *CELLULOSE SYNTHASE A2 (CESA2)*, *HKT1;1*, *SALT OVERLY SENSITIVE 1 (SOS1)*, *SOS2* and *WRKY8* (Table S3). Four days post salt imposition, *SOS1*, *SOS2* and *WRKY8* expression was significantly upregulated in the root of tomato plants treated with SynCom C compared to the non-inoculated control (Figure 5b). This effect was not observed in the roots of plants inoculated with the individual strains. Conversely, in the shoot there was a significant downregulation of *SOS2* for the individual strains but not SynCom C (Fig. S7f). Interestingly, *HKT1;1* was upregulated in the shoot by SynCom C and three of the individual strains though none were significantly different to the control. This stands in contrast to the expression of the same gene in the root tissue where *HKT1;1* is downregulated by four of the inoculums including SynCom C. The ion content of the shoot tissue from the control and SynCom C inoculated plants was measured at ten days post salt imposition. This revealed that the Na^+/K^+ ratio was significantly lower in SynCom C inoculated plants, when compared to control plants (Figure 5c). To determine whether this effect is also observed in presence of a soil microbiome, the experiment was repeated but now plants were grown in the 10% Mossel soil + 90% sand mixture. Again, this showed the growth promoting effect of SynCom C under saline conditions and with a significantly lower Na^+/K^+ ratio than the control plants

Chapter 5

(Fig. S8b & d). Taken together, these results demonstrate that SynCom C triggers increased resistance to salt stress in tomato plants grown in non-sterile conditions.

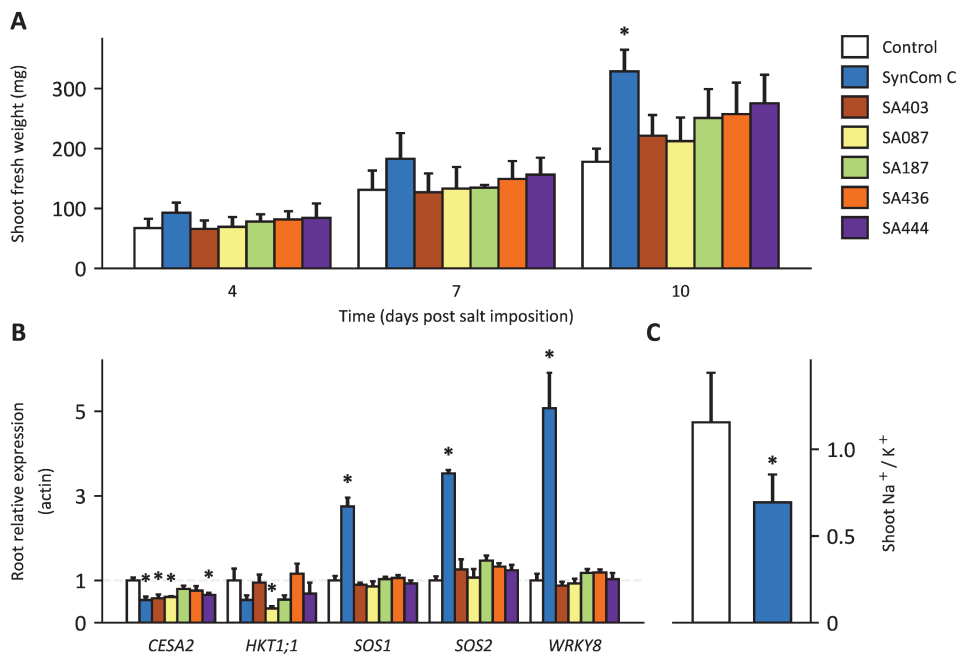


Figure 5: SynCom C induces salt stress tolerance related responses in tomato. Tomato seeds were sown in sterilized river sand and inoculated with the five-member SynCom C or the five individual strains. Plants were exposed to 200 mM NaCl on day seven. The root and shoot tissue were harvested on four, seven, and ten days post salt imposition. **(a)** Shoot fresh weight of the tomato plants for the three time points after salt imposition. A linear model was fitted to the biomass with the time points and inoculation as the explanatory variables. Only the SynCom C treated samples had a significantly different (p -value < 0.05) slope from the inoculum-free control samples. **(b)** Relative expression of salt stress resilience-related genes to Actin in the root tissue of tomato plants four days post salt imposition. An asterisk indicates a significant (p -value < 0.05) difference from the control, according to Dunnett's test. **(c)** The Na^+/K^+ ratio in the shoot of tomato plants ten days post salt imposition. SynCom C inoculated plants had a significantly lower ratio than the control (tested with Student's t -test). SynCom C is composed of the strains *Massilia* sp.

SA087, *Enterobacter* sp. SA187, *Ensifer* sp. SA403, *Bacillus* sp. SA436 and *Streptomyces* sp. SA444.

The Jizan SynCom colonized the root of tomato plants under non-sterile conditions

The degree of root colonization due to some treatment as an indicator of strain importance is the dominant approach taken in microbiome studies. This strategy also lends itself to the study of the inter-bacterial dynamics in either a native microbiome or, in our case, the interaction between a SynCom and its environment. As the 15 Jizan strains correspond to abundant OTUs in the root compartments of indigofera, their root colonization especially as a function of salt level could be a key factor leading to a successful plant phenotype.

To identify traits other than the growth promotion of single strains that can be used in the design of a SynCom, we conducted an experiment to measure the root colonization of the 15 Jizan strains in a non-sterile environment. Tomato plants were grown in the non-sterile substrate and half were inoculated with the Jizan SynCom. Plants were exposed to a single salt concentration ranging from 0 to 300 mM NaCl in 100 mM increments. The V4 16S rRNA gene region was sequenced with the Illumina HiSeq2500 platform on DNA isolated from the Soil, Rhizo and EC of each sample. Amplicon sequence variants (ASVs) were inferred from the sequencing reads and, after standard filtering, resulted in 10 029 248 reads distributed over 3 766 measurable ASVs.

With the V4 subregion from the 16S rRNA gene in the genome assemblies assumed as the expected sequence, the Jizan strains could be matched to ASVs which served as an indicator for strain presence and relative abundance (Table S4). This analysis showed that of the 15 Jizan strains, the ASVs of 8 strains were found among the measurable ASVs (designated as targeted ASVs). While the other seven strains, including two members of SynCom C (*Ensifer* sp. SA403 and *Streptomyces* sp. SA444), are not shown because they fell below the filtering criteria (Fig. S9). The relative abundances of each targeted ASVs in the three compartments were plotted along the salt gradient (Figure 6). Out of the eight targeted ASVs, ASV2 (*Pseudomonas* sp. SA244), ASV12 (*Enterobacter* sp. SA187), ASV13

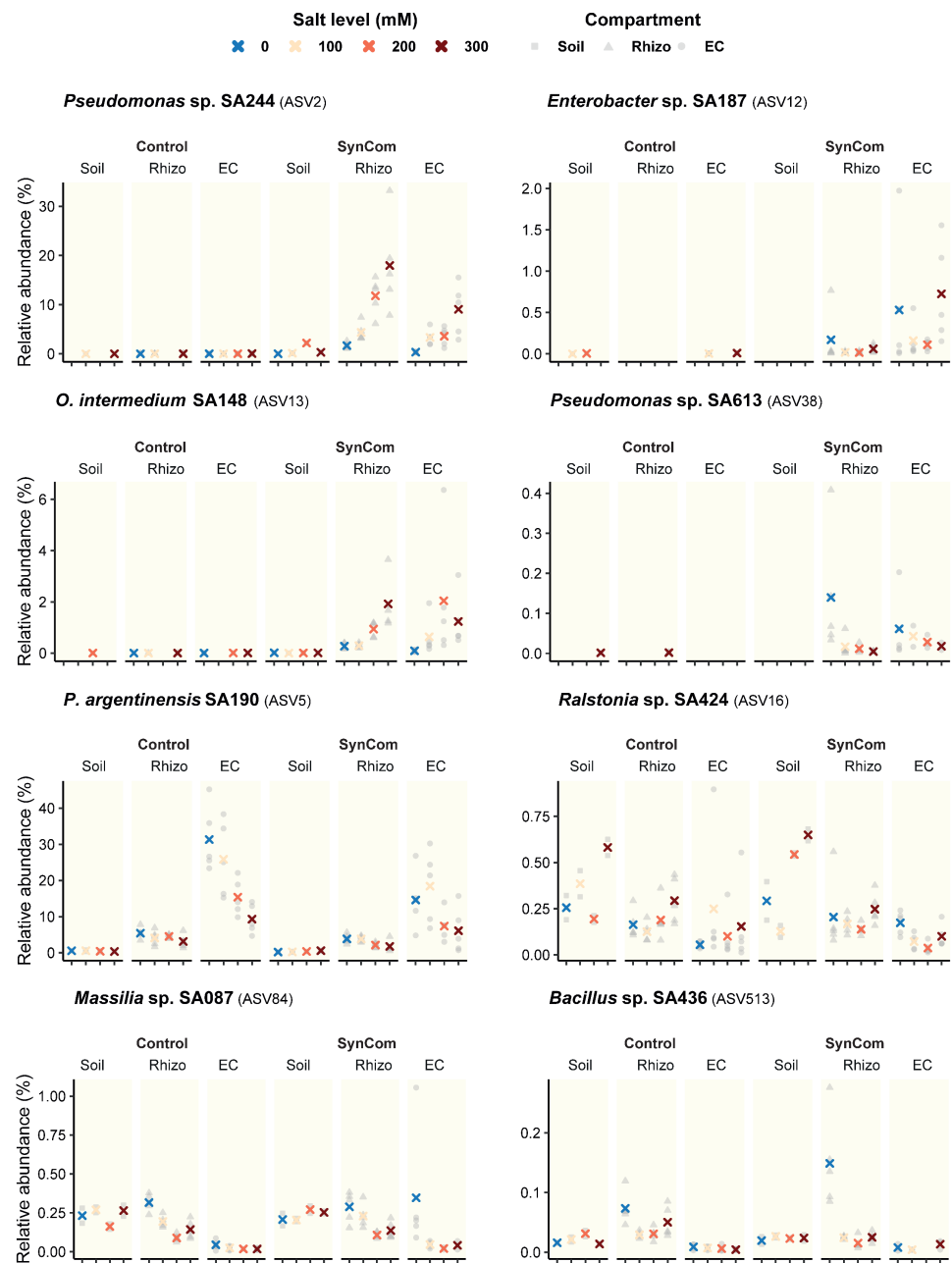


Figure 6: SynCom colonization at different salt levels in the soil and roots of tomato. Relative abundances of the bacterial ASVs in the Soil, Rhizo and EC of three-week-old tomato plants inoculated with or without the Jizan SynCom. Plants were grown in the non-

sterile substrate and were exposed to a salt gradient. The eight ASVs with a perfect match to the V4 region of the Jizan strains are shown here. The other strains fell below our filtering criteria (Fig. S8). The relative abundances of the replicates are shaded as gray symbols per compartment and the mean is shown as a cross with the color referring to the salt level.

(*O. intermedium* SA148) and ASV38 (*Pseudomonas* sp. SA613) as well as ASV91 (*Ensifer* sp. SA403) were not detected in the control but only in the soil inoculated with the Jizan SynCom. This indicated that the bacteria with these ASVs were likely not present in the non-sterile substrate and probably originated from the Jizan strains. Apart from the four targeted ASVs that were absent, ASV5 (*P. argentinensis* SA190), ASV16 (*Ralstonia* sp. SA424), ASV84 (*Massilia* sp. SA087), ASV513 (*Bacillus* sp. SA436) were detected both in the control and SynCom-inoculated samples. This prevents the differentiation of these four Jizan strains from the endogenous microbes present in the non-sterile substrate. Linear regression analysis showed that ASV2 (*Pseudomonas* sp. SA244) and ASV13 (*O. intermedium* SA148) significantly correlated with the salt level in the EC and, in the case of ASV2, also in the Rhizo (Fig. S10), which suggested the two strains belonging to these targeted ASVs were able to successfully colonize the roots under increasing saline conditions.

Moreover, bacterial network analysis was performed and the co-occurrence of targeted ASVs was determined as a function of the salt level. The bacterial co-occurrence analysis showed that ASV2 (*Pseudomonas* sp. SA244) and ASV13 (*O. intermedium* SA148) were always present in both root compartments; while ASV513 (*Bacillus* sp. SA436) and ASV84 (*Massilia* sp. SA087) were only present in the Rhizo and EC, respectively. The presence of the Jizan SynCom significantly increased the number of connections and, as a result, the average connectivity in the Rhizo and EC networks (Figure 7). As ASV2 and ASV13 were highly abundant in the root compartments, these two strains may have contributed to changes in the microbial networks, though their functions in the bacterial networks in the root compartment are yet unknown. Taken together, the presence of the SynCom C members was confirmed in this experiment, but only two of them could be definitively distinguished from the natural microbiome already present in the non-sterile substrate.

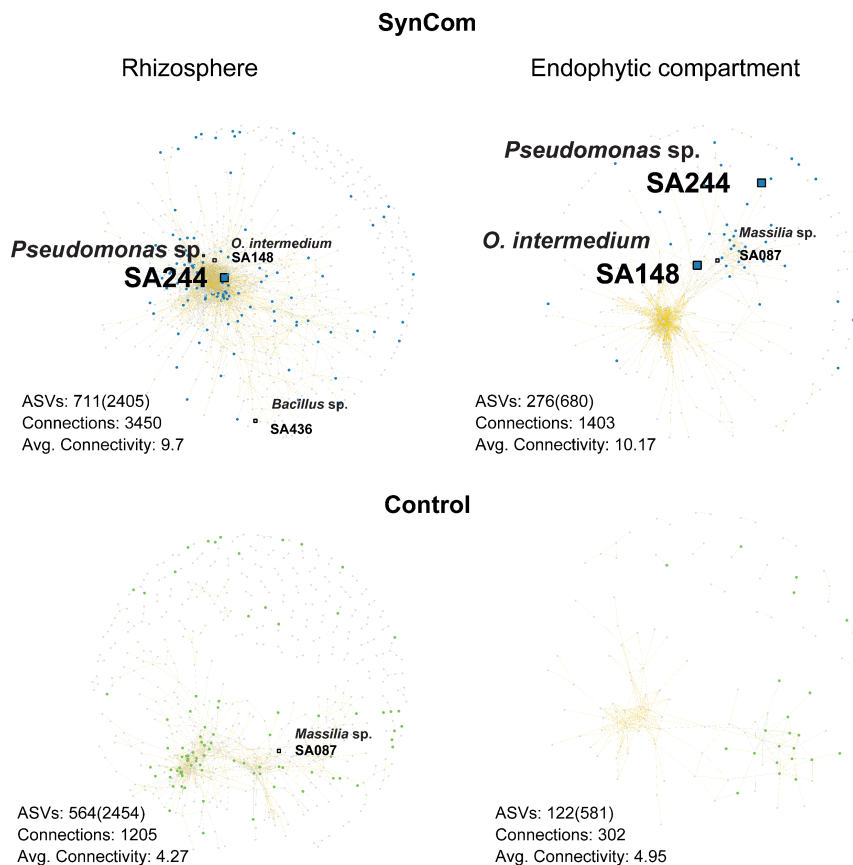


Figure 7: Bacterial co-occurrence networks in the root of tomato across a salt gradient.

Networks are based on Spearman's rank correlation between the ASVs in the Rhizo and EC of tomato growing in the non-sterile substrate with or without SynCom across a salt gradient from 0 to 300 mM NaCl. Only edges with a correlation score $|p| > 0.7$ and a $p < 0.001$ are shown. Positive and negative correlations are colored as gold and gray lines, respectively. Each node in a network is a detected ASV which means it passed these selection criteria. The square nodes are the ASVs belonging to a Jizan strain from the SynCom. A blue or green for the SynCom and control, respectively, indicates an ASV that was significantly enriched in any of the salt levels. The Jizan strains which were detected as well as enriched in a salt level are enlarged for clarity. Additional properties are shown below each network; ASVs: number of detected ASVs (initial number of ASVs), Connections: total number of edges, Avg. Connectivity: average number of edges per node.

Discussion

In this study, we showed that a bacterial SynCom originating from the Jizan desert plant *indigofera* promotes growth of the important economic crop tomato under salt stress in the presence of a non-sterile substrate that mimics a natural soil microbiome. Furthermore, we simplified this SynCom from the initial 15 to 5 strains. This simplified SynCom outperformed the plant growth promoting effect observed with the initial SynCom under the same experimental conditions. The five selected strains originate from the roots of the desert plant *indigofera* grown in a native soil. We argue that crop cultivation under abiotic stresses can be improved with microbiomes from such environments.

Some studies took a similar approach exploring desert microbiomes for the discovery of plant growth promoting rhizobacteria. For example, microbial communities have been analyzed from different desert regions, like Jizan, Thar, Atacama, Kalahari, Namib and Sahara deserts, as well as from various desert plant species (Mayak *et al.*, 2004; Rajput *et al.*, 2013; Sharma *et al.*, 2016; Singh & Jha, 2016; Eida *et al.*, 2018; Sarkar *et al.*, 2018; Bokhari *et al.*, 2019). Bacterial strains belonging to the genera *Pseudomonas*, *Bacillus*, *Klebsiella*, *Cupriavidus*, *Ochrobactrum*, *Isophtericola*, and *Enterobacter* were isolated and showed to promote growth of multiple plant species under saline conditions, including model plant species *arabidopsis* as well as crops like wheat (*Triticum aestivum*), rice (*Oryza sativa*), alfalfa (*Medicago sativa*) and tomato (de Zélicourt *et al.*, 2018; Shekhawat *et al.*, 2021).

In our opinion, confirming the plant growth promoting response of rhizobacteria is a critical step in determining the robustness of such a trait. Plant growth promoting responses under both abiotic and biotic stress induced by single strain inoculants has been well documented. Unfortunately, these strains often fail when they are applied individually in the field, which is attributed to competition by the local microbiome (Souza *et al.*, 2015). For this reason, there has been a shift from this so-called "one-microbe-at-a-time" approach to creating synthetic microbial communities (Raaijmakers, 2015). The general idea is that a community of microbes will be more competitive by forming a stable

Chapter 5

community and will be able to maintain the traits beneficial to plant growth in the field (Vorholt *et al.*, 2017). Other studies have attempted to combat salt stress with SynComs albeit in sterile conditions (Ahmad *et al.*, 2011; Egamberdieva *et al.*, 2017; Finkel *et al.*, 2020). However, to our knowledge there are no studies where a SynCom provides protection against salt stress to plants grown in the presence of a natural or local microbiome as seen under field conditions.

The quantification of shoot biomass was considered as the indicator for SynCom performance. From this data, it is unclear if the five member SynCom (SynCom C) leads to a higher biomass due to a specific microbe-mediated salt stress response or a general plant growth promotion. To verify, we measured the transcription of a selected list of salt stress related genes in tomato after SynCom C inoculation with a salt stress. This revealed that four days post salt imposition, the SynCom C mediated an early salt stress response in both the root and shoot tissues of tomato. For example, *SOS1*, *SOS2* and *WRKY8* were significantly upregulated in the root four days post salt imposition. The most common causes of salt stress on plant growth are ion toxicity (Flowers *et al.*, 2015), osmotic stress (Byrt *et al.*, 2018), and the accumulation of reactive oxygen species (ROS) (Ma *et al.*, 2012). As salt imposition causes large influxes of Na^+ into plant tissue, a critical step in the plant response is to recirculate and sequester Na^+ , as well as prevent further influx via the root (Wu *et al.*, 2019). The well-studied salt overly sensitive (SOS) pathway plays a crucial step in preventing Na^+ accumulation (Ji *et al.*, 2013). SOS3 is a calcium binding protein that senses cytosolic Ca^{2+} changes, caused by salt stress, and in turn interacts with SOS2, which belongs to the SnRK3/calcineurin-interacting protein kinase (CIPK) subfamily. The SOS3/SOS2 kinase complex phosphorylates the Na^+/H^+ exchanger SOS1, which is fundamental in Na^+ extrusion, distribution and long-distance transport in tomato (Olias, R. *et al.*, 2009). Mutant studies of *SOS1* show that it is essential for tomato NaCl tolerance, as gene silencing results in reduced growth (Olias, Raquel *et al.*, 2009). It is therefore interesting that we find an upregulation of *SOS1* in SynCom C inoculated plants in the presence of salt. Likewise, *SOS2* is highly upregulated four days post salt imposition, indicating that the SOS pathway is more active in SynCom C treated tomato plants than in the non-inoculated control. In addition, *HKT1-like* transporters are also essential in Na^+

recirculation and extrusion (Horie *et al.*, 2001). In arabidopsis and rice, ectopic expression of *HKT1;1* can increase Na^+ exclusion from the shoot (Moller *et al.*, 2009; Plett *et al.*, 2010). While the effect was not significant, there was an upregulation by SynCom C of *HKT1;1* in the shoot of tomato plants four days after the salt imposition (Zhao *et al.*, 2020). These findings suggest that SynCom C plays a role in the avoidance of ion toxicity, prompting an early activation of plant ion homeostasis mechanisms. This is in line with the lower Na^+/K^+ ratio in the shoot of SynCom C treated tomato plants. Additionally, none of the five SynCom C strains when applied as a separate inoculum showed a significant effect on plant biomass, nor was there a noticeable difference in the expression of genes that would indicate a salt stress response. This supports that SynCom C as a community is required for increasing salt stress resilience in tomato.

With the success of SynCom C, derived from the Jizan SynCom, we could evaluate the reported methods to design a suitable SynCom from a bacterial library. The key characteristics reported in literature rely on obvious traits such as plant growth promoting potential of single strains and, within the field of microbiome research, the presence of microbes in and around the roots (Vorholt *et al.*, 2017). A popular method to identify key species in a natural microbiome is based on the read counts of microbial sequences as an estimate of microbe presence (Muller *et al.*, 2016). This lends itself to the idea of a core microbiome and dominant OTUs, which we used to guide the isolation and selection of the original strains from the Jizan soil microbiome. The correlation between the abundance of a single strain and a triggered effect, such as abiotic stress tolerance, is considered to be indicative of a strain's relative importance (Naylor, D. *et al.*, 2017). By extending this idea to the interactions between strains, network analysis can reveal the effect of a treatment on microbiome structure, which can further guide the identification of key species (Faust & Raes, 2012). However, the key characteristics of the SynCom C strains did not meet the above expectations. Starting with the evaluation of plant growth promotion as a trait, only three of the five strains belonging to SynCom C significantly improved tomato growth under the same conditions when inoculated individually: namely *Massilia* sp. SA087, *Ensifer* sp. SA403, and *Bacillus* sp. SA436. The other two strains (*Enterobacter* sp. SA187 and *Streptomyces* sp. A444) showed a non-significant increase in

Chapter 5

biomass compared to the control. Interestingly, the community consisting of the best performing strains (SynCom A) did not significantly outperform the non-sterile control. This suggests that the selection criteria in the design of a SynCom should not solely rely on the plant growth promotion by a strain.

Shifting focus to the presence of microbes in or near the root, we would expect the five SynCom C strains to be dominant in relative abundance, positively correlated to the salt level and play a leading role in microbial network structure. Even though all SynCom C strains can be detected when added to a natural microbiome in combination with salt stress, none of the strains was dominant in abundance relative to the other strains detected from the Jizan SynCom. Interestingly, the only two strains (*Pseudomonas* sp. SA244 and *O. intermedium* SA148) that showed a positive correlation between read count and salt level did not belong to SynCom C. None of the SynCom C members showed a similar response to the salt gradient. Inoculation of the 15 strains from the Jizan SynCom influenced the microbial network of the natural microbiome by increasing the average connectivity. The network analysis revealed that only two members from SynCom C passed the detection threshold: *Bacillus* sp. SA436 and *Massilia* sp. SA087 in the rhizosphere and endophytic compartment, respectively. Both these strains were positioned in the periphery of their respective networks, which suggests a minor interaction with the natural microbiome. The SynComs containing *Pseudomonas* sp. SA244 and *O. intermedium* SA148, which were also present in the network and highly connected with the natural microbiome, did not perform as well as SynCom C. This suggests that solely relying on read count abundances from meta-amplicon sequencing is also not a reliable method for the design of a SynCom.

Overall, in this study, we isolated a core root bacterial microbiome of the desert plant indigofera and constructed a 15 strain SynCom that possesses a robust plant growth promoting effect on tomato when exposed to salt stress. The reduction of this Jizan SynCom led to a simplified version in the form of SynCom C, which retained its plant growth promoting effect. This SynCom was effective in specifically combating salt stress and did not lose effectiveness in a non-sterile environment. Our data suggests that a promising approach or strategy is in the combination of plant phenotype screening and

Salt tolerance conferred by a SynCom

more advanced and accurate methods, such as metagenomic, metatranscriptomics and metabolomics sequencing, to better model the predictive traits for a successful SynCom design.

Chapter 5

Materials and Methods

Bacterial strains and culture conditions

Bacterial strains were cultured in tryptic soy broth medium (TSB) at 28 °C. Fast growing strains were cultivated in 1/10th TSB for 1 day and slow growing strains were cultivated in ½ strength TSB for 5 days. Rhizobial strains were cultivated in yeast extract manitol (YEM) for 3-4 days. Bacterial cells were collected by centrifugation, washed three times with 0.9% NaCl and resuspended in appropriate solution according to the plant assay. The single strain cultures were adjusted to a final density of 0.5x10⁸ CFU ml⁻¹. The SynComs were an equimolar mixture of strains with a final concentration of 5x10⁸ CFU ml⁻¹ and each plant received in total 10⁹ cells.

Plant assay for indigofera and tomato

Indigofera seeds were surface sterilized by washing with ethanol and soaking in ¼ bleach for 10 minutes. Seeds were kept at 4 °C for three days followed by a seven-day incubation at 30°C. After germination, two seedlings were transplanted per pot containing either sterile river sand supplemented with *Bradyrhizobium* sp. SA281 or Jizan soil. The Jizan soil was collected from the Jizan desert in Saudi Arabia (Latitude 16.9405N; Longitude 42.6119E) and has a low nutrient content (Table S5). The river sand was sterilized by gamma radiation with a minimum dose of 25 kGy which is fatal to most microbes (Silliker, 1980). The water holding capacity (WHC) of the substrate was maintained at 30% with sterilized dH₂O. The climate room was configured at 35/25 °C day/night, 12 hours of light and 75% relative humidity to mimic the Jizan desert condition. The second indigofera experiment with the Jizan SynCom was identical in growing conditions and seed preparation. Two seedlings were transplanted to pots with sterile river sand inoculated with the Jizan SynCom or only with *Bradyrhizobium* sp. SA281 as a control. The sample size per treatment was four with two seedlings per replicate or pot. WHC was again maintained at 30% but *Fahräeus* medium was used once a week instead of sterile dH₂O. In both experiments, fresh and dry shoot weight were measured at day 42 post transplantation.

Tomato seeds of the MoneyMaker cultivar were sterilized with the same method. After vernalization, seeds were germinated in one day at 25 °C in the dark. The germinated seeds were sown into plastic cups containing, according to the experiment, either sterile river sand or the non-sterile substrate which was a 10/90% mixture of Mossel soil sourced from the Veluwe (the Netherlands) and sterile river sand. Inoculation by either a single Jizan strain or the 15-member Jizan SynCom followed immediately after sowing. Uniform seedlings were selected 7 days post sowing and the fresh weight recorded at day 21. Pots were randomly repositioned in the growing chamber (25 °C, 12hrs lighting, 60% relative humidity) several times throughout the growing period. Where applicable, the salt imposition always occurred on day 7 according to a modified protocol from a previous study (Awlia *et al.*, 2016) (Fig. S4). Pots were first watered to 60% WHC before soaking them in a saline solution for 30 minutes. The inflow of the saline solution will mix with the water present in the substrate and (after returning to 60% WHC) a target salt concentration is reached. For details refer to Fig. S4.

DNA extraction and sequencing

The soil, rhizosphere and endophytic compartment were isolated from the roots of tomato or indigofera following the procedure described previously (Schneijderberg *et al.*, 2020). In summary, the soil was defined as the sand easily removed from the roots by shaking. The roots were washed in sterile phosphate buffer (6.33 g $\text{NaH}_2\text{PO}_4 \cdot \text{H}_2\text{O}$, 16.5 g $\text{Na}_2\text{HPO}_4 \cdot 7\text{H}_2\text{O}$ & 200 μL Silwet L-77 in 1 L dH_2O , pH=7.0) and vortexed briefly. After removing the roots, the suspension was filtered through a 100 μm cell strainer and spun down for 10 min at 4,000 x g. Supernatant was discarded and the remaining pellet was the rhizosphere. For the EC: the roots were washed twice more with sterile phosphate buffer, transferred to a new tube with sterile phosphate buffer, sonicated for 10 min (with a 30 second pause in every minute) and dried on sterile filter paper. All samples were frozen in liquid nitrogen and stored at -80 °C. DNA from soil and rhizosphere samples was isolated using the Mo Bio PowerSoil kit (Qiagen) according to the manufacturer's instructions. According to the procedure described previously (Lundberg *et al.*, 2012), DNA from the EC samples was isolated using the Fast DNA Spin Kit for Soil (MP Biomedicals). Quality and quantity of the DNA was checked by nanodrop and gel electrophoresis. Per sample,

Chapter 5

around 400 ng was sent for 16S rRNA gene sequencing at Beijing Genomics Institute (BGI) with the V4 primers 515F and 806R. The samples from indigofera and tomato were sequenced with MiSeq and HiSeq, respectively.

Meta amplicon sequencing data processing

For the indigofera sequencing data, paired-end FASTQ reads were merged into contigs using PANDASeq (v.2.3) with a minimum overlap of 50 bp, minimum contig length of 100 bp and a Phred score of 25. Contigs were converted to FASTA format with the fastx-toolkit (v.0.0.13) into a single file. These reads were clustered into operational taxonomic units (OTUs) according to the UPARSE pipeline (Edgar, 2013) implemented in VSEARCH (v.1.1.3) (Rognes *et al.*, 2016). In short, the pipeline consisted of de-replication, sorting by abundance, and discarding singletons. OTUs were generated with the UPARSE algorithm and chimeric sequences were removed with the UCHIME algorithm. An OTU table was constructed by mapping reads back to the OTUs with the “usearch_global” algorithm from VSEARCH. Taxonomy based on the SILVA (V138) (Quast *et al.*, 2013) 16S rRNA gene dataset was assigned to the OTUs with the RDP classifier (v.2.10.1). All processing steps were implemented in a SnakeMake workflow.

For the tomato sequencing data, amplicon sequence variants (ASVs) were inferred from the Illumina paired-end FASTQ reads with the DADA2 pipeline (v.1.12.1) (Callahan *et al.*, 2016). FASTQ reads were filtered with the filterAndTrim function allowing for only one expected number of errors (maxEE=1) and discarding reads with any ambiguous nucleotides (maxN=0). Error rates were learned separately with the first 1×10^8 nucleotide bases of the filtered forward and reverse reads. The pseudo-pooling algorithm from the dada function together with the learned error rates predicted the ASVs in both orientations of the filtered reads after dereplication. The paired reads were merged with the mergePairs function and chimeras were removed by the consensus method with the removeBimeraDenovo function. The RDP Naive Bayesian Classifier algorithm (Wang *et al.*, 2007) as implemented in the assignTaxonomy function assigned the taxonomy of the ASVs against the SILVA (v138) dataset.

Meta amplicon sequencing data analysis

All analyses were performed in the R environment (v.3.6.3). The bacterial dataset of indigofera, which was the OTU table, was processed as described previously (Schneijderberg *et al.*, 2020). First, OTUs related to mitochondrial and chloroplast sequences were removed and it was named as “raw OTUs”. Next, the OTUs that have more than 25 reads in any sample were kept and they were named as “measurable OTUs”. The result was a table with 873 measurable OTUs with over 728 970 sequences divided over 11 samples (Dataset S4). Using the Bray-Curtis dissimilarity measure on a rarefied measurable OTU table, the soil, Rhizo and EC samples of indigofera were plotted with principal coordinate analysis (PCoA) in two-dimensional space. This was largely done with the vegan package (v.2.5.6).

For the bacterial dataset of tomato, which was the ASV table, ASVs related to mitochondrial and chloroplast sequences were removed. Then, ASVs with sequence length smaller than 253 or bigger than 254 bps were excluded. After this, data relating to our study were subset and named as “raw ASVs”. In order to track the SynCom members in our sequencing data, the V4 region of these strains were extracted and aligned with the sequences of “raw ASVs”. The “raw ASVs” table was then filtered and ASVs (which have more than 25 reads in at least 5 samples) and named as “measurable ASVs”. The custom R commands were used in these analyses, mainly retrieved from the R packages tidy (v.1.1.1), reshape2 (v.1.4.4), ggplot2 (v.3.3.2) and fmsb (v.0.7.0).

For differential abundance test, we used the same method as implemented in a previous study (Schneijderberg *et al.*, 2020). To test OTUs differently abundant between the Rhizo and EC in comparison to Soil, we used the default setting to create the normalized OTU table from “raw OTUs”. Next to it, the fitZig function and default settings in the metagenomeSeq package (v.1.28.2) (Paulson *et al.*, 2013) were used for differential abundance testing. This was the same for tomato where the “raw ASVs” were tested for differential abundance between no salt (0 mM) and each salt treatment (100, 200, 300 mM NaCl input) for all three compartments. Furthermore, for the enriched ASVs, the

Chapter 5

correlation between their abundance (log2-normalized reads) and increasing salt gradients was tested with linear regression.

We constructed co-occurrence networks between bacterial ASVs embedding all salt levels in three compartments in both control and SynCom inoculation conditions, using a custom implementation of publicly available scripts (Hartman, 2018). For these networks, we used the normalized ASV table and conducted Spearman rank correlations between ASVs. The networks were visualized with the Fruchterman-Reingold layout (50000 permutations) in igraph and show the strong and significant correlations ($|p| > 0.7$ and $p < 0.001$).

Bacteria isolation and correlation analysis

To isolate strains from the rhizosphere and endophytic compartment of indigofera grown in the Jizan soil, serial dilutions of the glycerol stocks obtained from these compartments were plated on 1/10th TSA, King's B, R2A and ISP3 agar media. Plates were incubated at 28 °C for 14 days. Colony appearance was monitored daily and independent colonies were re-streaked on 1/10th TSA plates. Colonies were re-streaked on fresh 1/10th TSA plates once more to ensure purity. The 16S rRNA gene was amplified with primers 63F 5'-CAGGCCTAACACATGCAAGTC-3' and 1389R 5'-ACGGGCGGTGTGTACAAG-3' (Hongoh *et al.*, 2003) of fresh colonies in replicate. PCR products were sequenced at Macrogen (Amsterdam, the Netherlands). All 16S rRNA sequences were processed with Geneious 8.1.9 (<https://www.geneious.com>) and submitted to RDP database for taxonomic identification. For the correlation analysis, the V4 region of the 16S rRNA gene sequences were aligned with the consensus sequences of the indigofera OTUs. Isolates with the V4 region matching OTUs with more than 97% identity were kept. Representative isolates of these OTUs were selected for strain level analysis by using BOX-PCR with primer BOXA1R 5'-CTACGGCAAGGCGACGCTGACG-3' (Selvakumar *et al.*, 2016) and repetitive strains were removed by comparing the genetic profiles. In the end, 11 strains were selected including 9 strains belonging to high abundant OTUs and 2 strains belonging to relatively low abundant OTUs but potentially promoting plant growth. Their glycerol stocks were prepared and stored at -80 °C.

Genome assemblies and phylogeny

Illumina paired-end FASTQ files were cleaned with Trimmomatic (v.0.38) (Bolger *et al.*, 2014) by clipping reads if the average Phred quality score within four consecutive bases dropped below 28 (SLIDINGWINDOW:4:28). The trimmed FASTQ files were then assembled into contigs by SPAdes (v.3.12.0) (Bankevich *et al.*, 2012) with the careful option turned on and k-mer sizes of 21, 33, 55, and 77 nt. A high amount of assembly contamination (up to 79%) was detected by CheckM (v.1.1.2) (Parks *et al.*, 2015) in the following genera: *Bacillus* (SA436), *Ensifer* (SA403), *Massilia* (SA087), *Pseudomonas* (SA613 and SA244), *Ralstonia* (SA424), and *Streptomyces* (SA113, SA444, SA619, SA670 and SA681). These assemblies were cleaned with K-means clustering (Python Scikit-learn) (Pedregosa *et al.*, 2011) on the tetranucleotide signatures of the contigs. A second round of CheckM indicated a drop in contamination to below two percent for all assemblies. Finally, assembly statistics and genome completeness were assessed with QUAST (v.5.0.0) (Gurevich *et al.*, 2013).

The phylogeny of the Jizan strains was inferred by maximum likelihood on concatenated AMPHORA gene alignments. For the nine genera, candidate accessions were selected from the NCBI RefSeq database based on several criteria. First, all the reference assemblies from each genus were included. Additional accessions were either plant root-associated or isolated from a desert habitat. The coding domain sequences and translated protein sequences were downloaded from NCBI in September 2020. For the Jizan strains, the open reading frames (ORFs) on the contigs were predicted by Prodigal (v.2.6.3) (Hyatt *et al.*, 2010). Hidden Markov Model profiles of the AMPHORA proteins were downloaded from the AMPHORA2 GitHub repository (Wu & Scott, 2012). These were used by hmmsearch (v.3.2) (Eddy, 2011) to identify the best protein hit in the translated ORFs with an E-value threshold below 0.001. Accessions without the full set of 31 AMPHORA genes were discarded from the analysis. The AMPHORA genes were aligned separately with Clustal Omega (v.1.2.4) (Madeira *et al.*, 2019) and inspected manually. A multiple sequence alignment (MSA) was constructed by concatenating the AMPHORA gene alignments per accession. Phylogeny was inferred on the MSA with IQTree (v.1.6.12) (Nguyen *et al.*, 2015). The affiliated tool ModelFinder (Kalyaanamoorthy *et al.*, 2017) identified the best-

Chapter 5

fit substitution model for each MSA. Finally, trees were visualized with the Python framework ETE3 (Huerta-Cepas *et al.*, 2016).

Gene expression and ion content assay

Tomato seeds were grown in sterile river sand, inoculated with either SynCom C, SA087, SA187, SA403, SA436 or SA444 and exposed to a 200 mM salt stress as described in Fig. S4. Plant shoot and root tissue were harvested at 4-, 7- and 10-days post salt imposition. The fresh shoot weight was recorded, and the root tissue was carefully extracted from the sand and vortexed briefly in phosphate buffer. All samples were frozen in liquid nitrogen and stored at -80 °C.

Five candidate genes for salt tolerance in tomato were chosen based on literature. The genes *HKT1;1*, *WRKY8*, *SOS1* and *SOS2* were previously shown to be associated with salt tolerance in tomato (Rus *et al.*, 2001; Olias, R. *et al.*, 2009; Huertas *et al.*, 2012; Kou *et al.*, 2019; Gao *et al.*, 2020). The gene *CESA2* was also included as it showed a high homology to *AtCESA6*, which is important to salt tolerance in *Arabidopsis thaliana* (Zhang *et al.*, 2016). Of these five genes, the primer sequences of *WRKY8* were taken from literature. For the others, custom primers were designed in silico on the RefSeq tomato assembly SL3.0 (GCF_000188115.4) with Geneious 11.1.5 (<https://www.geneious.com>). *Actin* was chosen as the housekeeping gene for normalization within samples (Lovdal & Lillo, 2009). Primer sequences, GC content, annealing temperature (T_m), expected amplicon length, NCBI GeneID, and references are shown in Table S3. Primer efficiencies were confirmed to be around 100% for all primer pairs using a range of serial dilutions.

Total RNA was extracted from the shoot and root tissue with the E.Z.N.A.® Plant RNA kit (OMEGA BioTek). An optimal on-membrane DNase digestion step was performed during the RNA extraction by adding 10 µL DNase 1 and 70 µL Buffer RDD from the Qiagen DNase 1 kit. RNA quantity and purity as well as integrity were checked by Nanodrop and agarose gel electrophoresis. cDNA was synthesized from 300 and 600 ng of root and shoot RNA, respectively, with the iScript™ Select cDNA Synthesis kit (Bio-Rad). The synthesis reaction was carried out at 25 °C for 5 minutes, 46 °C for 20 minutes followed by 1 minute at 95 °C. cDNA samples were diluted 5 times, aliquoted and stored at -20 °C. For the qPCR, each

reaction contained: 5 μ L IQ™ SYBR®, 2 μ L cDNA and 1.5 μ L of the forward and reverse primers with a total volume of 10 μ L. Samples were loaded into a CFX Connect™ system (Bio-Rad) and initialized at 95 °C for 3 minutes, followed by 40 rounds of thermocycling. Each cycle started at 95 °C for 15 seconds, followed by 30 seconds at the primer-specific T_m (average temperature of the forward and reverse primers). Melting curves of all samples (from 55 °C to 95 °C in 5 second intervals with a 0.5 °C increment after each cycle) showed primer specificity and no primer-dimer formation. Relative expression of target genes was calculated for shoot and root tissue per timepoint as described previously (Livak & Schmittgen, 2001). Calculations were based on the control treated plants with salt as the reference group and Actin as the reference gene. Relative expression level (fold change) was calculated by the $2^{-\Delta\Delta C_t}$ method. Statistical significance was determined by a Dunnett's test on the relative expression levels.

Ion concentrations was measured in tomato seedlings at ten days post salt imposition using an Ion Chromatography (IC) system 850 Professional (Metrohm, Switzerland), essentially as described previously (Roman *et al.*, 2020). Leaves of tomato seedlings were weighed in glass screw cap test tubes, dried and ashed in a furnace at 575 °C for 5 h. After cooling down to room temperature 1 mL formic acid (3M) was added to each tube. Samples were heated at 103 °C for 15 min with shaking at 600 rpm. The extracts were then diluted by adding 9 mL of milliQ water to each sample. The samples were again heated and mixed at 80 °C for 30 mins. After cooling down to room temperature all samples were measured in two dilutions 1/100 and 3/100 using a Metrohm 881 Compact IC pro ion chromatograph. Data was expressed in mg ion/mg dry weight.

A similar experiment was carried out with the same inoculums but in the non-sterile substrate. The shoot tissue of plants at ten days post salt imposition was harvested in order to record the fresh weight and to measure the ion content as described above.

Chapter 5

Acknowledgements

We thank the industrial partners BaseClear, BDS, Bejo Seeds, ENSA seeds, Incotec, Koppert, Plant Health Cure and Microlife Solutions, for their feedback on the project. This work was supported by the Netherlands Organisation for Scientific Research NWO-TTW (grant 14220, Microbial support of plant growth under abiotic stress to R.G. and T.B.).

Author contributions

LS, ZY, XC, MdR, RP, QZ, CF executed the experiments. LS, MS, ZY, RvV constructed and implemented the bioinformatics pipelines. LS, ZY, MS, XC conducted *in silico* analyses. AD and LMT performed ion content analysis. TB and RG initiated this project and helped setting up this study. LS, ZY, RG and XC wrote the manuscript.

Tables and legends:

Table 1: Selected bacterial strains of the root microbiome of *Indigofera argentea* grown in Jizan soil. Eleven strains were isolated in this study, including nine strains belonging to highly abundant OTUs representing ~40% and ~30% of rhizosphere and endophytic compartment, respectively, and two low abundant or rare strains with potential PGPR traits. Four additional strains with PGPR traits were collected from previous studies. These 15 strains together were used for SynCom construction.

Source	Strain Code	OTU	Class	Order	Family	Genus
Current work	Highly abundant					
	SA670	5	<i>Actinobacteria</i>	<i>Actinobacteria</i>	<i>Streptomycetaceae</i>	unclassified
	SA087	9	<i>Beta-Proteobacteria</i>	<i>Burkholderiales</i>	<i>Oxalobacteraceae</i>	<i>Massilia</i>
	SA424	14	<i>Beta-Proteobacteria</i>	<i>Burkholderiales</i>	<i>Burkholderiaceae</i>	<i>Ralstonia</i>
	SA444	30	<i>Actinobacteria</i>	<i>Actinobacteria</i>	<i>Streptomycetaceae</i>	<i>Streptomyces</i>
	SA613	71	<i>Gamma-Proteobacteria</i>	<i>Pseudomonadales</i>	<i>Pseudomonadaceae</i>	<i>Pseudomonas</i>
	SA244	136	<i>Gamma-Proteobacteria</i>	<i>Pseudomonadales</i>	<i>Pseudomonadaceae</i>	<i>Pseudomonas</i>
	SA619	203	<i>Actinobacteria</i>	<i>Actinobacteria</i>	<i>Streptomycetaceae</i>	<i>Streptomyces</i>
	SA681	326	<i>Actinobacteria</i>	<i>Actinobacteria</i>	<i>Streptomycetaceae</i>	unclassified
	SA113	171	<i>Actinobacteria</i>	<i>Actinobacteria</i>	<i>Actinomycetaceae</i>	unclassified
	Potential PGPRs					
	SA403	38	<i>Alpha-Proteobacteria</i>	<i>Rhizobiales</i>	<i>Rhizobiaceae</i>	<i>Ensifer</i>
	SA436	49	<i>Firmicutes</i>	<i>Bacillales</i>	<i>Bacillaceae</i>	<i>Bacillus</i>
Previous work	SA148	-	<i>Alpha-Proteobacteria</i>	<i>Rhizobiales</i>	<i>Brucellaceae</i>	<i>Ochrobactrum</i>
	SA187	955	<i>Gamma-Proteobacteria</i>	<i>Enterobacterales</i>	<i>Enterobacteriaceae</i>	<i>Enterobacter</i>
	SA188	17	<i>Gamma-Proteobacteria</i>	<i>Pseudomonadales</i>	<i>Moraxellaceae</i>	<i>Acinetobacter</i>
	SA190	1333	<i>Gamma-Proteobacteria</i>	<i>Pseudomonadales</i>	<i>Pseudomonadaceae</i>	<i>Pseudomonas</i>

Supplementary information:



Fig. S1: Former agricultural areas in the Jizan desert, which suffer from high salinity, are scarcely populated with indigofera.

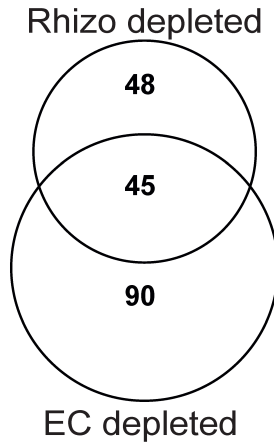


Fig. S2: Venn diagram showing number of depleted OTUs in the Rhizo and EC of *L. argentea* in comparison to the Soil. See Dataset S1.

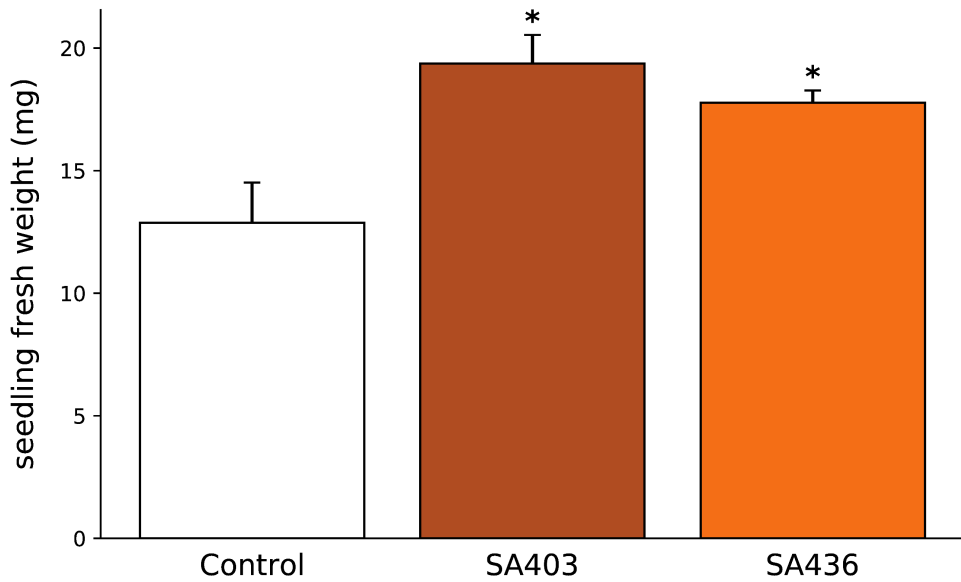
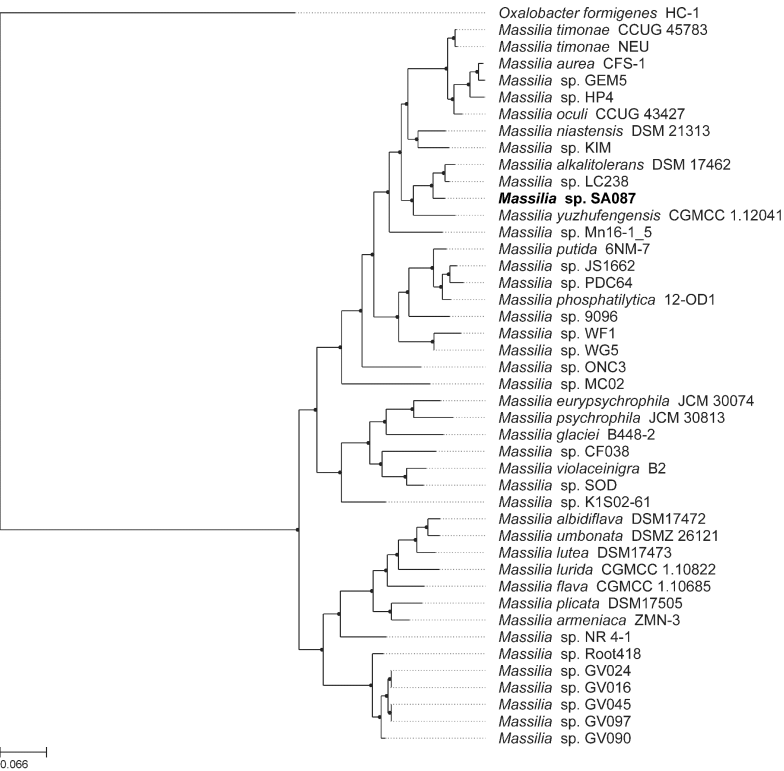
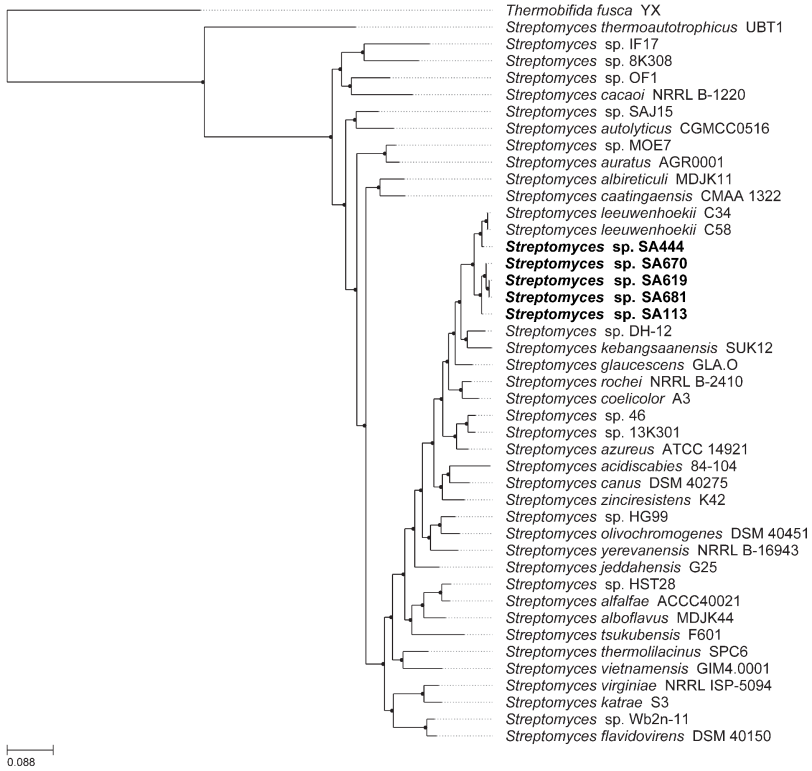


Fig. S3: Growth promotion of arabidopsis by the Jizan strains *Ensifer* sp. SA403 and *Bacillus* sp. SA436.

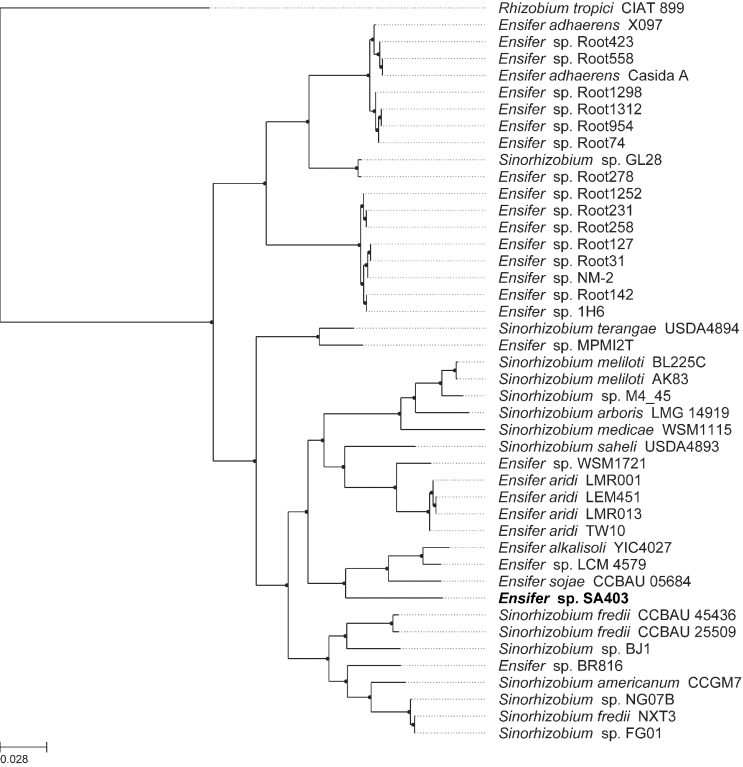
a



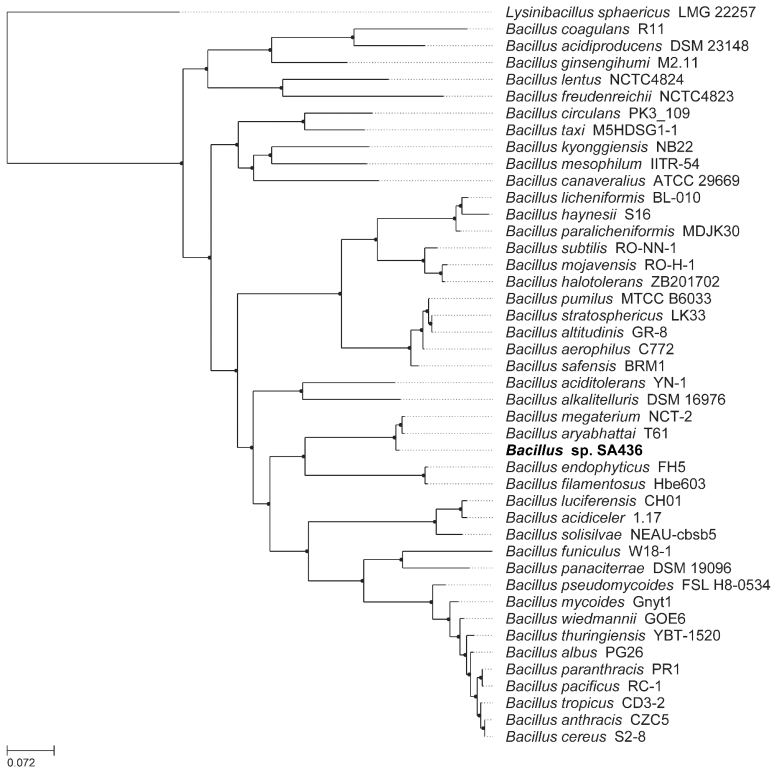
b

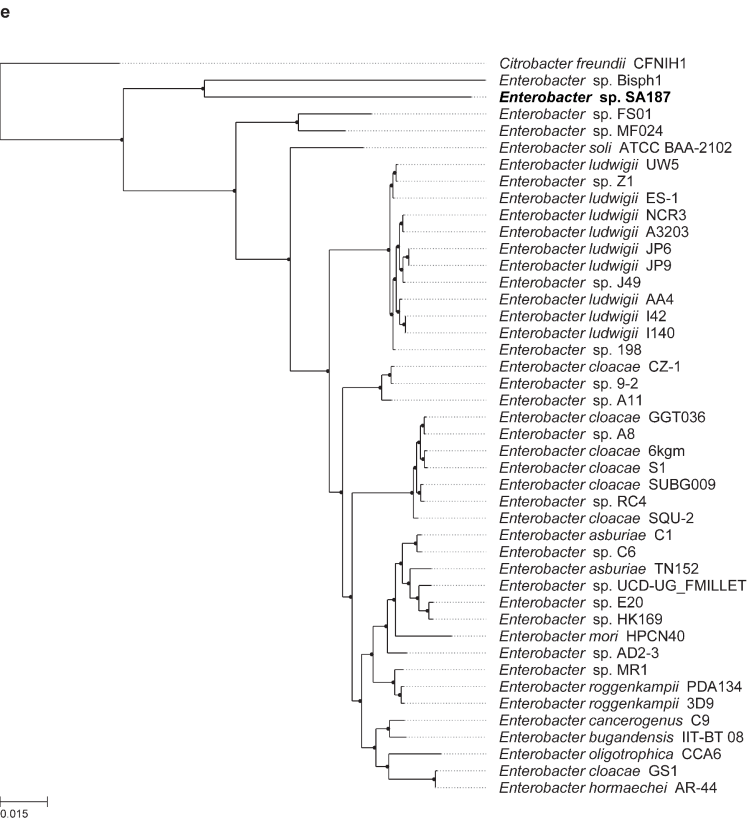


c

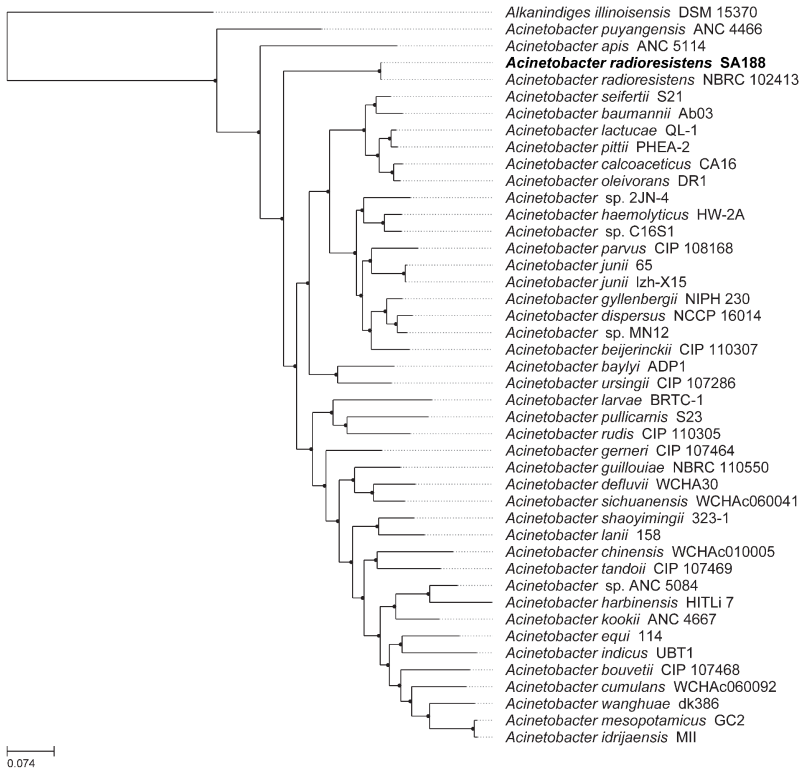


d

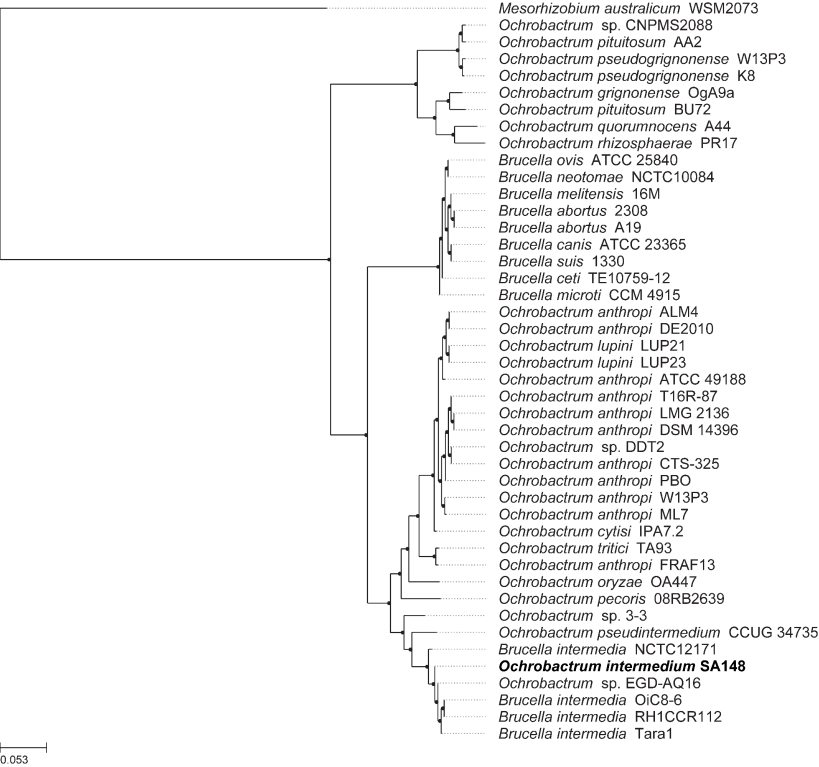




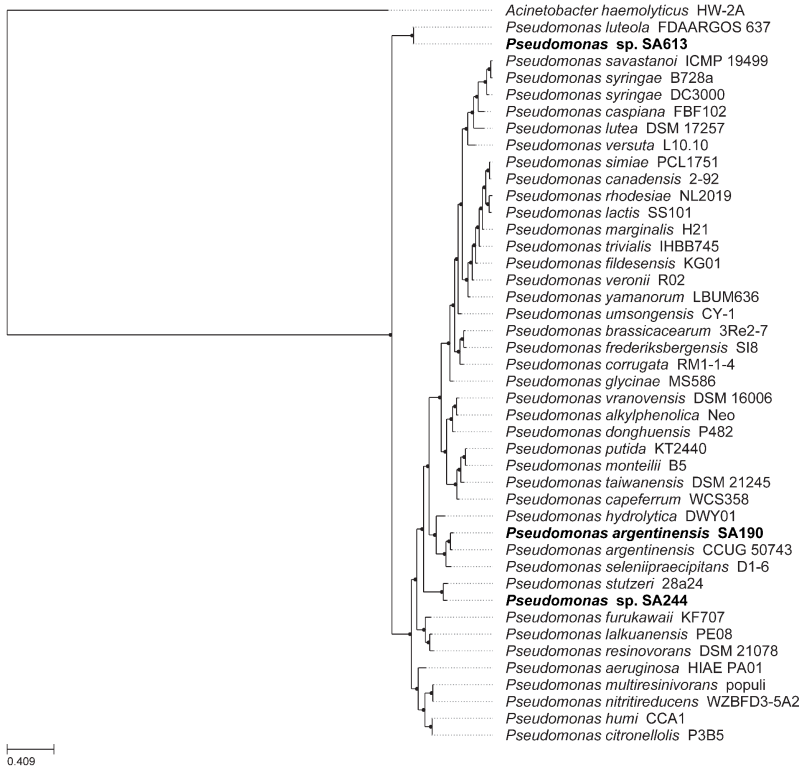
f



g



h



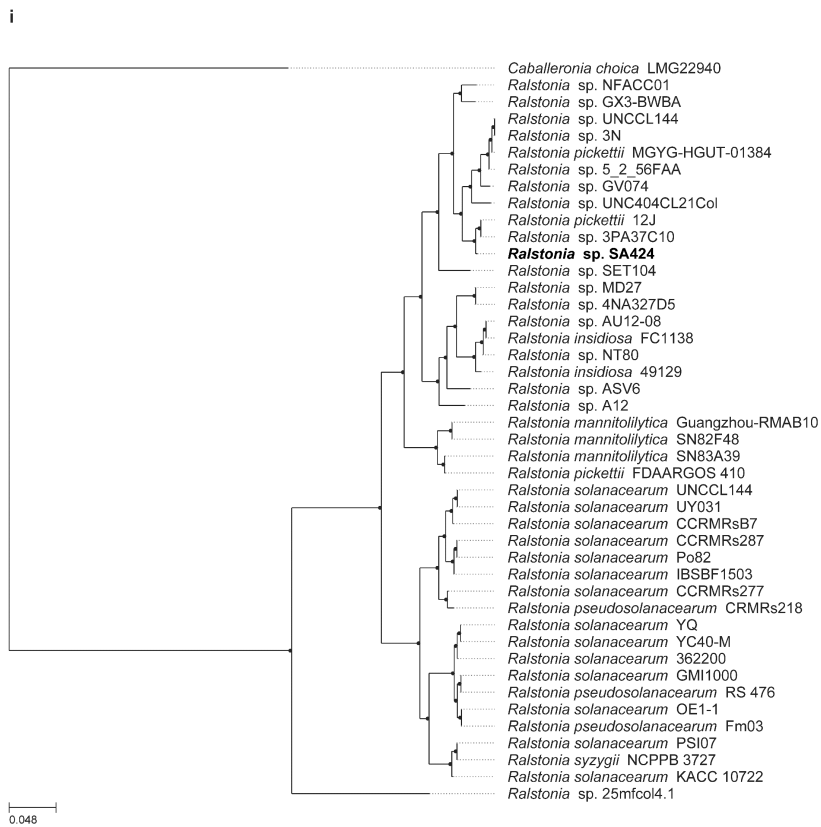


Fig. S4: Maximum likelihood trees based on the AMPHORA gene alignments of nine different genera. (a) *Massilia*, (b) *Streptomyces*, (c) *Ensifer*, (d) *Bacillus*, (e) *Enterobacter*, (f) *Acinetobacter*, (g) *Ochrobactrum*, (h) *Pseudomonas*, (i) *Ralstonia*. Each tree contains at least one of the strains found in the Jizan SynCom, representative genomes and plant-associated strains for that genus. All trees are rooted on a suitable outgroup and the Jizan strains are shown by bold font. The distance scale indicates the number of differences between sequences.

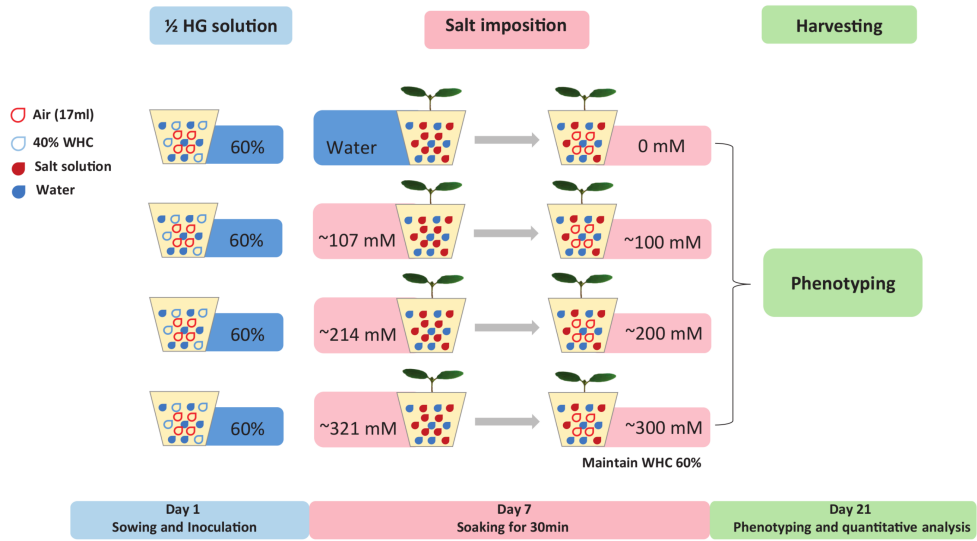


Fig. S5: Tomato salt stress assay. The salt stress assay was adapted from a protocol by *Awlia et al., 2016*. Pots with plants are soaked in a saline solution for about 30 minutes. As the WHC is always maintained at 60%, there is a certain volume of water already present in the substrate. When the saline solution enters through the bottom of the cups during the soaking, the salt concentration lowers as the solution is diluted by the water present in the substrate. The volume of saline solution that enters the pot is equal to the remaining 40% WHC plus extra air. This extra air volume is a result of the supersaturation by the soaking method which exceeds the amount predicted by 100% WHC. As the WHC returns to 60% due to evaporation and transpiration, the diluted saline solution will concentrate to a target concentration in the substrate.

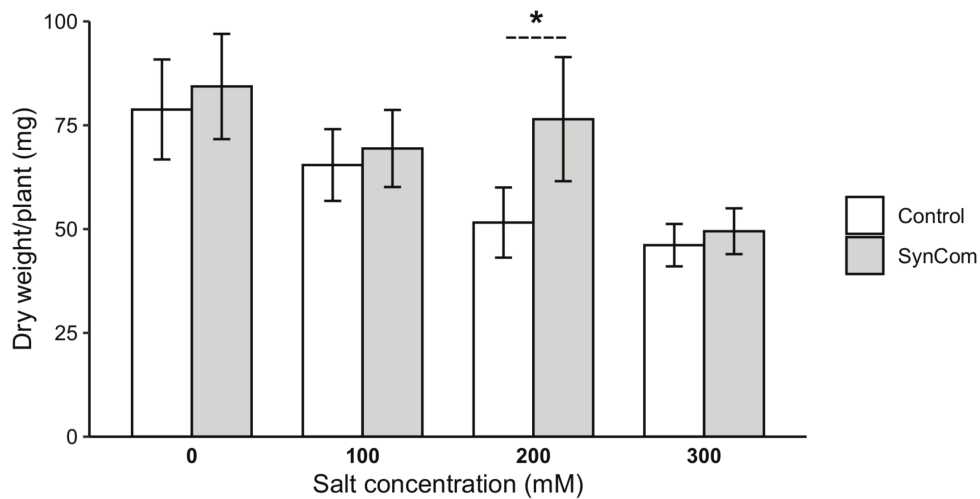
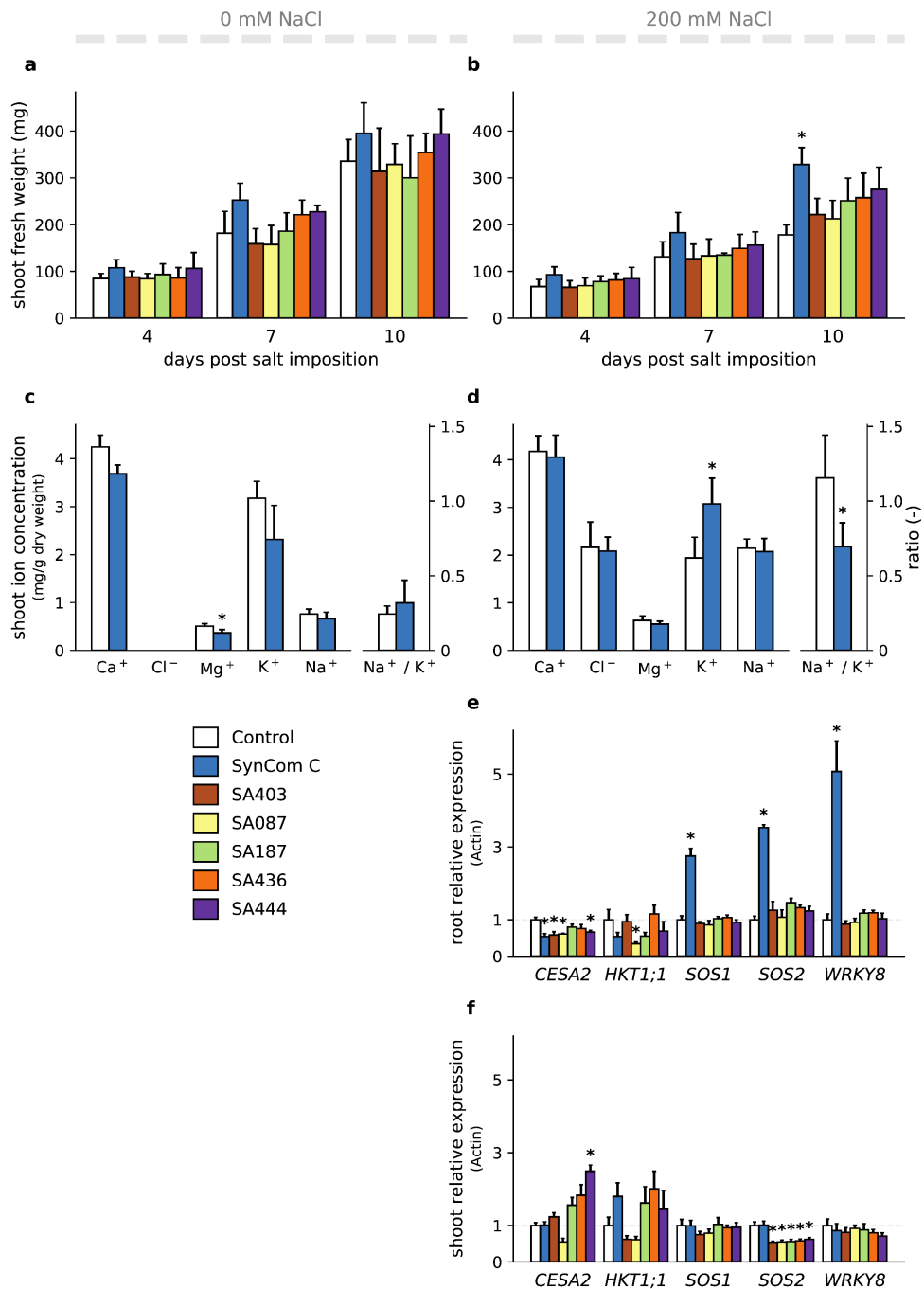


Fig. S6: Salt tolerance test of tomato plants grown with or without SynCom inoculation. Shoot dry weight of 21-day-old tomato plantlets exposed to 0, 100, 200, 300 mM NaCl (for 14 days) and inoculated with or without SynCom C. Plants were grown in the non-sterile substrate. An asterisk represents a statistically significant ($p < 0.05$) difference between the two inoculations per Student’s t-test.

Salt tolerance conferred by a SynCom



Chapter 5

Fig. S7: Tomato plants were grown in the sterile substrate and inoculated with SynCom C or individually with the five SynCom C strains. A control condition without inoculum was also included. Plants were exposed to 0 or 200 mM NaCl at 7 days post sowing. Shoot and root tissue was harvested at 4, 7 and 10 days post salt imposition. Unless otherwise indicated, error bars represent the standard deviation and an asterisk is a significant difference ($p < 0.05$) from the control per Dunnett's test. **(a & b)** Average shoot fresh weights ($n=5$) for each of the three time points and the 0 and 200 mM NaCl, respectively. **(c & d)** Average shoot ion content ($n=5$) as determined by ion chromatography ten days after the salt imposition for 0 and 200 mM NaCl, respectively. The left axis shows the average concentration in mg/g of dry weight for each ion. The right axis shows the dimensionless ratio between the concentrations of the Sodium and Potassium ions. Significance was determined by Student's t-test. **(e & f)** Relative expression against Actin in the root and shoot, respectively, of salt stress related genes in plants four days after being treated with 200 mM NaCl ($n=5$). The error bars represent the standard error of the mean of the fold changes per sample.

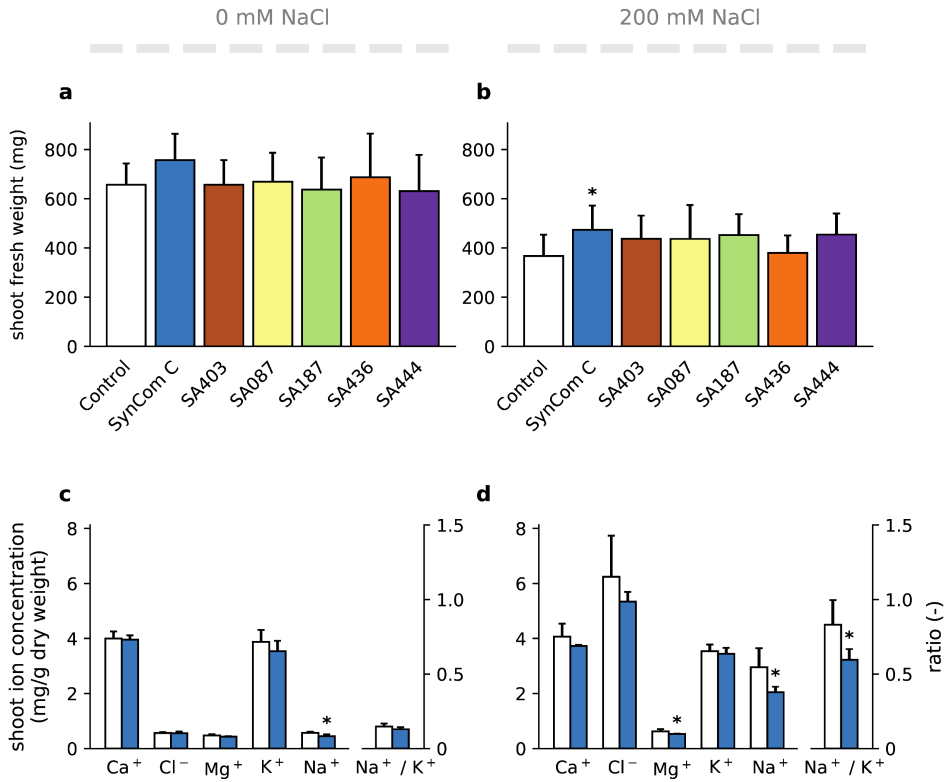


Fig. S8: Tomato plants were grown in the non-sterile substrate and inoculated with SynCom C or individually with the five SynCom C strains. A control condition without inoculum was also included. Plants were exposed to 0 or 200 mM NaCl one week after sowing. Shoot tissue was harvested at ten days post salt imposition for fresh weight and ion content analysis. The standard deviation is shown by the error bars. **(a & b)** Average shoot fresh weights ($n=15$) for the 0 & 200 mM NaCl treated plants, respectively. An asterisk indicates a significant difference ($p < 0.05$) from the control per Dunnett's test. **(c & d)** Average shoot ion content as determined by ion chromatography for the 0 & 200 mM NaCl salt levels, respectively. Five random plants were selected from the control and SynCom C inoculated plants. The left axis shows the concentration in mg/g of dry weight for each ion. The right axis shows the dimensionless ratio between the concentrations of the Sodium and Potassium ions. An asterisk is a significant difference ($p < 0.05$) per Student's t-test.

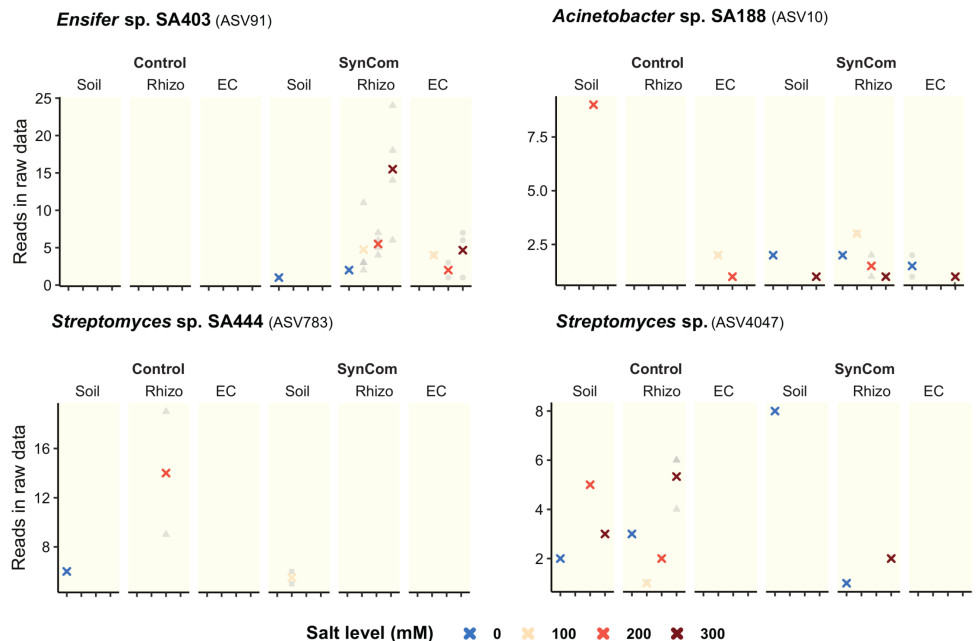


Fig. S9: ASVs of Jizan strains which did not pass the detection criteria for the root colonization of tomato.

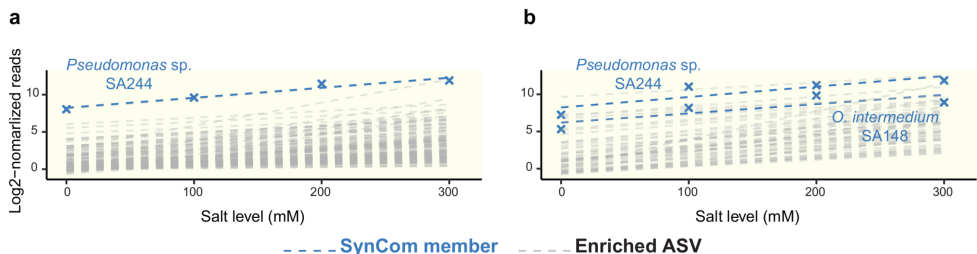


Fig. S10: Positive correlation between bacterial ASVs and salt concentration. Log2-transformed normalized read counts of ASVs found in the Rhizo (a) and EC (b) of tomato growing in the non-sterile substrate and inoculated with the Jizan SynCom. The ASVs that were enriched in any of the salt levels and with a positive correlation to the salt gradient are shown here. Crosses indicate mean log2-transformed normalized read counts of each ASV under each salt level. Blue crosses indicate ASVs matching a SynCom strain detected in this analysis.

Table S1: Genome quality and BUSCO completion of the Jizan strain draft assemblies.

strain number	contig count	largest contig (bp)	total length (bp)	N50 (bp)	L50	GC (%)	BUSCO (%)
SA087	175	543949	5765706	235133	9	66.03	97.3
SA113	45	621922	6368688	266747	9	73.21	93.92
SA244	27	738592	4869277	548984	4	61.07	99.32
SA403	55	791070	5827606	308192	6	61.53	96.62
SA424	49	561012	5422796	321413	6	63.45	97.97
SA436	92	876275	6512045	264159	6	36.77	99.32
SA444	147	243229	7832951	128819	23	73.42	93.92
SA613	27	859236	5493474	279279	6	55.5	99.32
SA619	61	642724	7060368	186344	11	73.14	94.59
SA670	1029	512909	8841294	143471	17	71.94	93.24
SA681	49	648396	6006283	234380	9	73.2	94.59

Table S2: Composition of simplified SynComs.

Strains		SynComs																			
		A	B	C	D	E	F	G	H	I	J	K	L	M	N	O	P	Q	R	S	T
<i>Massilia</i>	SA087	X	X	X	X				X	X	X	X	X	X	X		X	X	X	X	
<i>Ralstonia</i>	SA424	X																			
<i>Streptomyces</i>	SA444	X	X	X						X				X	X	X			X	X	X
<i>Ensifer</i>	SA403	X	X	X		X	X	X		X	X			X		X	X	X	X		X
<i>Bacillus</i>	SA436	X	X	X	X				X	X	X	X	X		X	X	X	X		X	X
<i>Pseudomonas</i>	SA613				X	X	X		X	X			X	X							
<i>Pseudomonas</i>	SA244					X	X	X													
<i>Ochrobactrum</i>	SA148				X	X	X	X			X	X									
<i>Enterobacter</i>	SA187			X	X		X	X	X		X	X	X					X	X	X	X
<i>Acinetobacter</i>	SA188					X		X	X				X								

Table S3: Information on primers used in the qPCR assay.

Gene	Primer orientation	Primer sequence (5' > 3')	GC (%)	Tm (°C)	length (bp)	GeneID	reference
Actin	forward	AATAGCATAAGATGGCAGACG	42.9	55.9	157	101260631	Lovdal & Lillo, 2009
Actin	reverse	ATACCCACCATCACACCACTAT	45.5	58.6			
WRKY8	forward	TAATTTCTGCCGAAAGCCTC	50	58.0	168	101259967	Gao <i>et al.</i> , 2020
WRKY8	reverse	ATGCTATTGCCGGTACTCGA	47.6	59.6			
HKT1;1	forward	CCGTGTTCTCTTCAACACCTT	47.6	58.4	210	101245180	Kou <i>et al.</i> , 2019
HKT1;1	reverse	TGGAGTGGACTCTAATGGTCT	45.5	58.2			
SOS1	forward	CTGCACCGTTACTGCCTTTG	55.0	59.8	168	778208	Olias, R. <i>et al.</i> , 2009
SOS1	reverse	GGAGACCCCTGCCTGATAGA	60.0	60.1			
SOS2	forward	TGGTAAACACCTTGCTGTGA	47.6	59.8	129	778340	Huertas <i>et al.</i> , 2012
SOS2	reverse	GTTTGTCACCTGGAGGAGAGC	55.0	58.2			
CESA2	forward	CATGGACCCCTAAGAAAGATTGG	43.5	57.2	199	101248382	Zhang <i>et al.</i> , 2016
CESA2	reverse	TCTCGAAAGTGGTTGCTTCC	47.6	57.9			

remarks: 1. Information on genes and primers used in the qPCR assay
2. GeneID refers to the RefSeq tomato assembly SL3.0 (GCF_000188115.4)
3. Primers highlighted in bold are of our own design

Table S4: ASV to Jizan strain 16S rRNA gene mapping to identify strains in the root colonization of tomato growing in the non-sterile substrate.

Strain	ASV
<i>Bacillus</i> sp. SA436	ASV513
<i>Massilia</i> sp. SA087	ASV84
<i>Ensifer</i> sp. SA403	ASV91
<i>Ralstonia</i> sp. SA424	ASV16
<i>Pseudomonas</i> sp. SA244	ASV2
<i>Pseudomonas</i> sp. SA613	ASV38
<i>Streptomyces</i> sp. SA619	ASV4047
<i>Streptomyces</i> sp. SA113	ASV4047
<i>Streptomyces</i> sp. SA681	ASV4047
<i>Streptomyces</i> sp. SA670	ASV4047
<i>Streptomyces</i> sp. SA444	ASV783
<i>Ochrobactrum intermedium</i> SA148	ASV13
<i>Enterobacter</i> sp. SA187	ASV12
<i>Acinetobacter radioresistens</i> SA188	ASV10
<i>Pseudomonas argentinensis</i> SA190	ASV5

Table S5: Jizan desert soil content analysis.

	Nt [g/kg]	K [mg/kg]	N-NH4 [mg/kg]	N-(NO3+NO2) [mg/kg]	Total Organic C [mg/kg]	P-Olsen [mg/kg]	pH
Jizan soil	N/A	33.00	1.10	0.70	11.00	2.06	7.28
Detection limit	0.30	3.00	1.00	0.50	3.00		

N/A: value below the detection limit, so no data was shown

Chapter 5

Dataset S1: Differentially abundant OTUs.

Dataset S2: NCBI assembly information on the accessions used for the AMPHORA phylogeny for the nine genera trees. The “display_name” column is the name used in the trees (see Fig. S3)

Dataset S3: NCBI assembly information on the accessions used for the AMPHORA phylogeny of the tree in figure 3b.

Dataset S4: OTU table from the meta-amplicon sequencing data of the soil, rhizosphere and endophytic compartment of indigofera.

These datasets could be accessed through <https://doi.org/10.1038/s41396-022-01238-3>.

Chapter 6

General discussion

Chapter 6

In this thesis, I have studied various aspects of root-associated microbiomes. Well studied root microbiomes are those of the rhizosphere and endophytic compartment. In line with previous studies, I have shown for several plant species that the composition of the microbiome of these compartments is distinct from that of bulk soil (chapters 2-5). We showed that, in addition to rhizosphere and endophytic compartment, xeric grasses can form a third compartment, the root-sleeve with its own distinct microbiome (chapter 2). The latter, in contrast to the other two compartments, appears to be the result of a highly controlled developmental process. I will discuss the mechanisms by which it might be formed and from which developmental processes it might be derived. The microbiomes of root-sleeve and endophytic compartment are more dissimilar from that of bulk soil than that of the rhizosphere and the plant genotype has a large effect on the composition of these two intraradical microbiomes. We further showed that the strength of the plant genotype effect depends on the environment (chapter 3). Using barley, we showed that salinity markedly reduced this plant genotype effect. I will discuss here that the underlying mechanism might involve the production of secondary metabolites which probably also affects the composition of the microbiome.

Most of my studies were performed with herbaceous plants, but one study was focussed on trees (chapter 4). This was done because tree species can become markedly older than herbaceous plants and some species can even reach ages of centuries. We studied whether the root microbiome could contribute to this longevity. By using a chrono-series of chestnut trees we showed that negative plant-soil feedback appears to be absent. Further, the chestnut root-associated microbiome harbours *Pseudomonas* strains with strong antagonist activities against major chestnut pathogens as well as a strain with growth promoting activity. As root microbiomes can also provide tolerance to abiotic stress, I used the microbiome of a legume adapted to a saline desert to study whether this can confer salt tolerance to tomato (chapter 5). We designed a simplified SynCom that improves salt tolerance of tomato even under non-sterile conditions. I will discuss potential mechanisms by which SynComs can confer salt tolerance as well as strategies by which SynComs can be engineered.

Development of root-sleeve and drought tolerance of xeric grasses

In Chapter 2 we described the formation of root-sleeves and we observed that it hosted a distinct bacterial microbiome. The root-sleeve can slide along the stele as the inner cortex was completely lysed as well as the radial walls of the endodermis. This was the case in *Agropyron* as well as *Stipa*. By investigating the cytology of root-sleeves from these two xeric grasses, we showed that the root-sleeve is formed by, from outside to inside, rhizosheath formation, formation of lacunae in the inner cortex and endodermal cell wall modification and hydrolysis.

The rhizosheath, in general, is a sticky layer of sand that adheres strongly to roots (Brown *et al.*, 2017). This is a property that is not restricted to xeric grass species, but shared by many species. In a study involving 58 species, more than 40 species, with a wide phylogenetic distribution, were shown to have the ability to form a rhizosheath (Brown *et al.*, 2017; Burak *et al.*, 2021; Karanja *et al.*, 2021). The rhizosheath is formed especially under dry conditions and this is correlated with modulation of the abscisic acid (ABA) and auxin levels to regulate root and root hair growth (Zhang *et al.*, 2020a). The longer the length of root hairs and the denser their distribution, the better root hairs facilitate rhizosheath formation (Zhang *et al.*, 2020a). A thicker rhizosheath retains more water and additionally it better prevents water loss by the root, protecting the plant against drought (Zhang *et al.*, 2020b; Burak *et al.*, 2021; Karanja *et al.*, 2021).

The lysis of cortical cells during the formation of the root-sleeve resembles the formation of cortical lacunae formed upon drought (Henrici, 1929; Beckel, 1956; Cuneo *et al.*, 2016). The formation of cortical lacunae has been well studied in fine roots of grapevine (Cuneo *et al.*, 2016). It was studied *in vivo* by a non-destructive imaging method. By applying different levels of drought it was shown that the formation of lacunae is a primary response to mild drought and osmotic stress. Their formation strictly correlates with reduced hydraulic conductivity. It is proposed that they especially reduce the radial flow of water from root to soil by which the hydraulic capacity of the vasculature is maintained. In our study, *Stipa* and *Agropyron* were collected from semi-arid regions which regularly face severe drought. Therefore, I hypothesize that the cortical lysis is related to lacunae

Chapter 6

formation and is induced by drought. However, there are also differences between lacunae formation in grapevine and cortical lysis in the xeric grasses we studied.

First, Cuneo *et al.* (2016) showed that the inner cortical cells in fine roots of grapevine were partly lysed, whereas in our study, they were completely lysed. This completely disconnected the epidermis/outer cortex and endodermis in the roots of *Agropyron* and *Stipa*. The complete lysis of inner cortex has been shown as well as in another xeric grass, *Bouteloua gracilis* (Beckel, 1956). By studying cytology along the longitudinal axis of the root, Beckel showed that lysis starts in the middle cortex and at a later stage, the outer cortex and epidermis were more or less completely disconnected from the stele. This lysis of the cortical cells is similar with what we have seen during the formation of the root-sleeve. The three xeric grasses, *Agropyron*, *Stipa* and *Bouteloua*, all belong to Poaceae and grow in (semi) arid regions. Whether this complete lysis of cortical cell layers is a specific trait for xeric Poaceae species or also occurs in other xeric grasses remains to be further studied.

Further, Cuneo *et al.* (2016) detected no visible difference in suberin or lignin deposition between well-watered and drought-stressed plants. However, in our study, suberin and lignin were deposited in cell walls of both endodermis and exodermis in lysed root. The latter might be a drought response controlled by ABA as signaling by this hormone triggers an increased suberin and lignin deposition (Barberon *et al.*, 2016; Liu *et al.*, 2021; Woolfson *et al.*, 2022).

We studied the microbiome composition in root-sleeves and showed that it is distinct from those in other compartments. In the root-sleeve, ASVs belonging to Actinobacteria were extremely dominant (Chapter 2). Recent studies, on a variety of monocot and dicot species from both natural and agricultural environments, have demonstrated an enrichment of Actinobacteria within the microbiomes of drought-stressed plants (Naylor, D. *et al.*, 2017; Fitzpatrick *et al.*, 2018; Marasco *et al.*, 2018; Xu, L *et al.*, 2018; Simmons *et al.*, 2020). This was also observed in root microbiomes of indigofera grown in arid regions (chapter 5). So what caused the enrichment of Actinobacteria in the root microbiome under drought condition? In our study, we noticed that among the most abundant

Actinobacteria, the genus *Streptomyces* occurred in both Agropyron and Stipa. Although *Streptomyces* are known to produce spores, spore-production cannot fully explain the enrichment of Actinobacteria under drought conditions as only about half of drought-enriched Actinobacteria have been shown to form spores (Naylor, Dan *et al.*, 2017).

The enrichment of Actinobacteria only occurs within roots exposed to drought but not across the whole root system, suggesting that the enrichment of Actinobacteria may be driven by a local hormone mediated response to drought (Simmons *et al.*, 2020). This is most likely ABA, which regulates the drought stress response and which accumulates to high levels within roots exposed to drought and not the whole root system (Purtolas *et al.*, 2015). Although the effect of ABA on the root microbiome has not yet been well studied, ABA is known to stimulate expression of genes encoding proteins whose activity results in ROS accumulation in the apoplast (Miller *et al.*, 2010). This most likely contributes to the enrichment of Actinobacteria as gram positive bacteria (e.g. Actinobacteria) are less sensitive to ROS than gram negative bacteria (e.g. Proteobacteria) (Xu & Coleman-Derr, 2019).

So the enrichment of Actinobacteria in the root microbiome, under drought conditions, is probably a response mediated by ABA, but whether this enrichment of Actinobacteria contributes to drought tolerance remains to be further studied.

So taken together, I hypothesize that the root-sleeve seems to create two strategies to improve tolerance to drought: 1. the rhizosheath retains more water and prevents water loss by the roots; 2. cortical lacunae, disconnecting the vascular bundle from dry soil, which reduces the backflow of water from root to soil.

Salinity induces conserved plant responses to recruit beneficial microbes that increase salt tolerance to the host plant

In chapter 3, we showed that salinity reduced the dissimilarity of the root-associated microbiomes of two barley genotypes, which is caused by a reduced plant genotype effect. Further, the salt-induced decrease in microbiome dissimilarity correlated with an increase of the relative abundance of *Pseudomonas*.

Chapter 6

The salt-induced decrease in microbiome dissimilarity is similar to what is observed with drought stress, as this decreases the effect of the plant genotype on the microbiome composition. This was shown by analyzing root-associated microbiomes of 18 Poaceae species (Naylor, Dan *et al.*, 2017). It is assumed that conserved plant responses to abiotic stress conditions, such as increased ABA and ethylene levels and production of organic acids, have larger effects on microbiome composition than genotype-specific adaptation. Emerging evidence indicates that these conserved responses of plant roots to abiotic stress could recruit specific root-associated bacterial communities (Rizaludin *et al.*, 2021). It is hypothesized that the recruited bacterial community is capable to increase the tolerance of the host plant to the stress condition (Naylor, Dan *et al.*, 2017; Li *et al.*, 2021; Rizaludin *et al.*, 2021). Hu *et al.* (2018) showed that secretion of benzoxazinoids in the soil alters the composition of the root-associated microbiome and this induces an increase of jasmonate signalling and plant defences. Xiong *et al.* (2020) showed that a root-associated bacterial community is recruited by *Limonum sinense* growing under salt stress. The growth and chemotaxis of *Bacillus flexus* KLBPM 491, a member of these recruited bacteria, could be promoted by several organic acids which are secreted by the roots of *L. sinense* during salinity. Inoculation of this strain into soil significantly promoted growth of *L. sinense* seedlings under salt stress. In our study (chapter 3), the soil microbiome from the same origin was shaped by host plants under three different salt levels, and this resulted in distinct root-associated microbiome. Whether the recruited microbiome under high salt levels could increase the tolerance of the host plant, needs to be further studied.

By analysing root-associated microbiomes of 12 *Curcubitaceae* genotypes growing under saline conditions, it was shown that the genus *Pseudomonas* was consistently enriched in rhizosphere and endophytic compartment of all host plants (Li *et al.*, 2021). This is in line with our results of chapter 3 and 5, as well as many recent studies showing that *Pseudomonas* was enriched in root microbiomes under salt stress condition (Kumar *et al.*, 2019; Etesami & Glick, 2020; Schmitz *et al.*, 2022). So the recruitment of *Pseudomonas* seems to be one of the conserved plant effects on root-associated microbiomes under salt stress.

This enrichment of *Pseudomonas* under saline conditions suggests that certain strains belonging to this genus can well adapt to these conditions and thereby have a potential to enhance plant tolerance to salt stress. This has been demonstrated by many studies and the production of ACC deaminase by *Pseudomonas* is suggested to be the major mechanism in alleviating salt stress in host plants (Glick, 2014; Kumar *et al.*, 2019; Etesami & Glick, 2020). However, a stimulation of plant growth by reducing ethylene levels has been shown to make plants more vulnerable to the stress condition (Achard *et al.*, 2006; Tao *et al.*, 2015). For example, EIN3 is the primary transcription factor for ethylene signal transduction and negatively controlled by genes EBF1-1, EBF2-1. In Arabidopsis, loss-of-function mutant *ein3-1* reduced the rate of survival to salinity whereas the double mutant *ebf1-1 ebf2-1* increased the rate of survival. This indicates a key role of ethylene in plant's survival during salinity (Achard *et al.*, 2006). Therefore, in chapter 1, it has been questioned whether bacteria capable of producing ACC deaminase, to reduce ethylene levels in the host plant, are real beneficial microbes.

A study with ACC deaminase producing bacteria, *Pseudomonas putida* UW4, showed that its ability to reduce ethylene levels has a similar effect on the host as mutations that disrupted Arabidopsis ethylene signaling; they both increased plant growth but at the cost of a strong sensitivity to stress (Achard *et al.*, 2006; Tao *et al.*, 2015; Ravanbakhsh *et al.*, 2019). It can be questioned whether this is beneficial to the plant. It seems unlikely that in a natural ecological system this would be beneficial. In contrast, under agricultural conditions it might be beneficial to the farmer that plants remain growing under stress conditions. In such case, applying these ACC deaminase producing bacteria may, to some extent, stimulate plant growth in agricultural practice. So in my opinion, the nature of ACC deaminase producing bacteria on altering plant ethylene balance, should not be considered simply as beneficial or deleterious, but it rather depends on the settings, i.e. from an ecological or agricultural perspective.

The absence of negative plant-soil feedback leads to similar root-associated microbiomes of chestnut, harbouring antagonistic and growth-promoting *Pseudomonas* strains

In chapter 4, we showed that the composition of root-associated microbiomes of chestnut trees, within a chrono-series ranging from 8 to 830 years, were rather similar and this is most likely caused by the absence of negative plant-soil feedback. A member of the core microbiome *Pseudomonas* OTU1, that represents more than 50% of the rhizosphere community, strongly inhibited growth of chestnut pathogens and stimulated plant growth. We hypothesized that such properties of root-associated microbiomes, together with the absence of negative plant-soil feedback, would contribute to longevity of chestnut.

Plant-mediated changes in the soil microbiome that can modulate local growth conditions for themselves, as well as for their own offspring and that of other plant species, are the result of "plant-soil feedback" (van der Putten *et al.*, 2013). In general plant-soil feedback is studied by growing monocultures of plant species on a certain soil and this is followed by successive cultivation of conspecific or heterospecific plant species. Parameters like biomass and seed production are used to determine the nature of the feedback (van der Putten *et al.*, 2013; Hannula *et al.*, 2021). For example, monocultures of six grassland species were maintained in soil mesocosms for 12 months and each mesocosm was divided into six physically separated sections, in which all six plant species were replanted. After five months of plant growth, plants were harvested and biomass measurements showed that all six plant species exhibited strong negative conspecific feedbacks, but also, some positive heterospecific feedbacks were observed (Hannula *et al.*, 2021).

It has been shown that negative/positive plant-soil feedback leads to changes in the soil microbiome and that these changes are the cause of the negative/positive effect on plant fitness (van der Putten *et al.*, 2013; Winkelmann *et al.*, 2019). In agricultural systems, rotation is often used to avoid conspecific negative feedback. However, for fruit production in orchards rotation on an annual basis is impossible. Therefore in orchards plant-soil feedback can be negative and strongly reduce plant/tree growth as well as yield (Mariotte *et al.*, 2018; Winkelmann *et al.*, 2019). This is indeed the case for apple and

other fruit trees belonging to the Rosacea and this causes the apple replant disease (Mazzola & Manici, 2012; Mariotte *et al.*, 2018). It is known that apple trees are pre-conditioning the soil by the formation of phenolic compounds which alter the soil microbiome into a dysbiosis state and affects its own growth and provides a legacy that negatively affects growth when a new apple tree is planted in such soil (Hofmann *et al.*, 2009; Balbín-Suárez *et al.*, 2021). The bacterial as well as fungal community composition, were different in apple replant disease affected soil in comparison to healthy soils from the same site (Franke-Whittle *et al.*, 2015; Balbín-Suárez *et al.*, 2020). A study in an orchard in Beijing showed that within 30 years a microbiome causing replant disease of apple trees had developed (Sun *et al.*, 2014).

In our study (chapter 4), chestnut trees have been cultivated in an orchard since the Ming dynasty. The trees are of different ages and plant-soil feedback has occurred at least during the lifespan of the tree. However, it is possible that trees younger than about 600 years were replanted at a site where another chestnut tree had been grown before. We studied whether a negative plant-soil feedback had (not) occurred by; 1 comparing the composition of the root-associated microbiomes of trees ranging from 8 to 830 years and 2. By studying the effect on chestnut growth by soil associated with trees of different ages.

Our results demonstrated that the composition of root-associated microbiomes of chestnut trees within a chrono-series were similar. Although we could not exclude that the composition of root-associated microbiomes of such chestnut trees has changed along the increasing tree age. However, such changes were in this case with a very slow speed (~1.5% per century, referring to Bray-Curtis dissimilarities). It is hard to compare the speed of microbiome changes between studies, since compositional analyses are relative values. However, our results show that within 30 years, a time span that apple replant disease can develop (Sun *et al.*, 2014), the dissimilarity values of the chestnut root-associated bacterial communities might increase with only about 0.4%. Furthermore, Hannula *et al.* (2021) showed that a one-year monoculture already created unique microbiomes, which negatively influence the growth of conspecific plants. Therefore the changes in soil microbiome induced by chestnut seem markedly smaller than, for example, apple or the six grassland species. In our study (chapter 4), we collected the soil around a young tree

Chapter 6

(10 years old) and two old trees (372 and 620 years old) as well as soil from an open field never cultivated with chestnut trees as control. All these soils contributed to a healthy and similar growth of young chestnut seedlings, indicating that the chestnut plant-soil feedback was neutral and not negative.

In our plant assay, replanted chestnut was grown for a relative short period and the seedlings were not exposed to pathogens. Therefore the antagonistic activities of, for example, the *Pseudomonas* strains of OTU1 could not contribute to a beneficial effect in this assay, although such strains could contribute to longevity in the orchard. We did not study the mechanisms by which our *Pseudomonas* strains had strong antagonistic activities. However, this has been studied for several other *Pseudomonas* species/strains. For example, *P. protegens* can produce secondary metabolites, like 2,4-diacetylphloroglucinol, hydrogen cyanide, and pyrrolnitrin, with a broad-spectrum antibiotic activity (Haas & Defago, 2005; Jousset *et al.*, 2014). In addition to the data described in chapter 4, some additional experiments were done to test the antagonistic activity of our isolated *Pseudomonas* strains on 4 well-known plant pathogens (the oomycete *Phytophthora infestans* and soil-borne fungal pathogens *Botrytis cinerea*, *Fusarium oxysporum* and *Verticillium dahliae*). Three *Pseudomonas* strains were shown to have strong antagonistic activity on all 6 pathogens, whereas the others have antagonistic activity on some of these pathogens. Phylogenetic analyses showed that these strains are close relatives to *P. protegens* CHA0 and *P. protegens* Pf-5. Our additional analyses showed that the latter have a bananamide as well as a pyrrolnitrin biosynthetic gene cluster. These two secondary metabolites, have previously been shown to have strong antifungal activity (Nguyen *et al.*, 2016; Quecine *et al.*, 2016; Omoboye *et al.*, 2019). However, only one of the three *Pseudomonas* strains had a bananamide biosynthetic gene cluster and neither of the three strains had pyrrolnitrin cluster. So it seems probable that the strong antagonistic activity of the three *Pseudomonas* strain depends on a different mechanism.

The *Pseudomonas* strain CM11 had a rather low antagonistic activity, but it was the only strain promoting Arabidopsis root and shoot growth. In a recent study its effect on root architecture has been studied in more detail (Li *et al.*, 2022). It was shown to promote

lateral root formation and to increase the shoot biomass. The latter seems to be independent of the increased root size. Although the underlying mechanisms remain to be solved it is clear that it is different from that of the well-studied *Pseudomonas* WCS417. The strong growth promoting effect of CM11 and its ability to colonize roots at a relatively high level may contribute to the longevity of chestnut trees. Li's study showed that CM11 also promotes the growth of crop species like lettuce and tomato, showing that its plant promoting effects are not species-specific and so this strain could be used to develop a new inoculum for agriculture.

Bottom-up and top-down approaches can be used to construct an effective SynCom under non-sterile conditions.

In chapter 5, we found that bacteria originating from roots of the desert plant *Indigofera argentea* (indigofera) can increase the salt tolerance of tomato plants. 15 bacterial strains were isolated from the root of indigofera including members of the core root microbiome and potential PGPR. The strains were first combined in one group as a full synthetic communities (SynCom), then randomly combined into groups as simplified SynComs. Under non-sterile conditions, the full SynCom and the simplified SynCom of five strains significantly increased tomato salt tolerance.

Studies have shown that microbiomes, that co-evolved with their host plant under stress conditions, could increase plant fitness under such conditions (Compant *et al.*, 2019; Fitzpatrick *et al.*, 2020; Rizaludin *et al.*, 2021). It was aimed to identify the members that contribute to the properties of such microbiomes, by isolating and studying individual microbes (Hussain *et al.*, 2018). However, in general the microbiomes as a whole have stronger growth promoting properties. So it is more the result of the collective activity of several members and also the interactions between them could be important. One approach to obtain better insight in the properties of complex microbiome is to establish a smaller community, for example, a SynCom, with the same properties as the microbiome (Carrión *et al.*, 2019). To construct such SynCom, several studies followed a bottom-up approach by piecing together single strains (Tsolakidou *et al.*, 2019; Zhuang *et al.*, 2021; Kaur *et al.*, 2022). In contrast, other studies also followed a top-down approach, by host-

Chapter 6

mediated selection, that aimed to reduce plant-microbial complexity to yield smaller communities with the desired phenotype (Niu *et al.*, 2017; Jochum *et al.*, 2019; Liu, YX *et al.*, 2019).

The bottom-up approach relied on knowledge of individual strains concerning their functional properties. This requires high-throughput platforms to isolate individual microbes and characterize their effect on plant hosts (Ahmad *et al.*, 2011; Egamberdieva *et al.*, 2017; Kaur *et al.*, 2022). With the development of high-throughput sequencing technologies additional selection criteria could be used. For example, core microbes of the root compartments could be selected for SynCom construction (Carrión *et al.*, 2019; Tsolakidou *et al.*, 2019). This is what we did to construct the SynCom described in chapter 5.

The top-down approach made use of host-mediated selection on microbiome. By several cycles of growth and selection a reduced microbiome is obtained with the desired beneficial property. Then by the help of sequencing data, best colonizers or keystone species in the reduced microbiome were selected to establish a SynCom (Niu *et al.*, 2017; Kaur *et al.*, 2022). We used an approach similar to host-mediated selection on microbiome in our study described in chapter 3, i.e. by cultivating barley on saline soil for two cycles, we had created a soil with a microbiome that stimulated growth of barley under saline conditions. The final microbiome composition showed that some bacteria with high abundance in the root compartments positively respond to high salt. These bacteria could be selected for a SynCom construction in future studies.

The construction of SynComs that have similar properties as the original microbiomes provide a good basis to study the underlying mechanisms and structure needed for survival as a community but also those involved in plant growth promotion. An analysis on SynCom structure was described by Niu *et al.* (2017), who cultivated germ-free maize seedlings in soil with two selective iterations to obtain a bacterial community with a reduced complexity. Afterwards, by selecting seven strains which represented the enriched and dominant genera in the maize root, a greatly simplified SynCom was constructed. The removal of one strain, namely *Enterobacter cloacae*, resulted in the

complete loss of microbial community structure in the maize roots, indicating the importance of microbe-microbe interactions and the existence of keystone species in the microbiome. Further, an example of functional analysis of SynCom was described by Carrión *et al.* (2019). They studied the root microbiome of sugar beet seedlings grown in the field soil suppressive to *Rhizoctonia solani* by the metagenomic method. The disease-suppressive phenotype was highly correlated with the abundance of *Chitinophaga* and *Flavobacterium*. A SynCom of two strains belonging to these two genera, respectively, provided the same disease protection as the original microbiome. Site-directed mutagenesis further confirmed the contribution of BGC298 in *Flavobacterium* to this phenotype.

In our study (chapter 5), qPCR-based analysis confirmed the success of 5 strain SynCom in increasing salt tolerance of tomato was correlated with the avoidance of ion toxicity, promoting an early activation of plant ion homeostasis mechanisms. In contrast, these effects were not present when any of the SynCom strains applied alone, suggesting that SynCom as a community is required for this phenotype. However, how these strains interact with each other is not known yet. In addition to the meta-amplicon sequencing, advanced methods like metagenomics, metatranscriptomics, metametabolomics as well as mutagenesis are promising to be applied in our future work to study the underlying mechanisms of the 5 strain SynCom.

Another advantage of SynComs in comparison to individual strains is that they might be more successful than individual strains in an agricultural setting. Under non-sterile condition, strains often fail when they were applied individually, which was attributed to the competition by the local microbiome (Souza *et al.*, 2015; Saad *et al.*, 2020). Although it is hypothesized that SynComs would have a better chance of surviving and functioning in the non-sterile condition (Raaijmakers, 2015; Vorholt *et al.*, 2017), efficient methods to construct a SynCom in the presence of a local microbiome as seen under field conditions, remains largely undefined. In our study (chapter 5), the 15 strain as well as the simplified 5 strain SynCom successfully improved tomato growth to salt imposition under non-sterile condition. The bottom-up approach was successful for the 15 strain SynCom construction. However the construction of 5 strain SynCom was not really driven by a strategy to obtain

Chapter 6

a well surviving SynCom under non-sterile conditions. Its success was more based on luck than rational.

It seems unlikely that a single SynCom can be designed that is suitable, for several crops and different field condition. More likely tailored SynComs have to be made for a specific crop and a certain field condition. The host-mediated selection might be used for a certain crop species on a mixture of a microbiome with the desired property, and the field soil. After each growth cycle, the roots and soil of the plot with best performance will be used as inoculum for the next-round of growth (Jochum *et al.*, 2019). Such tailored co-evolution process between the crop, candidate microbiome and field soil would reshape the root microbiome, but should maintains the desired phenotype and reduces its complexity. Subsequently, this information can be used to construct a SynCom, for example, by using core members, keystone species and microbes that are members of the original microbiome with growth promoting properties.

In relation to future research on root-associated microbiomes, major challenges will be to understand their functions and their underlying mechanisms in ecological as well as agricultural settings. In both cases, SynComs will be very useful to unravel such mechanisms. Such insight will hopefully result the development of a cost-effective and environmental-friendly strategies to improve crop cultivation.

References

- Abdenmour MA, Douaoui A, Barrena J, Pulido M, Bradaï A, Bennacer A, Piccini C, Alfonso-Torreño A. 2021.** Geochemical characterization of the salinity of irrigated soils in arid regions (Biskra, SE Algeria). *Acta Geochimica* **40**(2): 234-250.
- Achard P, Cheng H, Grauwe LD, Decat J, Schoutteten H, Moritz T, Straeten DVD, Peng J, Harberd NP. 2006.** Integration of Plant Responses to Environmentally Activated Phytohormonal Signals. *Science* **311**(5757): 91-94.
- Afzal I, Shinwari ZK, Sikandar S, Shahzad S. 2019.** Plant beneficial endophytic bacteria: Mechanisms, diversity, host range and genetic determinants. *Microbiological Research* **221**: 36-49.
- Ahmad M, Zahir ZA, Asghar HN, Asghar M. 2011.** Inducing salt tolerance in mung bean through coinoculation with rhizobia and plant-growth-promoting rhizobacteria containing 1-aminocyclopropane-1-carboxylate deaminase. *Can J Microbiol* **57**(7): 578-589.
- Alegria Terrazas R, Balbirnie-Cumming K, Morris J, Hedley PE, Russell J, Paterson E, Baggs EM, Fridman E, Bulgarelli D. 2020.** A footprint of plant eco-geographic adaptation on the composition of the barley rhizosphere bacterial microbiota. *Scientific Reports* **10**(1): 1-13.
- Andersen TG, Naseer S, Ursache R, Wybouw B, Smet W, De Rybel B, Vermeer JE, Geldner N. 2018.** Diffusible repression of cytokinin signalling produces endodermal symmetry and passage cells. *Nature* **555**(7697): 529-533.
- Andres-Barrao C, Lafi FF, Alam I, de Zelicourt A, Eida AA, Bokhari A, Alzubaidy H, Bajic VB, Hirt H, Saad MM. 2017.** Complete Genome Sequence Analysis of *Enterobacter* sp. SA187, a Plant Multi-Stress Tolerance Promoting Endophytic Bacterium. *Front Microbiol* **8**: 2023.
- Arnon DI. 1949.** Copper Enzymes in Isolated Chloroplasts. Polyphenoloxidase in *Beta Vulgaris*. *Plant Physiol* **24**(1): 1-15.

References

- Ashraf M, Hasnain S, Berge O, Mahmood T. 2004. Inoculating wheat seedlings with exopolysaccharide-producing bacteria restricts sodium uptake and stimulates plant growth under salt stress. *Biology and Fertility of Soils* **40**(3): 157-162.
- Aslam F, Ali B. 2018. Halotolerant bacterial diversity associated with Suaeda fruticosa (L.) forssk. improved growth of maize under salinity stress. *Agronomy* **8**(8): 131.
- Awlia M, Alshareef N, Saber N, Korte A, Oakey H, Panzarová K, Trtílek M, Negrão S, Tester M, Julkowska MM. 2021. Genetic mapping of the early responses to salt stress in Arabidopsis thaliana. *The Plant Journal* **107**(2): 544-563.
- Awlia M, Nigro A, Fajkus J, Schmoeckel SM, Negrão S, Santelia D, Trtílek M, Tester M, Julkowska MM, Panzarová K. 2016. High-throughput non-destructive phenotyping of traits that contribute to salinity tolerance in Arabidopsis thaliana. *Frontiers in Plant Science* **7**: 1414.
- Babalola OO, Fadiji AE, Enagbonma BJ, Alori ET, Ayilara MS, Ayangbenro AS. 2020. The nexus between plant and plant microbiome: Revelation of the networking strategies. *Frontiers in microbiology* **11**: 548037.
- Backer R, Rokem JS, Ilangumaran G, Lamont J, Praslickova D, Ricci E, Subramanian S, Smith DL. 2018. Plant Growth-Promoting Rhizobacteria: Context, Mechanisms of Action, and Roadmap to Commercialization of Biostimulants for Sustainable Agriculture. *Front Plant Sci* **9**(1473): 1473.
- Baez-Rogelio A, Morales-Garcia YE, Quintero-Hernandez V, Munoz-Rojas J. 2017. Next generation of microbial inoculants for agriculture and bioremediation. *Microb Biotechnol* **10**(1): 19-21.
- Bai Y, Muller DB, Srinivas G, Garrido-Oter R, Potthoff E, Rott M, Dombrowski N, Munch PC, Spaepen S, Remus-Emsermann M, et al. 2015. Functional overlap of the Arabidopsis leaf and root microbiota. *Nature* **528**(7582): 364-369.
- Bakker P, Berendsen RL, Van Pelt JA, Vismans G, Yu K, Li E, Van Bentum S, Poppeliers SWM, Sanchez Gil JJ, Zhang H, et al. 2020. The Soil-Borne Identity and

- Microbiome-Assisted Agriculture: Looking Back to the Future. *Mol Plant* **13**(10): 1394-1401.
- Bakker PA, Berendsen RL, Doornbos RF, Wiermants PC, Pieterse CM. 2013.** The rhizosphere revisited: root microbiomics. *Frontiers in Plant Science* **4**: 165.
- Bakker PA, Berendsen RL, Doornbos RF, Wiermants PC, Pieterse CM. 2013.** The rhizosphere revisited: root microbiomics. *Front Plant Sci* **4**(165): 165.
- Balbín-Suárez A, Jacquiod S, Rohr A-D, Liu B, Flachowsky H, Winkelmann T, Beerhues L, Nesme J, J. Sørensen S, Vetterlein D. 2021.** Root exposure to apple replant disease soil triggers local defense response and rhizoplane microbiome dysbiosis. *FEMS Microbiology Ecology* **97**(4): fiab031.
- Balbín-Suárez A, Lucas M, Vetterlein D, Sørensen SJ, Winkelmann T, Smalla K, Jacquiod S. 2020.** Exploring microbial determinants of apple replant disease (ARD): a microhabitat approach under split-root design. *FEMS Microbiology Ecology* **96**(12): fiae211.
- Bankevich A, Nurk S, Antipov D, Gurevich AA, Dvorkin M, Kulikov AS, Lesin VM, Nikolenko SI, Pham S, Prjibelski AD, et al. 2012.** SPAdes: a new genome assembly algorithm and its applications to single-cell sequencing. *J Comput Biol* **19**(5): 455-477.
- Barberon M, Vermeer JE, De Bellis D, Wang P, Naseer S, Andersen TG, Humbel BM, Nawrath C, Takano J, Salt DE, et al. 2016.** Adaptation of Root Function by Nutrient-Induced Plasticity of Endodermal Differentiation. *Cell* **164**(3): 447-459.
- Bashan Y, de-Bashan LE, Prabhu S, Hernandez J-P. 2014.** Advances in plant growth-promoting bacterial inoculant technology: formulations and practical perspectives (1998–2013). *Plant and soil* **378**(1): 1-33.
- Bassil E, Blumwald E. 2014.** The ins and outs of intracellular ion homeostasis: NHX-type cation/H⁺ transporters. *Current Opinion in Plant Biology* **22**: 1-6.

References

- Beckel DKB. 1956.** Cortical Disintegration in the Roots of *Bouteloua Gracilis* (H.B.K.) Lag.1. *New Phytologist* **55**(2): 183-190.
- Benidire L, El Khalloufi F, Oufdou K, Barakat M, Tulumello J, Ortet P, Heulin T, Achouak W. 2020.** Phytobeneficial bacteria improve saline stress tolerance in *Vicia faba* and modulate microbial interaction network. *Science of The Total Environment* **729**: 139020.
- Bent E, Loffredo A, Yang J-i, McKenry MV, Becker JO, Borneman J. 2009.** Investigations into peach seedling stunting caused by a replant soil. *FEMS Microbiology Ecology* **68**(2): 192-200.
- Berendsen RL, Vismans G, Yu K, Song Y, de Jonge R, Burgman WP, Burmølle M, Herschend J, Bakker PAHM, Pieterse CMJ. 2018.** Disease-induced assemblage of a plant-beneficial bacterial consortium. *ISME J* **12**(6): 1496-1507.
- Berg G, Smalla K. 2009.** Plant species and soil type cooperatively shape the structure and function of microbial communities in the rhizosphere. *FEMS Microbiol Ecol* **68**(1): 1-13.
- Berg G, Smalla K. 2009.** Plant species and soil type cooperatively shape the structure and function of microbial communities in the rhizosphere. *FEMS Microbiology Ecology* **68**(1): 1-13.
- Bisseling T, Geurts R. 2020.** Specificity in legume nodule symbiosis. *Science* **369**(6504): 620-621.
- Bokhari A, Essack M, Lafi FF, Andres-Barrao C, Jalal R, Alamoudi S, Razali R, Alzubaidy H, Shah KH, Siddique S. 2019.** Bioprospecting desert plant *Bacillus* endophytic strains for their potential to enhance plant stress tolerance. *Scientific Reports* **9**(1): 1-13.
- Bolger AM, Lohse M, Usadel B. 2014.** Trimmomatic: a flexible trimmer for Illumina sequence data. *Bioinformatics* **30**(15): 2114-2120.

- Bouffaud M-L, Poirier M-A, Muller D, Moëgne-Loccoz Y. 2014.** Root microbiome relates to plant host evolution in maize and other Poaceae. *Environmental microbiology* **16**(9): 2804-2814.
- Bouffaud ML, Poirier MA, Muller D, Moenne-Loccoz Y. 2014.** Root microbiome relates to plant host evolution in maize and other Poaceae. *Environ Microbiol* **16**(9): 2804-2814.
- Branch MP 1999.** A Garden of Bristlecones: Tales of Change in the Great Basin: JSTOR.
- Brown LK, George TS, Neugebauer K, White PJ. 2017.** The rhizosheath – a potential trait for future agricultural sustainability occurs in orders throughout the angiosperms. *Plant and soil* **418**(1): 115-128.
- Bulgarelli D, Garrido-Oter R, Munch PC, Weiman A, Droge J, Pan Y, McHardy AC, Schulze-Lefert P. 2015.** Structure and function of the bacterial root microbiota in wild and domesticated barley. *Cell Host Microbe* **17**(3): 392-403.
- Bulgarelli D, Rott M, Schlaeppi K, Ver Loren van Themaat E, Ahmadinejad N, Assenza F, Rauf P, Huettel B, Reinhardt R, Schmelzer E, et al. 2012.** Revealing structure and assembly cues for Arabidopsis root-inhabiting bacterial microbiota. *Nature* **488**(7409): 91-95.
- Burak E, Quinton JN, Dodd IC. 2021.** Root hairs are the most important root trait for rhizosheath formation of barley (*Hordeum vulgare*), maize (*Zea mays*) and *Lotus japonicus* (Gifu). *Ann Bot* **128**(1): 45-57.
- Burian A, Barbier de Reuille P, Kuhlemeier C. 2016.** Patterns of Stem Cell Divisions Contribute to Plant Longevity. *Curr Biol* **26**(11): 1385-1394.
- Byrt CS, Munns R, Burton RA, Gilliham M, Wege S. 2018.** Root cell wall solutions for crop plants in saline soils. *Plant Sci* **269**: 47-55.
- Callahan B, McMurdie P, Rosen M, Han A, Johnson A. 2016.** JA, Holmes SP. 2016. DADA2: high-resolution sample inference from Illumina amplicon data. *Nature Methods* **13**(7): 581-583.

References

- Caporaso JG, Kuczynski J, Stombaugh J, Bittinger K, Bushman FD, Costello EK, Fierer N, Pena AG, Goodrich JK, Gordon JI, et al. 2010. QIIME allows analysis of high-throughput community sequencing data. *Nat Methods* 7(5): 335-336.
- Cardinale M, Ratering S, Suarez C, Montoya AMZ, Geissler-Plaum R, Schnell S. 2015. Paradox of plant growth promotion potential of rhizobacteria and their actual promotion effect on growth of barley (*Hordeum vulgare* L.) under salt stress. *Microbiological Research* 181: 22-32.
- Carrion VJ, Cordovez V, Tyc O, Etalo DW, de Bruijn I, de Jager VCL, Medema MH, Eberl L, Raaijmakers JM. 2018. Involvement of Burkholderiaceae and sulfurous volatiles in disease-suppressive soils. *ISME J* 12(9): 2307-2321.
- Carrión VJ, Perez-Jaramillo J, Cordovez V, Tracanna V, Hollander Md, Ruiz-Buck D, Mendes LW, Ijcken WJv, Gomez-Exposito R, Elsayed SS, et al. 2019. Pathogen-induced activation of disease-suppressive functions in the endophytic root microbiome. *Science* 366(6465): 606-612.
- Castrillo G, Teixeira PJPL, Paredes SH, Law TF, de Lorenzo L, Feltcher ME, Finkel OM, Breakfield NW, Mieczkowski P, Jones CD, et al. 2017. Root microbiota drive direct integration of phosphate stress and immunity. *Nature* 543(7646): 513-518.
- Chang P, Gerhardt KE, Huang X-D, Yu X-M, Glick BR, Gerwing PD, Greenberg BM. 2014. Plant Growth-Promoting Bacteria Facilitate the Growth of Barley and Oats in Salt-Impacted Soil: Implications for Phytoremediation of Saline Soils. *International Journal of Phytoremediation* 16(11): 1133-1147.
- Chatterjee P, Samaddar S, Anandham R, Kang Y, Kim K, Selvakumar G, Sa T. 2017. Beneficial soil bacterium *Pseudomonas frederiksbergensis* OS261 augments salt tolerance and promotes red pepper plant growth. *Frontiers in Plant Science* 8: 705.
- Chen L, Liu Y, Wu G, Veronican Njeri K, Shen Q, Zhang N, Zhang R. 2016. Induced maize salt tolerance by rhizosphere inoculation of *Bacillus amyloliquefaciens* SQR9. *Physiol Plant* 158(1): 34-44.

- Cheng X, de Bruijn I, van der Voort M, Loper JE, Raaijmakers JM. 2013.** The Gac regulon of *Pseudomonas fluorescens* SBW 25. *Environmental microbiology reports* **5**(4): 608-619.
- Cheng X, Etalo DW, van de Mortel JE, Dekkers E, Nguyen L, Medema MH, Raaijmakers JM. 2017.** Genome-wide analysis of bacterial determinants of plant growth promotion and induced systemic resistance by *Pseudomonas fluorescens*. *Environ Microbiol* **19**(11): 4638-4656.
- Chu TN, Tran BTH, Van Bui L, Hoang MTT. 2019.** Plant growth-promoting rhizobacterium *Pseudomonas* PS01 induces salt tolerance in *Arabidopsis thaliana*. *BMC research notes* **12**(1): 1-7.
- Clauw P, Coppens F, De Beuf K, Dhondt S, Van Daele T, Maleux K, Storme V, Clement L, Gonzalez N, Inzé D. 2015.** Leaf responses to mild drought stress in natural variants of *Arabidopsis*. *Plant Physiol* **167**(3): 800-816.
- Cole JR, Wang Q, Fish JA, Chai B, McGarrell DM, Sun Y, Brown CT, Porras-Alfaro A, Kuske CR, Tiedje JM. 2014.** Ribosomal Database Project: data and tools for high throughput rRNA analysis. *Nucleic Acids Res* **42**(Database issue): D633-642.
- Coleman-Derr D, Desgarennes D, Fonseca-Garcia C, Gross S, Clingenpeel S, Woyke T, North G, Visel A, Partida-Martinez LP, Tringe SG. 2016.** Plant compartment and biogeography affect microbiome composition in cultivated and native *Agave* species. *New Phytol* **209**(2): 798-811.
- Compant S, Samad A, Faist H, Sessitsch A. 2019.** A review on the plant microbiome: Ecology, functions, and emerging trends in microbial application. *J Adv Res* **19**: 29-37.
- Cook RJ, Thomashow LS, Weller DM, Fujimoto D, Mazzola M, Banger G, Kim DS. 1995.** Molecular mechanisms of defense by rhizobacteria against root disease. *Proc Natl Acad Sci U S A* **92**(10): 4197-4201.

References

- Cordovez V, Carrion VJ, Etalo DW, Mumm R, Zhu H, van Wezel GP, Raaijmakers JM. 2015.** Diversity and functions of volatile organic compounds produced by *Streptomyces* from a disease-suppressive soil. *Front Microbiol* **6**: 1081.
- Csardi G, Nepusz T. 2006.** The igraph software package for complex network research. *InterJournal, complex systems* **1695**(5): 1-9.
- Cuneo IF, Knipfer T, Brodersen CR, McElrone AJ. 2016.** Mechanical Failure of Fine Root Cortical Cells Initiates Plant Hydraulic Decline during Drought. *Plant Physiol* **172**(3): 1669-1678.
- De Cáceres M, Legendre P, Moretti M. 2010.** Improving indicator species analysis by combining groups of sites. *Oikos* **119**(10): 1674-1684.
- de Souza JT, Weller DM, Raaijmakers JM. 2003.** Frequency, Diversity, and Activity of 2,4-Diacetylphloroglucinol-Producing Fluorescent *Pseudomonas* spp. in Dutch Take-all Decline Soils. *Phytopathology* **93**(1): 54-63.
- de Zélicourt A, Synek L, Saad MM, Alzubaidy H, Jalal R, Xie Y, Andres-Barrao C, Rolli E, Guerard F, Mariappan KG. 2018.** Ethylene induced plant stress tolerance by *Enterobacter* sp. SA187 is mediated by 2 - keto - 4 - methylthiobutyric acid production. *PLOS Genetics* **14**(3): e1007273.
- Dobbelaere S, Croonenborghs A, Thys A, Vande Broek A, Vanderleyden J. 1999.** Phytostimulatory effect of *Azospirillum brasilense* wild type and mutant strains altered in IAA production on wheat. *Plant and soil* **212**(2): 153-162.
- Dobbelaere S, Vanderleyden J, Okon Y. 2003.** Plant growth-promoting effects of diazotrophs in the rhizosphere. *Critical reviews in plant sciences* **22**(2): 107-149.
- Dubrovsky JG, Sauer M, Napsucialy-Mendivil S, Ivanchenko MG, Friml J, Shishkova S, Celenza J, Benková E. 2008.** Auxin acts as a local morphogenetic trigger to specify lateral root founder cells. *Proceedings of the National Academy of Sciences* **105**(25): 8790-8794.
- Eddy SR. 1998.** Profile hidden Markov models. *Bioinformatics* **14**(9): 755-763.

- Eddy SR. 2011.** Accelerated Profile HMM Searches. *PLoS Comput Biol* **7**(10): e1002195.
- Edgar RC. 2013.** UPARSE: highly accurate OTU sequences from microbial amplicon reads. *Nat Methods* **10**(10): 996-998.
- Edgar RC, Haas BJ, Clemente JC, Quince C, Knight R. 2011.** UCHIME improves sensitivity and speed of chimera detection. *Bioinformatics* **27**(16): 2194-2200.
- Edwards J, Johnson C, Santos-Medellin C, Lurie E, Podishetty NK, Bhatnagar S, Eisen JA, Sundaresan V. 2015.** Structure, variation, and assembly of the root-associated microbiomes of rice. *Proc Natl Acad Sci U S A* **112**(8): E911-920.
- Egamberdieva D, Jabborova D, Hashem A. 2015.** Pseudomonas induces salinity tolerance in cotton (*Gossypium hirsutum*) and resistance to Fusarium root rot through the modulation of indole-3-acetic acid. *Saudi Journal of Biological Sciences* **22**(6): 773-779.
- Egamberdieva D, Kucharova Z, Davranov K, Berg G, Makarova N, Azarova T, Chebotar V, Tikhonovich I, Kamilova F, Validov SZ. 2011.** Bacteria able to control foot and root rot and to promote growth of cucumber in salinated soils. *Biology and Fertility of Soils* **47**(2): 197-205.
- Egamberdieva D, Wirth S, Bellingrath-Kimura SD, Mishra J, Arora NK. 2019.** Salt-Tolerant Plant Growth Promoting Rhizobacteria for Enhancing Crop Productivity of Saline Soils. *Frontiers in microbiology* **10**(2791).
- Egamberdieva D, Wirth S, Jabborova D, Räsänen LA, Liao H. 2017.** Coordination between Bradyrhizobium and Pseudomonas alleviates salt stress in soybean through altering root system architecture. *Journal of Plant Interactions* **12**(1): 100-107.
- Eida AA, Ziegler M, Lafi FF, Michell CT, Voolstra CR, Hirt H, Saad MM. 2018.** Desert plant bacteria reveal host influence and beneficial plant growth properties. *PLoS One* **13**(12): e0208223.

References

- Etesami H, Emami S, Alikhani HA. 2017.** Potassium solubilizing bacteria (KSB):: Mechanisms, promotion of plant growth, and future prospects A review. *Journal of soil science and plant nutrition* **17**(4): 897-911.
- Etesami H, Glick BR. 2020.** Halotolerant plant growth–promoting bacteria: Prospects for alleviating salinity stress in plants. *Environmental and Experimental Botany* **178**.
- Fårhreaus G. 1952.** Formation of laccase by Polyporus versicolor in different culture media. *Physiologia Plantarum* **5**(2): 284-291.
- Fatima T, Arora NK. 2021.** Pseudomonas entomophila PE3 and its exopolysaccharides as biostimulants for enhancing growth, yield and tolerance responses of sunflower under saline conditions. *Microbiological Research* **244**: 126671.
- Faust K, Raes J. 2012.** Microbial interactions: from networks to models. *Nat Rev Microbiol* **10**(8): 538-550.
- Fernández-González AJ, Villadas PJ, Gómez-Lama Cabanás C, Valverde-Corredor A, Belaj A, Mercado-Blanco J, Fernández-López M. 2019.** Defining the root endosphere and rhizosphere microbiomes from the World Olive Germplasm Collection. *Scientific Reports* **9**(1): 1-13.
- Fierer N. 2017.** Embracing the unknown: disentangling the complexities of the soil microbiome. *Nat Rev Microbiol* **15**(10): 579-590.
- Finkel OM, Salas-Gonzalez I, Castrillo G, Conway JM, Law TF, Teixeira P, Wilson ED, Fitzpatrick CR, Jones CD, Dangl JL. 2020.** A single bacterial genus maintains root growth in a complex microbiome. *Nature* **587**(7832): 103-108.
- Finkel OM, Salas-González I, Castrillo G, Spaepen S, Law TF, Teixeira PJPL, Jones CD, Dangl JL. 2019.** The effects of soil phosphorus content on plant microbiota are driven by the plant phosphate starvation response. *PLoS Biology* **17**(11): e3000534.

- Fitzpatrick CR, Copeland J, Wang PW, Guttman DS, Kotanen PM, Johnson MTJ. 2018.** Assembly and ecological function of the root microbiome across angiosperm plant species. *Proc Natl Acad Sci U S A* **115**(6): E1157-E1165.
- Fitzpatrick CR, Salas-Gonzalez I, Conway JM, Finkel OM, Gilbert S, Russ D, Teixeira P, Dangl JL. 2020.** The Plant Microbiome: From Ecology to Reductionism and Beyond. *Annu Rev Microbiol* **74**: 81-100.
- Flowers TJ, Munns R, Colmer TD. 2015.** Sodium chloride toxicity and the cellular basis of salt tolerance in halophytes. *Ann Bot* **115**(3): 419-431.
- Fonseca-Garcia C, Coleman-Derr D, Garrido E, Visel A, Tringe SG, Partida-Martinez LP. 2016.** The Cacti Microbiome: Interplay between Habitat-Filtering and Host-Specificity. *Front Microbiol* **7**: 150.
- Franke-Whittle IH, Manici LM, Insam H, Stres B. 2015.** Rhizosphere bacteria and fungi associated with plant growth in soils of three replanted apple orchards. *Plant and soil* **395**(1): 317-333.
- Fukami J, Nogueira MA, Araujo RS, Hungria M. 2016.** Accessing inoculation methods of maize and wheat with *Azospirillum brasilense*. *Amb Express* **6**(1): 1-13.
- Gao YF, Liu JK, Yang FM, Zhang GY, Wang D, Zhang L, Ou YB, Yao YA. 2020.** The WRKY transcription factor WRKY8 promotes resistance to pathogen infection and mediates drought and salt stress tolerance in *Solanum lycopersicum*. *Physiol Plant* **168**(1): 98-117.
- Glick BR. 2005.** Modulation of plant ethylene levels by the bacterial enzyme ACC deaminase. *FEMS Microbiol Lett* **251**(1): 1-7.
- Glick BR. 2014.** Bacteria with ACC deaminase can promote plant growth and help to feed the world. *Microbiological Research* **169**(1): 30-39.
- Gould IJ, Wright I, Collison M, Ruto E, Bosworth G, Pearson S. 2020.** The impact of coastal flooding on agriculture: A case - study of Lincolnshire, United Kingdom. *Land Degradation & Development* **31**(12): 1545-1559.

References

- Gran-Scheuch A, Trajkovic M, Parra L, Fraaije MW. 2018.** Mining the Genome of *Streptomyces leeuwenhoekii*: Two New Type I Baeyer-Villiger Monooxygenases From Atacama Desert. *Front Microbiol* **9**: 1609.
- Gurevich A, Saveliev V, Vyahhi N, Tesler G. 2013.** QUASt: quality assessment tool for genome assemblies. *Bioinformatics* **29**(8): 1072-1075.
- Haas D, Defago G. 2005.** Biological control of soil-borne pathogens by fluorescent pseudomonads. *Nat Rev Microbiol* **3**(4): 307-319.
- Hacquard S, Spaepen S, Garrido-Oter R, Schulze-Lefert P. 2017.** Interplay Between Innate Immunity and the Plant Microbiota. *Annu Rev Phytopathol* **55**: 565-589.
- Han Q-Q, Lü X-P, Bai J-P, Qiao Y, Paré PW, Wang S-M, Zhang J-L, Wu Y-N, Pang X-P, Xu W-B, et al. 2014.** Beneficial soil bacterium *Bacillus subtilis* (GB03) augments salt tolerance of white clover. *Frontiers in Plant Science* **5**(525).
- Hannula SE, Heinen R, Huberty M, Steinauer K, De Long JR, Jongen R, Bezemer TM. 2021.** Persistence of plant-mediated microbial soil legacy effects in soil and inside roots. *Nat Commun* **12**(1): 5686.
- Haroon U, Khizar M, Liaquat F, Ali M, Akbar M, Tahir K, Batool SS, Kamal A, Chaudhary HJ, Munis MFH. 2021.** Halotolerant Plant Growth-Promoting Rhizobacteria Induce Salinity Tolerance in Wheat by Enhancing the Expression of SOS Genes. *Journal of Plant Growth Regulation*.
- Hartman K. 2018.** Cropping practices manipulate abundance patterns of root and soil microbiome members paving the way to smart farming_additional file. *Microbiome*.
- Hartman K, Tringe SG. 2019.** Interactions between plants and soil shaping the root microbiome under abiotic stress. *Biochemical Journal* **476**(19): 2705-2724.
- Hartman K, van der Heijden MGA, Wittwer RA, Banerjee S, Walser JC, Schlaeppi K. 2018.** Cropping practices manipulate abundance patterns of root and soil microbiome members paving the way to smart farming. *Microbiome* **6**(1): 14.

- Hartmann A, Schmid M, Van Tuinen D, Berg G. 2009.** Plant-driven selection of microbes. *Plant and soil* **321**(1): 235-257.
- Hartney SL, Mazurier S, Kidarsa TA, Quecine MC, Lemanceau P, Loper JE. 2011.** TonB-dependent outer-membrane proteins and siderophore utilization in *Pseudomonas fluorescens* Pf-5. *Biometals* **24**(2): 193-213.
- Hassani A, Azapagic A, Shokri N. 2020.** Predicting long-term dynamics of soil salinity and sodicity on a global scale. *Proceedings of the National Academy of Sciences* **117**(52): 33017-33027.
- Hauser F, Horie T. 2010.** A conserved primary salt tolerance mechanism mediated by HKT transporters: a mechanism for sodium exclusion and maintenance of high K⁺/Na⁺ ratio in leaves during salinity stress. *Plant, Cell & Environment* **33**(4): 552-565.
- Hayat R, Ali S, Amara U, Khalid R, Ahmed I. 2010.** Soil beneficial bacteria and their role in plant growth promotion: a review. *Annals of Microbiology* **60**(4): 579-598.
- Henrici M. 1929.** Structure of the cortex of grass roots in the more arid regions of South Africa. Union S. Africa, Dept. Agric. Sci. Bull **85**(1).
- Hesse C, Schulz F, Bull CT, Shaffer BT, Yan Q, Shapiro N, Hassan KA, Varghese N, Elbourne LDH, Paulsen IT, et al. 2018.** Genome-based evolutionary history of *Pseudomonas* spp. *Environ Microbiol* **20**(6): 2142-2159.
- Hofmann A, Wittenmayer L, Arnold G, Schieber A, Merbach W. 2009.** Root exudation of phloridzin by apple seedlings (*Malus domestica* Borkh.) with symptoms of apple replant disease. *Journal of Applied Botany and Food Quality* **82**(2): 193-198.
- Hongoh Y, Yuzawa H, Ohkuma M, Kudo T. 2003.** Evaluation of primers and PCR conditions for the analysis of 16S rRNA genes from a natural environment. *FEMS Microbiol Lett* **221**(2): 299-304.
- Horie T, Yoshida K, Nakayama H, Yamada K, Oiki S, Shinmyo A. 2001.** Two types of HKT transporters with different properties of Na⁺ and K⁺ transport in *Oryza sativa*. *Plant J* **27**(2): 129-138.

References

- Hu L, Robert CAM, Cadot S, Zhang X, Ye M, Li B, Manzo D, Chervet N, Steinger T, van der Heijden MGA, et al. 2018.** Root exudate metabolites drive plant-soil feedbacks on growth and defense by shaping the rhizosphere microbiota. *Nature communications* **9**(1): 2738.
- Huang AC, Jiang T, Liu Y-X, Bai Y-C, Reed J, Qu B, Goossens A, Nützmann H-W, Bai Y, Osbourn A. 2019.** A specialized metabolic network selectively modulates *Arabidopsis* root microbiota. *Science* **364**(6440).
- Huerta-Cepas J, Serra F, Bork P. 2016.** ETE 3: Reconstruction, Analysis, and Visualization of Phylogenomic Data. *Mol Biol Evol* **33**(6): 1635-1638.
- Huertas R, Olias R, Eljakaoui Z, Galvez FJ, Li J, De Morales PA, Belver A, Rodriguez-Rosales MP. 2012.** Overexpression of SISOS2 (SICIPK24) confers salt tolerance to transgenic tomato. *Plant Cell Environ* **35**(8): 1467-1482.
- Hussain SS, Mehnaz S, Siddique KHM 2018.** Harnessing the Plant Microbiome for Improved Abiotic Stress Tolerance. In: Egamberdieva D, Ahmad P eds. *Plant Microbiome: Stress Response*. Singapore: Springer Singapore, 21-43.
- Hyatt D, Chen GL, Locascio PF, Land ML, Larimer FW, Hauser LJ. 2010.** Prodigal: prokaryotic gene recognition and translation initiation site identification. *BMC Bioinformatics* **11**(1): 119.
- Ilangumaran G, Smith DL. 2017.** Plant growth promoting rhizobacteria in amelioration of salinity stress: a systems biology perspective. *Frontiers in Plant Science* **8**: 1768.
- Iniguez AL, Dong Y, Carter HD, Ahmer BM, Stone JM, Triplett EW. 2005.** Regulation of enteric endophytic bacterial colonization by plant defenses. *Molecular Plant-Microbe Interactions* **18**(2): 169-178.
- Isayenkov SV, Maathuis FJ. 2019.** Plant salinity stress: many unanswered questions remain. *Frontiers in Plant Science* **10**: 80.

- Jacoby R, Peukert M, Succurro A, Koprivova A, Kopriva S. 2017.** The role of soil microorganisms in plant mineral nutrition—current knowledge and future directions. *Frontiers in Plant Science* **8**: 1617.
- Jatan R, Chauhan PS, Lata C. 2019.** *Pseudomonas putida* modulates the expression of miRNAs and their target genes in response to drought and salt stresses in chickpea (*Cicer arietinum* L.). *Genomics* **111**(4): 509-519.
- Ji H, Pardo JM, Batelli G, Van Oosten MJ, Bressan RA, Li X. 2013.** The Salt Overly Sensitive (SOS) pathway: established and emerging roles. *Mol Plant* **6**(2): 275-286.
- Jia Y, Yuan Y, Zhang Y, Yang S, Zhang X. 2015.** Extreme expansion of NBS-encoding genes in Rosaceae. *BMC Genet* **16**(1): 48.
- Jochum MD, McWilliams KL, Pierson EA, Jo YK. 2019.** Host-mediated microbiome engineering (HMME) of drought tolerance in the wheat rhizosphere. *PLoS One* **14**(12): e0225933.
- Jousset A, Schuldes J, Keel C, Maurhofer M, Daniel R, Scheu S, Thuermer A. 2014.** Full-genome sequence of the plant growth-promoting bacterium *Pseudomonas protegens* CHA0. *Genome announcements* **2**(2): e00322-00314.
- Julkowska MM, Koevoets IT, Mol S, Hoefsloot H, Feron R, Tester MA, Keurentjes JJ, Korte A, Haring MA, de Boer G-J. 2017.** Genetic components of root architecture remodeling in response to salt stress. *The Plant Cell* **29**(12): 3198-3213.
- Julkowska MM, Testerink C. 2015.** Tuning plant signaling and growth to survive salt. *Trends in Plant Science* **20**(9): 586-594.
- Jun S-R, Wassenaar TM, Nookaew I, Hauser L, Wanchai V, Land M, Timm CM, Lu T-YS, Schadt CW, Doktycz MJ. 2016.** Diversity of *Pseudomonas* genomes, including *Populus*-associated isolates, as revealed by comparative genome analysis. *Applied and environmental microbiology* **82**(1): 375-383.

References

- Kalyaanamoorthy S, Minh BQ, Wong TKF, von Haeseler A, Jermiin LS. 2017.** ModelFinder: fast model selection for accurate phylogenetic estimates. *Nat Methods* **14**(6): 587-589.
- Karanja JK, Aslam MM, Qian Z, Yankey R, Dodd IC, Weifeng X. 2021.** Absciscic Acid Mediates Drought-Enhanced Rhizosheath Formation in Tomato. *Front Plant Sci* **12**: 658787.
- Karlova R, Boer D, Hayes S, Testerink C. 2021.** Root plasticity under abiotic stress. *Plant Physiol* **187**(3): 1057-1070.
- Kaur S, Egidi E, Qiu Z, Macdonald CA, Verma JP, Trivedi P, Wang J, Liu H, Singh BK. 2022.** Synthetic community improves crop performance and alters rhizosphere microbial communities. *Journal of Sustainable Agriculture and Environment* **1**(2): 118-131.
- Kecskés M, Choudhury A, Casteriano A, Deaker R, Roughley R, Lewin L, Ford R, Kennedy I. 2016.** Effects of bacterial inoculant biofertilizers on growth, yield and nutrition of rice in Australia. *Journal of Plant Nutrition* **39**(3): 377-388.
- Keel C, Schnider U, Maurhofer M, Voisard C, Laville J, Burger U, Wirthner PJ, Haas D, Défago G. 1992.** Suppression of root diseases by *Pseudomonas fluorescens* CHA0: importance of the bacterial secondary metabolite 2, 4-diacetylphloroglucinol. *Molecular Plant-Microbe Interactions* **5**(1): 4-13.
- Köster J, Rahmann S. 2012.** Snakemake—a scalable bioinformatics workflow engine. *Bioinformatics* **28**(19): 2520-2522.
- Kou X, Chen X, Mao C, He Y, Feng Y, Wu C, Xue Z. 2019.** Selection and mechanism exploration for salt-tolerant genes in tomato. *The Journal of Horticultural Science and Biotechnology* **94**(2): 171-183.
- Kronzucker HJ, Britto DT. 2011.** Sodium transport in plants: a critical review. *New Phytol* **189**(1): 54-81.

- Kumar M, Etesami H, Kumar V. 2019.** *Saline soil-based agriculture by halotolerant microorganisms*: Springer.
- Lafi FF, Alam I, Bisseling T, Geurts R, Bajic VB, Hirt H, Saad MM. 2017a.** Draft Genome Sequence of the Plant Growth-Promoting Rhizobacterium *Acinetobacter radioresistens* Strain SA188 Isolated from the Desert Plant *Indigofera argentea*. *Genome Announc* **5**(9): e01708-01716.
- Lafi FF, Alam I, Geurts R, Bisseling T, Bajic VB, Hirt H, Saad MM. 2016.** Draft Genome Sequence of the Phosphate-Solubilizing Bacterium *Pseudomonas argentinensis* Strain SA190 Isolated from the Desert Plant *Indigofera argentea*. *Genome Announc* **4**(6): e01431-01416.
- Lafi FF, Alam I, Geurts R, Bisseling T, Bajic VB, Hirt H, Saad MM. 2017b.** Draft Genome Sequence of *Enterobacter* sp. Sa187, an Endophytic Bacterium Isolated from the Desert Plant *Indigofera argentea*. *Genome Announc* **5**(7): e01638-01616.
- Lafi FF, Alam I, Geurts R, Bisseling T, Bajic VB, Hirt H, Saad MM. 2017c.** Draft Genome Sequence of *Ochrobactrum intermedium* Strain SA148, a Plant Growth-Promoting Desert Rhizobacterium. *Genome Announc* **5**(9): e01707-01716.
- Lamers J, Van Der Meer T, Testerink C. 2020.** How plants sense and respond to stressful environments. *Plant Physiol* **182**(4): 1624-1635.
- Lebeis SL, Paredes SH, Lundberg DS, Breakfield N, Gehring J, McDonald M, Malfatti S, Glavina del Rio T, Jones CD, Tringe SG, et al. 2015.** Salicylic acid modulates colonization of the root microbiome by specific bacterial taxa. *Science* **349**(6250): 860-864.
- Lemanceau P, Blouin M, Muller D, Moenne-Loccoz Y. 2017.** Let the Core Microbiota Be Functional. *Trends Plant Sci* **22**(7): 583-595.
- Lennon JT, Jones SE. 2011.** Microbial seed banks: the ecological and evolutionary implications of dormancy. *Nat Rev Microbiol* **9**(2): 119-130.

References

- Li H, La S, Zhang X, Gao L, Tian Y. 2021. Salt-induced recruitment of specific root-associated bacterial consortium capable of enhancing plant adaptability to salt stress. *ISME J*.
- Li Q, Li H, Yang Z, Cheng X, Zhao Y, Qin L, Bisseling T, Cao Q, Willemsen V. 2022. Plant Growth-Promoting rhizobacterium *Pseudomonas* sp. CM11 Specifically Induces Lateral Roots. *New Phytol* **n/a**(n/a).
- Liu C, Yu H, Rao X, Li L, Dixon RA. 2021. Absciscic acid regulates secondary cell-wall formation and lignin deposition in *Arabidopsis thaliana* through phosphorylation of NST1. *Proc Natl Acad Sci U S A* **118**(5).
- Liu YX, Qin Y, Bai Y. 2019. Reductionist synthetic community approaches in root microbiome research. *Curr Opin Microbiol* **49**: 97-102.
- Liu Z, Li L, Zhuo G, Xue B. 2019. Characterizing structure and potential function of bacterial and fungal root microbiota in hullless barley cultivars. *Journal of soil science and plant nutrition* **19**(2): 420-429.
- Livak KJ, Schmittgen TD. 2001. Analysis of relative gene expression data using real-time quantitative PCR and the 2^{(-Delta Delta C(T))} Method. *Methods* **25**(4): 402-408.
- Ljubuncic P, Reznick AZ. 2009. The evolutionary theories of aging revisited--a mini-review. *Gerontology* **55**(2): 205-216.
- Lovdal T, Lillo C. 2009. Reference gene selection for quantitative real-time PCR normalization in tomato subjected to nitrogen, cold, and light stress. *Anal Biochem* **387**(2): 238-242.
- Lugtenberg B, Kamilova F. 2009. Plant-growth-promoting rhizobacteria. *Annu Rev Microbiol* **63**: 541-556.
- Lugtenberg B, Kamilova F. 2009. Plant-growth-promoting rhizobacteria. *Annual review of microbiology* **63**: 541-556.

- Lundberg DS, Lebeis SL, Paredes SH, Yourstone S, Gehring J, Malfatti S, Tremblay J, Engelbrektson A, Kunin V, Del Rio TG, et al. 2012.** Defining the core Arabidopsis thaliana root microbiome. *Nature* **488**(7409): 86-90.
- Ma L, Zhang H, Sun L, Jiao Y, Zhang G, Miao C, Hao F. 2012.** NADPH oxidase AtrbohD and AtrbohF function in ROS-dependent regulation of Na⁺/K⁺ homeostasis in Arabidopsis under salt stress. *J Exp Bot* **63**(1): 305-317.
- Madeira F, Park YM, Lee J, Buso N, Gur T, Madhusoodanan N, Basutkar P, Tivey ARN, Potter SC, Finn RD, et al. 2019.** The EMBL-EBI search and sequence analysis tools APIs in 2019. *Nucleic Acids Res* **47**(W1): W636-W641.
- Marasco R, Mosqueira MJ, Fusi M, Ramond J-B, Merlino G, Booth JM, Maggs-Kölling G, Cowan DA, Daffonchio D. 2018.** Rhizosheath microbial community assembly of sympatric desert speargrasses is independent of the plant host. *Microbiome* **6**(1): 215.
- Marchesi JR, Ravel J. 2015.** The vocabulary of microbiome research: a proposal. *Microbiome* **3**: 31.
- Mariotte P, Mehrabi Z, Bezemer TM, De Deyn GB, Kulmatiski A, Drigo B, Veen GFC, van der Heijden MGA, Kardol P. 2018.** Plant-Soil Feedback: Bridging Natural and Agricultural Sciences. *Trends Ecol Evol* **33**(2): 129-142.
- Masella AP, Bartram AK, Truszkowski JM, Brown DG, Neufeld JD. 2012.** PANDAseq: paired-end assembler for illumina sequences. *BMC Bioinformatics* **13**(1): 31.
- Maser P, Hosoo Y, Goshima S, Horie T, Eckelman B, Yamada K, Yoshida K, Bakker EP, Shinmyo A, Oiki S, et al. 2002.** Glycine residues in potassium channel-like selectivity filters determine potassium selectivity in four-loop-per-subunit HKT transporters from plants. *Proc Natl Acad Sci U S A* **99**(9): 6428-6433.
- Mayak S, Tirosh T, Glick BR. 2004.** Plant growth-promoting bacteria confer resistance in tomato plants to salt stress. *Plant Physiol Biochem* **42**(6): 565-572.

References

- Mazzola M, Manici LM. 2012.** Apple replant disease: role of microbial ecology in cause and control. *Annu Rev Phytopathol* **50**: 45-65.
- McMurdie PJ, Holmes S. 2013.** phyloseq: an R package for reproducible interactive analysis and graphics of microbiome census data. *PLoS One* **8**(4): e61217.
- Mendes R, Garbeva P, Raaijmakers JM. 2013.** The rhizosphere microbiome: significance of plant beneficial, plant pathogenic, and human pathogenic microorganisms. *FEMS Microbiol Rev* **37**(5): 634-663.
- Mendes R, Kruijt M, de Bruijn I, Dekkers E, van der Voort M, Schneider JH, Piceno YM, DeSantis TZ, Andersen GL, Bakker PA. 2011.** Deciphering the rhizosphere microbiome for disease-suppressive bacteria. *Science* **332**(6033): 1097-1100.
- Meyers BC, Kozik A, Griego A, Kuang H, Michelmore RW. 2003.** Genome-wide analysis of NBS-LRR-encoding genes in Arabidopsis. *The Plant Cell* **15**(4): 809-834.
- Miller G, Suzuki N, Ciftci-Yilmaz S, Mittler R. 2010.** Reactive oxygen species homeostasis and signalling during drought and salinity stresses. *Plant Cell Environ* **33**(4): 453-467.
- Mitter EK, de Freitas JR, Germida JJ. 2017.** Bacterial root microbiome of plants growing in oil sands reclamation covers. *Frontiers in microbiology* **8**: 849.
- Moller IS, Gilliam M, Jha D, Mayo GM, Roy SJ, Coates JC, Haseloff J, Tester M. 2009.** Shoot Na⁺ exclusion and increased salinity tolerance engineered by cell type-specific alteration of Na⁺ transport in Arabidopsis. *Plant Cell* **21**(7): 2163-2178.
- Morgan PW, Drew MC. 1997.** Ethylene and plant responses to stress. *Physiologia Plantarum* **100**(3): 620-630.
- Mueller UG, Sachs JL. 2015.** Engineering microbiomes to improve plant and animal health. *Trends in microbiology* **23**(10): 606-617.
- Muller DB, Vogel C, Bai Y, Vorholt JA. 2016.** The Plant Microbiota: Systems-Level Insights and Perspectives. *Annu Rev Genet* **50**: 211-234.

- Munns R, Tester M. 2008.** Mechanisms of salinity tolerance. *Annual review of plant biology* **59**: 651.
- Naseer S, Lee Y, Lapierre C, Franke R, Nawrath C, Geldner N. 2012.** Casparian strip diffusion barrier in Arabidopsis is made of a lignin polymer without suberin. *Proceedings of the National Academy of Sciences* **109**(25): 10101-10106.
- Nautiyal CS. 1999.** An efficient microbiological growth medium for screening phosphate solubilizing microorganisms. *FEMS Microbiol Lett* **170**(1): 265-270.
- Nautiyal CS, Srivastava S, Chauhan PS, Seem K, Mishra A, Sopory SK. 2013.** Plant growth-promoting bacteria *Bacillus amyloliquefaciens* NBRISN13 modulates gene expression profile of leaf and rhizosphere community in rice during salt stress. *Plant Physiology and Biochemistry* **66**: 1-9.
- Naylor D, DeGraaf S, Purdom E, Coleman-Derr D. 2017.** Drought and host selection influence bacterial community dynamics in the grass root microbiome. *ISME J* **11**(12): 2691-2704.
- Naylor D, DeGraaf S, Purdom E, Coleman-Derr D. 2017.** Drought and host selection influence bacterial community dynamics in the grass root microbiome. *ISME J* **11**(12): 2691-2704.
- Nguyen DD, Melnik AV, Koyama N, Lu X, Schorn M, Fang J, Aguinaldo K, Lincecum TL, Ghequire MG, Carrion VJ. 2016.** Indexing the *Pseudomonas* specialized metabolome enabled the discovery of poaeamide B and the bananamides. *Nature Microbiology* **2**(1): 1-10.
- Nguyen LT, Schmidt HA, von Haeseler A, Minh BQ. 2015.** IQ-TREE: a fast and effective stochastic algorithm for estimating maximum-likelihood phylogenies. *Mol Biol Evol* **32**(1): 268-274.
- Niu B, Paulson JN, Zheng X, Kolter R. 2017.** Simplified and representative bacterial community of maize roots. *Proc Natl Acad Sci U S A* **114**(12): E2450-E2459.

References

- North GB, Nobel PS. 1991.** Changes in hydraulic conductivity and anatomy caused by drying and rewetting roots of *Agave deserti* (Agavaceae). *American Journal of Botany* **78**(7): 906-915.
- North GB, Nobel PS. 1992.** Drought-induced changes in hydraulic conductivity and structure in roots of *Ferocactus acanthodes* and *Opuntia ficus-indica*. *New Phytologist* **120**(1): 9-19.
- Oleńska E, Małek W, Wójcik M, Swiecicka I, Thijs S, Vangronsveld J. 2020.** Beneficial features of plant growth-promoting rhizobacteria for improving plant growth and health in challenging conditions: A methodical review. *Science of The Total Environment* **743**: 140682.
- Olias R, Eljakaoui Z, Li J, De Morales PA, Marin - Manzano MC, Pardo JM, Belver A. 2009.** The plasma membrane Na⁺/H⁺ antiporter SOS1 is essential for salt tolerance in tomato and affects the partitioning of Na⁺ between plant organs. *Plant, Cell & Environment* **32**(7): 904-916.
- Olias R, Eljakaoui Z, Pardo JM, Belver A. 2009.** The Na⁽⁺⁾/H⁽⁺⁾ exchanger SOS1 controls extrusion and distribution of Na⁽⁺⁾ in tomato plants under salinity conditions. *Plant Signal Behav* **4**(10): 973-976.
- Omoboye OO, Geudens N, Duban M, Chevalier M, Flahaut C, Martins JC, Leclère V, Oni FE, Höfte M. 2019.** *Pseudomonas* sp. COW3 produces new bananamide-type cyclic lipopeptides with antimicrobial activity against *Pythium myriotylum* and *Pyricularia oryzae*. *Molecules* **24**(22): 4170.
- Otlewska A, Migliore M, Dybka-Stępień K, Manfredini A, Struszczyk-Świta K, Napoli R, Białkowska A, Canfora L, Pinzari F. 2020.** When salt meddles between plant, soil, and microorganisms. *Frontiers in Plant Science*: 1429.
- Park YG, Mun BG, Kang SM, Hussain A, Shahzad R, Seo CW, Kim AY, Lee SU, Oh KY, Lee DY, et al. 2017.** *Bacillus aryabhattai* SRB02 tolerates oxidative and nitrosative stress and promotes the growth of soybean by modulating the production of phytohormones. *PLoS One* **12**(3): e0173203.

- Parks DH, Imelfort M, Skennerton CT, Hugenholtz P, Tyson GW. 2015.** CheckM: assessing the quality of microbial genomes recovered from isolates, single cells, and metagenomes. *Genome Res* **25**(7): 1043-1055.
- Patten CL, Glick BR. 1996.** Bacterial biosynthesis of indole-3-acetic acid. *Canadian Journal of Microbiology* **42**(3): 207-220.
- Paulson JN, Stine OC, Bravo HC, Pop M. 2013.** Differential abundance analysis for microbial marker-gene surveys. *Nat Methods* **10**(12): 1200-1202.
- Pedregosa F, Varoquaux G, Gramfort A, Michel V, Thirion B, Grisel O, Blondel M, Prettenhofer P, Weiss R, Dubourg V. 2011.** Scikit-learn: Machine learning in Python. *the Journal of machine Learning research* **12**: 2825-2830.
- Peiffer JA, Spor A, Koren O, Jin Z, Tringe SG, Dangl JL, Buckler ES, Ley RE. 2013.** Diversity and heritability of the maize rhizosphere microbiome under field conditions. *Proc Natl Acad Sci U S A* **110**(16): 6548-6553.
- Pérez-Jaramillo JE, Carrión VJ, de Hollander M, Raaijmakers JM. 2018.** The wild side of plant microbiomes. *Microbiome* **6**(1): 1-6.
- Pfeiffer S, Mitter B, Oswald A, Schlöter-Hai B, Schlöter M, Declerck S, Sessitsch A. 2017.** Rhizosphere microbiomes of potato cultivated in the High Andes show stable and dynamic core microbiomes with different responses to plant development. *FEMS Microbiology Ecology* **93**(2): fiw242.
- Philippot L, Raaijmakers JM, Lemanceau P, van der Putten WH. 2013.** Going back to the roots: the microbial ecology of the rhizosphere. *Nat Rev Microbiol* **11**(11): 789-799.
- Phour M, Sindhu SS. 2020.** Amelioration of salinity stress and growth stimulation of mustard (*Brassica juncea* L.) by salt-tolerant *Pseudomonas* species. *Applied Soil Ecology* **149**: 103518.

References

- Pieterse CM, Zamioudis C, Berendsen RL, Weller DM, Van Wees SC, Bakker PA. 2014. Induced systemic resistance by beneficial microbes. *Annu Rev Phytopathol* **52**: 347-375.
- Pieterse CMJ, Berendsen RL, de Jonge R, Stringlis IA, Van Dijken AJH, Van Pelt JA, Van Wees SCM, Yu K, Zamioudis C, Bakker PAHM. 2021. *Pseudomonas simiae* WCS417: star track of a model beneficial rhizobacterium. *Plant and soil* **461**(1): 245-263.
- Plett D, Safwat G, Gilliham M, Skrumsager Møller I, Roy S, Shirley N, Jacobs A, Johnson A, Tester M. 2010. Improved salinity tolerance of rice through cell type-specific expression of AtHKT1; 1. *PLoS One* **5**(9): e12571.
- Plomion C, Aury JM, Amselem J, Leroy T, Murat F, Duplessis S, Faye S, Francillon N, Labadie K, Le Provost G, et al. 2018. Oak genome reveals facets of long lifespan. *Nat Plants* **4**(7): 440-452.
- Puértolas J, Conesa MR, Ballester C, Dodd IC. 2015. Local root abscisic acid (ABA) accumulation depends on the spatial distribution of soil moisture in potato: implications for ABA signalling under heterogeneous soil drying. *J Exp Bot* **66**(8): 2325-2334.
- Qin Y, Druzhinina IS, Pan X, Yuan Z. 2016. Microbially Mediated Plant Salt Tolerance and Microbiome-based Solutions for Saline Agriculture. *Biotechnology Advances* **34**(7): 1245-1259.
- Qiu QS, Guo Y, Quintero FJ, Pardo JM, Schumaker KS, Zhu JK. 2004. Regulation of vacuolar Na⁺/H⁺ exchange in *Arabidopsis thaliana* by the salt-overly-sensitive (SOS) pathway. *J Biol Chem* **279**(1): 207-215.
- Quast C, Pruesse E, Yilmaz P, Gerken J, Schweer T, Yarza P, Peplies J, Glockner FO. 2013. The SILVA ribosomal RNA gene database project: improved data processing and web-based tools. *Nucleic Acids Res* **41**(Database issue): D590-596.
- Quecine MC, Kidarsa TA, Goebel NC, Shaffer BT, Henkels MD, Zabriskie TM, Loper JE. 2016. An interspecies signaling system mediated by fusaric acid has parallel

- effects on antifungal metabolite production by *Pseudomonas protegens* strain Pf-5 and antibiosis of *Fusarium* spp. *Applied and environmental microbiology* **82**(5): 1372-1382.
- Raaijmakers JM 2015.** The minimal rhizosphere microbiome. *Principles of plant-microbe interactions*: Springer, 411-417.
- Raaijmakers JM, Paulitz TC, Steinberg C, Alabouvette C, Moënné-Loccoz Y. 2008.** The rhizosphere: a playground and battlefield for soilborne pathogens and beneficial microorganisms. *Plant and soil* **321**(1-2): 341-361.
- Rademaker JL. 1997.** Characterization and classification of microbes by rep-PCR genomic fingerprinting and computer assisted pattern analysis. *DNA markers: protocols, applications, and overviews*: 151-171.
- Rahman MM, Flory E, Koyro H-W, Abideen Z, Schikora A, Suarez C, Schnell S, Cardinale M. 2018.** Consistent associations with beneficial bacteria in the seed endosphere of barley (*Hordeum vulgare* L.). *Systematic and applied microbiology* **41**(4): 386-398.
- Rajput L, Imran A, Mubeen F, Hafeez FY. 2013.** Salt-tolerant PGPR strain *Planococcus rifietensis* promotes the growth and yield of wheat (*Triticum aestivum* L.) cultivated in saline soil. *Pak J Bot* **45**(6): 1955-1962.
- Ravanbakhsh M, Kowalchuk GA, Jousset A. 2019.** Root-associated microorganisms reprogram plant life history along the growth-stress resistance tradeoff. *ISME J* **13**(12): 3093-3101.
- Ravanbakhsh M, Sasidharan R, Voeseinek L, Kowalchuk GA, Jousset A. 2018.** Microbial modulation of plant ethylene signaling: ecological and evolutionary consequences. *Microbiome* **6**(1): 52.
- Remans R, Croonenborghs A, Gutierrez RT, Michiels J, Vanderleyden J 2007.** Effects of plant growth-promoting rhizobacteria on nodulation of *Phaseolus vulgaris* L. are dependent on plant P nutrition. *New perspectives and approaches in plant growth-promoting Rhizobacteria research*: Springer, 341-351.

References

- Richardson AD, Duigan SP, Berlyn GP. 2002.** An evaluation of noninvasive methods to estimate foliar chlorophyll content. *New Phytologist* **153**(1): 185-194.
- Richardson AE, Simpson RJ. 2011.** Soil microorganisms mediating phosphorus availability update on microbial phosphorus. *Plant Physiol* **156**(3): 989-996.
- Rigling D, Prospero S. 2018.** Cryphonectria parasitica, the causal agent of chestnut blight: invasion history, population biology and disease control. *Mol Plant Pathol* **19**(1): 7-20.
- Rizaludin MS, Stopnisek N, Raaijmakers JM, Garbeva P. 2021.** The Chemistry of Stress: Understanding the 'Cry for Help' of Plant Roots. *Metabolites* **11**(6).
- Rognes T, Flouri T, Nichols B, Quince C, Mahe F. 2016.** VSEARCH: a versatile open source tool for metagenomics. *PeerJ* **4**: e2584.
- Rojas-Tapias D, Moreno-Galván A, Pardo-Díaz S, Obando M, Rivera D, Bonilla R. 2012.** Effect of inoculation with plant growth-promoting bacteria (PGPB) on amelioration of saline stress in maize (*Zea mays*). *Applied Soil Ecology* **61**: 264-272.
- Roman VJ, den Toom LA, Gamiz CC, van der Pijl N, Visser RG, van Loo EN, van der Linden CG. 2020.** Differential responses to salt stress in ion dynamics, growth and seed yield of European quinoa varieties. *Environmental and Experimental Botany* **177**: 104146.
- Rubio F, Gassmann W, Schroeder JI. 1995.** Sodium-driven potassium uptake by the plant potassium transporter HKT1 and mutations conferring salt tolerance. *Science* **270**(5242): 1660-1663.
- Rus A, Lee BH, Munoz-Mayor A, Sharkhuu A, Miura K, Zhu JK, Bressan RA, Hasegawa PM. 2004.** AtHKT1 facilitates Na⁺ homeostasis and K⁺ nutrition in planta. *Plant Physiol* **136**(1): 2500-2511.
- Rus A, Yokoi S, Sharkhuu A, Reddy M, Lee B-h, Matsumoto TK, Koiwa H, Zhu J-K, Bressan RA, Hasegawa PM. 2001.** AtHKT1 is a salt tolerance determinant that controls

- Na⁺ entry into plant roots. *Proceedings of the National Academy of Sciences* **98**(24): 14150-14155.
- Saad MM, Eida AA, Hirt H. 2020.** Tailoring plant-associated microbial inoculants in agriculture: a roadmap for successful application. *J Exp Bot* **71**(13): 3878-3901.
- Sadeghi A, Karimi E, Dahaji PA, Javid MG, Dalvand Y, Askari H. 2012.** Plant growth promoting activity of an auxin and siderophore producing isolate of *Streptomyces* under saline soil conditions. *World Journal of Microbiology and Biotechnology* **28**(4): 1503-1509.
- Saikia J, Sarma RK, Dhandia R, Yadav A, Bharali R, Gupta VK, Saikia R. 2018.** Alleviation of drought stress in pulse crops with ACC deaminase producing rhizobacteria isolated from acidic soil of Northeast India. *Scientific Reports* **8**(1): 3560.
- Samad A, Trognitz F, Compant S, Antonielli L, Sessitsch A. 2017.** Shared and host-specific microbiome diversity and functioning of grapevine and accompanying weed plants. *Environmental microbiology* **19**(4): 1407-1424.
- Sandrini M, Nerva L, Sillo F, Balestrini R, Chitarra W, Zampieri E. 2022.** Abiotic stress and belowground microbiome: The potential of omics approaches. *International Journal of Molecular Sciences* **23**(3): 1091.
- Santos-Medellín C, Edwards J, Liechty Z, Nguyen B, Sundaresan V. 2017.** Drought stress results in a compartment-specific restructuring of the rice root-associated microbiomes. *mBio* **8**(4): e00764-00717.
- Santos SS, Rask KA, Vestergård M, Johansen JL, Priemé A, Frøslev TG, González AMM, He H, Ekelund F. 2021.** Specialized microbiomes facilitate natural rhizosphere microbiome interactions counteracting high salinity stress in plants. *Environmental and Experimental Botany* **186**.
- Sarkar A, Ghosh PK, Pramanik K, Mitra S, Soren T, Pandey S, Mondal MH, Maiti TK. 2018.** A halotolerant *Enterobacter* sp. displaying ACC deaminase activity promotes rice seedling growth under salt stress. *Res Microbiol* **169**(1): 20-32.

References

- Sasse J, Martinoia E, Northen T. 2018.** Feed your friends: do plant exudates shape the root microbiome? *Trends in Plant Science* **23**(1): 25-41.
- Schachtman DP, Schroeder JI. 1994.** Structure and transport mechanism of a high-affinity potassium uptake transporter from higher plants. *Nature* **370**(6491): 655-658.
- Schlaeppi K, Dombrowski N, Oter RG, Ver Loren van Themaat E, Schulze-Lefert P. 2014.** Quantitative divergence of the bacterial root microbiota in *Arabidopsis thaliana* relatives. *Proc Natl Acad Sci U S A* **111**(2): 585-592.
- Schmitz L, Yan Z, Schnejderberg M, de Roij M, Pijnenburg R, Zheng Q, Franken C, Dechesne A, Trindade LM, van Velzen R, et al. 2022.** Synthetic bacterial community derived from a desert rhizosphere confers salt stress resilience to tomato in the presence of a soil microbiome. *ISME J*.
- Schnejderberg M, Cheng X, Franken C, de Hollander M, van Velzen R, Schmitz L, Heinen R, Geurts R, van der Putten WH, Bezemer TM, et al. 2020.** Quantitative comparison between the rhizosphere effect of *Arabidopsis thaliana* and co-occurring plant species with a longer life history. *ISME J* **14**(10): 2433-2448.
- Schnejderberg M, Schmitz L, Cheng X, Polman S, Franken C, Geurts R, Bisseling T. 2018.** A genetically and functionally diverse group of non-diazotrophic *Bradyrhizobium* spp. colonizes the root endophytic compartment of *Arabidopsis thaliana*. *BMC Plant Biol* **18**(1): 61.
- Schreiber M, Barakate A, Uzrek N, Macaulay M, Sourdille A, Morris J, Hedley PE, Ramsay L, Waugh R. 2019.** A highly mutagenised barley (cv. Golden Promise) TILLING population coupled with strategies for screening-by-sequencing. *Plant methods* **15**(1): 1-14.
- Schreiber M, Mascher M, Wright J, Padmarasu S, Himmelbach A, Heavens D, Milne L, Clavijo BJ, Stein N, Waugh R. 2020.** A genome assembly of the barley 'transformation reference' cultivar golden promise. *G3: Genes, Genomes, Genetics* **10**(6): 1823-1827.

- Schrire BD, Lavin M, Barker NP, Forest F. 2009.** Phylogeny of the tribe Indigofereae (Leguminosae – Papilionoideae): Geographically structured more in succulent - rich and temperate settings than in grass - rich environments. *American Journal of Botany* **96**(4): 816-852.
- Schwyn B, Neilands JB. 1987.** Universal chemical assay for the detection and determination of siderophores. *Anal Biochem* **160**(1): 47-56.
- Selvakumar G, Krishnamoorthy R, Kim K, Sa TM. 2016.** Genetic Diversity and Association Characters of Bacteria Isolated from Arbuscular Mycorrhizal Fungal Spore Walls. *PLoS One* **11**(8): e0160356.
- Sessitsch A, Pfaffenbichler N, Mitter B. 2019.** Microbiome Applications from Lab to Field: Facing Complexity. *Trends Plant Sci* **24**(3): 194-198.
- Sharma S, Kulkarni J, Jha B. 2016.** Halotolerant Rhizobacteria Promote Growth and Enhance Salinity Tolerance in Peanut. *Front Microbiol* **7**(1600): 1600.
- Shekhawat K, Saad MM, Sheikh A, Mariappan K, Al-Mahmoudi H, Abdulhakim F, Eida AA, Jalal R, Masmoudi K, Hirt H. 2021.** Root endophyte induced plant thermotolerance by constitutive chromatin modification at heat stress memory gene loci. *EMBO Rep* **22**(3): e51049.
- Shi Z, Li Y, Wang R, Makeschine F. 2005.** Assessment of temporal and spatial variability of soil salinity in a coastal saline field. *Environmental Geology* **48**(2): 171-178.
- Shukla PS, Agarwal PK, Jha B. 2012.** Improved Salinity Tolerance of *Arachis hypogaea* (L.) by the Interaction of Halotolerant Plant-Growth-Promoting Rhizobacteria. *Journal of Plant Growth Regulation* **31**(2): 195-206.
- Si P, Shao W, Yu H, Shi X, Zhang Y, Du G. 2017.** Soil Microbial Community Development in a Cherry Replant Site.
- Silliker JH. 1980.** *Microbial ecology of foods*: Academic Press.

References

- Simmons T, Styer AB, Pierroz G, Goncalves AP, Pasricha R, Hazra AB, Bubner P, Coleman-Derr D. 2020.** Drought Drives Spatial Variation in the Millet Root Microbiome. *Front Plant Sci* **11**: 599.
- Singh RP, Jha PN. 2016.** The Multifarious PGPR *Serratia marcescens* CDP-13 Augments Induced Systemic Resistance and Enhanced Salinity Tolerance of Wheat (*Triticum aestivum* L.). *PLoS One* **11**(6): e0155026.
- Souza Rd, Ambrosini A, Passaglia LM. 2015.** Plant growth-promoting bacteria as inoculants in agricultural soils. *Genetics and molecular biology* **38**: 401-419.
- Spaepen S, Vanderleyden J. 2011.** Auxin and plant-microbe interactions. *Cold Spring Harb Perspect Biol* **3**(4).
- Stringlis IA, Yu K, Feussner K, de Jonge R, Van Bentum S, Van Verk MC, Berendsen RL, Bakker PAHM, Feussner I, Pieterse CMJ. 2018.** MYB72-dependent coumarin exudation shapes root microbiome assembly to promote plant health. *Proceedings of the National Academy of Sciences* **115**(22): E5213.
- Su C, Lei L, Duan Y, Zhang K-Q, Yang J. 2012.** Culture-independent methods for studying environmental microorganisms: methods, application, and perspective. *Applied Microbiology and Biotechnology* **93**(3): 993-1003.
- Sun J, Zhang Q, Zhou J, Wei Q. 2014.** Illumina amplicon sequencing of 16S rRNA tag reveals bacterial community development in the rhizosphere of apple nurseries at a replant disease site and a new planting site. *PLoS One* **9**(10): e111744.
- Tang M, Liu J, Hou W, Stubbendieck RM, Xiong H, Jin J, Gong J, Cheng C, Tang X, Liu Y. 2021.** Structural variability in the bulk soil, rhizosphere, and root endophyte fungal communities of *Themeda japonica* plants under different grades of karst rocky desertification. *Plant and soil*: 1-18.
- Tao JJ, Chen HW, Ma B, Zhang WK, Chen SY, Zhang JS. 2015.** The Role of Ethylene in Plants Under Salinity Stress. *Front Plant Sci* **6**: 1059.

- Tian B, Zhang C, Ye Y, Wen J, Wu Y, Wang H, Li H, Cai S, Cai W, Cheng Z, et al. 2017.** Beneficial traits of bacterial endophytes belonging to the core communities of the tomato root microbiome. *Agriculture, Ecosystems & Environment* **247**: 149-156.
- Trifonova R, Babini V, Postma J, Ketelaars J, Van Elsas J. 2009.** Colonization of torrefied grass fibers by plant-beneficial microorganisms. *Applied Soil Ecology* **41**(1): 98-106.
- Trivedi P, Leach JE, Tringe SG, Sa T, Singh BK. 2020.** Plant-microbiome interactions: from community assembly to plant health. *Nat Rev Microbiol* **18**(11): 607-621.
- Tsolakidou MD, Stringlis IA, Fanega-Sleziak N, Papageorgiou S, Tsalakou A, Pantelides IS. 2019.** Rhizosphere-enriched microbes as a pool to design synthetic communities for reproducible beneficial outputs. *FEMS Microbiol Ecol* **95**(10).
- Uozumi N, Kim EJ, Rubio F, Yamaguchi T, Muto S, Tsuboi A, Bakker EP, Nakamura T, Schroeder JI. 2000.** The Arabidopsis HKT1 gene homolog mediates inward Na(+) currents in xenopus laevis oocytes and Na(+) uptake in Saccharomyces cerevisiae. *Plant Physiol* **122**(4): 1249-1259.
- Ursache R, Andersen TG, Marhavý P, Geldner N. 2018.** A protocol for combining fluorescent proteins with histological stains for diverse cell wall components. *The Plant Journal* **93**(2): 399-412.
- van de Mortel JE, de Vos RC, Dekkers E, Pineda A, Guillod L, Bouwmeester K, van Loon JJ, Dicke M, Raaijmakers JM. 2012.** Metabolic and transcriptomic changes induced in Arabidopsis by the rhizobacterium Pseudomonas fluorescens SS101. *Plant Physiol* **160**(4): 2173-2188.
- Van der Ent S, Verhagen BWM, Van Doorn R, Bakker D, Verlaan MG, Pel MJC, Joosten RG, Proveniers MCG, Van Loon LC, Ton J, et al. 2008.** MYB72 Is Required in Early Signaling Steps of Rhizobacteria-Induced Systemic Resistance in Arabidopsis *Plant Physiol* **146**(3): 1293-1304.

References

- van der Putten WH, Bardgett RD, Bever JD, Bezemer TM, Casper BB, Fukami T, Kardol P, Klironomos JN, Kulmatiski A, Schweitzer JA, et al. 2013. Plant–soil feedbacks: the past, the present and future challenges. *Journal of Ecology* **101**(2): 265-276.
- Van Loon L 2007. Plant responses to plant growth-promoting rhizobacteria. *New perspectives and approaches in plant growth-promoting Rhizobacteria research*: Springer, 243-254.
- Van Zelm E, Zhang Y, Testerink C. 2020. Salt tolerance mechanisms of plants. *Annual review of plant biology* **71**: 403-433.
- Verbon EH, Trapet PL, Stringlis IA, Kruijs S, Bakker P, Pieterse CMJ. 2017. Iron and Immunity. *Annu Rev Phytopathol* **55**: 355-375.
- Vettraino A, Morel O, Perlerou C, Robin C, Diamandis S, Vannini A. 2005. Occurrence and distribution of Phytophthora species in European chestnut stands, and their association with Ink Disease and crown decline. *European Journal of Plant Pathology* **111**(2): 169-180.
- Vieira S, Sikorski J, Dietz S, Herz K, Schrumpf M, Bruelheide H, Scheel D, Friedrich MW, Overmann J. 2020. Drivers of the composition of active rhizosphere bacterial communities in temperate grasslands. *ISME J* **14**(2): 463-475.
- Vives-Peris V, Gómez-Cadenas A, Pérez-Clemente RM. 2018. Salt stress alleviation in citrus plants by plant growth-promoting rhizobacteria *Pseudomonas putida* and *Novosphingobium* sp. *Plant cell reports* **37**(11): 1557-1569.
- Volkens G. 1887. *Die Flora der aegyptisch-arabischen Wüste auf Grundlage anatomisch-physiologischer Forschungen*: Borntraeger.
- Vorholt JA, Vogel C, Carlstrom CI, Muller DB. 2017. Establishing Causality: Opportunities of Synthetic Communities for Plant Microbiome Research. *Cell Host Microbe* **22**(2): 142-155.

- Wagner MR, Lundberg DS, Del Rio TG, Tringe SG, Dangl JL, Mitchell-Olds T. 2016.** Host genotype and age shape the leaf and root microbiomes of a wild perennial plant. *Nat Commun* **7**(1): 12151.
- Wang M, Yang P, Falcão Salles J. 2016.** Distribution of root-associated bacterial communities along a salt-marsh primary succession. *Frontiers in Plant Science* **6**: 1188.
- Wang Q, Garrity GM, Tiedje JM, Cole JR. 2007.** Naive Bayesian classifier for rapid assignment of rRNA sequences into the new bacterial taxonomy. *Applied and environmental microbiology* **73**(16): 5261-5267.
- Wang Y, Wu W-H. 2017.** Regulation of potassium transport and signaling in plants. *Current Opinion in Plant Biology* **39**: 123-128.
- Weller DM, Raaijmakers JM, Gardener BB, Thomashow LS. 2002.** Microbial populations responsible for specific soil suppressiveness to plant pathogens. *Annu Rev Phytopathol* **40**(1): 309-348.
- Winkelmann T, Smalla K, Amelung W, Baab G, Grunewaldt-Stocker G, Kanfra X, Meyhofer R, Reim S, Schmitz M, Vetterlein D, et al. 2019.** Apple Replant Disease: Causes and Mitigation Strategies. *Curr Issues Mol Biol* **30**(1): 89-106.
- Woolfson KN, Esfandiari M, Bernards MA. 2022.** Suberin Biosynthesis, Assembly, and Regulation. *Plants (Basel)* **11**(4).
- Wu H, Shabala L, Zhou M, Su N, Wu Q, Ul - Haq T, Zhu J, Mancuso S, Azzarello E, Shabala S. 2019.** Root vacuolar Na⁺ sequestration but not exclusion from uptake correlates with barley salt tolerance. *The Plant Journal* **100**(1): 55-67.
- Wu M, Scott AJ. 2012.** Phylogenomic analysis of bacterial and archaeal sequences with AMPHORA2. *Bioinformatics* **28**(7): 1033-1034.
- Wullstein LH, Bruening ML, Bollen WB. 1979.** Nitrogen Fixation Associated with Sand Grain Root Sheaths (Rhizosheaths) of Certain Xeric Grasses. *Physiologia Plantarum* **46**(1): 1-4.

References

- Xing Y, Liu Y, Zhang Q, Nie X, Sun Y, Zhang Z, Li H, Fang K, Wang G, Huang H, et al. 2019. Hybrid de novo genome assembly of Chinese chestnut (*Castanea mollissima*). *GigaScience* **8**(9): giz112.
- Xiong Y-W, Li X-W, Wang T-T, Gong Y, Zhang C-M, Xing K, Qin S. 2020. Root exudates-driven rhizosphere recruitment of the plant growth-promoting rhizobacterium *Bacillus flexus* KLBMP 4941 and its growth-promoting effect on the coastal halophyte *Limonium sinense* under salt stress. *Ecotoxicology and Environmental Safety* **194**: 110374.
- Xu J, Zhang Y, Zhang P, Trivedi P, Riera N, Wang Y, Liu X, Fan G, Tang J, Coletta-Filho HD, et al. 2018. The structure and function of the global citrus rhizosphere microbiome. *Nat Commun* **9**(1): 4894.
- Xu L, Coleman-Derr D. 2019. Causes and consequences of a conserved bacterial root microbiome response to drought stress. *Curr Opin Microbiol* **49**: 1-6.
- Xu L, Naylor D, Dong Z, Simmons T, Pierroz G, Hixson KK, Kim Y-M, Zink EM, Engbrecht KM, Wang Y. 2018. Drought delays development of the sorghum root microbiome and enriches for monoderm bacteria. *Proceedings of the National Academy of Sciences* **115**(18): E4284-E4293.
- Yaish MW, Al-Lawati A, Jana GA, Vishwas Patankar H, Glick BR. 2016. Impact of soil salinity on the structure of the bacterial endophytic community identified from the roots of caliph medic (*Medicago truncatula*). *PLoS One* **11**(7): e0159007.
- Yang H, Hu J, Long X, Liu Z, Rengel Z. 2016. Salinity altered root distribution and increased diversity of bacterial communities in the rhizosphere soil of Jerusalem artichoke. *Scientific Reports* **6**(1): 1-10.
- Yang J, Kloepper JW, Ryu CM. 2009. Rhizosphere bacteria help plants tolerate abiotic stress. *Trends Plant Sci* **14**(1): 1-4.
- Yeoh YK, Paungfoo - Lonhienne C, Dennis PG, Robinson N, Ragan MA, Schmidt S, Hugenholtz P. 2016. The core root microbiome of sugarcane cultivated under

- varying nitrogen fertilizer application. *Environmental microbiology* **18**(5): 1338-1351.
- Zamioudis C, Hanson J, Pieterse CM. 2014.** β -Glucosidase BGLU42 is a MYB72-dependent key regulator of rhizobacteria-induced systemic resistance and modulates iron deficiency responses in Arabidopsis roots. *New Phytol* **204**(2): 368-379.
- Zarraonaindia I, Owens SM, Weisenhorn P, West K, Hampton-Marcell J, Lax S, Bokulich NA, Mills DA, Martin G, Taghavi S, et al. 2015.** The soil microbiome influences grapevine-associated microbiota. *mBio* **6**(2): e02527-02514.
- Zhang H, Kim MS, Sun Y, Dowd SE, Shi H, Pare PW. 2008.** Soil bacteria confer plant salt tolerance by tissue-specific regulation of the sodium transporter HKT1. *Mol Plant Microbe Interact* **21**(6): 737-744.
- Zhang SS, Sun L, Dong X, Lu SJ, Tian W, Liu JX. 2016.** Cellulose synthesis genes CESA6 and CSI1 are important for salt stress tolerance in Arabidopsis. *J Integr Plant Biol* **58**(7): 623-626.
- Zhang Y, Du H, Gui Y, Xu F, Liu J, Zhang J, Xu W. 2020a.** Moderate water stress in rice induces rhizosheath formation associated with abscisic acid and auxin responses. *J Exp Bot* **71**(9): 2740-2751.
- Zhang Y, Du H, Xu F, Ding Y, Gui Y, Zhang J, Xu W. 2020b.** Root-Bacteria Associations Boost Rhizosheath Formation in Moderately Dry Soil through Ethylene Responses. *Plant Physiol* **183**(2): 780-792.
- Zhao C, Zhang H, Song C, Zhu JK, Shabala S. 2020.** Mechanisms of Plant Responses and Adaptation to Soil Salinity. *Innovation (N Y)* **1**(1): 100017.
- Zhao X, Zhen W, Qi Y, Liu X, Yin B. 2009.** Coordinated effects of root autotoxic substances and *Fusarium oxysporum* Schl. f. sp. *fragariae* on the growth and replant disease of strawberry. *Frontiers of Agriculture in China* **3**(1): 34.

References

- Zhou D, Huang X-F, Chaparro JM, Badri DV, Manter DK, Vivanco JM, Guo J. 2016.** Root and bacterial secretions regulate the interaction between plants and PGPR leading to distinct plant growth promotion effects. *Plant and soil* **401**(1): 259-272.
- Zhuang L, Li Y, Wang Z, Yu Y, Zhang N, Yang C, Zeng Q, Wang Q. 2021.** Synthetic community with six *Pseudomonas* strains screened from garlic rhizosphere microbiome promotes plant growth. *Microb Biotechnol* **14**(2): 488-502.

Summary

Plants sustain microorganisms, for example, bacteria, around and inside their roots. These communities of microorganisms are referred to as root-associated microbiomes. The research on root-associated microbiomes includes, among others, a systematic analysis of their composition, understanding of mechanisms underlying their beneficial effect and robust application of beneficial microbes in agricultural settings. In this thesis, I made use of culture-dependent and -independent methods to study the root-associated microbiomes of different plant species. I analysed the root-associated microbiomes of; a new root compartment of grasses that grow in arid areas, two barley genotypes that grow under saline conditions and a chrono-series of chestnut trees. Furthermore, I constructed synthetic bacterial communities that increased salt tolerance to tomato seedlings that grow in a non-sterile substrate.

In **Chapter 1**, I gave an overview of the current knowledge concerning root-associated bacterial microbiomes and focused on their role in conferring tolerance to abiotic stress.

In **Chapter 2**, we described the developmental and cell biological process underlying the formation of the compartment named root-sleeve. It was studied in two desert grass species, agropyron and stipa. The microbiome composition in the root-sleeve was markedly different from that in the bulk soil (SO) and rhizosphere (RH) and it was more similar to that in the endophytic compartment (EC), although they were significantly different. Actinobacteria were enriched in the root microbiomes with the highest abundance in the root-sleeve and this was probably a plant response to drought. We hypothesized that the formation of root-sleeve and the microbiome community recruited in this compartment would improve tolerance to drought.

In **Chapter 3**, we showed that high salinity reduced the dissimilarity of the root-associated microbiomes of two barley genotypes, Algerian barley landrace and Golden Promise. It is assumed that conserved plant responses to abiotic stress conditions, such as salinity and drought, have larger effects on microbiome composition than genotype-specific adaptation. The salt-induced decrease in microbiome dissimilarity correlated with an

Summary

increase in the relative abundance of *Pseudomonas*. It has previously been well studied that the production of ACC deaminase by *Pseudomonas* could reduce the ethylene level in host plants. We hypothesized that such *Pseudomonas* strains could stimulate the growth of barley under salt stress.

In **Chapter 4**, we used a chrono-series of chestnut trees, ranging from 8 to 830 years, grown in an orchard next to the Great Wall. We observed that the composition of root-associated microbiomes of these chestnut trees was rather similar although we could not exclude that there were small changes correlated with increasing tree age. To test whether such small changes were the result of a negative feedback, chestnut seedlings were replanted on soils associated with trees of different ages or from a control area without trees. Growth was not different, suggesting that such small changes in the composition of the root-associated microbiome did not lead to negative effect. Furthermore, a member of the core microbiome, *Pseudomonas* OTU1, which represented more than 50% of the rhizosphere community, strongly inhibited the growth of chestnut pathogens and stimulated plant growth. We hypothesized that such properties of root-associated microbiome together with the absence of negative plant-soil feedback could contribute to longevity of chestnuts.

In **Chapter 5**, we created a bacterial synthetic community (SynCom), using the core members and verified plant-growth promoting rhizobacteria of the root-associated microbiome of desert plant indigofera. We showed that it promoted the growth of tomato seedlings, under the saline condition in the presence of a non-sterile substrate that mimicked a natural soil microbiome. Furthermore, we simplified this SynCom from the initial 15 to 5 strains by creating random combinations. Such simplified SynCom outperformed the plant growth promoting effect observed from the initial SynCom. Recently often used criteria for SynCom construction could not explain the success of our simplified SynCom. We proposed that more advanced methods, such as metagenomics, metatranscriptomics and metabolomics sequencing, should be used to unveil the mechanism of such phenotype.

In **Chapter 6**, I integrated the findings described in this thesis and the knowledge from literature and proposed methods to construct effective SynComs that can be used under field conditions.

Acknowledgements

I arrived in the Netherlands on 13th August 2013 and started my MSc and new life in this peaceful and lovely town Wageningen. Beautiful time always flies and now it is time to look back and express my gratitude to all those people whom I met and who helped me in this period.

First, I would like to express the deepest appreciation to my promotor Prof. Ton Bisseling, who gave me the chance to join MolBi to do my second MSc thesis on March 2015. That was the beginning of this long march. After my master study, you supported me to work in the lab as a Research Assistant. During this period, I developed great interest in root-associated microbiome studies and with your help, I successfully applied for a doctoral grant from the Chinese Scholarship Council which made it possible for me to continue as a PhD candidate from September 2016. In the beginning of my PhD study, you encouraged me to learn, and apply all kinds of expertise's I was interested in. Further you stimulated me to cooperate with researchers in and outside the Netherlands. With your support, we have created so many good opportunities and some of them have been well finished. Thank you for giving me so much guidance on critical thinking, oral presentations and scientific writing. Your efforts on revising my thesis are very much appreciated. I have to say, without you, I could not have finished it. Furthermore, your wisdom and enthusiasm for science stimulated me to continue scientific career. In this thesis, the last proposition is related to you as I noticed how great your cognitive functioning is in comparison to other elder people. This encourages me to learn all lifelong, just like you do.

I would like to give my sincere gratitude also to my co-promotor, and as my daily supervisor Xu Cheng (程旭) for the continuous support and guidance during my PhD period and life, and for his patience and immense knowledge. I came to you for my second master thesis because you were known as a kind person. However, I didn't expected your demands for extreme high standard for our work. So it was quite tough in the beginning. But thanks for your patience and time-consuming guiding, I developed and could achieve what is described in this thesis. Further, you are such a charming man with great

Acknowledgements

leadership. The Rhizo team, you initiated with Ton, was wonderful. The atmosphere in this team was so nice. Everybody was willing to share knowledge and to help each other. The periods that we were working and enjoying social activities will be my most treasurable memories. Cooperation to create win-win conditions is the most important thing you have taught me. It is my great honor to be able to learn from you, work with you and live with you for such a long period.

Except my daily supervisors, there are two people who also helped me a lot in my projects. They are Martinus Schneijderberg and Carolien Franken. Martinus is one of the cleverest persons I have ever met. He is the first PhD candidate supervised by Xu and he acts like a big brother in our Rhizo team. I was supervised by him during my second MSc thesis in the lab. You actually initiated my critical and logical thinking by teaching me to challenge myself three times for a question. It was hard in the very beginning, but now, I can use it to train the people who accept my supervision. Personally, we are good friends. Your first time to China was to join my wedding in Wuhan. You experienced that a PhD was not what you aspired, but feel happy that you can have found a new way of life. Carolien, thanks for all your support during the experiments, i.e. the design, application and operation as well as taking care of them. It was a wonderful period that we and Martinus worked in the Rhizolab upstairs, with nice music and interesting chats. The size of the experiments were huge, but with a nice arrangement from you, together with other colleagues, we finished it very well. Furthermore, I would like to thank you for all the suggestions on baby care. Believe me, Lu and I have spoiled Zhizhi just a little bit.

I would like to thank other colleagues in Rhizo team, thanks for providing a friendly and open environment, and also thanks for all the supports from you throughout these years. Rene Geurts, thanks for offering me valuable suggestions on my projects. You really good at summarizing others' works and your talks are always so charming, which I tried to follow but still, a long way to go. Lucas Schmitz, thanks for helping us to process the raw data of sequencing and teaching me the very 'pure' and 'local' English writing, fantastic. Most importantly, I enjoyed discussing politics with you, although all are non-sense, but they let us know and understand each other better in a 'local' way. Yuda Roswanjaya, my

buddy, thanks for guiding me with mycorrhizal staining and observation. We made boring and dirty jokes on each other and I was surprised that we both enjoy that. Wow, I really love you, my Yuda. Jing Wang (王璟), thank you for helping me with numerous field and lab works. Also thanks for playing games with me for a long period until Zhizhi was born. So you really should play more before your baby is born. Asma Nacer, thanks for your kindness and it is my pleasure to co-operate with you. Robin van Velzen, thanks for initiating the bioinformatics pipeline for analysing the microbiome data, it is essential for our projects. I also want to thank Amina Bouherama and Said Amrani, as I appreciated to work with you in the Rhizo team.

Outside our small team, I would like to thank all my former and current colleagues. Viola Willemsen, thanks for supporting me to be able to have an online defense. Henk Franssen, thanks for organizing the lab cleaning and the messages with humor. Although, sometimes I did not get your black humors, you successfully delivered happiness to us. Olga Kulikova, thanks for your nice words and encouragements on my study and life. They indeed helped me to finish this work. I wish you and Henk a healthy and happy life. Rik Huisman and Titis Wardhani, thanks for sharing us the lovely music, I still remembered the song of MolBi from you and Martinus, amazing. Guusje Bonnema, thanks for advising me during my master study. You helped me to start the new life in Wageningen and guided me through a totally different education system. Without your guidance, I could not have reached so far. Xiaoxue Sun (孙晓雪), thanks for your daily supervision on my first master thesis. I learnt great lab technics from you and the amount of work we finished together is still impressive. Also, thanks for leading me during the dark moments of my life. Wish you always happiness. Johan Bucher, thanks for helping me with the experiments for my first masters thesis. I really like your dramatic change in dressing style, respect! I also want to thank Erik Limpens, Luuk Rutten, Wouter Kohlen, Rens Holmer, Sultan Alhusayni, Jac Aarts, Renze Heidstra, Tijs Ketelaar, Wilma van Esse, Joan Wellink, Jan Verver, Jan Hontelez, Simon Dupin, Sidney Linders, Arjan van Zeijl, Kevin Magne as I appreciated to work with you.

Acknowledgements

I would like to thank all the Chinese colleagues, besides professional supports on my study, you also help me a lot in my daily life. Siqi Yan (闫思奇), a beautiful, decent and forever 18-years-old girl, thanks for being my paranymp. Although I am in China, I still miss a lot the spicy beef you prepared for the hot pot, so delicious. Jundi Yan (闫俊迪), a handsome and warm-hearted man, thanks for being my paranymp, too. I always appreciate the support from you and Yueyang Ge (葛月阳) on the chestnut project, and being the best man and bridesmaid, respectively, on my wedding. Tian Zeng (曾添), my buddy, thanks for your love and kiss, so sweet. Next time, we still drink, eat crab and vomit together. Jieyu Liu (刘洁宇), thanks for taking care of us together with Lu when Tian and I were hangover. Hanging a garbage bag on our ears was a gorgeous idea to hold the vomit. Also, thanks for such a long company in MolBi. Defeng Shen (申德峰), thanks for trusting my expertise on your project, most importantly, without you, we could not 'fish' my keys from my window with your clothesline pole and fridge magnet, amazing! It must be even colder in Cologne, so please do remember to wear your long johns. Huchen Li (李虎臣), thanks for your supports on our Root-sleeve work and playing Gouji with us, your bluffing skills on this poker game is super. Wang Peng (王鹏), thanks for your suggestions on my proposition and also for helping our move. You did great in riding the tricycle. Haolin Zhang (张昊琳), together with Jieyu and Siqi, thanks for visiting us when Zhizhi was born. I wish you and your families a happy and healthy life. Qian Li (李茜), thanks for sharing your R scripts and working experience with me, see you in Shanghai soon. My thanks are also going to Tingting Xiao (肖婷婷), Fengjiao Bu (卜凤娇), Qi Zheng (郑琪), Jianyong An (安剑勇), Zhouwen Kun (周文焜), Jun Zhao (赵君老师), Qingqin Cao (曹庆芹老师), Mengli Zhao (赵萌莉老师), Fang Tang (唐芳), Min Li (李敏), Mengmeng Hou (侯蒙蒙), Yinshan Jiao (焦银山), I am glad I have been able to work with you.

Many thanks also go to the secretaries of MolBi, Marie-Jose van Iersel and Maria Augustijn for helping with administrative matters. Thank you both for helping me to start my study in the lab and prepare all the necessary documents and materials in time. Together with Carolien, you visited us when Zhizhi was born and delivered the nice gifts and warm

greetings from our lovely colleagues. All my friends from other groups envy our super nice secretaries, as you are always helpful.

Of course, without the help from the plant caretakers in Unifarm and Klima, I could not have finished my work. I need to apologize that I forgot your names, but I do really appreciate your help.

Special thanks goes to Johan Specken, Gerard Hoekzema, Herman van Eck and Bart Timmermans who helped me with field work at Marwijksoord and Zonnehoeve. It is a pity that these studies have not been published yet, but your visions on the development of agriculture really inspired me a lot.

I would like to recognize the invaluable assistance from the students involved in my project. Martijn de Roij and Mara Langeveld, many thanks for all your work and I am lucky to work with you. Wishing you the best in your future scientific careers.

Life during a PhD is not only about work, but also includes wonderful personal time with ‘families’. Therefore, I want to give my thanks to Xu again, the big brother of me and Lu, and the uncle of my daughter. Thanks for your care and guidance in our life, and thanks for choosing us to be part of your family. Peicheng Sun (孙培成) and Xi Bai (白溪), my brother and sister, how lucky I am to be so close with you. Thanks for taking care of us in our daily life and especially after Lu’s delivery. I have to say, the noodles you cooked are the best in the world. Junnan Ma (马俊南), our big ‘daughter’, we love you so much. We deeply appreciate your company and until now, you still deliver goods for Zhizhi to China. The cuisine Dapanji from you is the best in the world, I miss it so much. Xiao Dong (董笑), thanks for your company and guiding me during the master study. I could hardly graduate without you. I feel so lucky to have you around me when we were new in the Netherlands. You took good care of me and you also educated me when I did wrong. Wish you have a nice and successful period, for sure you will, in Cologne. Zhengyi Lin (林正仪) and Jialun Wu (吴加伦), thanks for all the delicious food and nice drinks from you. I feel very warm to stay with you for your kindness and nice tempers. Especially thanks to Zhengyi for expressing the “Jumbo” blue barriers from Yunnan to Nanjing. Wow,

Acknowledgements

that was the taste of our second home, Wageningen. Liu Liu (刘浏), you are such an independent girl with fancy ideas. Thanks for all the funny time with you.

I would like to express my thanks to friends sharing great time with me: Xiangdan Meng (孟祥丹), Juncai Chen (陈俊才), Hui Tian (田卉), Shuqing Yang (杨叔青), Beibei Jiang (蒋贝贝), Feng Zhu (朱峰), Qiqi Lu (鲁琦琦), Yiqian Fu (傅伊倩), Kaile Sun (孙凯乐), Zhongnan Chen (陈中南), Qi Liu (刘奇), Jing Li (李静) and your lovely daughter Jiajia (加加), Qinmei Yang (杨秦妹), Yuzhi Chen (陈禹志), Ying Liu (刘颖), Yue Zhao (赵越), Yongran Ji (季永然), Lili Wei (魏丽莉), Wenbo Wu (伍文博), Liuchang Nie (聂浏畅), Xing Fu (付星), Yuanyuan Zhang (张媛园), Jun Zhao (赵君), Hao Feng (冯昊).

I would like to thank my football teammates for your supports: Shiyang Wang (王诗阳), Geng Suo (索庚), Jie Lu (卢杰), Jiapeng Li (李佳蓬), Qiuyu Wang (王秋宇), Bo Wang (王博), Peng Wang (王鹏), Han Xia (夏涵), Ziqiu Su (苏子秋), Xi Zhao (赵溪), Shuyuan Wang (王书苑), Xiao Pan (潘晓), Baibing Yan (闫白冰), Jimmy (李俊明), Siyuan Xing (邢思远), Wenbiao Shi (石文标), Weixin Huang (黄炜鑫), Yue Sun (孙岳), Zongyao Huan (呼延宗尧), Xinrou Huang (黄心柔), Da Wei (伟达), Xiao Luo (罗霄), Qizhi Ren (任齐智), Cheng Liu (刘骋), Xu Li (李旭), Yi Chen (陈毅).

Also, I would like to thank friends playing games with me. Although I am the 'carry' in the game, you are the 'carry' of my life: Hy (贺远), 488 (王璟), Cj (常江), Wind (朱枫), CY (陈晔), Yu Guan (关羽), OB, dantikun, 城城, 如来, 大黄, 李为鲲, 430, X, CNDY.

I further thank my best friends in China: Ke Wu (可可), Ning Zhang (妞妞), Bo Fu (傅爹爹), Tao Liu (涛儿), Xiao Liu (骁儿), Chensheng Zhang (孙子), Jing Huang (星儿), Zhipeng Ge (葛儿), Zecheng Yin (泽儿), Lan Lu (二妹). Especially I would like to thank Lan, who spend a full day to finish my thesis's cover, which I believe that everyone loves it. We have been friends for 10 years or even longer. No matter when and where I need your support, you guys are always there. Thank you so much! 爱你们!

Acknowledgements

Well, my darling, my beloved wife, Lu Luo (罗露)! Without you, I cannot imagine how hard my life would be. You not only share your life with me, but also you guide me in our lives. You are the only one who suggested me to give up as you realize my struggles. Although the price of giving up is extreme, you are brave to accept it because you want me to be happy. Thanks for your care, support and love. Happy wife, happy life, this is the true happiness of mine. 妞啊，谢谢你!

My dear daughter, Zhizhi Yan (严知之), thanks for choosing me to be your dad. I once made a joke about my graduation when you were born, i.e. it is possible that I would get my diploma even after you can ask me why I haven't graduated yet. Well, you have the ability to do so now, but luckily, you did not do it. After your birth, besides work, I spend most of my time with you, instead of my favorite game and football. I have no regret at all. I am so happy to share my time with you, your mom, and all the people loving you. I am so proud to be your dad. 谢谢你，六一!

At last, I would like to thank my parents and my mother-in-law. Without your support, I could not have reached so far. The most important thing you taught me, is to receive love from others, and to love others. 最后，我要感谢我的爸爸和妈妈们。没有你们的支持，我走不到今天。谢谢你们教会我，学会接受别人的爱，学会去爱别人。愿您们都健康平安，以后的日子让我，露露和六一来守护您们。

Zhichun Yan

严志纯

2nd December 2022

Curriculum Vitae

Zhichun Yan was born on 12th of June, 1991 in Hubei Province, China. In 2013, he obtained his bachelor's degree at the College of Horticulture & Forestry Sciences in Huazhong Agricultural University, Hubei. He was curious about the world abroad, so he came to the Netherlands and continued his master study in Wageningen University & Research, Wageningen. His major was plant breeding and genetic resources, supervised by Dr Guusje Bonnema. He graduated in August 2015 with two MSc theses: Morphological and molecular characterization of heading traits in



Chinese cabbage (*Brassica rapa*) and Creation of CRISPR/Cas9 root mutants in the Arabidopsis Mossel accession, respectively. Except for plants, he showed great interest in CRISPR-Cas9 gene editing technology and root-microbiome studies. So, he decided to stay in the Laboratory of Molecular Biology and worked on construction of plant mutant and microbiome data analysis as a Research Assistant. In the meantime, he searched for related PhD projects. Together with his supervisors, he successfully applied for a CSC grant to start his PhD in this lab in September 2016, aiming to investigate the composition of root-associated microbiomes and their beneficial effects on plant growth under stress conditions. Main findings obtained during his doctoral study are presented in this thesis.

Publications

Schmitz, L. [#], **Yan, Z.** [#], Schneijderberg, M. *et al.* (2022) A synthetic bacterial community derived from a desert rhizosphere confers salt stress resilience to tomato in the presence of a soil microbiome. **THE ISME J.**

Kherfi-Nacer, A. [#], **Yan, Z.** [#], Bouherama, A. *et al.* (2022) High salt levels reduced dissimilarities in root-associated microbiomes of two barley genotypes. **MPMI.**

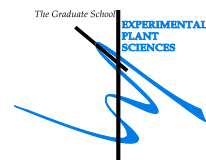
Sun, X., Basnet, R.K., **Yan, Z.** *et al.* (2019) Genome-wide transcriptome analysis reveals molecular pathways involved in leafy head formation of Chinese cabbage (*Brassica rapa*). **Horticulture research.**

Yan, Z. [#], Li, H. [#], Zhang, B. *et al.* (2022) Root-sleeve, an adaptation to drought and a niche for a distinct microbiome. In preparation.

Cheng, X. [#], **Yan, Z.** [#], Li, Q. *et al.* (2022) Longevity correlates with similar root bacterial microbiome compositions in a chrono-series of Chinese chestnut. In preparation.

Education Statement of the Graduate School

Experimental Plant Sciences



Issued to: Zhichun Yan
Date: 02 December 2022
Group: Laboratory of Molecular Biology
University: Wageningen University & Research

1) Start-Up Phase	<u>date</u>	<u>cp</u>
► First presentation of your project Microbial communities supporting potato growth against abiotic stresses	16 Dec 2016	1.5
► Writing or rewriting a project proposal Microbial communities supporting potato growth against abiotic stresses	2016/2017	6.0
► MSc courses		

Subtotal Start-Up Phase

7.5

2) Scientific Exposure	<u>date</u>	<u>cp</u>
► EPS PhD student days EPS PhD student days 'Get2Gether', Soest (NL)	09-10 Feb 2017	0.6
EPS PhD student days 'Get2Gether', Soest (NL)	15-16 Feb 2018	0.6
► EPS theme symposia EPS Theme 1 Symposium 'Developmental Biology of Plants', Leiden (NL)	28 Feb 2017	0.3
EPS Theme 1 Symposium 'Developmental Biology of Plants', Wageningen (NL)	30 Jan 2018	0.3
EPS Theme 1 Symposium 'Developmental Biology of Plants' (online)	28 Jan 2021	0.2
EPS Theme 2 Symposium & Willie Commelin Scholten day 'Interactions between Plants and Biotic Agents', Wageningen (NL)	23 Jan 2017	0.3
EPS Theme 2 Symposium & Willie Commelin Scholten day 'Interactions between Plants and Biotic Agents', Amsterdam (NL)	24 Jan 2018	0.3
EPS Theme 2 Symposium & Willie Commelin Scholten day 'Interactions between Plants and Biotic Agents' (online)	09 Feb 2021	0.2
EPS Theme 3 Symposium 'Metabolism and Adaptation', Wageningen (NL)	14 Mar 2017	0.3
EPS Theme 3 Symposium 'Metabolism and Adaptation' (online)	30 Oct 2020	0.2
► Lunteren Days and other national platforms Annual Meeting 'Experimental Plant Sciences', Lunteren (NL)	10-11 Apr 2017	0.6
Annual Meeting 'Experimental Plant Sciences', Lunteren (NL)	09-10 Apr 2018	0.6
Annual Meeting 'Experimental Plant Sciences', Lunteren (NL)	08-09 Apr 2019	0.6
Annual Meeting 'Experimental Plant Sciences', Lunteren (NL)	12-13 Apr 2021	0.5
► Seminars (series), workshops and symposia 1st Symposium WURomics: Technology-Driven Innovation for Plant Breeding	15 Dec 2016	0.3
'B2R get together' symposium	15 Nov 2017	0.3
Symposium - Root zone phenomics, physiology and ecology: creating space for the better half	02 Oct 2018	0.3
Plant-RX symposium online event "Artificial intelligence in plant science and breeding"	24 Feb 2021	0.2
Seminar Michael Nodine "RNA Biology of Plant Embryos"	25 Feb 2021	0.1
Seminar by Wilma van Esse "From gene discovery to molecular network analysis: unraveling transcription factor networks that control cereal crop yield"	26 Mar 2021	0.1
Seminar by the Research Unit "Plant Growth and Development"	29 Oct 2021	0.2
► Seminar plus		
► International symposia and congresses 2nd Plant Microbiome Symposium, Amsterdam (NL)	19-21 Feb 2018	0.9
International Symposium on Microbe-assisted Crop Production - Opportunities, Challenges & Needs (miCROPe 2019), Vienna (AT)	02-05 Dec 2019	1.2
► Presentations 2nd Plant Microbiome Symposium (poster)	19-21 Feb 2018	1.0
Annual Meeting 'Experimental Plant Sciences' (online, poster)	12-13 Apr 2021	1.0
► 3rd year interview		
► Excursions		

Subtotal Scientific Exposure

11.2

3) In-Depth Studies	<u>date</u>	<u>cp</u>
► Advanced scientific courses & workshops EPS course 'Data Analyses and Visualizations in R'	11-12 May 2017	0.6
VLAg course 'Applied Statistics'	15-21 Jun 2017	1.0
VLAg course 'Chemometrics'	26-30 Jun 2017	1.5
EPS course 'The Power of RNA-Seq'	11-13 Jun 2018	0.9
PE&RC/EPS/WIMEK course 'Introduction to machine learning'	28 Jun - 2 Jul 2021	1.5
► Journal club Literature discussion - Laboratory of Molecular Biology	2016 - 2021	3.0
► Individual research training		

Subtotal In-Depth Studies

8.5

4) Personal Development	<u>date</u>	<u>cp</u>
► General skill training courses		
EPS Introduction course	16 Feb 2017	0.3
WGS course 'Brain training'	11 Apr 2018	0.3
WGS workshop 'Critical thinking and argumentation'	19 Sep 2019	0.3
WGS workshop 'Scientific Publishing'	15 Oct 2019	0.3
WUR workshop 'Scientific Integrity'	20 Feb 2020	0.1
Lunch webinar 'A Beautiful Thesis In 6 Steps'	30 Jul 2020	0.1
WUR Library course 'Searching and Organising Literature' (online training)	16-17 Feb 2021	0.6
WGS course 'Career Orientation' (online training)	18 May - 15 Jun 2021	1.5
► Organisation of meetings, PhD courses or outreach activities		
► Membership of EPS PhD Council		

Subtotal Personal Development

3.5

5) Teaching & Supervision Duties	<u>date</u>	<u>cp</u>
► Courses		
Molecular aspects of Bio-interactions PHP-30806	2017, 2018, 2020	1.0
► Supervision of BSc/MSc students		
BSc project "Salinity tolerance conferred to Barley by microbiome", Martijn de Roij	2018	0.7
BSc project "Induced salt tolerance in barley based on Rhizobium isolates", Mara Langeveld	2019	0.7

Subtotal Teaching & Supervision Duties

2.4

TOTAL NUMBER OF CREDIT POINTS*	33.1
Herewith the Graduate School declares that the PhD candidate has complied with the educational requirements set by the Educational Committee of EPS with a minimum total of 30 ECTS credits.	
* A credit represents a normative study load of 28 hours of study.	

The research described in this thesis was financially supported by the Laboratory of Molecular Biology, Wageningen University, and from China Scholarship Council (201607720004).

Financial support from Wageningen University for printing this thesis is gratefully acknowledged.

Cover design by: Lan Lu (卢兰), Lu Luo & Zhichun Yan

Layout design by: Zhichun Yan

Printed by: ProefschriftMaken